



UNIVERSIDADE FEDERAL DE PERNAMBUCO
CENTRO DE TECNOLOGIA E GEOCIÊNCIAS
DEPARTAMENTO DE OCEANOGRÁFIA
PROGRAMA DE PÓS-GRADUAÇÃO EM OCEANOGRÁFIA

LISANA FURTADO CAVALCANTI LIMA

**DIVERSIDADE, ESTRUTURA E BIOMASSA FITOPLANCTÔNICA AO LONGO DE
UM *CONTINUUM* ESTUÁRIO-OCEANO, SÍTIO RAMSAR - COSTA NORTE
AMAZÔNICA: UMA ABORDAGEM TEMPORAL E ESPACIAL**

Recife

2023

LISANA FURTADO CAVALCANTI LIMA

**DIVERSIDADE, ESTRUTURA E BIOMASSA FITOPLANCTÔNICA AO LONGO DE
UM *CONTINUUM* ESTUÁRIO-OCEANO, SÍTIO RAMSAR - COSTA NORTE
AMAZÔNICA: UMA ABORDAGEM TEMPORAL E ESPACIAL**

Tese apresentada ao Programa de Pós-Graduação em Oceanografia da Universidade Federal de Pernambuco, como requisito parcial para obtenção do título de doutor em Oceanografia.

Área de concentração: Oceanografia Biológica

Orientador: Prof. Dr. Fernando Antônio do Nascimento Feitosa

Coorientador: Prof. Dr. Marco Valério Jansen Cutrim

Coorientador: Prof. Dr. Manuel de Jesus Flores-Montes

Recife

2023

Catalogação na fonte
Bibliotecário Gabriel Luz, CRB-4 / 2222

- L732d Lima, Lisana Furtado Cavalcanti.
Diversidade, estrutura e biomassa fitoplânctonica ao longo de um *continuum* estuarino-oceano, Sítio Ramsar - Costa Norte Amazônica: uma abordagem temporal e espacial / Lisana Furtado Cavalcanti Lima, 2023.
172 f.: il.
- Orientador: Prof. Dr. Fernando Antônio do Nascimento Feitosa.
Coorientador: Prof. Dr. Marco Valério Jansen Cutrim.
Coorientador: Prof. Dr. Manuel de Jesus Flores-Montes.
Tese (Doutorado) – Universidade Federal de Pernambuco. CTG. Programa de Pós-Graduação em Oceanografia. Recife, 2023.
Inclui referências, apêndices e anexo.
1. Oceanografia. 2. Diatomáceas. 3. Fitoplâncton indicador. 4. Diversidade beta. 5. Reentrâncias Maranhenses. 6. Plataforma Continental. I. Feitosa, Fernando Antônio do Nascimento (Orientador). II. Cutrim, Marco Valério Jansen (Coorientador). III. Flores-Montes, Manuel de Jesus (Coorientador). IV. Título.

UFPE

551.46 CDD (22. ed.)

BCTG / 2023 - 137

LISANA FURTADO CAVALCANTI LIMA

**DIVERSIDADE, ESTRUTURA E BIOMASSA FITOPLANCTÔNICA AO LONGO DE
UM *CONTINUUM* ESTUÁRIO-OCEANO, SÍTIO RAMSAR - COSTA NORTE
AMAZÔNICA: UMA ABORDAGEM TEMPORAL E ESPACIAL**

Tese apresentada ao Programa de Pós-Graduação em Oceanografia da Universidade Federal de Pernambuco, como requisito parcial para obtenção do título de doutor em Oceanografia.

Área de concentração: Oceanografia Biológica

Aprovado em: 14/02/2023.

BANCA EXAMINADORA

Prof. Dr. Fernando Antônio do Nascimento Feitosa (Orientador)
Universidade Federal de Pernambuco - UFPE

Prof. Dra. Sigrid Neumann Leitão (Examinador Interno)
Universidade Federal de Pernambuco - UFPE

Prof. Dr. Pedro Augusto Mendes de Castro Melo (Examinador Interno)
Universidade Federal de Pernambuco - UFPE

Prof. Dra. Andrea Christina Gomes de Azevedo Cutrim (Examinador Externo)
Universidade Estadual do Maranhão – UEMA

Prof. Dra. Luci Cajueiro Carneiro Pereira (Examinador Externo)
Universidade Federal do Pará - UFPA

*Dedico à minha família amada, meu porto seguro, onde
encontro razão para viver
Ao meu esposo e melhor amigo, Fernando
Ao meu avô tão querido, Teodulino (in memoriam)
Devo tudo a vocês!*

AGRADECIMENTOS

Como é gratificante chegar à etapa final desse tão sonhado ciclo e ao mesmo tempo chega a ser difícil tentar resumir em poucas palavras toda a minha gratidão. Desde a graduação sonhava em fazer doutorado, desbravar o mundo fitoplânctônico marinho, lecionar e seguir fazendo pesquisa científica. Naquela época, tudo isso parecia muito distante e hoje, finalizando esse ciclo, vejo o quanto que aprendi e quantas pessoas incríveis fizeram parte dessa longa jornada. Então, quero registrar os meus agradecimentos mais sinceros àqueles que foram essenciais para o meu crescimento pessoal e profissional:

Primeiramente, agradeço a *Deus* pelo seu infinito amor e compaixão. Não sei o que seria de mim sem os Teus cuidados. Toda a honra seja dada ao Senhor!

À minha família, especialmente, a minha mãe *Rosana* que cuida de mim sem medir esforços, nunca serei capaz de recompensá-la por tanto amor. Ao meu pai *José Liraelson*, irmãos *Philip* e *Clisman* e irmãs *Karol* e *Thaiane* pela torcida e incentivo. Todo esse amor e torcida me deram força para prosseguir.

Ao meu melhor amigo, inicialmente namorado, noivo e hoje esposo *Fernando* que sempre esteve ao meu lado dando suporte, força e incentivo. Obrigada por ser meu porto seguro e por aceitar embarcar comigo em mais um grande desafio que foi o doutorado. Sem você não teria chegado até aqui!

À *Universidade Federal de Pernambuco, Departamento de Oceanografia* e ao *Programa de Pós-graduação em Oceanografia*, pelas oportunidades concedidas e por proporcionar suporte estrutural e técnico possibilitando a realização deste trabalho durante o Curso de Pós-Graduação em Oceanografia.

À *Coordenação de Aperfeiçoamento de Pessoal de Nível Superior (CAPES)*, pela concessão da bolsa de doutorado.

Ao meu querido orientador *Prof. Fernando Feitosa*, que me conduziu ao longo desses anos, compartilhando seu precioso conhecimento e experiência sobre Oceanografia na sua forma mais bela. Obrigada por todo cuidado e atenção sem igual, sou imensamente grata por tê-lo conhecido além das citações (que não foram poucas). Serei eternamente honrada por fazer parte da longa lista de “maguinhas” orientadas pelo senhor!

Ao meu querido coorientador *Prof. Marco Cutrim*, que considero, além de orientador, meu pai científico. Muito obrigada por sempre acreditar em mim! Obrigada por ser parte fundamental do meu crescimento profissional e pessoal, foram muitos os momentos de

aprendizagem desde o mestrado até o fim deste ciclo. Ao meu eterno pai científico toda a minha gratidão.

Ao meu coorientador *Prof. Manuel Flores-Montes*, também foi um enorme prazer conhecer além das publicações científicas. Obrigada por todo incentivo e apoio.

Aos laboratórios de *Fitoplâncton (LabFic)* e *Física (Lhiceai)* da Universidade Federal do Maranhão, representados pelos coordenadores *Prof. Marco Cutrim* e *Prof. Francisco Dias*, por todo suporte técnico e científico que viabilizaram as coletas de campo e análises em laboratório para o aperfeiçoamento do conhecimento sobre a comunidade fitoplanctônica.

Aos laboratórios de *Fitoplâncton (LABFITO)* e *Química (LOQuim)* da Universidade Federal de Pernambuco, representados pelos coordenadores *Prof. Fernando Feitosa* e *Prof. Manuel Flores-Montes* e amigos *Jamerson* e *Brenno*, que nos auxiliaram nas análises químicas.

Aos professores do Programa de Pós-graduação em Oceanografia, em especial à *Profa. Maria da Glória Cunha*, *Prof. Pedro Melo*, *Profa. Tereza Araújo* e *Prof. Marius Muller*, pela atenção e conhecimentos compartilhados durante o doutorado e a todos os funcionários que me ajudaram de forma direta e indireta com a realização deste trabalho.

À *Prof. Andrea Christina Azevedo Cutrim*, minha eterna orientadora, obrigada por me apresentar a beleza da Ficologia durante a graduação em Ciências Biológicas (UEMA). Meus sinceros agradecimentos por ter sido minha mãe científica e por ter construído fortes laços de amizade.

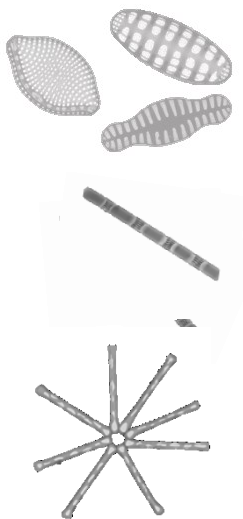
Ao meu querido amigo *Prof. Caio Brito*, pelo suporte, conselhos e sugestões na finalização deste trabalho. Seu apoio foi muito importante.

Aos meus amigos de turma *Mariana*, *Juliana*, *Brenno*, *Rodolfo* e *Silvio* que estiveram comigo durante essa caminhada. Ao *Gabriel* pelos ensinamentos sobre GAM, *Leidiane* por despertar a minha paixão pela diversidade beta e *Claudeilton* pelos ensinamentos sobre o tratamento de imagens científicas.

De forma especial, às minhas amigas de laboratório *Taiza*, *Quediane*, *James*, *Cybelle*, *Adryanne*, *Denise*, *Jacyara* e amigo *Daniel*, pela amizade construída, momentos de descontração, por serem tão parceiros na etapa de campo e auxílio nas análises de laboratório. Às minhas queridas “xubas” *Jordana*, *Bethânia*, *Amanda*, *Francinara* e *Nágela*, vocês foram fundamentais nesta jornada, onde estudamos e crescemos juntas. Em especial agradeço à minha amiga e parceira de vida, *Karol*, obrigada por compartilhar cada emoção vivida durante a nossa caminhada no doutorado. A todos, obrigada por essa linda amizade!

Aos meus grandes amigos da minha terrinha São Luís: *Adaylza, Diego, Lilian, Adriano, Jordan, Nilza, Rhaysa, Débora e Rannyele*, e aos presentes mais que especiais que ganhei durante o curso de doutorado em Recife: *Neto, Karina, Rita, Roberta, Nathan, Ilmaria e Nadja*. A vocês meu muito obrigada!

Registro aqui minha eterna gratidão a todos que contribuíram de alguma forma durante essa minha jornada tão sonhada.



*"I've learned that you are never too small
to make a difference"*

Greta Thunberg

*"Your grace abounds in deepest waters
Your sovereign hand will be my guide
Where feet may fail and fear surrounds me
You've never failed and You won't start now..."*

Oceans – Hillsong United

RESUMO

A manutenção da biodiversidade, fator chave na ecologia, tem sido um dos maiores desafios na atualidade. Entender os processos que influenciam a diversidade e estrutura fitoplanctônica pode auxiliar no estabelecimento de medidas de conservação cada vez mais precisas. Devido a isto, a pesquisa foi desenvolvida na Plataforma Continental Maranhense (PCM), setor leste da Costa Norte Amazônica, considerada *hotspot* mundial para conservação por apresentar elevada produtividade e diversidade biológica. Este estudo teve como objetivo investigar os padrões temporais e espaciais da diversidade, estrutura e biomassa fitoplancônica na PCM, evidenciando sua relação com a variabilidade climática, ciclo de maré e hidrologia ao longo de um *continuum* estuário-oceano. Para isso, foram realizadas análises temporais e espaciais das variáveis físicas, químicas e biológicas entre os anos de 2019 e 2020, totalizando 13 pontos amostrais considerando duas abordagens. A primeira (menor escala espacial) investigou padrões eco-hidrológicos ao longo de cinco pontos em uma baía de macromaré (Baía de Cumã). A segunda (maior escala espacial) abrangeu desde os pontos mais internos da baía até a isóbata de 60 m próximo a quebra da plataforma, caracterizando um *continuum* estuário-oceano. Como resultados, 192 táxons foram identificados na baía de Cumã e 189 ao longo do *continuum* estuário-oceano, com o predomínio do filo Bacillariophyta (diatomáceas) em ambas as escalas, seguido por Miozoa e Cyanobacteria. A dinâmica hidrológica na PCM foi caracterizada espacialmente pela elevada contribuição continental que resultou em uma maior influência da pluma estuarina (salinidade < 30) alcançando cerca de 60 km da linha de costa. Esta dinâmica, associada ao regime de macromaré, resultou em uma heterogeneidade ambiental marcada por zonas funcionalmente distintas. Sazonalmente, a maior influência da pluma estuarina e disponibilidade de luz na Baía de Cumã, durante os primeiros meses do ano, favoreceram o aumento da densidade e biomassa fitoplancônica, com ocorrência de *blooms* da diatomácea *Skeletonema costatum* ($> 10^6$ cell L⁻¹) e redução de diversidade taxonômica. Durante a estiagem, a maior penetração da água marinha no sistema associada a maior intensidade dos ventos e dinâmica de macromarés resultaram em águas mais turvas, limitando a disponibilidade de luz e atividade fotossintética do fitoplâncton. A análise de cluster identificou a formação de oito grupos fitoplancônicos associados à variabilidade espaço-temporal do *continuum* estuário-oceano. A partir desses grupos, 39 espécies foram selecionadas como indicadoras da PCM. A diversidade beta apresentou um gradiente crescente ao longo da escala temporal e espacial. Por fim, o presente estudo evidenciou que processos determinísticos governaram a estrutura comunidade e diversidade fitoplancônica da PCM, e reforça a importância da manutenção de

séries temporais para melhor compreensão da dinâmica do fitoplâncton em ambientes de alta complexidade como os encontrados na Costa Norte Amazônica.

Palavras-chave: Diatomáceas; Fitoplâncton indicador; Diversidade beta; Reentrâncias Maranhenses; Plataforma Continental.

ABSTRACT

Biodiversity maintenance, a key factor in ecology, is one of the biggest challenges nowadays. Understanding the processes that influence phytoplankton diversity and structure can help to establish accurate conservation measures. Therefore, this research was developed in the Maranhense Continental Shelf (MCS), the eastern sector of the North Amazon Coast, which is considered a world hotspot for conservation due to its high productivity and biological diversity. This study aimed to investigate the temporal and spatial patterns of phytoplankton diversity, structure, and biomass in the MCS, evidencing their relationship with climate variability, tidal cycle, and hydrology along an estuary-ocean continuum. For this, temporal and spatial analyses of the physical, chemical, and biological variables were carried out between 2019 and 2020, totaling 13 stations considering two approaches. The first (smaller spatial scale) investigated ecohydrological patterns along five stations in a macrotidal bay (Baía de Cumã). The second (larger spatial scale) included stations from the innermost portion of the bay to stations at the 60 m isobath near the shelf break, characterizing an estuary-ocean continuum. As a result, 192 taxa were identified in Cumã Bay and 189 along the estuary-ocean continuum, with a predominance of Bacillariophyta (diatoms) at both scales, followed by Miozoa and Cyanobacteria. The hydrological dynamics in the PCM were characterized spatially by the high continental contribution that resulted in a greater influence of the estuarine plume (salinity < 30) reaching approximately 60 km from the coastline. This dynamic, associated with the macrotidal regime, resulted in an environmental heterogeneity marked by functionally distinct zones. Seasonally, the influence of the estuarine plume and light availability in the Cumã Bay, during the first months of the year, favored the increase in phytoplankton abundance and biomass, with the occurrence of blooms of the diatom *Skeletonema costatum* ($> 10^6$ cell L⁻¹) and reduction of the taxonomic diversity. During the dry season, the greater penetration of marine water into the system associated with high wind intensity and macrotidal dynamics resulted in turbid waters, which limited the light availability and photosynthetic activity of phytoplankton. Cluster analysis depicted eight phytoplankton groups associated with the spatiotemporal variability of the estuary-ocean continuum. From these groups, 39 species were selected as indicators of the MCS. Beta diversity showed an increasing temporal and spatial trend across the shelf. Finally, the present study pointed out that deterministic processes governed the community structure and phytoplankton diversity of the coastal shelf and highlighted the importance of maintaining time series for a better understanding of

phytoplankton dynamics in highly complex environments such as those found in the North Coast of the Amazon.

Keywords: Diatoms; Phytoplankton indicator; Beta diversity; Reentrâncias Maranhenses; Continental shelf.

LISTA DE FIGURAS

Figura 1 - Representação esquemática da definição de zona costeira de acordo com Holligan e Boois (1993)	21
Figura 2 - Distribuição das Ecorregiões Marinhas e suas respectivas províncias com destaque para o Oceano Atlântico Tropical e Plataforma Norte do Brasil. Fonte: Adaptado de Spalding et al. (2007) e Tosetto et al. (2022).....	23
Figura 3 - Localização dos 27 Sítios Ramsar localizados no Brasil. Fonte: https://www.gov.br/mma/pt-br	24
Figura 4 - Diagrama de blocos esquemáticos indicando as categorias e os serviços ecossistêmicos fornecidos pelo fitoplâncton. Fonte: Adaptado de Naselli-Flores e Padisák (2022).	25
Figura 5 - Plataforma Continental Amazônica incluindo os estados do Maranhão, Pará e Amapá. Fonte: Silva (2019).....	30
Figura 6 - Distribuição horizontal das principais correntes na Plataforma Continental Amazônica. CNB - Corrente Norte do Brasil, CCNE - Contra-Corrente Norte Equatorial. Fonte: Adaptado de Chérubin e Richardson (2007).	31
Figura 7 - Localização da Plataforma Continental Maranhense, incluindo as Reentrâncias Maranhenses na costa oeste, o Golfão Maranhense no setor central e o Parque dos Lençóis Maranhenses na costa leste. Fonte: Autoria própria.....	33
Figura 8 - Localização da Baía de Cumã e seus principais tributários, Reentrâncias Maranhenses, Plataforma Continental Maranhense - Brasil. Fonte: Autoria própria.....	35
Figura 9 - Distribuição vertical e longitudinal de salinidade na Baía de Cumã durante o período chuvoso e de estiagem, considerando o regime de maré enchente e vazante. Fonte: Autoria própria	37
Figura 10 - Fluxograma metodológico do procedimento de pesquisa e análise de dados referentes ao capítulo 5.....	39
Figura 1 - Fluxograma metodológico do procedimento de pesquisa e análise de dados referentes ao capítulo 6.....	40

ARTIGO 1 - Drivers of phytoplankton biomass and diversity in a macrotidal bay of the Amazon Mangrove Coast, a Ramsar site

Fig. 1 -	Map of study area, including the determination of functional zones based on Cluster analysis according to water quality during rainy and dry seasons in Cumã Bay, Amazon Macrotidal Mangrove Coast.....	45
Fig. 2 -	Historical average of precipitation, total monthly precipitation and wind speed for study period (2019-2020) (a). Monthly flow rate average of the Pericumã river basin (b). Meteorological data were obtained from National Institute of Meteorology (www.portal.inmet.gov.br).	46
Fig. 3 -	Spatial and seasonal variation of environmental variables in Cumã Bay, Amazon Macrotidal Mangrove Coast.....	54
Fig. 4 -	Synthesis of phytoplankton biomass (a), nutritional status (b), contribution of phytoplankton fractions (microphytoplankton: < 20 µm and nanophytoplankton: > 20 µm) (c), and light limiting factors (d) in Cumã Bay.	
	55
Fig. 5 -	Relative abundance (%), total richness (right diagram) and richness by zones (FIZ, MIZ) and seasonal periods (rainy and dry seasons) (top diagram) of the phytoplankton distribution by divisions (Bacillariophyta, Miozoa, Chrysophyta, Cyanobacteria, Euglenophyta, and Chlorophyta) in Cumã Bay. Note: FIZ - freshwater influence zone; MIZ - marine influence zone.....	56
Fig. 6 -	Generalized Additive Models (GAMs) results describing the main factors that influenced the phytoplankton diversity (H') (a), Skeletonema costatum and Thalassiosira subtilis as critical species (b), and chlorophyll-a (c). Solid lines represent smoothed mean relationships from GAM's and shaded areas are 95% confidence intervals. Points represent residuals. Other details are provided in Table 6.	62
Fig. 7 -	Ecohydrologic conceptual diagram for the Cumã Bay, integrating hydrological, ecological and anthropogenic factors and processes during the rainy and dry seasons.....	64

ARTIGO 2 - Effects of climate, spatial and hydrological processes on shaping phytoplankton community structure and β -diversity in an estuary-ocean continuum (Amazon continental shelf, Brazil)

Fig. 1 -	Map of the study area, including the positions of the 13 stations along the estuary-ocean continuum in the Amazon continental shelf (eastern sector). The North Brazil Current (NBC) is indicated in the map (a). The historical average and monthly rainfall (28-year historical series) (b) and wind speed (c) during the study period (January 2019 – December 2020). Monthly river discharge of the main rivers of Cumã Bay (CB), São Marcos Bay (SMB) and São José Bay (SJB) (c)	85
Fig. 2 -	Dispersion of environmental variables through principal coordinate analysis (PCoA) and boxplot based on distance to centroid (environmental heterogeneity) considering the temporal scale in Cumã Bay (a) and spatial scale along the estuary-ocean continuum (b).	92
Fig. 3 -	Temporal distribution of salinity (a) and nutrients (b–e) in Cumã Bay. Monthly distribution is indicated through boxplots.....	94
Fig. 4 -	Vertical profile of salinity gradient (a) and depth-referenced T-S diagram (b) from the data collected during the cruise over the estuary-ocean continuum. Located at different water depths, three water masses are identified, the estuarine water (EW) in the upper water column, the coastal water (CW) at mid-depth, and the tropical water (TW) in the lower water column.....	96
Fig. 5 -	Spatial distribution of salinity (a), water temperature (b), DO (c), pH (d), SPM (f) and nutrients (f–i) along the estuary-ocean continuum.....	98
Fig. 6 -	Redfield ratios (DIN:DIP:DSi) in Cumã Bay (a-b) and along the estuary-ocean continuum (c). The potentially limiting nutrients are indicated in the three areas delimited by the Redfield ratio (P-limited: blue; N-limited: yellow; Si-limited: pink). (For interpretation of the references to colour in this figure legend, the reader is referred to the web version of this article.).....	100
Fig. 7-	Spatiotemporal distribution of phytoplankton abundance (a-b) and chlorophyll-a (c-d) in the MCS. Note: The pizza graphs attached to the abundance profiles represent the phytoplankton groups and those attached to the chlorophyll-a profiles represent the chlorophyll-a fractions.....	102

Fig. 8 -	Synthesis of phytoplankton associations in Cumā Bay and MCS. Hierarchical clustering dendrogram of the phytoplankton assemblages (a), horizontal profiles of phytoplankton groups defined by cluster analysis (b), and morphological traits for each cluster group (c).....	105
Fig. 9 -	Taxonomic β -diversity (β_{Sor}) partitioned into turnover (β_{Sim}) and nestedness (β_{Nes}) components considering the temporal scale in Cumā Bay (a) and spatial scale in the estuary-ocean continuum (b) for phytoplankton community. β -diversity heatmap comparing the groups depicted in the cluster analysis. Numbers under the arches on the temporal scale indicate total β -diversity. Upper and bottom arrowheads in spatial scale represent turnover and nestedness, respectively.....	107
Fig. 10 -	Variation partitioning-based Venn diagrams showing the relative contribution of environmental variables (Env), spatial AEM eigenvectors (Spa), climatic variables (Cli) and local hydrodynamic factors (Hyd) for phytoplankton β -diversity (a) and community structure (b). Values represent the adjusted R^2 values. Negative fraction values are not presented. Statistical significance: * p <0.05; ** p <0.01; *** p <0.001.....	103

LISTA DE TABELAS

Tabela 1 - Resumo das publicações atuais sobre o fitoplâncton com foco na diversidade beta nas regiões do Brasil	28
ARTIGO 1: Drivers of phytoplankton biomass and diversity in a macrotidal bay of the Amazon Mangrove Coast, a Ramsar site	
Table 1 - Diversity measures used to estimate the phytoplankton richness, diversity and evenness in an Amazon macrotidal bay.	49
Table 2 - Summary of results of permutational multivariate analysis of variance (PERMANOVA) of the hydrological variables, considering Seasonal periods (Sea), Zones of similar influence (ZSI) and Sampling depth (Sd) as factors... .	51
Table 3 - Descriptive statistics (mean and standard deviation) for physical, chemical and biological variables of Cumã Bay and Kruskal-Wallis test with <i>p</i> values for the analyzed treatments (seasons, zones, and sampling depth). Note: FIZ = freshwater influence zone; MIZ = marine influence zone; Sea. = seasonal periods; Spa. = Spatial variation; Sd. = Sampling depth.....	53
Table 4 - Correlation coefficients (Pearson, r) between alpha diversity indices, number of taxa (S) and cell abundance (Ca). The grey shading indicates that the indices are from the same group: richness (light grey), diversity (white) or evenness (dark grey).....	59
Table 5 - Correlation coefficients (Pearson, r) between the Principal Components (PC) that were calculated from rainy season data and dry season and diversity indices for Cumã Bay, Amazon Macrotidal Mangrove Coast. Statistically significant values (<i>p</i> <0.001) are indicated with an asterisk (*).	60
Table 1 - Statistical summary of generalized additive models (GAMs) between phytoplankton diversity (Shannon index), critical species (<i>S. costatum</i> and <i>T. subtilis</i>), chlorophyll <i>a</i> and environmental parameters for Cumã bay (n=60).....	61
ARTIGO 2: Effects of climate, spatial and hydrological processes on shaping phytoplankton community structure and β-diversity in an estuary-ocean continuum (Amazon continental shelf, Brazil)	
Table 1 - Main physical and ecological characteristics of the Maranhão Continental Shelf and Cumã Bay.....	85

Table 2 - Summary of the permutational multivariate analysis of variance (PERMANOVA) results evaluating the variability of environmental conditions along the temporal scale (seasonal periods and months) and between tides cycle (flood and ebb) in Cumã Bay and the spatial scale (bay, plume and outer) in the estuary-ocean continuum in Maranhão continental shelf (MCS).	911
Table 3 - Descriptive statistics (mean and standard deviation) of hydrological and biological variables and nutrients in Cumã Bay. Note: Ti: Tides. Temporal included seasonal (Se.) periods (rainy and dry) and months (Mo) (May to December).	95
Table 4 - Descriptive statistics (mean and standard deviation) and multiple comparisons (pairwise test) of hydrological and biological variables and nutrients along the estuary-ocean continuum.	99
Table 5 - Indicator values (IndVal), phytoplankton abundance, functional traits, ecology and occurrence of phytoplankton species in the MCS.....	110

SUMÁRIO

1	INTRODUÇÃO	20
1.1	Região costeira	20
1.2	Plataformas continentais e Sítios Ramsar	22
1.3	Diversidade do fitoplâncton marinho.....	24
2	DESCRIÇÃO DA ÁREA.....	29
2.1	Costa Norte Amazônica	29
2.2	Plataforma Continental Maranhense	31
2.3	Baía de Cumã	34
3	OBJETIVOS E HIPÓTESES	38
3.1	Objetivo Geral.....	38
3.2	Objetivos Específicos.....	38
3.3	Hipóteses.....	38
4	ESTRUTURA DA TESE	39
5	ARTIGO 1 - DRIVERS OF PHYTOPLANKTON BIOMASS AND DIVERSITY IN A MACROTIDAL BAY OF THE AMAZON MANGROVE COAST, A RAMSAR SITE	41
6	ARTIGO 2 - EFFECTS OF CLIMATE, SPATIAL AND HYDROLOGICAL PROCESSES ON SHAPING PHYTOPLANKTON COMMUNITY STRUCTURE AND B-DIVERSITY IN AN ESTUARY-OCEAN CONTINUUM (AMAZON CONTINENTAL SHELF, BRAZIL).....	81
7	CONSIDERAÇÕES FINAIS	139
	REFERÊNCIAS	141
	APÊNDICE A – IMPLICAÇÕES ECOLÓGICAS DA COMUNIDADE FITOPLANCTÔNICA GERAL (DISTRIBUIÇÃO TAXONÔMICA, FREQUÊNCIA DE OCORRÊNCIA E ECOLOGIA) E DISTRIBUIÇÃO TAXONÔMICA POR CLASSES AO LONGO DO CONTINUUM ESTUÁRIO-OCEANO.....	151
	APÊNDICE B – SINOPSE DOS TÁXONS IDENTIFICADOS NA BAÍA DE CUMÃ E PLATAFORMA CONTINENTAL MARANHENSE	153
	APÊNDICE C – DISTRIBUIÇÃO E IMPLICAÇÕES ECOLÓGICAS DO FITOPLÂNCTON NA BAÍA DE CUMÃ E PLATAFORMA CONTINENTAL MARANHENSE	156
	APÊNDICE D – ARTIGO 1.....	163

APÊNDICE E - ARTIGO 2.....	167
ANEXO A - DESENVOLVIMENTO DE ENSINO E PESQUISA DURANTE O DOUTORADO QUE CONTRIBUIU PARA A EXECUÇÃO DESTA TESE	170

1 INTRODUÇÃO

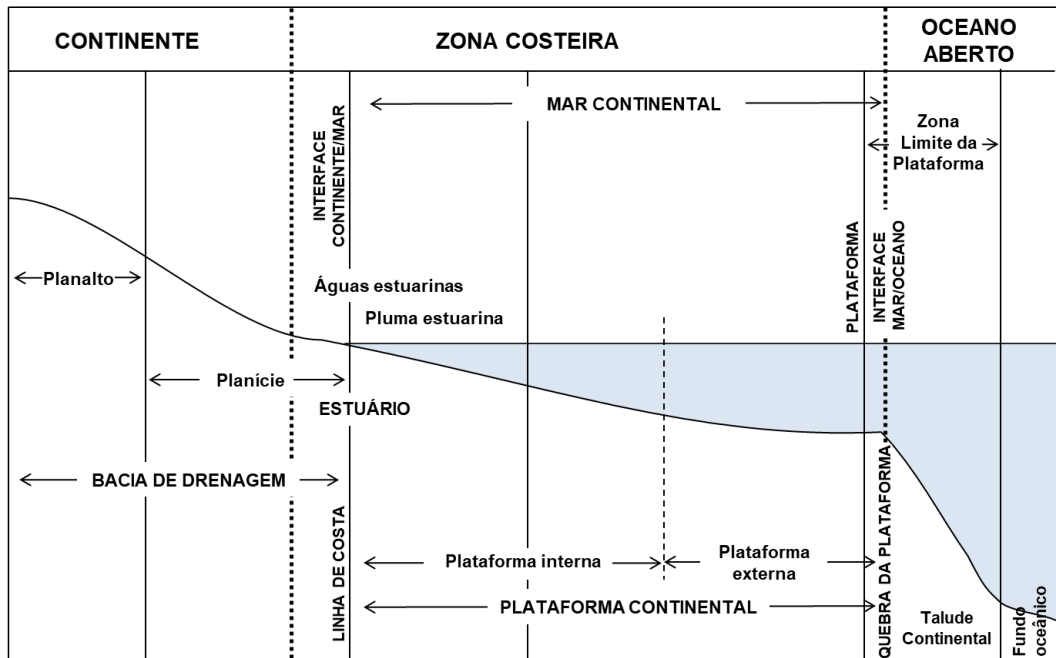
Este trabalho de Tese de Doutorado está organizado em formato de artigos científicos, abordando discussões sobre a diversidade, estrutura e biomassa fitoplanctônica em escala temporal e espacial e os efeitos dos processos climáticos e hidrológicos na Plataforma Continental Maranhense, setor leste da Costa Norte Amazônica, considerada *hotspot* mundial para conservação por apresentar elevada produtividade e diversidade biológica. Além disso, o presente trabalho é o primeiro estudo a fornecer importantes informações científicas sobre os padrões da diversidade da comunidade fitoplancônica (diversidade alfa e beta) nas Reentrâncias Maranhenses – Sítio Ramsar, maior faixa contínua de manguezais do mundo.

1.1 Região costeira

As regiões costeiras do mundo formam uma estreita zona de interface entre as áreas marinhas e terrestres, nas quais estão localizadas grandes e crescentes proporções da população humana e da atividade econômica global. Este ambiente sustenta ecossistemas sensíveis que fornecem habitat crítico para muitas espécies ameaçadas e serviços ecossistêmicos altamente importantes na forma de proteção costeira, pesca e outros recursos vivos, terras agrícolas ricas, áreas de alto valor estético, e é comumente considerado como patrimônio público (RAMESH et al., 2015).

Apesar de nos últimos anos as zonas costeiras serem foco de muitas economias nacionais, não existe uma definição clara desta zona que seja aceita pelas diferentes áreas e segmentos envolvidos nos problemas costeiros. No entanto, no ramo das Ciências Naturais, a definição apresentada pelo programa de Interações Continente-Oceano na Zona Costeira (*Land-Ocean Interactions in the Coastal Zone* – LOICZ) é amplamente aceita (Figura 1).

Figura 2 - Representação esquemática da definição de zona costeira



Fonte: Adaptado de Holligan e Boois (1993).

Uma abordagem fundamental apresentada pelo LOICZ é o reconhecimento de que “... a zona costeira não é apenas um limite geográfico de interação entre a terra e o mar, mas sim um compartimento global de significado especial para os ciclos e processos biogeoquímicos e cada vez mais para a habitação humana e economias” (HOLLIGAN e BOOIS, 1993).

As regiões costeiras contribuem substancialmente para a produtividade primária marinha global, respondendo por aproximadamente 25% dessa produção anual (RYTHER, 1969). Tais ecossistemas costeiros abrigam as mais diversas comunidades biológicas, as quais se encontram interligadas em complexas cadeias tróficas (FALKOWSKI, 2002).

Estes ecossistemas estão entre as regiões mais produtivas e dinâmicas do oceano, sendo sujeitos a descargas fluviais de grandes rios que podem ter um impacto considerável no oceano aberto, retendo, trocando ou transformando nutrientes e carbono orgânico (SHARPLES et al., 2017). No entanto, esses ambientes têm sido pouco investigados nos trópicos em comparação com as regiões temperadas, embora muitos dos maiores estuários do mundo estejam localizados nas regiões costeiras tropicais e contribuem com mais de 50% de toda a água de origem fluvial nos oceanos (BRUNSKILL, 2010; ARAUJO et al., 2017; AQUINO et al., 2022).

1.2 Plataformas continentais e Sítios Ramsar

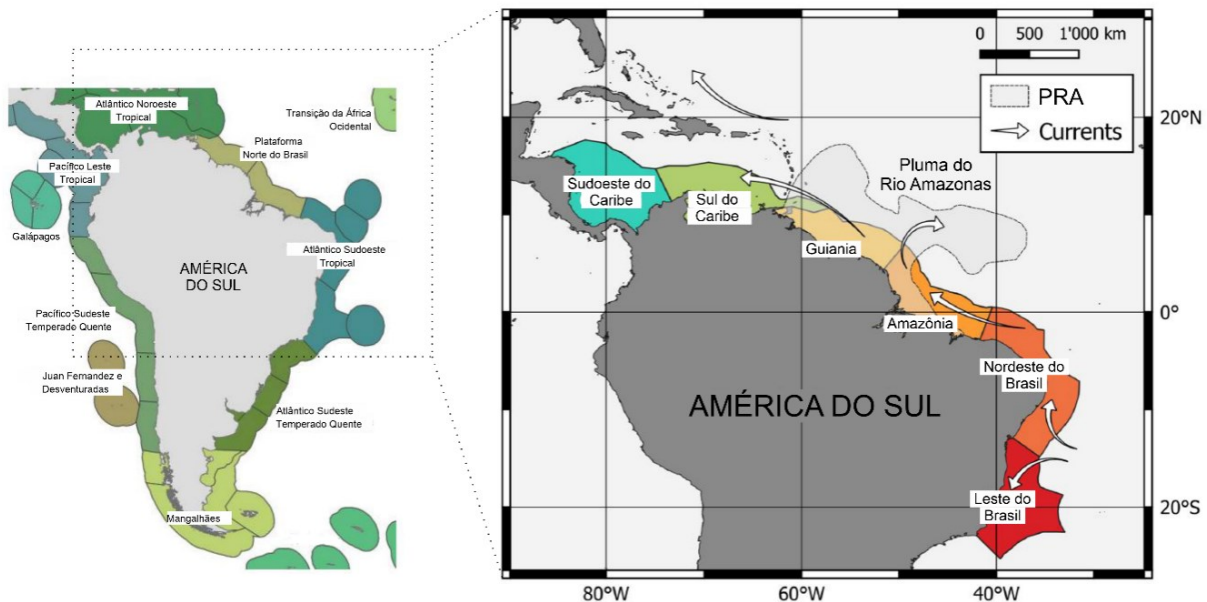
Plataformas continentais funcionam como um receptor final de água e materiais de origem continental, os quais são transportados principalmente através da descarga dos rios e estuários. Do ponto de vista dinâmico, essa descarga resulta em uma massa de água flutuante com menor densidade que a encontrada nas águas costeiras, denominada pluma de rio ou pluma fluvial (KOURAFALOU et al., 1996).

As condições físicas e químicas resultantes da interação entre essas massas de água fluvial e oceânica podem servir como fonte de nutrientes biologicamente importantes e influenciar diretamente no crescimento fitoplanctônico, criando uma zona de transição altamente produtiva e propícia para alta transferência trófica do fitoplâncton para os demais níveis tróficos (SMITH JR e DEMASTER, 1996; DAGG et al., 2004).

Além disso, plumas fluviais associadas a limitações de nicho ecológico podem atuar como barreiras aquáticas permeáveis, limitando a distribuição de organismos marinhos (LUIZ et al., 2011). Essas barreiras reduzem o potencial de colonização ao longo de todo o oceano por organismos costeiros, servindo como filtros de dispersão que afetam espécies selecionadas com características fisiológicas, morfológicas e/ou ecológicas limitadas (BRADBURY et al., 2008; TOSETTO et al., 2022). Isto é particularmente observado na Costa Norte do Brasil, onde são encontrados rios extensos e com grande volume de água, como por exemplo, o rio Amazonas que possui a maior descarga global com média de $150.000 \text{ m}^3 \text{ s}^{-1}$, sendo responsável por aproximadamente metade de toda a descarga fluvial no Oceano Atlântico Tropical (LENTZ, 1995; GOES et al., 2014; ARAUJO et al., 2017).

A Costa Norte do Brasil está inserida na ecorregião Amazônica a qual faz parte da Plataforma Norte do Brasil (Atlântico Tropical) (Figura 2).

Figura 3 - Distribuição das Ecorregiões Marinhas e suas respectivas províncias com destaque para o Oceano Atlântico Tropical e Plataforma Norte do Brasil



Fonte: Adaptado de Spalding et al. (2007) e Tosetto et al. (2022).

De acordo com estudos de classificação biogeográfica para as áreas costeiras e de plataforma realizado por Spalding et al. (2007), ecorregiões são as unidades de menor escala no Sistema de Ecorregiões Marinhas do mundo, sendo definidas como “áreas de composição de espécies relativamente homogênea, claramente distinta dos sistemas adjacentes”. As forçantes biogeográficas dominantes que as definem variam localmente, mas podem incluir isolamento, ressurgência, disponibilidade de nutrientes, influxo de água fluvial, regimes de temperatura, exposição, sedimentos, correntes e complexidade batimétrica ou costeira.

Um dos usos do sistema de classificação da ecorregiões marinhas é o mapeamento de áreas para conservação, onde são selecionadas as coberturas de Sítios Ramsar ao longo das regiões costeiras e marinhas (SPALDING et al., 2007). Sítios Ramsar são áreas úmidas de relevante importância internacional, os quais fazem parte de uma lista de habitats aquáticos importantes para conservação estabelecida pela Convenção Ramsar em fevereiro de 1971. Esta é um tratado intergovernamental que incorpora os compromissos de seus países membros para manter o caráter ecológico de suas zonas úmidas e planejar o seu uso racional e sustentável (van der MOST e MARCHAND, 2011).

Sítios Ramsar abrangem ecossistemas altamente produtivos e ricos em biodiversidade. No território brasileiro foram estabelecidos 27 Sítios Ramsar, sendo cinco destes pertencentes a Costa Norte Amazônica: Parque Nacional do Cabo Orange (AP), Sítio Ramsar Regional

Estuário do Amazonas e seus manguezais (AM, PA, MA), Área de Proteção Ambiental das Reentrâncias Maranhenses (MA) e Parque Estadual Marinho do Parcel de Manuel Luiz (MA) (Figura 3).

Figura 4 - Localização dos 27 Sítios Ramsar localizados no Brasil



Fonte: <https://www.gov.br/mma/pt-br>.

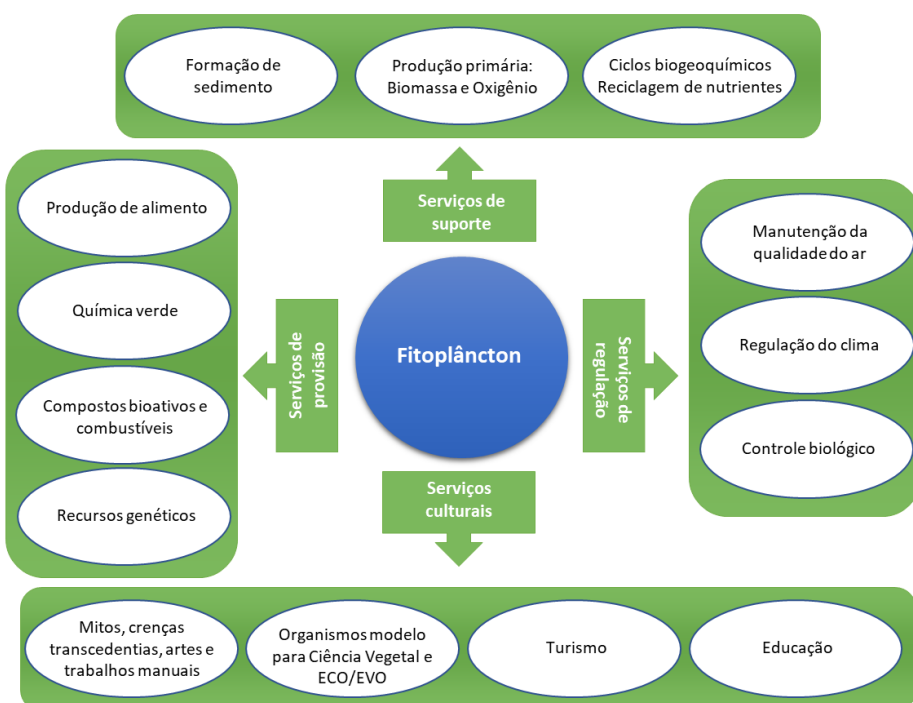
Considerando a importância ecológica dos ecossistemas costeiros, há uma necessidade urgente de compreender os principais processos responsáveis pela dinâmica local, além de entender a melhor forma de gerir estes ecossistemas de forma sustentável, para que possam continuar a prestar os serviços dos quais a sociedade depende.

1.3 Diversidade do fitoplâncton marinho

Entre os produtores primários que sustentam as demais cadeias tróficas nos ecossistemas costeiros, encontra-se o fitoplâncton, contribuindo com cerca de $250 \text{ gC m}^{-2} \text{ ano}^{-1}$ na produção primária anual (CLOERN et al., 2014). O fitoplâncton marinho é essencial não só para os ecossistemas marinhos, mas também para toda a biosfera (LIU et al., 2022). Eles fornecem oxigênio que permeia a atmosfera (FALKOWSKI, 2012), além de desempenhar papel importante na ciclagem do carbono, abastecendo a bomba de carbono biológico do oceano global, e nutrientes, incluindo nitrogênio, fósforo, sílica, ferro e entre outros elementos (JARDILLIER et al., 2010; REYNOLDS, 2006).

Naselli-Flores e Padisák (2022), em estudos recentes, identificaram cerca de 20 serviços ecossistêmicos diferentes fornecidos pelo fitoplâncton em uma escala global (Figura 4). Dentre estes, os serviços de suporte têm sustentado significativamente o funcionamento de grande parte da biosfera há milhares de anos. A eficiência do uso dos recursos do fitoplâncton, ou seja, a fixação de carbono está diretamente ligada à sua diversidade, a qual contribui fortemente para a estabilidade global dos ecossistemas aquáticos e reforça o papel do fitoplâncton como provedor de serviços reguladores para a biosfera (PTACNIK et al., 2008).

Figura 5 - Diagrama de blocos esquemáticos indicando as categorias e os serviços ecossistêmicos fornecidos pelo fitoplâncton



Fonte: Adaptado de Naselli-Flores e Padisák (2022).

Tais serviços foram alcançados em virtude da diversidade biológica que esse grupo de organismos apresenta em seu sentido mais amplo, ou seja, em termos de espécies, genes e diversidade funcional (REYNOLDS et al., 2002; PADISÁK et al., 2009; KRUK et al., 2021; ABONYI et al., 2021).

O fitoplâncton marinho representa um grupo de microrganismos eucariontes e procariônicos altamente diversos, abundantes e cosmopolitas. Estes compreendem os grupos autotróficos mais frequentes, incluindo Bacillariophyta, Chlorophyta, Cyanobacteria, Haptophyta e Cryptophyta, bem como Miozoa com representantes autotróficos, heterotróficos e mixotróficos (SIMON et al., 2009). Estes organismos planctônicos possuem grande

significado ecológico por responderem rapidamente às mudanças ecológicas, sendo considerado um bom indicador biológico para avaliar as alterações dos ecossistemas aquáticos e qualidade da água (PAERL et al., 2003; SATHICQ et al., 2017; KANG et al., 2021).

A estrutura da comunidade fitoplânctonica, em termos de composição, abundância e biomassa, pode ser influenciada por fatores climáticos, físicos, químicos e biológicos, bem como pelas interações entre eles (PAERL et al., 2010; THOMPSON et al., 2015). Dentre estes, a disponibilidade de luz, nutrientes e variações de salinidade atuam como fatores-chave na regulação da comunidade fitoplânctonica em escalas espaciais e temporais (AZHIKODAN et al., 2016; ZHONG et al., 2021; NWE et al., 2022).

Entender as mudanças na composição e nos padrões de distribuição das espécies, ao longo do tempo ou no espaço, é um fator-chave na ecologia permitindo auxiliar em medidas de conservação frente às mudanças globais (SOCOLAR et al., 2016). Estudos sobre padrões espaço-temporais na organização de comunidades biológicas também são importantes para descrever padrões de diversidade de espécies em função de gradientes ambientais e geográficos (LANSAC-TÔHA et al., 2019). Estes incluem a heterogeneidade ambiental, que tende a promover a diversidade de espécies (TONKIN et al., 2015).

Na costa maranhense, onde se encontra o sítio Ramsar Reentrâncias Maranhenses, a comunidade fitoplânctonica apresenta uma alta diversidade de diatomáceas em resposta a elevada hidrodinâmica local e condições ambientais, como disponibilidade de luz e nutrientes. Informações sobre o fitoplâncton e condições hidrológicas em ecossistemas estuarinos têm sido investigadas por estudos pioneiros para o estado do Maranhão, com destaque para Azevedo et al. (2008), Rodrigues e Cutrim (2010), Duarte-dos-Santos et al. (2017), Cavalcanti et al. (2018), Cavalcanti et al. (2020), Costa e Cutrim (2021), Queiroz et al. (2022) e Sá et al. (2022).

Atualmente, estudos de diversidade abrangem diferentes escalas, desde a escala local (diversidade alfa) que revela a riqueza de espécies medida apropriadamente como o número de espécies em uma amostra de tamanho padrão (WHITTAKER, 1972), as mudanças na composição da comunidade entre escalas espaciais e temporais (diversidade beta) e a diversidade regional (diversidade gama) (BASELGA, 2010).

Efeitos de dispersão e heterogeneidade podem ser identificados por meio da diversidade beta (ANDERSON, 2006). Estudos têm mostrado que a partição da diversidade beta em seus respectivos componentes de rotatividade (substituição de espécies entre locais) e aninhamento (perda ou ganho de espécies) facilitam a detecção de padrões ecológicos no espaço e no tempo (BASELGA, 2010). Essas informações sobre a variação espacial e temporal na diversidade beta

também são essenciais para a compreensão da biogeografia, ecologia e questões de conservação, além de orientar decisões práticas de manejo (BASELGA, 2010; LEGENDRE, 2014).

Recentemente, estudos sobre diversidade beta têm sido amplamente aplicados para entender os processos ecológicos determinantes dos padrões espaciais e temporais da biodiversidade fitoplânctonica em ecossistemas tropicais e sub-tropicais (JYRKÄNKALLIO-MIKKOLA et al., 2018; ZHANG et al., 2018; KAHSAY et al., 2022; XU et al., 2022; FRAU et al., 2023) e temperados (MOUSING et al., 2016; ROMBOUTS et al., 2019; STEFANIDOU et al., 2020; BAO et al., 2022; OLLI et al., 2022; RUSANOV et al., 2022). No Brasil, estudos que utilizam essa abordagem ainda são incipientes e a maioria é aplicada aos ecossistemas limnéticos tais como rios, lagos e reservatórios (Tabela 1). A partir disso, foi proposta a realização deste trabalho aplicando uma abordagem de análise da diversidade (alfa e beta), estrutura da comunidade e traços funcionais do fitoplâncton como ineditismo para a região costeira amazônica devido a sua relevante importância ecológica, econômica e social.

Tabela 1 - Resumo das publicações atuais sobre o fitoplâncton com foco na diversidade beta nas regiões do Brasil

	Área de estudo	Coeficientes de dissimilaridade	Componente dominante	Referência
Norte e Nordeste	Lagos de Parauapebas, Canãa dos Carajás e Curionópolis - PA	Bray–Curtis e Jaccard	Não aplicado	Lopes et al. (2011)
	Rio Negro - AM	Sørensen	Substituição de espécies	Wetzel et al. (2012)
	Bacias do Apodi-Mossoró e Piranhas-Açu - RN	Bray–Curtis e Jaccard	Não aplicado	Brasil et al. (2019)
	Rio Tocantins - PA	Sørensen	Substituição de espécies	Castro et al. (2021)
	Rio Araguaia - GO, MT	Índice β -1	Não aplicado	Nabout et al. (2006)
Centro-Oeste	Reservatórios hidroelétricos - MG, GO, TO	Bray-Curtis	Não aplicado	Santos et al. (2015)
	Lagoa de estabilização/Trindade - GO	Índice de Whittaker	Não aplicado	D'Alessandro et al. (2020)
	Bacia de Santa Teresa - GO	Contribuição Local para a diversidade-beta (LCBD) e Jaccard	Substituição de espécies	Oliveira et al. (2020)
Sul e Sudeste	Rios Tigre e Retiro - SC	Índice β -1	Não aplicado	Schuster et al. (2015)
	Reservatórios subtropicais - PR	Sørensen	Substituição de espécies	Wojciechowski et al. (2017)
	Rio Paraná - PR, SP	Jaccard	Substituição de espécies	Lansac-Tôha et al. (2019)
	Bacia do Rio Tramandaí - RS	Sørensen, Bray-Curtis e Gower	Não aplicado	Costa et al. (2020)
	Reservatórios - SP	Sørensen	Substituição de espécies	Zorral-Almeida et al. (2021)
	Rio Paraíba do Sul – SP, RJ, MG	Sørensen, Gower	Substituição de espécies	Graco-Roza et al. (2021)
	Bacia do Rio Iguaçu - PR	Contribuição Local para a diversidade-beta (LCBD)	Substituição de espécies	Moura et al. (2022)
	Rio Guaraguaçu - PR	Bray-Curtis	Não aplicado	Sampaio et al. (2023)

Fonte: Autoria própria (2023).

2 DESCRIÇÃO DA ÁREA

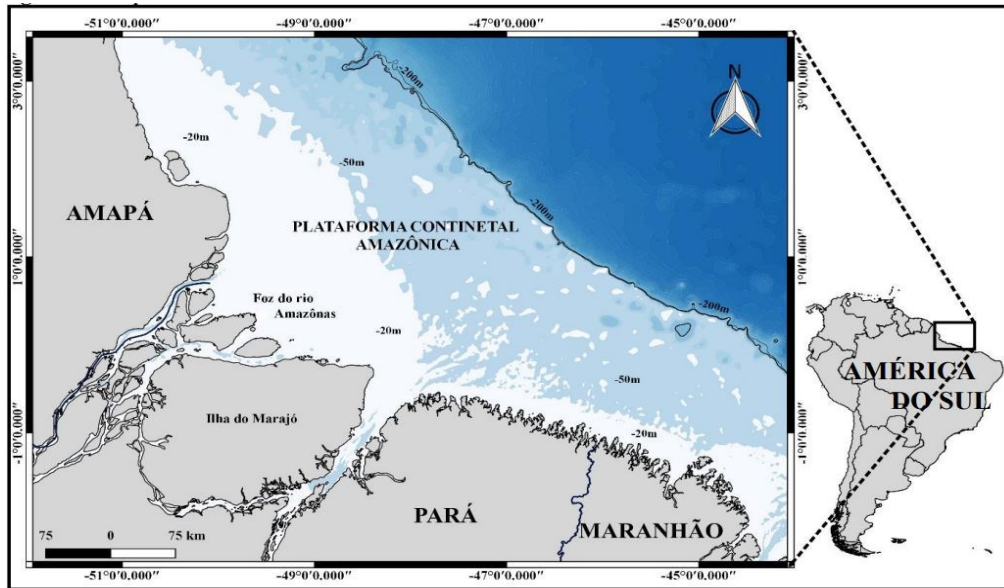
Informações sobre a descrição da área abordando uma visão geral sobre a Costa Norte Amazônica, Plataforma Continental Maranhense e Baía de Cumã são apresentadas nesta seção, região onde foi desenvolvida a etapa de campo e análise dos dados amostrais.

2.1 Costa Norte Amazônica

O Brasil possui uma linha de costa de aproximadamente 8.500 km de extensão, dos quais cerca de 35% são ocupados pelo litoral amazônico brasileiro, onde estão inseridos diversos ecossistemas como estuários, praias, ilhas, deltas, florestas tropicais e manguezais (PEREIRA et al., 2009). A Zona Costeira Amazônica Brasileira estende-se desde o Cabo Orange (Amapá) até o Delta do Parnaíba (Piauí), entre as latitudes 4°N e 3°S (EKAU e KNOPPERS, 1999).

Situada na Costa Norte do Brasil, a Plataforma Continental Amazônica (PCA) é considerada a principal feição oceanográfica da região, devido à elevada descarga de rios caudalosos, como por exemplo, o rio Amazonas, que influencia diretamente os processos biogeoquímicos da região costeira e oceano adjacente (LOURENÇO, 2017; OTSUKA et al., 2022). A PCA situa-se entre as latitudes 5°N e 2°S, abrangendo os estados do Amapá, Pará e Maranhão (Figura 5), e destaca-se como a porção mais larga da margem continental brasileira com largura variada ao longo da sua extensão alcançando máxima de 320 km na foz do rio Amazonas e decrescendo para aproximadamente 100 km tanto a noroeste quanto a sudoeste no Amapá e Maranhão, respectivamente (BRANDINI et al., 1997; CASTRO e MIRANDA, 1998; PRESTES et al., 2020).

Figura 6 - Plataforma Continental Amazônica incluindo os estados do Maranhão, Pará e Amapá

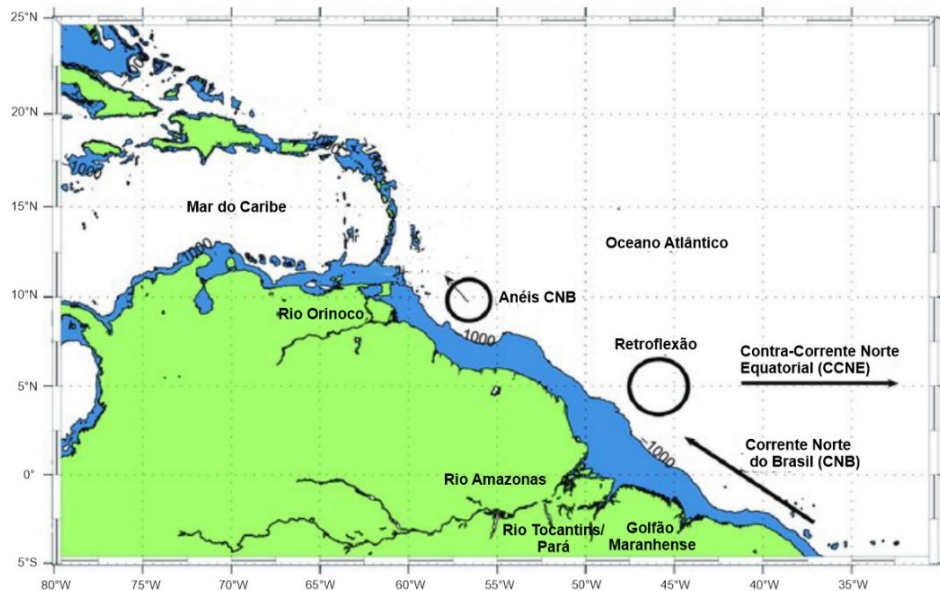


Fonte: Silva (2019).

Caracterizada como uma plataforma pouco profunda, a profundidade da quebra de plataforma varia ao longo da costa entre as isóbatas de 75 e 115m, sendo a maior parte desta com isóbata de 20 m ao longo de mais de 200 km da costa na região da foz do Rio Amazonas (NETO e SILVA, 2004; LOURENÇO, 2017). Além disso, a PCA apresenta um extenso ambiente de deposição sedimentar, representado por um delta submarino decorrente do grande aporte fluvial e de correntes oceânicas presentes na região (NETO et al., 2009).

Este é um ambiente altamente dinâmico sujeito a regimes de hipermarés e macromarés, fortes correntes oceânicas e ventos alísios associados à migração sazonal da Zona de Convergência Intertropical (ZCIT) (NITTROUER e DEMASTER, 1996; AQUINO et al., 2022). A principal corrente oceânica atuante na PCA é a Corrente Norte do Brasil (CNB) e sua componente Subcorrente Norte do Brasil, formadas a partir da bifurcação da Corrente Sul Equatorial (CSE) (SILVEIRA et al., 2000). Entre os meses de fevereiro e junho, a CNB apresenta um fluxo contínuo no sentido noroeste ao longo da quebra da PCA e entre julho a janeiro, a migração para norte dos ventos alísios resulta na retroflexão da CNB, alimentando a Contra-Corrente Norte Equatorial (CCNE) com águas enriquecidas da pluma do Rio Amazonas as quais são transportadas para o leste entre as latitudes 5°N e 10°N (FLAGG et al., 1986; COLES et al., 2013; ARAUJO et al., 2017) (Figura 6).

Figura 7 - Distribuição horizontal das principais correntes na Plataforma Continental Amazônica. CNB - Corrente Norte do Brasil, CCNE - Contra-Corrente Norte Equatorial



Fonte: Adaptado de Chérubin e Richardson (2007).

A PCA recebe a maior descarga fluvial do mundo, representando cerca de 15 a 20% da descarga fluvial global no Oceano Atlântico Equatorial (COLES et al., 2013; OTSUKA et al., 2022). As principais fontes de nutrientes para a zona eufótica são a regeneração bêntica e a drenagem continental dos rios de grande porte como o Rio Amazonas, Rio Parnaíba e os principais rios que desembocam no Golfão Maranhense (BRANDINI et al., 1997). Esta plataforma recebe uma descarga fluvial na ordem de 10^5 a $10^6 \text{ m}^3 \text{ s}^{-1}$ dos rios Amazonas e Pará, cujas plumas se estendem até 250 km e 165 km, respectivamente, no Oceano Atlântico (LENTZ, 1995; MASCARENHAS et al., 2016). Assim, a elevada descarga do rio Amazonas e de dezenas de outros sistemas estuarinos encontrados ao longo da PCA torna-se um fator crucial que influencia na dinâmica dos processos oceanográficos da costa amazônica (NITTROUER et al., 1991).

2.2 Plataforma Continental Maranhense

Situada no setor leste da PCA, encontra-se a Plataforma Continental Maranhense (PCM) localizada entre as coordenadas $01^{\circ}01'S$ e $02^{\circ}36'S$ e $41^{\circ}48'W$ e $48^{\circ}40'W$. A PCM apresenta o segundo maior litoral da costa brasileira com 640 km de extensão, estendendo-se desde a foz do Rio Gurupi até a foz do Rio Parnaíba (Figura 7), com uma superfície de $55,70 \text{ km}^2$ sendo limitada pela isóbata de 80 m (GUALBERTO e EL-ROBRINI, 2005; PEREIRA et al., 2018).

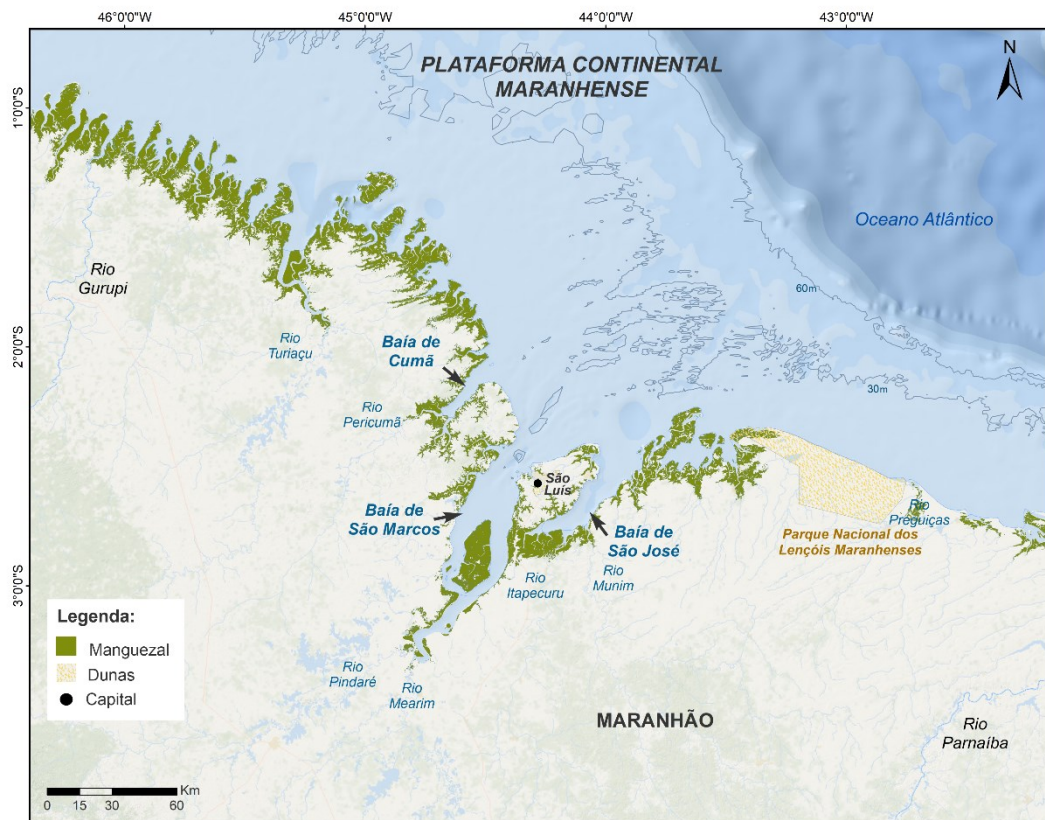
Apresenta geomorfologia irregular, evidenciada pelos campos de bancos arenosos submersos e pelo Parcel Manuel Luís (sítio Ramsar e parque marinho), extensa formação coralina onde ocorrem diversas associações entre organismos bentônicos (algas coralinas) e sésseis (por exemplo, cnidários e poríferos) (CORDEIRO et al., 2020). Esta é caracterizada pela influência de ventos alíseos e variabilidade espaço-temporal da Zona de Convergência Intertropical (ZCIT) resultando na ocorrência de dois períodos sazonais ao ano, período chuvoso e de estiagem (GUALBERTO e EL-ROBRINI, 2005).

A partir da classificação geológica, a PCM é subdividida em: plataforma interna, média e externa. A plataforma interna é limitada pela isóbata de 40 m, com um relevo complexo típico de regiões com elevada energia de maré, tendo o Golfo Maranhense como feição geomorfológica com maior influência sobre a plataforma. Nesta zona, verifica-se a ocorrência de sucessões de campos de bancos arenosos submarinos alongados transversalmente à linha de costa, possuindo até 70 km de comprimento, 10 km de largura e alturas que podem atingir 20 m, associados à ação das correntes de maré durante a transgressão marinha holocênica. A distribuição de sedimento é caracterizada por areia e cascalho esparsos como classe dominante. A plataforma média é a área com maior inclinação situada entre as isóbatas de 40 e 60 m, onde é encontrado o parque marinho Parcel Manuel Luís. As classes de sedimentos dominantes são o cascalho esparsos, cascalho arenoso e areia. A plataforma externa está compartimentada entre a isóbata de 60 e 80 m, com morfologia que sugere uma natureza carbonática, possivelmente uma formação de bancos de algas paralelos à quebra do talude, onde ocorre uma série de reentrâncias, configurando pequenos canais de relevo irregular. Cascalho esparsos e areia com cascalho são os sedimentos dominantes da área (PALMA, 1979; GOES et al., 2017; GUALBERTO e EL-ROBRINI, 2005).

Caracteriza-se por um complexo mosaico de ecossistemas como estuários, baías, campos inundados, restingas, praias arenosas, dunas, bem como extensas faixas de manguezais (GUALBERTO e EL-ROBRINI, 2005). Os manguezais correspondem às áreas úmidas costeiras do litoral maranhense, formando a maior faixa contínua de manguezais mais bem preservados do mundo com aproximadamente 1.200 km de extensão desde o litoral do Amapá até o Maranhão (SOUZA-FILHO et al., 2005; HAYASHI et al., 2019). Os manguezais da região são dominados pelas espécies *Rhizophora mangle*, *R. racemosa*, *R. harrisonii*, *Avicennia germinans*, *A. schaueriana*, *Laguncularia racemosa* e *Conocarpus erectus* (MENEZES et al., 2008; NASCIMENTO et al., 2013).

O litoral maranhense está dividido em três setores considerando as peculiaridades das condições climáticas, drenagem fluvial e circulação oceânica, onde se destacam a costa oeste, a costa leste e entre elas, o Golfão Maranhense no setor central (AZEVEDO et al., 2008). A costa oeste se estende por 520 km desde a fronteira do estado no estuário do Gurupi (1°) até a margem do Golfão Maranhense ($2,1^{\circ}$), sendo caracterizada pela presença de uma ampla faixa de manguezais ($\sim 4.000 \text{ km}^2$) recortada externamente por pontões lodosos e ilhas que se formaram pela força das marés - Reentrâncias Maranhenses, com inúmeras rias e cerca de 20 estuários dominados pela maré em forma de漏il separados por penínsulas baixas dominadas por manguezais (SOUZA-FILHO et al., 2005; PEREIRA et al., 2018).

Figura 8 - Localização da Plataforma Continental Maranhense, incluindo as Reentrâncias Maranhenses na costa oeste, o Golfão Maranhense no setor central e o Parque dos Lençóis Maranhenses na costa leste



Fonte: Autoria própria (2023).

No setor central encontra-se o Golfão Maranhense, com uma orla externa de 490 km incluindo a Baía de Cumã, Baía de São Marcos e Baía de São José (PEREIRA et al., 2018). Esta região apresenta uma costa irregular, incluindo inúmeros estuários, praias, ilhas e manguezais que ocupam uma área de 1.622 km^2 (SOUZA-FILHO et al., 2005), além da cidade de São Luís - região metropolitana e capital do Maranhão. Trata-se de um complexo estuarino com características de transição entre as duas costas, além de ser a feição geomorfológica com

maior influência sobre a plataforma e o principal coletor do sistema hidrográfico do estado (MARANHÃO, 2002; GUALBERTO e EL-ROBRINI, 2005). Nesta região, a amplitude das marés pode chegar a 7 m durante marés de sizígia e as correntes de maré podem chegar a 2 m s⁻¹ (PEREIRA et al., 2011).

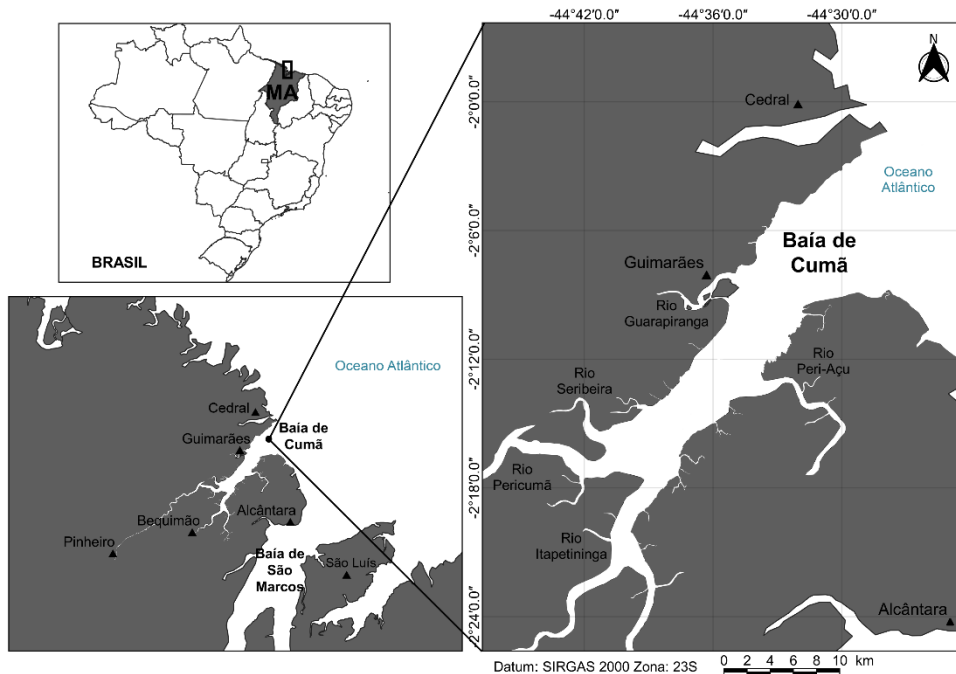
O Golfão é abastecido pelas descargas fluviais de inúmeros rios, dentre eles destacam-se: o rio Pericumã (~115 km) desaguando na Baía de Cumã; os rios Mearim (~966 km), Grajaú (~690 km) e Pindaré (~468 km) na Baía de São Marcos, e os rios Itapecuru (~1.050 km) e Munim (~120 km) na Baía de São José (MACEDO, 1989; LIMA et al., 2021), apresentando ainda um canal de mistura (Estreito dos Mosquitos) das massas de água da Baía de São Marcos e de São José (SANTOS et al., 2020).

A costa leste se estende por 230 km desde o Golfão Maranhense até a divisa do estado no Delta do Parnaíba. Este litoral é caracterizado pelo predomínio de praias dominadas por ondas, ausência de reentrâncias, relativamente reto, e alturas de onda (Hs) que podem chegar a 3 m de altura, enquanto as marés diminuem de 7 a 3 m em direção ao Delta do Parnaíba. Nesta área é encontrado o Parque Nacional dos Lençóis Maranhenses que possui extensos campos de dunas e lagoas costeiras (PEREIRA et al., 2018).

2.3 Baía de Cumã

A Baía de Cumã está situada na Mesorregião Norte Maranhense e Microrregião Litoral Ocidental Maranhense, delimitando as Reentrâncias Maranhenses e o setor central (IBGE, 2017). Constitui o Golfão Maranhense, juntamente com a Baía de São Marcos e Baía de São José (CZIZEWESKI et al., 2020), sendo o segundo maior recorte da costa oeste do litoral do Maranhão. Com uma área aproximada de 205,72 km² e 33,92 km de extensão, essa baía é caracterizada pela influência de macromarés semi-diurnas (amplitude média > 4m) associadas ao intenso aporte fluvial dos rios Pericumã, Itapetinga, Guarapiranga, Peri-Açu e Seribeira (Figura 8).

Figura 9 - Localização da Baía de Cumã e seus principais tributários, Reentrâncias Maranhenses, Plataforma Continental Maranhense - Brasil



Fonte: Autoria própria (2023).

A Baía de Cumã caracteriza-se por um sistema amazônico costeiro-marinho conectado diretamente com o Oceano Atlântico Tropical. A corrente de maré nesta região apresenta uma direção de WSW - SW perpendicular à costa, durante a enchente, e N - NE durante a vazante (GUALBERTO e EL-ROBRINI, 2005; IBGE, 2017).

Este ambiente costeiro recebe influência continental de centros urbanos (pequenos e médios) localizados às margens da baía, destacando os municípios de: Guimarães ($479,56\text{ km}^2$; 12.030 hab.), Alcântara ($1.168,24\text{ km}^2$; 22.097 hab.), Pinheiro ($1.512,96\text{ km}^2$; 83.387 hab.) e Bequimão ($790,22\text{ km}^2$; 21.280 hab.). Dentro das principais atividades antrópicas presentes na região, pode-se citar a pecuária (criação de gado e búfalo), a agricultura (cultivo de mandioca e arroz) e a intensa atividade de pesca e cultivo de mariscos (CARVALHO et al., 2011; IBGE, 2017).

A bacia hidrográfica do rio Pericumã é o principal tributário da Baía de Cumã percorrendo cerca de 13 municípios da Baixada Maranhense. Esta possui uma área de 10.800 km^2 que anualmente transborda e inunda as planícies baixas da região, formando um grande número de lagos temporários e permanentes (ALMEIDA-FUNO et al., 2010). A descarga do rio Pericumã é caracterizada por um ciclo sazonal marcante, com as maiores vazões registradas

no período chuvoso alcançando média de $113,69 \pm 94,30 \text{ m}^3 \text{ s}^{-1}$ (MARTINS e OLIVEIRA, 2011).

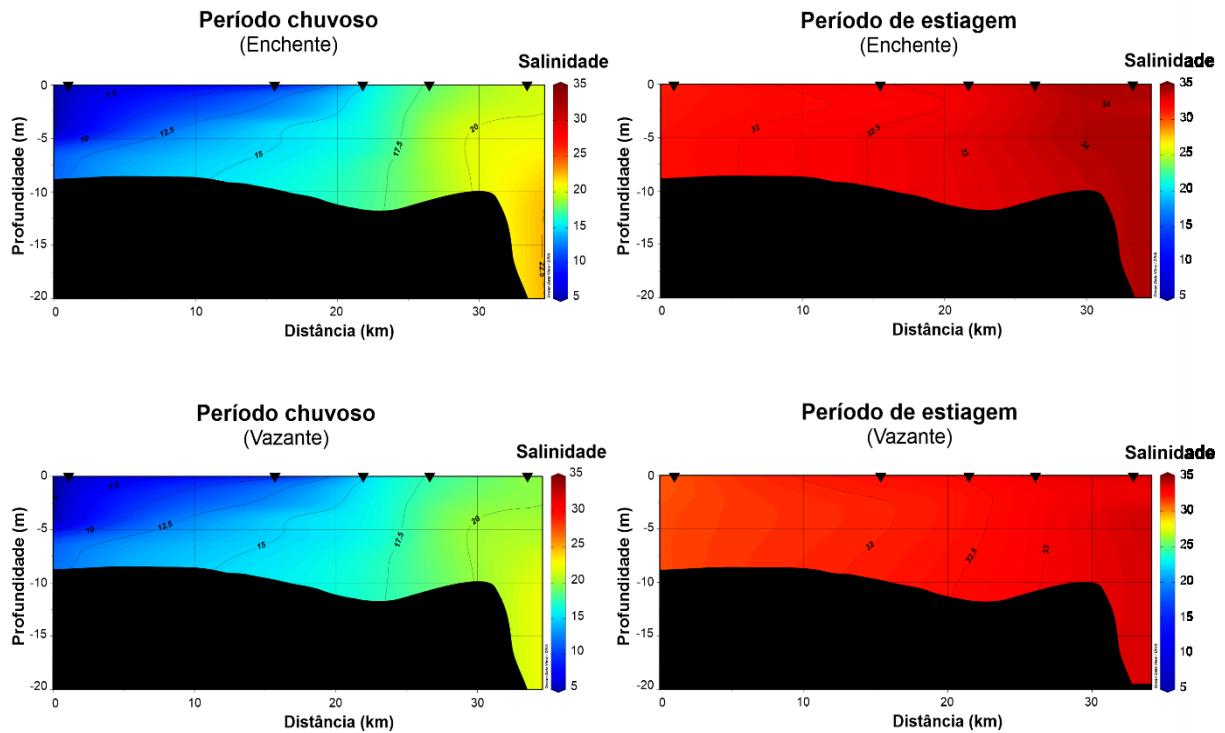
No curso médio do rio Pericumã, a 40 km da foz do rio e a 11 km da cidade de Pinheiro, encontra-se a construção de uma barragem (comprimento = 275 m; largura = 39 m; altura máxima = 29,3 m) com vazão controlada através de comportas verticais. Sua construção teve como objetivo minimizar a penetração da água salgada, reduzir as enchentes em áreas urbanas e agrícolas e regularizar as vazões de água no período de estiagem e chuvoso (BRASIL, 1991; CARVALHO et al., 2011). Tal intervenção antrópica, juntamente com as principais atividades econômicas supracitadas, são consideradas potenciais tensores antrópicos para a saúde do ecossistema.

O clima da região é tropical quente com chuvas de verão (Aw), de acordo com a classificação de Köppen. Situado entre o super-úmido da Amazônia e o semi-árido do nordeste, apresenta características intrínsecas tais como elevadas temperaturas ($\sim 26^\circ\text{C}$) e precipitação média ($> 2.000 \text{ mm}$) durante todo o ano, resultando em dois períodos sazonais bem definidos e fortemente marcados pela precipitação (LEFÈVRE et al., 2017).

Tal dinâmica resulta na formação de gradientes ambientais com variação sazonal marcante. A distribuição vertical e longitudinal de salinidade obtida a partir de dados coletados na Baía de Cumã é descrita na Figura 9.

A distribuição vertical de salinidade, baseada em valores medidos *in situ* através de perfilagem vertical da coluna d'água, não apontou diferenças bem definidas indicando ser um sistema verticalmente bem misturado. Sazonalmente, é observado um predomínio de águas estuarinas (salinidade < 30) durante o período chuvoso, em ambos os cenários de maré (enchente e vazante). Enquanto que na estiagem, ocorre maior intrusão de águas marinhas (salinidade > 30) na extensão da baía.

Figura 10 - Distribuição vertical e longitudinal de salinidade na Baía de Cumã durante o período chuvoso e de estiagem, considerando o regime de maré enchente e vazante



Fonte: Autoria própria (2023).

3 OBJETIVOS E HIPÓTESES

Os objetivos gerais, objetivos específicos e hipóteses serão apresentados nesta seção.

3.1 Objetivo Geral

Avaliar o efeito das condições climáticas, hidrológicas e regime de maré sobre a diversidade, biomassa e estrutura da comunidade fitoplanctônica ao longo de um *continuum* estuário-oceano na Costa Norte Amazônica.

3.2 Objetivos Específicos

- Examinar os padrões espaciais e sazonais da diversidade alfa e biomassa do fitoplâncton, determinando os principais fatores ambientais que influenciam a dinâmica fitoplanctônica na Baía de Cumã;
- Analisar a estrutura da comunidade fitoplanctônica a fim identificar os seus traços funcionais e espécies indicadoras de mudanças ecológicas ao longo de um *continuum* estuário-oceano amazônico;
- Determinar os padrões de diversidade beta em diferentes escalas espaciais e temporais na Plataforma Continental Maranhense;
- Investigar quais processos (climáticos, espaciais, hidrodinâmicos e ambientais) influenciam a diversidade e estrutura da comunidade fitoplanctônica na Plataforma Continental Maranhense.

3.3 Hipóteses

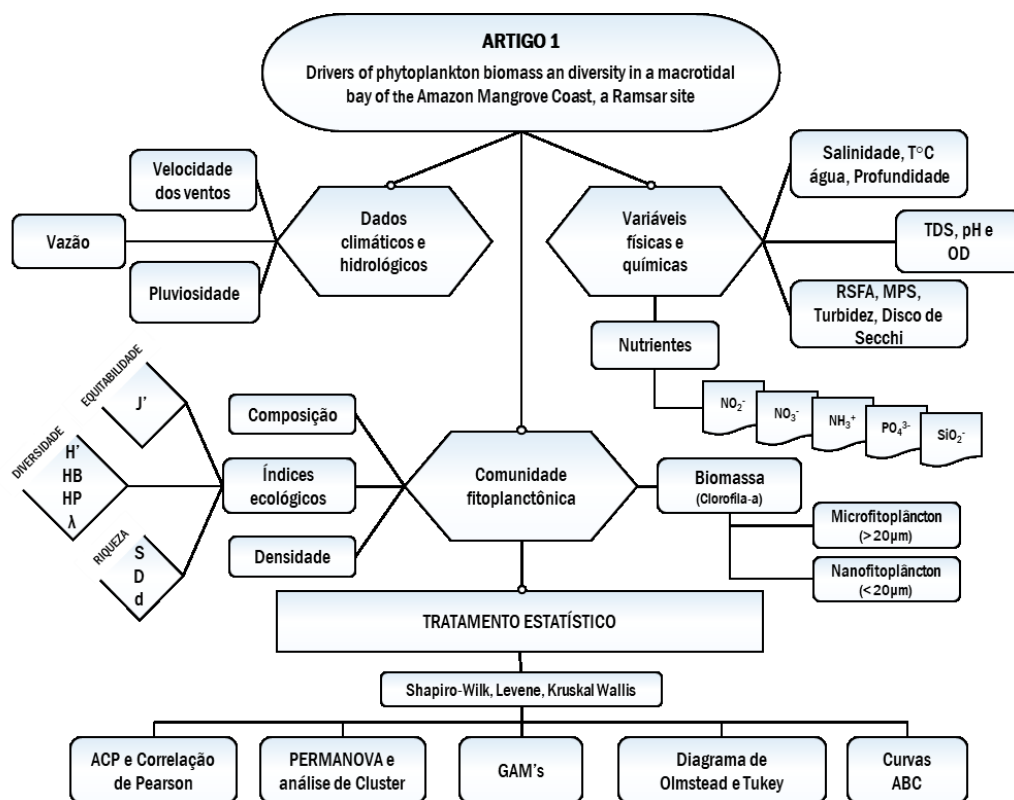
- Mudanças hidrológicas sazonais nos ecossistemas costeiros amazônicos promovem um crescimento do fitoplâncton podendo resultar em uma redução na diversidade fitoplanctônica da Baía de Cumã.
- A intensa drenagem continental amazônica promove uma heterogeneidade ambiental resultando em mudanças na estrutura da comunidade fitoplanctônica e diversidade beta ao longo de um *continuum* estuário-oceano amazônico.

4 ESTRUTURA DA TESE

De acordo com os objetivos e resultados obtidos ao longo da realização do presente estudo, esta tese foi dividida em cinco capítulos. O capítulo 1 com a Introdução, o capítulo 2 referente a Descrição da Área, o capítulo 3 se refere aos Objetivos e Hipóteses, o capítulo 4 apresenta a Estrutura da Tese, o capítulo 5 se refere ao artigo científico (*Original Article* e/ou *Research Paper*) publicado na revista *Ecohydrobiology and Hydrobiology* (artigo 1), o capítulo 6 ao artigo científico (*Original Article* e/ou *Research Paper*) submetido a *Journal of Sea Research* (artigo 2) e o capítulo 7 referente às Considerações Finais.

Artigo 1: Drivers of phytoplankton biomass and diversity in a macrotidal bay of the Amazon Mangrove Coast, a Ramsar site. Fatores determinantes da biomassa e diversidade fitoplânctonica em uma baía de macromaré da Costa de Manguezais Amazônica, sítio Ramsar. Este estudo objetivou analisar os padrões de distribuição da clorofila-a e diversidade alfa na Baía de Cumã, avaliando os principais fatores ambientais que influenciam na dinâmica do fitoplâncton através da combinação de análises estatísticas tradicionais e modelos aditivos generalizados (Figura 10).

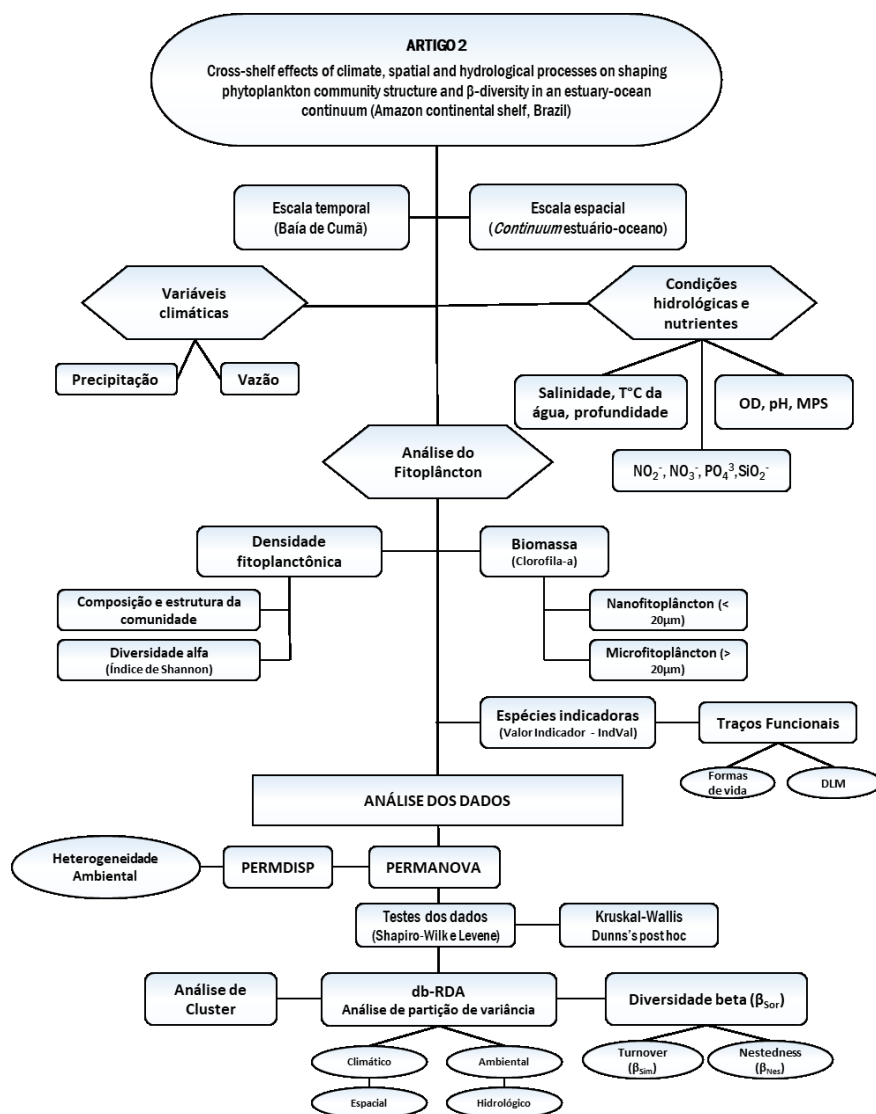
Figura 11 - Fluxograma metodológico do procedimento de pesquisa e análise de dados referentes ao capítulo 5



Fonte: Autoria própria (2023).

Artigo 2: Effects of climate, spatial and hydrological processes on shaping phytoplankton community structure and β -diversity in an estuary-ocean continuum (Amazon continental shelf, Brazil). Efeitos dos processos climáticos, espaciais e hidrológicos ao longo da plataforma modulando a estrutura da comunidade fitoplânctonica e da diversidade beta em um *continuum* estuário-oceano (Plataforma Continental Amazônica, Brasil). Este estudo produziu informações importantes sobre a distribuição dos gradientes ambientais ao longo da plataforma maranhense e sua influência sobre a estrutura da comunidade fitoplânctonica e diversidade beta considerando escalas temporais e espaciais, além de selecionar indicadores ecológicos como uma ferramenta para a avaliação de alterações dos ecossistemas aquáticos e qualidade da água (Figura 11).

Figura 12 - Fluxograma metodológico do procedimento de pesquisa e análise de dados referentes ao capítulo 6



Fonte: Autoria própria (2023).

5 ARTIGO 1

Drivers of phytoplankton biomass and diversity in a macrotidal bay of the Amazon Mangrove Coast, a Ramsar site

Manuscript published in Ecohydrobiology and Hydrobiology

Published: 26 Feb 2022

<https://doi.org/10.1016/j.ecohyd.2022.02.0027>



ABSTRACT

Biodiversity maintenance is a main goal in ecology. Hence, phytoplankton diversity and biomass were analyzed in a coastal bay (Cumã Bay) of the Amazon Macrotidal Mangrove Coast, which has been designated as an international hotspot for conservation (Ramsar site) with high biological productivity and diversity that provides crucial ecosystem services and elevated fish production. An ecohydrology-based approach was applied to identify the main factors that drive the patterns of phytoplankton diversity and biomass, considering spatio-temporal analyses of physical, chemical, and biological variables from May 2019 to June 2020. Phytoplankton dynamics were investigated using multivariate analyses, correlations, and generalized additive models. Seven indices were tested to select the most efficient biodiversity metric. The hydrological conditions of Cumã Bay were governed primarily by elevated precipitation and macrotidal dynamics, resulting in two different functional zones based on environmental variability: the freshwater influence zone and marine influence zone. Seasonally, the maximum freshwater discharge, low salinity and light availability promoted cell abundance and biomass increase, with blooms of *Skeletonema costatum*, which reduced the taxonomic diversity of the community in the rainy season. During the dry season, turbid waters resulting from macrotidal dynamics and wind speed limited light penetration and phytoplankton photosynthesis, leading to a higher uniformity in the species distribution. Shannon index was the most sensitive biodiversity metric to environmental changes. This study found that deterministic processes governed the community, which rainfall on the Amazon coast, along with wind speed, salinity, light availability and nutrients were the main controlling factors for phytoplankton diversity and richness.

Keywords: Maranhão Reentrâncese; ecohydrology; diversity hotspot; phytoplankton; Generalized Additive Model; chlorophyll *a*

Introduction

Biodiversity is a key factor in ecology that is directly related to the regulation and functioning of ecosystems (Cardinale et al., 2012; Chalar, 2009), and its maintenance and integrity at multiple scales is of great interest to the scientific community (Konar et al., 2013; Wilsey and Potvin, 2000).

Studies evaluating the factors influencing species diversity and richness in aquatic ecosystems have been a hot topic on ongoing ecological researchers in recent years due to declining biodiversity at the global level through anthropogenic effects on the goods and services that humans rely on that are provided by these ecosystems (Chai et al., 2020; Hooper et al., 2012; Knapp et al., 2017; Korhonen et al., 2011; Yang et al., 2021).

Coastal environments are important aquatic ecosystems because they are highly productive and dynamic, providing essential ecosystem services such as bioremediation, food production, nutrient cycling, and recreational activities that aid in the maintenance of both marine life and humanity (Attrill and Rundle, 2002; Lillebø et al., 2016). However, these environments are exposed to anthropogenic and natural influences, which often results in declining water quality (eutrophication) and reduced ecosystem productivity and structure (Carstensen et al., 2011; Wetz and Yoskowitz, 2013).

The successful management of estuarine and coastal waters requires an Ecohydrology-based, basin-wide management approach (Chícharo et al., 2009). The ecohydrological principles recognize the integration of hydrological and ecological aspects and human intervention (Wolanski and Elliott, 2015), being regarded as a new scientific approach to water management and conservation of aquatic systems that search for the understanding of ecosystem processes and functioning to increase its carrying capacity and natural resilience to support anthropogenic impacts, as a basis for the development of ecological integrated low costs solutions to mitigate or restore degraded aquatic ecosystems (Chícharo et al., 2009).

Diversity metrics may be useful for conservation practice and management purposes (Rombouts et al., 2019; Yang et al., 2021; Ye et al., 2019) since they summarize the abundance data for numerous species in an assemblage into a single number to describe the state of the community (Kwak and Peterson, 2007). In this respect, ecologists study deterministic and stochastic processes to better understand the dynamics of communities (Wang et al., 2013; Zhang et al., 2016). Several plankton species can coexist despite the limited resources for which they compete (i.e., the Paradox of Plankton; Hutchinson, 1961); however, the essential

factors and processes controlling biodiversity have not been clarified, especially in coastal ecosystems subject to constant changes.

Furthermore, served as a crucial tool, the traditional statistical analysis can help us to elucidate the knowledge from the monitoring of complex environments (Zhong et al, 2018; Zhang et al., 2021). For instance, Principal Components Analysis (PCA) and other multivariate techniques provide a means to identify stressor gradients in the data, including their correlation with each other (Ewaid et al, 2018; Feld et al, 2016). These methods are reliable on account of their capacity to efficiently and practically quantify the situation (Béjaoui et al., 2016). Nevertheless, they often suffer from the limits like outlier sensitivity and implicit assumptions on data distribution (Pavlidou et al., 2015).

The Generalized Additive Model (GAM) is able to reflect the specific response relationships between the response variable and explanatory variables, by using multiple spline smooth functions and relaxing parametric assumptions (Liu et al., 2016; Zhang et al., 2021). Nonetheless, the combination of traditional techniques and sophisticated models to explain the ecohydrological interactions still lacks study now in coastal systems (Wolanski and Elliott, 2015).

Cumã Bay, located on the northern Amazon coast, is known for its high productivity and biological diversity. It is a spawning area and nursery for numerous species of fish, shellfish, and migratory birds. Due to its importance for conservation has been considered under the Ramsar Convention as an internationally important wetland (Hazin, 2008). Cumã Bay provides relevant ecosystem services for the Amazon coast; however, information based on ecosystem functionality is currently scarce. In fact, the challenges presented by the Cumã Bay represent a number of opportunities for the application of ecohydrological principles.

From an ecological point of view, the interpretation of the effects of hydrological processes on biology is straightforward, because mechanistic relationship can be hypothesized (Poff, 1997). However, this is different and more difficult in complex environments, for example Cumã bay, which renders the interpretation of pressure effects on ecological functioning a challenge. Thus, an application of multivariate analysis and additive models can solve this problem. We hypothesized that hydrological seasonal changes in coastal ecosystems promote massive growth of phytoplankton which may lead to a reduction in overall biodiversity. From this point, our study combined traditional techniques and Generalized Additive Model (GAM) to evaluate the influence of environmental factors on phytoplankton diversity and biomass in the Amazon coastal system (Cumã Bay). Traditional techniques (PCA

and correlations analysis) were used to select the most appropriated biodiversity metric that reflects seasonal changes, and GAM was applied to determine the main environmental factors that drive phytoplankton diversity and biomass in an Amazon macrotidal bay. Hence, the present work is able to provide a new perspective to support conservation and management programs in Amazon aquatic ecosystems.

Material and methods

Study area and climatology

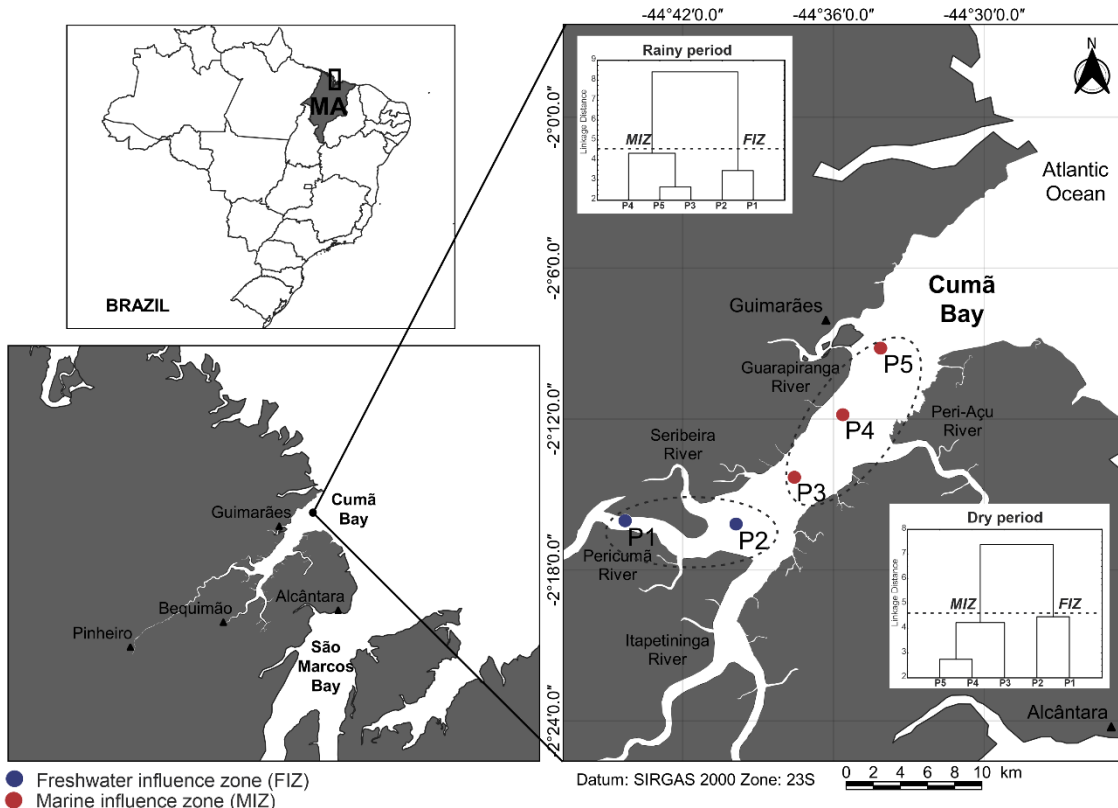
The Brazilian Amazon coast, also known as the Amazon Macrotidal Mangrove Coast (AMCC), is located between the Amapá and Maranhão states and contains a complex mosaic of vitally important aquatic ecosystems, sheltering bays, islands, estuaries (Nascimento et al., 2013). It is characterized by complex hydrodynamic processes (Nittrouer and DeMaster, 1996) and large volumes of river water, solutes, and particulate matter from the Amazon and Maranhão rivers (Araujo et al., 2017; Matos et al., 2016a; Pereira et al. 2013), as well as dozens of other smaller estuaries that surround the Maranhão coastline known as the Maranhão Reentrances.

Maranhão Reentrances was declared as “Ramsar site number 640” and based on its ecological and socio-cultural importance, the government of Brazil declared the study area as “Wetland of international importance” under the Ramsar convention in the year 1993 (Hazin, 2008). The AMCC is a large wetland that features bays, inlets and estuaries, low and flat areas, as well as extensive mangroves. It covers almost 2.7 million hectares and is connected to four other wetlands (Cabo Orange National Park, Baixada Maranhense Environmental Protection Area, Amazon Estuary and its mangroves, and State Park of Parcel Manuel Luís) of international importance forming the largest continuous and best-preserved worldwide mangrove belt (1,200 km long). Mangroves in the region are dominated by *Rhizophora mangle*, *R. racemosa*, *R. harrisonii*, *Avicennia germinans*, *A. schaueriana*, *Laguncularia racemosa*, and *Conocarpus erectus* (Martins and Oliveira, 2011). However, the ecosystem has been undergoing continuous anthropogenic pressures from fishing, agriculture (cassava and rice farming), livestock (cattle and buffalo breeding), dam construction, and domestic sewage discharge from the main urban centers.

As part of the Maranhão Reentrances, Cumã Bay is the second largest water body on the western coast of Maranhão, with an area of approximately 205.72 km² and a length of 33.92 km (Fig. 1). This bay has semidiurnal macrotides (tidal range mean > 4 m) associated with high

river discharge of the Pericumã (Pinheiro city), Itapetininga (Bequimão city), Guarapiranga and Seribeira (Guimarães city), and Peri-Açu (Alcântara city) rivers.

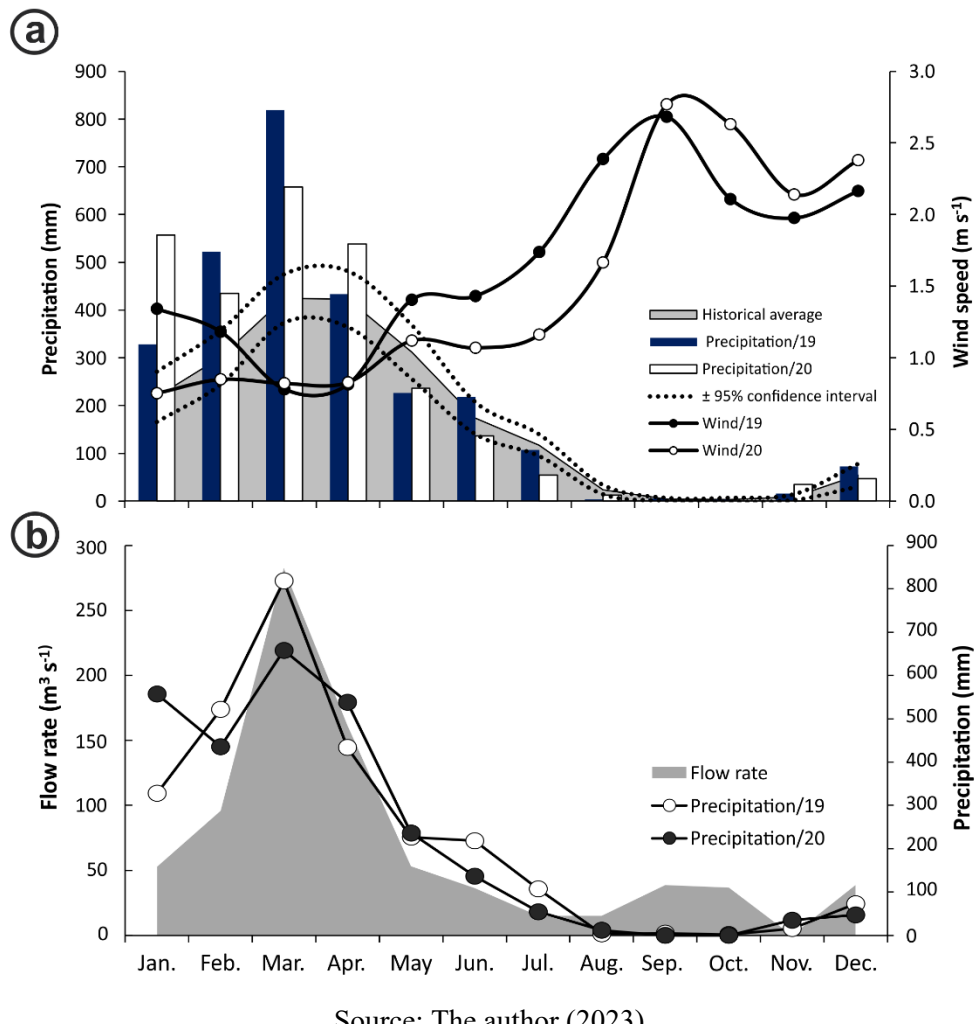
Fig. 1. Map of study area, including the determination of functional zones based on Cluster analysis according to water quality during rainy and dry seasons in Cumã Bay, Amazon Macrotidal Mangrove Coast.



Source: The author (2023).

According to the Köppen classification, the climate in the region is a tropical wet-dry climate (Aw). It is situated between the Amazon super-wet and semi-arid Northeastern Brazil and has as high temperatures ($\sim 26^{\circ}\text{C}$) and average precipitation of $> 2,000$ mm throughout the year (Cutrim et al., 2019). The total precipitation in 2019 (2,753 mm) and 2020 (2,708 mm) followed the trend of the historical annual average (2,200 mm) based on the last 28 years, and the climatological data showed two well-defined seasonal periods. The rainy season extends from January to July with the highest precipitation in March 2019 (818.2 mm) and the lowest wind speed (0.75 m s^{-1}) in January 2020. The dry season begins in August and extends to mid-December, with less than 1 mm of accumulated precipitation in September and October 2020 and a higher wind speed in September 2020 (2.77 m s^{-1}) (Fig. 2a).

Fig. 2. Historical average of precipitation, total monthly precipitation and wind speed for study period (2019-2020) (a). Monthly flow rate average of the Pericumã river basin (b). Meteorological data were obtained from National Institute of Meteorology (www.portal.inmet.gov.br).



Source: The author (2023).

The Pericumã river basin is the main tributary of Cumã Bay and covers approximately 13 municipalities in the pre-Amazonian floodplain, recognized as Baixada Maranhense. This region has a high diversity and covers $10,800 \text{ km}^2$ with a seasonal flooding cycle that annually overflows and inundates the lowland components of the fluvial network, resulting in the formation of temporary and permanent lakes (Almeida-Funo et al., 2010; Ibañez et al., 2000). Its discharge is marked by a seasonal cycle (Martins and Oliveira, 2011). The maximum flow rate ($113.69 \pm 94.30 \text{ m}^3 \text{ s}^{-1}$) is clearly observed in the rainy season, with March recording the highest average flow rate ($282.5 \text{ m}^3 \text{ s}^{-1}$). In contrast, the dry season has the lowest flow rate ($24.04 \pm 16.28 \text{ m}^3 \text{ s}^{-1}$) (Fig. 2b).

Sampling strategy

To analyze the spatiotemporal fluctuations of the phytoplankton community and environmental variables, six surveys were conducted from May 2019 to June 2020, with a total of 60 collected samples ($n=60$). The sampling period included the rainy (May, March, and June) and dry (August, October, and December) seasons at five sampling sites along the bay. Sampling was performed on the sub-surface water as well as at a 2 m depth with a van Dorn oceanographic bottle during the daytime ebb tide and the neap tide.

Cumã Bay was divided into two functional zones with spatial patterns of water quality (physical and chemical variables) during each season of either (Fig. 1): (i) the freshwater influence zone (FIZ; sites 1 to 2, depth < 9 m); and (ii) the marine influence zone (MIZ; sites 3 to 5, depth 12–17 m). Zone identification was based on cluster analysis, following the approach of Boyer et al. (1997), Boyer (2006), and Varona-Cordeiro et al. (2010) for coastal ecosystems, to better understand and classify the bay into spatially distributed stations with similar water quality characteristics (zones of similar influence; ZSI).

Physical and chemical variables and light limiting factors

To physically characterize the Cumã Bay, a Conductivity, Temperature, and Depth (CTD) probe (Castway, Sontek Inst. Co) was used to measure salinity (resolution = 0.01, accuracy = ± 0.1), temperature (resolution = 0.01, accuracy = ± 0.05 °C) and pressure (resolution = 0.01 m, accuracy = $\pm 0.25\%$ scale) *in situ* by a vertical profile of the water column.

Total dissolved solids (TDS), pH and dissolved oxygen (DO) concentrations were measured with a Hanna multi-parametric probe (HI-9828). In order to evaluate the light limiting factors, measurements of Photosynthetically Active Radiation (PAR) were obtained using an underwater radiation quantum sensor (LI-COR LI 1500), water turbidity with a turbidity meter (MS Tecnopom - TB 1000P) and suspended particulate matter (SPM) was determined according to gravimetric analysis as described by Strickland and Parsons (1972). Water transparency was estimated based on Secchi depth, and the light extinction coefficient (k) from the formula described by Poole and Atkins (1929).

Water samples (350-500 mL) were filtered through Whatman GF/F glass fiber filters (0.7 µm porosity and 47 mm diameter) to determine dissolved inorganic nutrients. The determination of ammonium ion (NH_3^-) followed the methodology described by Koroleff (1983). The concentrations of nitrite (NO_2^-) and nitrate (NO_3^-) were based

on Strickland and Parsons (1972); whereas orthophosphate (PO_4^{3-}) and silicate (SiO_2^-) measurements were derived according to Grasshoff et al. (1983). The precision was $\pm 0.02 \mu\text{mol}$ for NO_3^- , $\pm 0.02 \mu\text{mol}$ for NO_2^- , $\pm 0.02 \mu\text{mol}$ for NH_3^- , and $0.01 \mu\text{mol}$ for PO_4^{3-} . The accuracy was $\pm 2\%$ for PO_4^{3-} , $\pm 3\%$ for NO_3^- and NO_2^- , and $\pm 5\%$ for NH_3^- .

Phytoplankton community, biomass, and nutritional status

Phytoplankton in Cumā Bay were analyzed in terms of composition, cell abundance, biomass, and diversity. For biological analysis, water samples (250 mL) were collected from the sub-surface and at 2 m depth, and preserved with Lugol's iodine solution at a final concentration of 1%. In the laboratory, identification and cell counts (20–200 μm cell size) were performed using an inverted microscope (ZEISS Axiovert 100) at $400 \times$ magnification, following Utermöhl's technique (Utermöhl, 1958). The equation of Villafañe and Reid (1995) was applied to calculate the cell abundance (cells L^{-1}). Phytoplankton were identified at the lowest taxonomic level, and updated using the AlgaeBase international database (Guiry and Guiry, 2020).

Chlorophyll *a* was used as a reliable proxy for total phytoplankton biomass. Water samples (150 - 350 mL) were filtered through Whatman GF/F glass fiber filters (0.7 μm porosity and 47 mm diameter), and to separate the microphytoplankton ($>20 \mu\text{m}$) from the nanophytoplankton ($<20 \mu\text{m}$) fraction, chlorophyll *a* sub-samples were passed through 20 μm mesh, and then filtered. Pigment extraction was performed in 10 mL of 90% (v/v) acetone in the dark at -18°C for 24 h, and the fluorescence was measured both before and after acidification with 5% (v/v) HCl using a Turner Designs Trilogy Laboratory fluorimeter (Parsons et al., 1984), with the results expressed in mg m^{-3} .

The ratio of light absorption at 480 and 665 nm by 90% acetone extracts of phytoplankton pigments was used, as proposed by Heath et al. (1990) as a potential indicator of the phytoplankton nutritional status ratio. The optical density at 480 nm was used as an index of total carotenoid content (Strickland and Parsons, 1972). As a result, the absorption ratio A_{480}/A_{665} (the 480/665 ratio) was used as an index of the carotenoid/chlorophyll *a* ratio. Values of 0.5 - 1.5 indicate a good physiological status of phytoplankton cells, while those close to 2 reflect a potential nutrient limitation, and ratios higher than 2.4 indicate severe nutritional depletion.

Estimation of diversity measures

A number of the most commonly used diversity measures were used to estimate the phytoplankton diversity (alpha diversity). In terms of ecological information, three aspects of diversity indices were considered, including richness (number of taxa (S), Margalef index (d) and Menhinick index (D)), diversity (Shannon index (H')), Simpson index (λ), Brillouin index (HB), and Berger-Parker index (BP)) and evenness index (J') (Table 1).

Table 2. Diversity measures used to estimate the phytoplankton richness, diversity and evenness in an Amazon macrotidal bay.

Diversity measures	Formula	References
Richness		
Number of taxa (S)	S	
Margalef (d)	$d = \frac{S-1}{\ln N}$	Margalef (1958)
Menhinick (D)	$D = \frac{S}{\sqrt{N}}$	Menhinick (1964)
Diversity		
Shannon (H')	$H' = - \sum_{i=1}^S \frac{N_i}{N} \ln \times \frac{N_i}{N}$	Shannon and Weaver (1949)
Simpson (λ)	$\lambda = 1 - \sum_{i=1}^S \frac{N_i^2}{N}$	Simpson (1949)
Brillouin (HB)	$HB = \frac{\ln N! - \sum \ln N_i!}{N}$	Brillouin (1956)
Berger-Parker (BP)	$BP = \frac{N_{max}}{N}$	Berger and Parker (1970)
Evenness		
Pielou (J')	$J' = \frac{H'}{\ln S}$	Pielou (1975)

Source: The author (2023).

The terms used are given below:

S = the total number of species at any sampling point.

N = the total number of individuals found.

N_i = the number of individuals of one particular species found.

N_{max} = the number of individuals of the most abundant species.

Data analysis

Identification of environmental patterns and zones

Significant differences in physicochemical and biological variables were analyzed using a permutational multivariate analysis of variance (PERMANOVA) with three factors: season, ZSI, and sampling depth. After checking the normality and homogeneity of variances, a non-parametric analysis (Kruskal-Wallis test) was used to test statistical differences for each

variable, considering p values of ≤ 0.05 as significant. Cluster analysis was used to aggregate sampling points and identify zones with similar water quality (ZSI), using Euclidean distance as a measure of distance and Ward's method to construct the algorithm (Pielou, 1984), based on a standardized data matrix, in which the value was converted to a Z-value (values in a standardized normal distribution).

Relationship between phytoplankton abundance and biomass

To categorize the phytoplankton species, the frequency (% of sampling sites where a species occurred) was correlated with the abundance of each taxon and presented as an Olmstead-Tukey diagram, which classifies the species as dominant, frequent, occasional, or rare based on Sokal and Rohlf (1994) criteria. The relationship between phytoplankton biomass (chlorophyll *a* content) and abundance was analyzed using abundance–biomass comparison (ABC) curves, which determine the level of disturbance in the phytoplankton community. The W-statistic was used, which ranges from -1 (dominance in abundance or disturbed community) to 1 (dominance in biomass or undisturbed community) according to Clarke (1990) and Clarke and Warwick (2001).

Selection of diversity indices and link with hydrological conditions

Biodiversity metrics that respond differently to hydrological conditions can be considered complementary (Rombouts et al., 2019). Hence, we investigated the extent to which the selected biodiversity measures reflected changes in the environmental conditions and if these indices were interrelated. A standardized Principal Component Analysis (PCA) was used to identify the spatial and seasonal patterns of the environmental variables and chlorophyll *a*. Subsequently, the scores of the principal components (which summarize the explanation of environmental variability) were then correlated with diversity metrics to investigate how the phytoplankton diversity reflect changes in the environmental conditions of Cumă Bay. Linear Pearson's correlations were calculated to assess the relationship between each PC and the phytoplankton diversity indices.

Additionally, to evaluate nonlinear interactions between environmental factors and phytoplankton biomass and diversity and critical species, we used Generalized Additive Models (GAMs). GAMs have several advantages in analyzing nonlinear and nonmonotonic relationships between a response variable and fitted predictors (Hastie and Tibshirani, 1986) and allow one response variable to be fitted by several predictors in additive models, having

the advantage of not requiring an a priori specification of functional relationships, which is suitable for describing complex ecological interactions (Farias et al., 2022). We modeled the response of phytoplankton biomass and diversity to the effect of main environmental variables (salinity, temperature, SPM, PAR) and nutrients using the *gam* function in the R package *mgcv* (Wood, 2011). The estimated degrees of freedom (edf) indicate the degree of nonlinearity of the GAMs, where values close to 1 implies a linear relationship, and > 1 implies a progressively higher-order relationship (Xiong et al., 2021). Previously, the Draftsman plot from the Spearman correlation was used for evaluating variable collinearity ($R^2 > 0.6$). Multivariate statistical analyses were performed using IBM SPSS Statistics (version 24), R software (version 4.1.0), STATISTIC software (version 10.0), PRIMER (version 6.0), and CANOCO (version 4.5). The interpolation maps were constructed by QGIS software (version 2.18) using the Inverse Distance Weighting (IDW) method.

Results

Hydrological conditions

Spatial and seasonal fluctuations of physical and chemical variables in Cumã Bay were detected. Based on PERMANOVA analysis, the environmental variables showed significant differences among seasonal periods, spatial variations, and sampling depths ($p = 0.05$, Table 2). However, the interaction between them was not statistically significant ($p > 0.05$).

Table 3. Summary of results of permutational multivariate analysis of variance (PERMANOVA) of the hydrological variables, considering Seasonal periods (Sea), Zones of similar influence (ZSI) and Sampling depth (Sd) as factors.

Source	df	SS	MS	Pseudo-F	P(perm)	Unique perms
Sea	1	86.686	86.686	22.965	0.001	998
ZSI	1	11.273	11.273	2.9864	0.033	998
Sd	1	98.84	98.84	26.185	0.001	999
Sea vs ZSI	1	8.2153	8.2153	2.1764	0.081	998
Sea vs Sd	1	8.2049	8.2049	2.1737	0.088	998
ZSI vs Sd	1	1.0784	1.0784	0.2857	0.871	998
Sea vs ZSI vs Sd	1	1.0147	1.0147	0.26882	0.883	999
Res	52	196.28	3.7747			
Total	59	422.74				

Source: The author (2023).

Significant P values are indicated in bold text ($P < 0.05$).

Spatial and seasonal variations of hydrological variables are shown in Table 3 and Figure 3. In relation to depth sampling (sub-surface and 2 m), only PAR was significantly different ($p < 0.001$).

Salinity in the bay ranged from 8.22 to 29.24, with a significant difference between seasonal and spatial variation ($p < 0.05$). The seasonal dynamics of the freshwater-marine system are main factors driving the salinity distribution, with an increasing gradient from FIZ (8.22) to MIZ (18.56) in the rainy season, and between 22.45 (FIZ) and 29.24 (MIZ) in the dry season (Fig. 3 a-d). Water temperature showed a regular interannual cycle with slight fluctuations from 31.20°C (MIZ) to 32.66°C (FIZ), and no significant differences among the analyzed factors (Fig. 3 e-h).

Dissolved oxygen concentrations ranged from 3.00 mg L⁻¹ to 4.91 mg L⁻¹, with higher values recorded in MIZ during the rainy season, and the spatial factor differed significantly ($p < 0.02$) (Fig. 3 i-l). TDS followed the pattern of salinity distribution (7.161 mg L⁻¹–22.710 mg L⁻¹), both showing increasing gradients from FIZ to MIZ ($p = 0.01$), highest values during the dry season ($p < 0.01$) (Fig. 3 u-x), neutral pH values (6.9–7.5), and significant variation among zones and seasonal periods ($p < 0.05$) (Fig. 3 m-p).

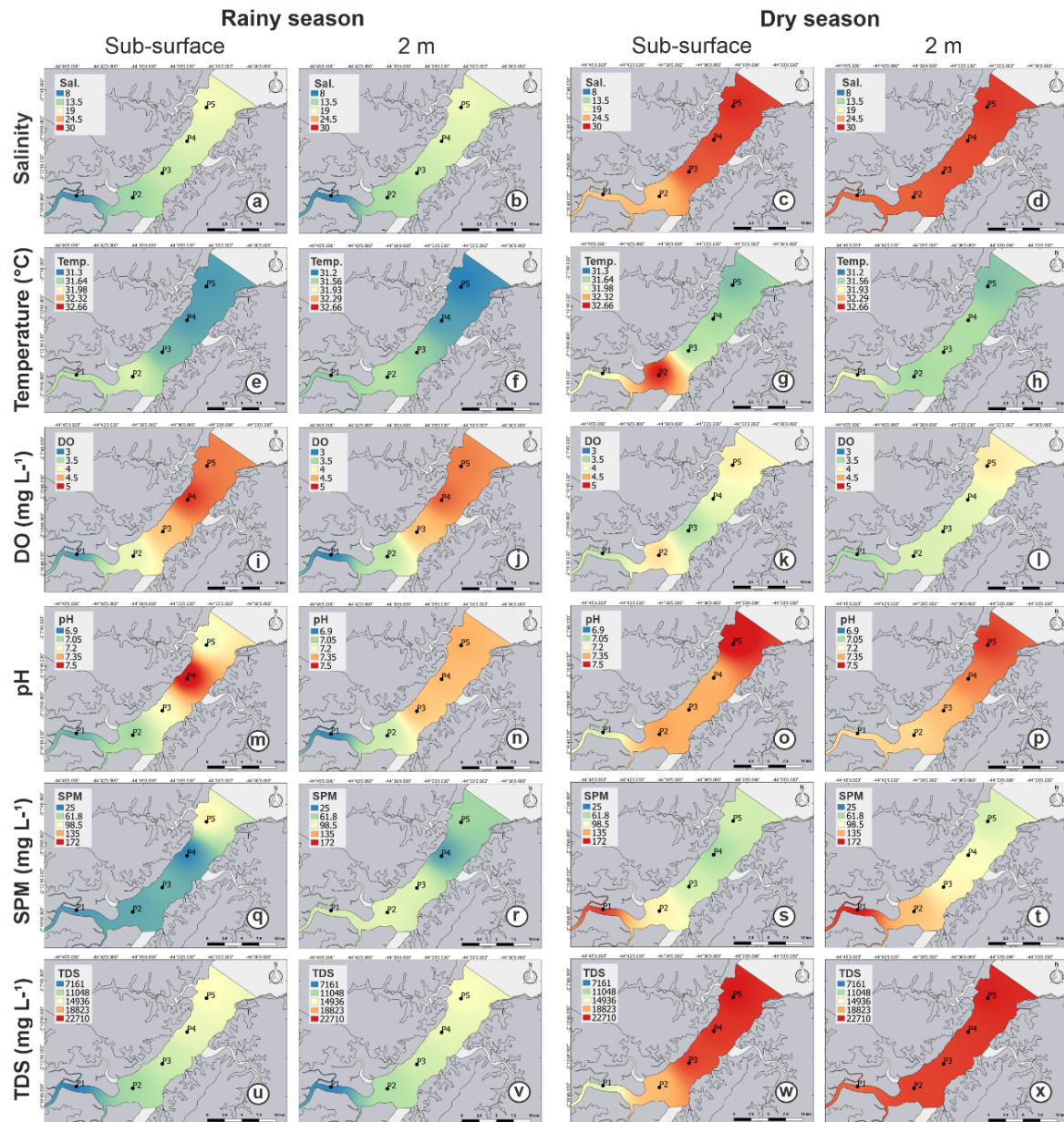
Table 4. Descriptive statistics (mean and standard deviation) for physical, chemical and biological variables of Cumă Bay and Kruskal-Wallis test with *p* values for the analyzed treatments (seasons, zones, and sampling depth). Note: FIZ = freshwater influence zone; MIZ = marine influence zone; Sea. = seasonal periods; Spa. = Spatial variation; Sd. = Sampling depth.

Variables	Units	Rainy season		Dry season		<i>p</i> value		
		FIZ	MIZ	FIZ	MIZ	Sea.	Spa.	Sd.
Salinity	--	10.95± 5.68	16.98±2.45	24.86±7.89	28.03±4.88	0.000	0.032	0.979
Temperature	°C	31.67± 0.93	31.39±0.54	32.00±1.42	31.57±0.90	0.223	0.160	0.482
DO	mg L ⁻¹	3.40±0.55	4.63±0.47	3.79±1.63	3.89±1.48	0.371	0.017	0.785
pH	--	7.01±0.29	7.32±0.25	7.25±0.29	7.40±0.21	0.038	0.004	0.988
TDS	mg L ⁻¹	9180±4431	13952±1803	18455±5446	22098±3420	0.000	0.010	0.492
NO ₃ ⁻	µmol L ⁻¹	4.34±3.03	4.67±3.81	10.55±3.31	6.91±2.47	0.000	0.233	0.559
NO ₂ ⁻	µmol L ⁻¹	0.06±0.05	0.05±0.02	0.05±0.02	0.06±0.04	0.356	0.564	0.760
NH ₃ ⁻	µmol L ⁻¹	1.41±1.21	1.42±1.56	0.71±0.67	0.59±0.47	0.070	0.521	0.391
PO ₄ ³⁻	µmol L ⁻¹	0.44±0.14	0.51±0.27	1.02±0.35	0.91±0.23	0.000	0.958	0.145
SiO ₂ ⁻	µmol L ⁻¹	35.10±6.01	37.34±15.02	64.31±17.76	46.09±13.01	0.000	0.287	0.217
Chlorophyll <i>a</i>	mg m ⁻³	15.59±7.41	12.62±5.78	7.35±1.49	8.26±3.45	0.000	0.916	0.074
Cell abundance	× 10 ⁵ cells L ⁻¹	18.37±20.47	11.30±11.51	2.85±0.71	3.20±1.28	0.000	0.880	0.308
Margalef (d)	--	4.45±1.62	4.78±2.33	4.87±0.72	4.71±0.97	0.076	0.763	0.723
Menhinick (D)	--	1.57±0.75	1.67±0.83	2.47±0.52	2.16±0.45	0.002	0.635	0.779
Shannon (H')	bits cell ⁻¹	1.77±1.00	1.78±1.04	2.59±0.28	2.47±0.31	0.011	0.786	0.871
Simpson (λ)	--	0.61±0.34	0.58±0.32	0.88±0.05	0.86±0.06	0.002	0.798	0.813
Brillouin (H _B)	--	1.62±0.91	1.62±0.96	2.25±0.19	2.20±0.25	0.022	0.774	0.739
Berger-Parker (BP)	--	0.52±0.32	0.55±0.31	0.25±0.09	0.27±0.10	0.000	0.844	0.953
Pielou evenness (J')	--	0.32±0.22	0.31±0.22	0.60±0.12	0.53±0.14	0.000	0.451	0.595

Source: The author (2023).

Significant *p* values are indicated in bold text (*p* < 0.05).

Fig. 3. Spatial and seasonal variation of environmental variables in Cumã Bay, Amazon Macrotidal Mangrove Coast.



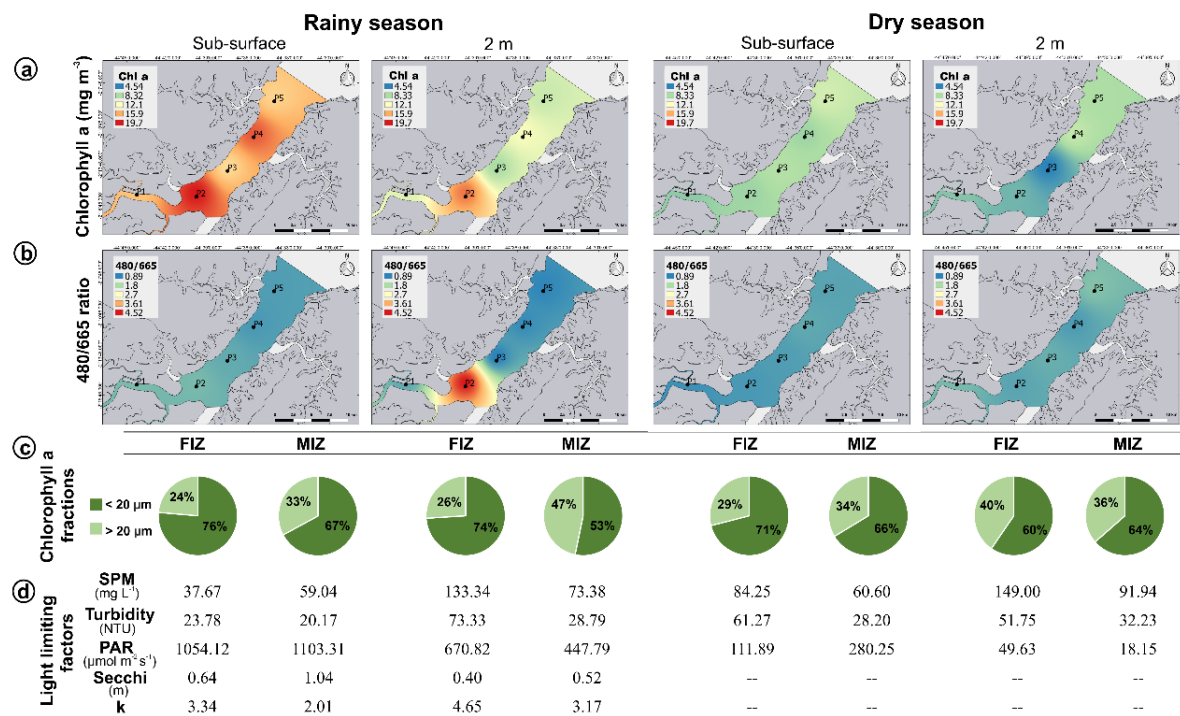
Source: The author (2023).

Nitrate ($10.55 \pm 3.31 \mu\text{mol L}^{-1}$), phosphate ($1.02 \pm 0.35 \mu\text{mol L}^{-1}$), and silicate ($64.31 \pm 17.76 \mu\text{mol L}^{-1}$) concentrations were significantly higher ($p < 0.001$) in the FIZ during the dry period while ammonium ($1.42 \pm 1.56 \mu\text{mol L}^{-1}$) was greater in the MIZ during the rainy period. Nitrite concentrations were lower than $0.06 \pm 0.05 \mu\text{mol L}^{-1}$ across the functional zones and seasonal periods.

Phytoplankton biomass, nutritional status, and light limiting factors

The distribution of chlorophyll *a* concentration along the bay showed a seasonal pattern (Fig. 4a), with values significantly higher ($p < 0.001$) in the rainy season (overall mean $13.81 \pm 6.53 \text{ mg m}^{-3}$) than in the dry season (overall mean $7.90 \pm 2.83 \text{ mg m}^{-3}$). A spatial gradient ($8.35 \text{ mg m}^{-3} - 19.67 \text{ mg m}^{-3}$) was identified with higher concentrations in the FIZ, even with no significant spatial difference ($p > 0.05$). From the average of the chlorophyll *a* fractions, nanophytoplankton ($< 20 \mu\text{m}$) was the dominant fraction with a contribution of 53% to 76% and was more representative in the FIZ during both seasons (Fig. 4c).

Fig. 4. Synthesis of phytoplankton biomass (a), nutritional status (b), contribution of phytoplankton fractions (microphytoplankton: $< 20 \mu\text{m}$ and nanophytoplankton: $> 20 \mu\text{m}$) (c), and light limiting factors (d) in Cumā Bay.



Source: The author (2023).

Seasonality was not a significant factor in the phytoplankton nutritional state (480/665 ratio; $p > 0.05$); however, a significant spatial gradient ($p < 0.05$) was observed with a minimum value in the MIZ (0.89) and maximum in the FIZ (4.52) during the rainy season (Fig. 4b). A good physiological status of the phytoplankton cells was recorded with 73% of the data within

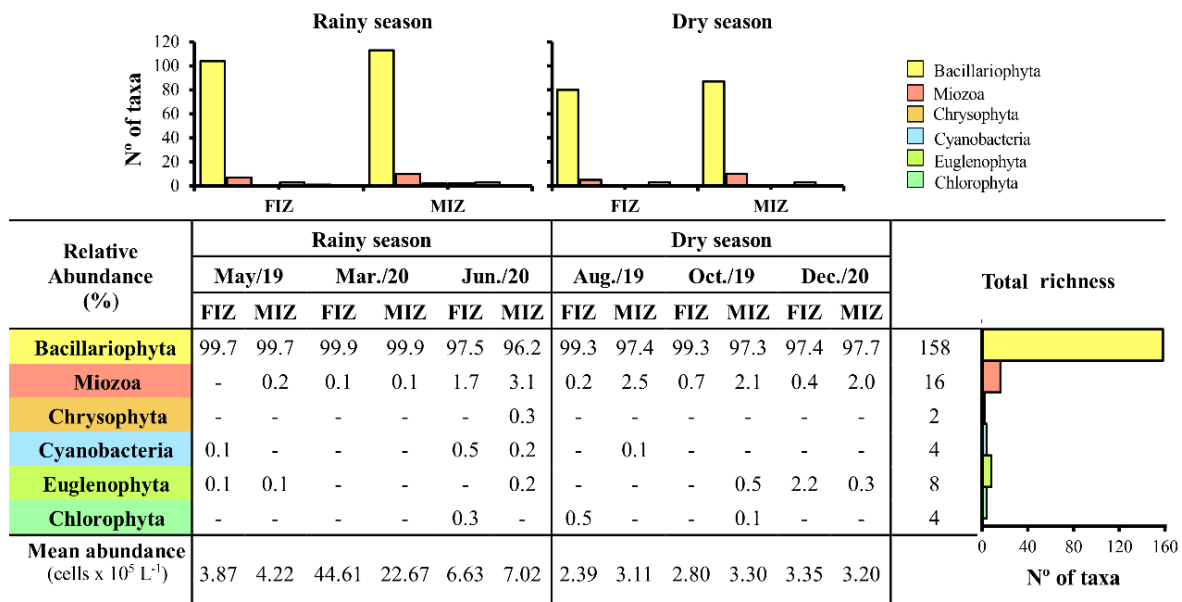
to the reference limits (0.5–1.5), except in the P2 (FIZ) during the rainy season, which reached an average of 4.51 ± 5.32 .

The lowest concentrations of SPM ($< 40 \text{ mg L}^{-1}$) and turbidity ($< 60 \text{ NTU}$) were recorded on the sub-surface water of the FIZ during the rainy season, which promoted a higher light availability ($\text{PAR} > 1,000 \mu\text{mol m}^{-2} \text{s}^{-1}$) and water transparency (Secchi $> 0.6 \text{ m}$) and consequently, greater phytoplankton biomass (Fig. 4d). By contrast, the dry season was characterized by turbid water with a higher light extinction coefficient ($k > 3$) and lower phytoplankton biomass.

Phytoplankton diversity

Between May 2019 and December 2020, 192 taxa were identified in Cumã Bay, distributed in six divisions: Bacillariophyta, Miozoa, Chrysophyta, Cyanobacteria, Euglenophyta, and Chlorophyta (Fig. 5). Diatoms were the most representative (82.29%; 158 taxa) in both seasons and zones (FIZ, MIZ), with relative abundances ranging between 96% and 99%. Miozoa had the second highest contribution (8.33%; 16 taxa) and relative abundance ($\leq 3\%$), while species of Chrysophyta were observed exclusively during the rainy season.

Fig. 5. Relative abundance (%), total richness (right diagram) and richness by zones (FIZ, MIZ) and seasonal periods (rainy and dry seasons) (top diagram) of the phytoplankton distribution by divisions (Bacillariophyta, Miozoa, Chrysophyta, Cyanobacteria, Euglenophyta, and Chlorophyta) in Cumã Bay.



Note: FIZ - freshwater influence zone; MIZ - marine influence zone.

Source: The author (2023).

Out of 158 diatoms species identified, 83 were centric where 40 showed ecological strategies of solitary and 43 formed chains, while 75 were pennate including 60 solitaries and only 15 formed chains. Based on the seasonal variability of the community, higher species richness (165) were observed in the rainy season, whereby 29% (48 taxa) were classified as dominant (abundance $> 2.5 \times 10^5$ cells L^{-1} and frequency $> 16.9\%$) and 58% (96 taxa) rare. During the dry season, of the 126 taxa recorded, 28% (36 taxa) were dominant (abundance $> 0.78 \times 10^5$ cells L^{-1} and frequency $> 19.1\%$) and 55% (69 taxa) were rare. The diatoms *Skeletonema costatum*, *Thalassiosira rotula*, *Thalassiosira subtilis*, and *Cyclotella litoralis* were the most dominant species along the study period. The significant increasing abundance in the rainy season is due to blooms of *S. costatum* ($10.39 \pm 16.17 \times 10^5$ cells L^{-1}) in the FIZ during March 2020, while *T. subtilis* ($0.47 \pm 0.51 \times 10^5$ cells L^{-1}) showed an abundance increasing from FIZ to MIZ during the dry season. More details on species dominance are available in the supplementary material (Supplementary Fig. 1).

Cell abundance was associated with phytoplankton distribution in response to seasonal variability of the environmental variables in the bay. The minimum abundance was recorded in the dry season (overall mean $3.06 \pm 1.08 \times 10^5$ cells L^{-1}) with a significant increase in the rainy season (overall mean $14.13 \pm 15.77 \times 10^5$ cells L^{-1}). Spatially, a decreasing gradient was observed from the FIZ to the MIZ, particularly in the rainy season (Table 3).

The alpha diversity also reflected a seasonal pattern with space-time changes but showed only significant differences between seasons ($p < 0.05$). The phytoplankton richness was assessed using Margalef (d) and Menhinick (D) indices, while evenness was based on the Pielou (J') index, and both showed higher means in the dry season, especially in the FIZ (4.87 ± 0.72 ; 2.47 ± 0.52 ; and 0.60 ± 0.12 , respectively) indicating higher homogeneity of the phytoplankton distribution in this period. In addition, higher fluctuations were recorded during the rainy season (Table 3).

The diversity indices, Shannon (H'), Brillouin (H_B), and Simpson (λ) showed similar distributions with higher means in the inner part of the bay (FIZ) during the dry season (2.59 ± 0.28 bits $cell^{-1}$; 2.25 ± 0.19 ; and 0.88 ± 0.05 , respectively), which implies in higher diversity in this period. However, the Berger-Parker (BP) index exhibited the opposite behavior, with a higher mean in the outer part of the bay (MIZ) during the rainy season (0.52 ± 0.32), in response to the greatest contribution of the dominant species (Table 3).

The level of disturbance in the phytoplankton community was indicated by ABC curves, which the W index indicated a pronounced disturbed condition during the rainy season

($W = -0.285$) and more elevated k-dominance curves denoting lower diversity. In contrast, k-dominance curves did not show a marked difference during the dry season, indicating a tendency toward a lower stressed environment ($W = 0.005$). Blooms of the opportunistic species *S. costatum* were the main factors responsible for the disturbance level in the period of higher precipitation. ABC curve plot and cell abundance of the *S. costatum* are provided as Supplementary Fig. 2.

Inter-relationships among phytoplankton diversity metrics

From the correlation analysis using seven indices widely used to measure alpha diversity, strong correlations among diversity measures were found (Table 4). For the richness metrics, the Margalef index (d) and taxa number (S) were highly and positively correlated ($r = 0.91$), while the Menhinick index (D) was correlated with cell abundance ($r = -0.66$). For the dominance group, Shannon (H'), Simpson (λ), and Brillouin (H_B) were strongly correlated ($r \geq 0.97$). Between categories, D was highly and positively correlated ($r \geq 0.90$) to H' , λ , and H_B indices, suggesting that these metrics carry similar ecological information. The Pielou (J') index was significantly related to Berger-Parker (BP) ($r = -0.92$), but presented a negative relationship. In addition, regression coefficients between richness and H' and H_B were significantly higher in comparison to evenness, indicating a greater effect of the taxa number under the diversity measurements, and that the λ and BP variations were primarily caused by relative abundance.

Table 5. Correlation coefficients (Pearson, r) between alpha diversity indices, number of taxa (S) and cell abundance (Ca). The grey shading indicates that the indices are from the same group: richness (light grey), diversity (white) or evenness (dark grey).

	S	Ca	d	D	H'	λ	H _B	BP	J
Nº of taxa (S)									
Cell abundance (Ca)	-0.045								
Margalef (d)	0.918	-0.363							
Menhinick (D)	0.492	-0.668	0.795						
Shannon (H')	0.448	-0.765	0.737	0.928					
Simpson (λ)	0.264	-0.830	0.575	0.849	0.971				
Brillouin (H_B)	0.498	-0.755	0.761	0.902	0.995	0.963			
Berger-Parker (BP)	-0.247	0.761	-0.561	-0.850	-0.959	-0.979	-0.945		
Pielou evenness (J')	-0.005	-0.698	0.360	0.805	0.850	0.882	0.804	-0.922	

Source: The author (2023).

Coefficients > 0.8 and with a significant level of p < 0.05 are indicated in bold.

Environmental conditions as driving factors of phytoplankton biomass and diversity

Principal Component Analysis (PCA) investigated the relationships among environmental descriptors (hydrological and meteorological variables) and ordination of the sampling sites for rainy and dry seasons in Cumã Bay (Supplementary Fig. 3).

The PCA applied for investigating the relationship among the hydrological data and chlorophyll *a* from the rainy season summarized 51.47% of the total variation in the first two axes. The PC1 axis explains 47.28% and related rainfall, temperature, SPM and NO₃⁻ negatively to wind, salinity, DO and pH. That confirms that the highest freshwater influence increases SPM concentrations and water temperature and decreases salinity and DO. The PC2 (17.70%) axis suggests that high chlorophyll *a* values are related to low PO₄³⁻ and SiO₂⁻ concentrations.

A contrary scenario was observed in the PCA performed with abiotic data from the dry season, with 62.30% of the total variation explained in the first two axes. The PC1 axis accounted for 42.27% of the variance and related wind speed negatively to salinity, rainfall, pH, DO, SPM, NH₃⁻ and PO₄³⁻, in response to greater marine influence into the bay. The PC2 axis, showing an additional 20.03% of the variance, highlighted the positive correlation between nutrients (SiO₂⁻, NO₃⁻, NO₂⁻) and PAR.

We investigated the relationships of the PC with phytoplankton diversity to select the most efficient biodiversity measure for assessing environmental changes (Table 5). Significant correlations were found mainly between PC1 and richness and diversity groups suggesting that fluctuations of the environmental descriptors regulate the pattern identified by the diversity indices. D was the most effective metric for richness and best explained the environmental fluctuations ($r = 0.83$; $p < 0.000$), while H' best reflected the diversity and evenness of the environmental conditions in the bay ($r = 0.86$; $p < 0.000$). This sensitivity shared by D and H' in relation to changes in aquatic ecosystems corroborates the strong interrelationships previously detected in Table 4.

Table 6. Correlation coefficients (Pearson, r) between the Principal Components (PC) that were calculated from rainy season data and dry season and diversity indices for Cumã Bay, Amazon Macrotidal Mangrove Coast. Statistically significant values ($p < 0.001$) are indicated with an asterisk (*).

α diversity	Rainy season		Dry season	
	PC1	PC2	PC1	PC2
Nº of taxa (S)	0.57	-0.28	0.07	-0.01
Margalef (d)	0.71	-0.25	0.19	0.09
Mehnhinick (D)	0.83	-0.15	0.28	0.17
Shannon (H')	0.86*	-0.14	0.16	0.09
Simpson (λ)	0.83	-0.05	0.04	0.13
Brillouin (H_B)	0.85	-0.15	0.09	0.06
Berger-Parker (BP)	-0.78	0.11	0.15	-0.10
Pielou evenness (J')	0.66	-0.04	0.09	0.07

Source: The author (2023).

GAMs analysis evaluating the response of phytoplankton diversity and chlorophyll *a* to the combined effects of the main drivers (environmental factors) explained at least 59% of the total variance (Table 6). The predictor variables were salinity, temperature, PAR, SPM, and the responses variables were Shannon index (H'), critical species (*Skeletonema costatum* and *Thalassiosira subtilis*) and chlorophyll *a* for four GAMs, respectively (Fig. 6).

The GAM explained 84.8% of the variance in diversity phytoplankton. The most significant predictor variables for phytoplankton diversity were salinity ($F = 14.78$, $p = < 0.0001$), SPM ($F = 10.12$, $p = < 0.0001$), and temperature ($F = 5.92$, $p = 0.0001$) where increases in salinity, concentrations of SPM up to $< 100 \text{ mg L}^{-1}$ and temperature around 32°C induced positive effects on phytoplankton diversity.

Table 7. Statistical summary of generalized additive models (GAMs) between phytoplankton diversity (Shannon index), critical species (*S. costatum* and *T. subtilis*), chlorophyll *a* and environmental parameters for Cumă bay (n=60).

Model 1			
$H' = s(\text{Sal}) + s(\text{Temp}) + s(\text{SPM})$		$R^2 = 0.79$	Dev. expl. = 84.8%
Predictors	edf	F	p - value
s(Sal)	8.76	14.78	< 0.0001***
s(Temp)	3.99	5.92	0.0003***
s(SPM)	3.00	10.12	< 0.0001***
Model 2			
$S. costatum = s(\text{Sal}) + s(\text{SPM}) + s(\text{PAR})$		$R^2 = 0.75$	Dev. expl. = 80.9%
Predictors	edf	F	p - value
s(Sal)	1.00	23.55	< 0.0001***
s(SPM)	2.81	11.14	< 0.0001***
s(PAR)	8.53	10.27	< 0.0001***
Model 3			
$T. subtilis = s(\text{Sal}) + s(\text{PAR}) + s(\text{SPM})$		$R^2 = 0.53$	Dev. expl. = 59.1%
Predictors	edf	F	p - value
s(Sal)	2.10	15.58	< 0.0001***
s(PAR)	4.64	3.77	0.004**
s(SPM)	1.00	3.76	0.05
Model 4			
$\text{Chla} = s(\text{Sal}) + s(\text{Temp}) + s(\text{PAR})$		$R^2 = 0.58$	Dev. expl. = 67.3%
Predictors	edf	F	p - value
s(Sal)	7.81	4.53	0.0003***
s(Temp)	4.83	4.33	0.001**
s(PAR)	1.01	5.53	0.023*

Source: The author (2023).

Note: R^2 is the adjusted proportion of total variability explained by the model; Dev. expl.: Deviance explained; edf: Estimated degrees of freedom; H' : (Shannon index); *S. costatum*: *Skeletonema costatum*; *T. subtilis*: *Thalassiosira subtilis*; Chla: chlorophyll *a*.

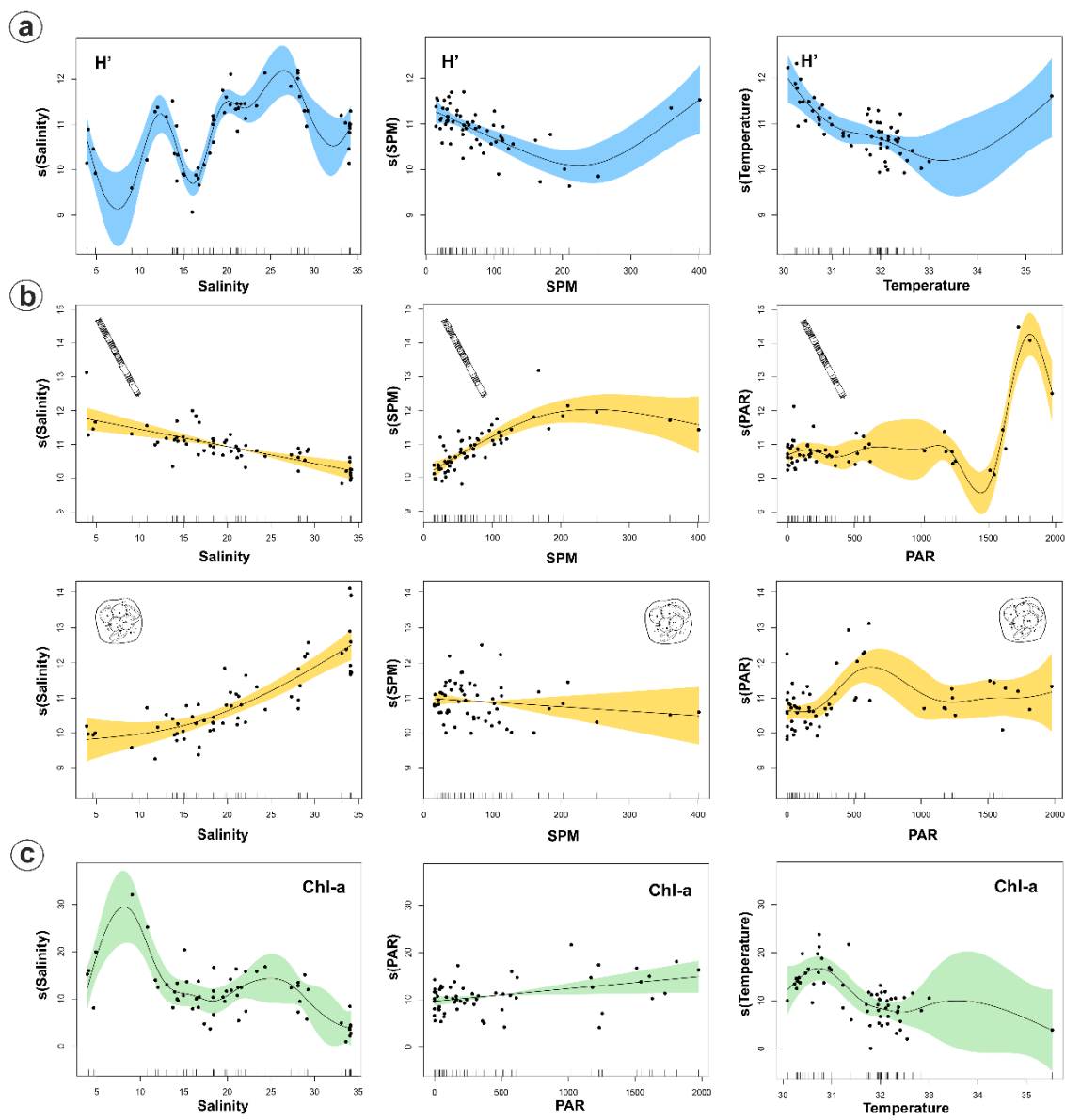
*: $p < 0.05$

**: $p < 0.01$

***: $p < 0.001$.

The GAM explained 80.9% and 59.1% of the deviance for *S. costatum* and *T. subtilis*, respectively. The most significant drivers for *S. costatum* were salinity ($F = 23.55$, $p = < 0.0001$), SPM ($F = 11.14$, $p = < 0.0001$), and PAR ($F = 10.27$, $p = < 0.0001$). Blooms of *S. costatum* occurred when salinity ranged between 10 to 25, and SPM and PAR reached values up to 100 mg L^{-1} and $500 \mu\text{mol m}^{-2} \text{ s}^{-1}$, respectively. *T. subtilis* were influenced mainly by salinity ($F = 15.58$, $p = < 0.0001$) and PAR ($F = 3.77$, $p = 0.004$) with significant and positive non-linear correlations, while SPM fluctuations implied a linear relationship ($F = 3.76$, $p = 0.05$) but values up to 100 mg L^{-1} promoted an increase of *T. subtilis* abundance.

Fig. 6. Generalized Additive Models (GAMs) results describing the main factors that influenced the phytoplankton diversity (H') (a), Skeletonema costatum and Thalassiosira subtilis as critical species (b), and chlorophyll-a (c). Solid lines represent smoothed mean relationships from GAM's and shaded areas are 95% confidence intervals. Points represent residuals. Other details are provided in Table 6.



Source: The author (2023).

GAM results showed the response of phytoplankton biomass (chlorophyll *a*) to salinity ($F = 4.53$, $p = 0.0003$), temperature ($F = 4.33$, $p = 0.001$) and PAR ($F = 5.53$, $p = 0.023$), with a combined explanation of 67.3%. The highest chlorophyll *a* concentrations were observed at salinity around 10, under light availability $< 500 \mu\text{mol m}^{-2} \text{s}^{-1}$ and temperature values ranging

between 30° C and 32° C. Thus, salinity, PAR and SPM were the main predictors for all biological variables investigated (phytoplankton diversity, chlorophyll *a*, critical species).

Discussion

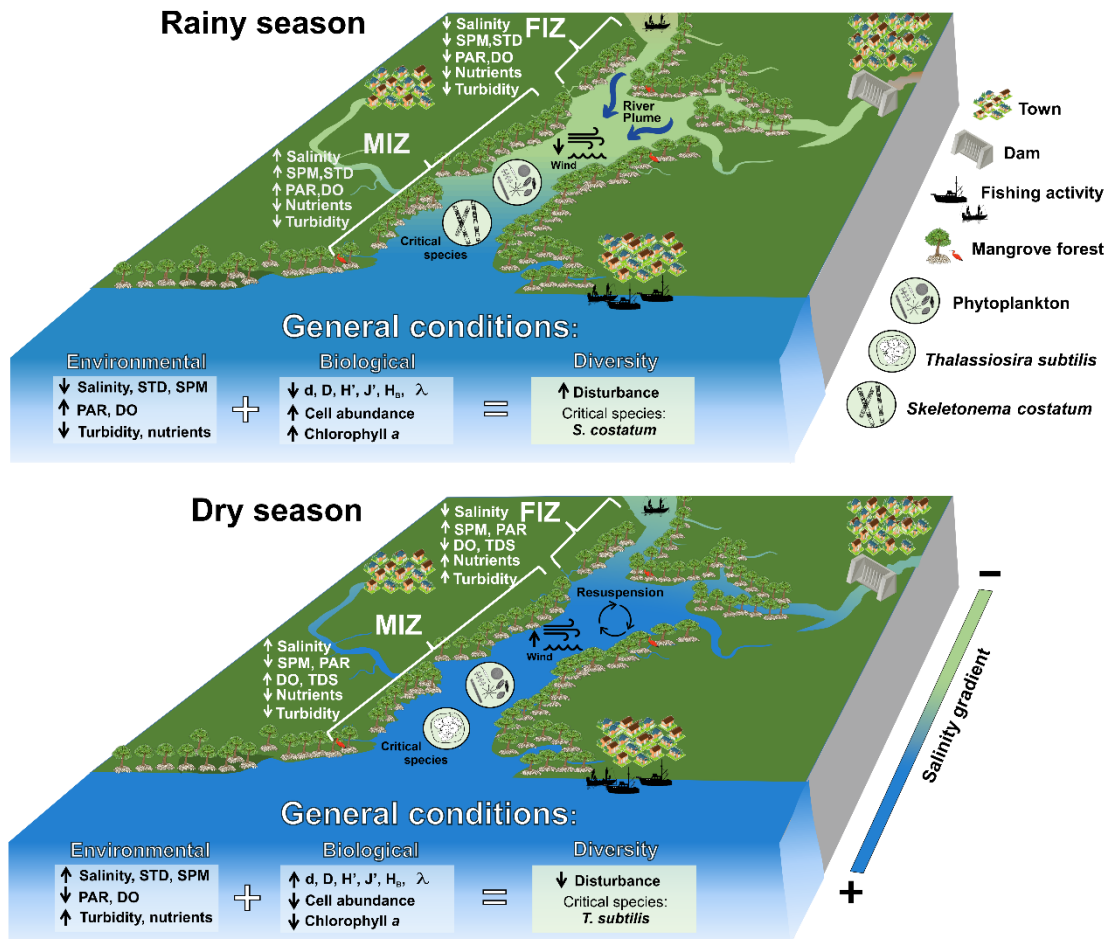
Seasonality as a controlling factor for phytoplankton dynamics

Cumã Bay, a wetland of international importance (Ramsar site), is inserted in the latitudinal band, which contains the world's wettest region and is characterized by high influence of macrotides (> 4 m) associated with a high freshwater contribution (Pericumã, Itapetininga, Guarapiranga, Peri-Açu, and Seribeira rivers).

In marine ecosystems, such as bays and estuaries, the spatiotemporal variations of biological processes (phytoplankton biomass) are associated with physical factors such as tidal cycle, solar energy input, fluvial input dilution, wind intensity, and vertical mixing of the water column (Cloern, 1996; Wirtz and Wiltshire, 2005; Yin et al., 2004). The seasonality of the water balance (rainfall and river flow) and the variability of environmental descriptors and nutrients subjected to the macrotidal regime controls the patterns of biomass and phytoplankton diversity in this tropical area and produce accentuated gradients environmental Broecker (1998). confirms that the water cycle among the land, sea, and atmosphere in the tropics is the main driving engine for ocean circulation of heat, salt, and water vapor.

Freshwater cycle is an important external factor that controls nutrient inputs, fertilizer runoff, and organic matter from urban margins (Gameiro et al., 2007; Thompson et al., 2015). The rainfall distribution along the Maranhão coast was similar to the historical annual average (last 28 years), with higher than average volumes in the first four months of the year. The high rainfall in Maranhão ($> 2,300$ mm), located on the Amazon coast, changed the hydrological conditions of the bay, increasing the flow rate of its main contributors and nutrient inputs, and decreasing salinity, SPM, and water turbidity, which favored phytoplankton growth. An ecohydrologic conceptual diagram showing the relationships between phytoplankton biomass, abundance, and diversity, the main hydrological variables, physical conditions and anthropogenic processes are summarized in Fig. 7.

Fig. 7. Ecohydrologic conceptual diagram for the Cumã Bay, integrating hydrological, ecological and anthropogenic factors and processes during the rainy and dry seasons.



Source: The author (2023).

Increased precipitation from January to June is a consequence of the Intertropical Convergence Zone (ITCZ), which is the controlling mechanism of the meteorological variables in northern and northeastern Brazil (Araujo et al., 2017; Fu et al., 2001). In response to the lower rainfall contribution (negative water balance) during the rest of the year, greater wind intensity and marine water intrusion are determining factors for the dynamics of the environmental (Santos et al., 2020) and biological descriptors (Cavalcanti et al., 2020).

Seasonal variability in Cumã Bay directly influenced the dynamics and diversity of primary producers. Therefore, our results corroborate the use of phytoplankton as an efficient indicator of water quality and ecological changes, as they are sensitive to environmental

stressors and respond quickly to changes in the water column (Cabrita, 2014; Lemley et al., 2017; Paerl et al., 2007; Santana et al., 2018).

Phytoplankton biomass and environmental conditions

Two functional zones were identified in both seasonal periods: freshwater and marine influence zones. This zonation of the bay reflects its spatial heterogeneity, the strong effect of external factors acting in bays and estuaries (freshwater and marine water entering), and local climatic conditions (Goes et al., 2014; Varona-Cordero et al., 2010) influencing the photosynthetic process and phytoplankton abundance.

Based on the fluctuations of thermohaline variables, a river plume originating from the tributaries of Cumã Bay extended into the superficial layer of the inner zone of the bay (FIZ), which has a greater positive water balance (high freshwater input), less salinity (<18), and warmer water ($>31^{\circ}\text{C}$) than the adjacent zone (MIZ). During the period of negative water balance (dry season), the macrotidal effects overlap with the flow rate of the main tributaries along the bay, resulting in a higher intrusion of marine water (salinity >22 ; temperature $<32^{\circ}\text{C}$).

The variation of the thermohaline structure has been discussed with regard to two bays on the north Amazon coast: São Marcos (Cavalcanti et al., 2018; Lefèvre et al., 2017) and São José (Santos et al., 2020), both of which showed similar patterns to those of Cumã Bay. These outcomes confirm the typical dynamics of the equatorial coastal zone, which is influenced by local water balance with relevant fluvial contributions in the rainy season and intrusion of the coastal water mass in the dry season. This seasonal variability directly influenced the phytoplankton community, since salinity and nutrients are the main factors affecting phytoplankton distribution, biochemistry, and control in coastal systems (Brand, 1984; Papry et al., 2020), and they are unique hydrological aspects because they are markers of freshwater influx into coastal ecosystems (Lancelot and Muylaert, 2011).

Phosphorus concentration significantly influences phytoplankton behavior because it is an essential macronutrient for these species (Jin et al., 2021), contributing $\sim 0.87\%$ of the phytoplankton cell dry weight (Redfield, 1958), and participating in metabolism, nucleic acid replication, and cellular constitution (Pasek et al. 2015; Reed et al., 2016). Land uses may directly influence N and P delivery to coastal waters, and concentrations of total N and P, and biomass (chlorophyll *a*) are often higher within the inner zones of coastal areas, thereby affecting phytoplankton composition.

Our findings confirmed the ecological importance of salinity, light, and nutrients on chlorophyll *a* distribution, mainly on spatial and seasonal scales (Fig. 4a), since multivariate

analyses and generalized additive models showed significant correlations with freshwater input and marine water influence. The higher extension of the river plume in the rainy season reduces salinity promoting a favorable condition for the significant increase in phytoplankton biomass (Azhikodan and Yokoyama, 2016; Cabral et al., 2020; Howarth et al., 2000; Leach et al., 2018). Higher light availability in the water column in this season also contributed for phytoplankton growth, and it is a result of the lower values of water turbidity, SPM, and light extinction coefficient that favored light penetration (PAR) and water transparency. This scenario resulted in a greater depth of the photic layer, which promoted a necessary condition for phytoplankton growth in terms of abundance and biomass (Fig. 7).

In contrast, during the months in which the wind speed was intensified and precipitation was scarce (dry season), higher salinity and SPM concentrations reduced the light penetration in the water column and consequently limited phytoplankton growth. The increased SPM load into the bay and higher water turbidity, are likely the result of the higher wind speed associated with greater permanence of coastal waters in the bay, which causes resuspension of the previously deposited material and/or erosion of the margins (Dias et al., 2016; Santos et al., 2020, Vale and Sundby, 1987), which is intensified by tidal flux in macrotidal systems (Wolanski and Spagnol, 2003; Yellen et al., 2017).

The average chlorophyll *a* concentration recorded in the present study ($10.85 \pm 5.80 \text{ mg m}^{-3}$) was typical of coastal ecosystems with anthropogenic effects, such as domestic and industrial pollutants (Smith et al., 1999). In addition, the nutritional state assessed by the 480/665 ratio did not identify phytoplankton cells under nutritional depletion (values > 2.0), indicating a good physiological status (Heath et al., 1990). Chlorophyll is commonly used as a proxy for water quality because it provides consistent insights on eutrophication; therefore, it should be considered with changes in community composition and structure (Bužančić et al., 2016; McQuatters-Gollop et al., 2009).

Previous studies world-wide have investigated the major factors that affect chlorophyll *a* distribution, and the significant influence of seasonality was observed with phytoplankton along the northern Bay of Bengal (Jyothibabu et al., 2018), the Mississippi delta (Lane et al., 2007), the southern North Sea (Van der Hout et al., 2017), the Brazilian coastal bays (Cabral et al., 2020; Cavalcanti et al., 2018), and the Amazon river plume (Goes et al., 2014).

Ecological status of the phytoplankton community

Identifying factors that control species diversity in a community is a key question in ecology (Sommer and Worm, 2002; Stein et al., 2014). Our results showed significant correlations between alpha diversity indices and environmental distribution patterns (Table 5), suggesting that the variability of environmental descriptors affects phytoplankton diversity. These finding showed deterministic processes governed the phytoplankton community in Cumã Bay and rainfall on the Amazon coast was the main controlling factor for phytoplankton diversity and richness.

Species diversity can enhance ecosystem productivity at higher levels of species richness (Cardinale et al., 2012; Korhonen et al., 2011; Tilman et al., 2012). In Cumã Bay, the high number of taxa identified (192 taxa) contributed to a significant species richness and biological diversity, thereby preserving the ecosystem integrity. Similar data were found in bays (Cavalcanti et al., 2018), estuaries (Cavalcanti et al., 2020, Duarte-dos-Santos et al., 2017), and beaches (Matos et al., 2016a; Matos et al., 2016b) governed by macrotides along the northern Amazon coast.

Diatoms were the dominant phytoplankton group (> 80%) found at all sampling sites and throughout the seasonal cycle. Recent meta-analysis studies suggest that the interaction between estuarine and coastal environments function as diatom-producing systems (Carstensen et al., 2015), which are well-adapted to environmental conditions and responsible for numerous ecosystem functions (Alexander et al., 2015; Malviya et al., 2016). Diatom dominance followed by dinoflagellates is consistent with studies on phytoplankton diversity in marine and coastal environments (Bužančić et al., 2016; Cavalcanti et al., 2020; Goes et al., 2014; Madhu et al., 2006; Olli et al., 2015; Zhou et al., 2016).

Blooms of *Skeletonema costatum* ($10.39 \pm 16.17 \times 10^5$ cells L⁻¹) recorded in rainy period (March 2020) contributed to the maximum abundance and biomass in the rainy season and decreased the local diversity and richness. *S. costatum* is a common bloom-forming diatom with long chains and small cells (usually <10 µm) (Shikata et al., 2008) that has a preference for waters with higher freshwater influences such as a diatom adaptable that thrives in coastal waters globally and is most common at salinities between 14 and 28 (Carstensen et al., 2015). Typical estuarine phytoplankton *S. costatum* was found as the most critical species responsible for higher dissimilarity among the seasons during this study.

The environmental conditions present in the dry period (high wind intensity, salinity and turbidity) favored the predominance of *Thalassiosira subtilis*, a critical species which causes a dissimilarity in the community due to its higher abundance. This dominance reflects

the ability of this colonial diatom to associate with detrital and inorganic particles, which is an ecological response to minimize stress by such conditions in turbulent and turbid environments (Kang et al., 2019; Verity et al., 1998). Shifts in diatom dominance and niche partitioning enhance resource use efficiency (Ye et al., 2019), such as light and nutrient availability, which is reflected in the good physiological state of phytoplankton cells. These results demonstrate the importance of interspecific and nutritional relationships in ecosystem homeostasis and resilience.

The phytoplankton diversity (H' , H_B , λ), richness (D), and evenness (J') varied significantly ($p < 0.05$) among the seasons, and the highest values were recorded during the dry season, while the lowest values were recorded during the rainy season. Therefore, the observed highest diversity during the dry season could be linked to the diverse species composition observed during this period combined with higher marine water intrusion that favors the co-occurrence of a greater number of species. Moreover, the advantageous environmental circumstances with an elevated nutrient level in water could have explained another reason for the higher diversity indices during this season, as Haque et al. (2021) reported. During the rainy season, the highest freshwater discharge and the occurrence of diatom blooms led to a destabilization of the phytoplankton population structure, which was reflected in the decrease in alpha diversity, except for in the Berger-Parker (BP) index, which showed higher values due to the numerical importance of the most abundant species (Berger and Parker, 1970).

According to Francé et al. (2021), environmental stress often decreases taxonomic diversity of affected communities by selecting only the most stress-tolerant taxa. In phytoplankton communities, light and nutrient availability associated with hydrological dynamics frequently promote blooms of a few dominant species. Cozzoli et al. (2017) stated that taxonomically rich and diverse phytoplankton communities are considered indicators of good environmental status.

The final selection of the most appropriated biodiversity metric that reflects the community ecological information was based on multivariate and comparative analyses, including its sensitivity to environmental changes. The Menhinick (D) and Shannon (H') indices were the most effective metrics to describe the pattern of species richness and diversity. These two indices were also sensitive to environmental stress with significant fluctuations at spatiotemporal scales, showing a more optimistic characterization of water quality in Cumã Bay.

Similar studies in coastal systems corroborate that D is an efficient tool for the assessment of water quality because it shows changes across environmental gradients (Bužančić et al., 2016; Rombouts, et al., 2019; Spatharis and Tsirtsis, 2010). Similarly, H' was selected here because it is a commonly used diversity index that includes both richness and diversity traits, and it is not significantly affected by rare species (Francé et al., 2021). Heip et al. (1998) suggested that caution must be taken when interpreting indices based on estimates of the number of species in the community since these are biased; however, we are more interested in the overall state and the relative changes in the community structure. The application of different and combined ecological metrics could be an efficient approach to better understand ecological changes for the implementation of phytoplankton monitoring, which can reflect the true taxonomic diversity in the community.

Conclusions

This study shows the importance of this tropical area and their influences in the land–ocean boundary that could extend beyond the shelf edge, influencing the marine biogeochemical cycles. In the Maranhão Reentrances this was the first study to provide fundamental information on the phytoplankton species diversity, biomass and the influence of physicochemical parameters of water on phytoplankton community. We found that deterministic processes governed the phytoplankton communities in Cumã Bay. Among the environmental variables, rainfall on the Amazon coast, along with wind speed, salinity, light availability, and nutrients were the main controlling factors conducive to specific phytoplankton community. As a result of these abiotic interactions, it was possible to identify two functionally distinct zones: the freshwater influence zone (FIZ) and the marine influence zone (MIZ). The phytoplankton biomass and abundance reached the maximum in the rainy season with a decreasing gradient to the MIZ, while the dry season showed a homogeneous distribution due to higher synergetic species interactions. The metric diversity responded to environmental and biological shifts, and Menhinick and Shannon indices were the most sensitive to environmental changes. The phytoplankton community varied as a function of the seasonal cycle along the two zones, highlighting the colonial diatoms *S. costatum* and *T. subtilis* as critical species. Thus, these findings demonstrate the connectivity of phytoplankton diversity and hydrological conditions, elucidating the relationship not yet described in Brazilian Amazon ecosystem. In summary, Cumã Bay revealed a high phytoplankton diversity, good physiological status of the cells, and chlorophyll *a* concentration as an indicator of good environmental status. However, further studies of phytoplankton and seasonal bloom

monitoring will provide directions for the sustainable management of Amazon coastal ecosystems using ecohydrology principles.

Acknowledgements

This research was supported by grant given by Coordination for the Improvement of Higher Education Personnel (CAPES) through the granting/concession of a doctoral scholarship to the first author. The authors would like to thank the Postgraduate Program in Oceanography (PPGO) as well as the Laboratory of Phytoplankton of Federal University of Pernambuco (UFPE) and Federal University of Maranhão (UFMA) for technical and structural support. We would like to thank Editage (www.editage.com) for English language editing.

References

- ALEXANDER, H., JENKINS, B. D., RYNEARSON, T. A., DYHRMAN, S. T., 2015. Metatranscriptome analyses indicate resource partitioning between diatoms in the field. *Proceedings of the National Academy of Sciences*, 112(17), E2182–E2190. doi: 10.1073/pnas.1421993112.
- ALMEIDA-FUNO, I. C. S., PINHEIRO, C. U. B., MONTELES, J. S., 2010. Identificação de tensores ambientais nos ecossistemas aquáticos da área de proteção ambiental (APA) da Baixada Maranhense. *Revista Brasileira de Agroecologia*. 5(1), 74-85.
- ARAUJO, M., NORIEGA, C., HOUNSOU-GBO, G. A., VELEDA, D., ARAUJO, J., BRUTO, L., FEITOSA, F., FLORES-MONTES, M., LEFÈVRE, N., MELO, P., OTSUKA, A., TRAVASSOS, K., SCHWAMBORN, R., NEUMANN-LEITÃO, S., 2017. A Synoptic Assessment of the Amazon River-Ocean Continuum during Boreal Autumn: From Physics to Plankton Communities and Carbon Flux. *Frontiers in Microbiology*. 8. doi: 10.3389/fmicb.2017.01358.
- ATTRILL, M., RUNDLE, S., 2002. Ecotone or Ecocline: Ecological Boundaries in Estuaries. *Estuarine, Coastal and Shelf Science*, 55(6), 929–936. doi:10.1006/ecss.2002.1036
- AZHIKODAN, G., YOKOYAMA, K., 2016. Spatio-temporal variability of phytoplankton (Chlorophyll-a) in relation to salinity, suspended sediment concentration, and light intensity in a macrotidal estuary. *Continental Shelf Research*, 126, 15–26. doi:10.1016/j.csr.2016.07.006
- BÉJAoui, B., ARMI, Z., OTTAVIANI, E., BARELLI, E., GARGOURI-ELLOUZ, E., CHÉRIF, R., TURKI, S., SOLIDORO, C., ALEYA, L., 2016. Random Forest model and TRIX used in combination to assess and diagnose the trophic status of Bizerte Lagoon, southern Mediterranean. *Ecological Indicators*, 71, 293–301.
- BERGER, W.H., PARKER, F.L., 1970. Diversity of planktonic foraminifera in deep-sea sediments. *Science*, 168, 1345–1347.

- BOYER, J. N., FOURQUREAN, J. W., JONES, R. D., 1997. Spatial characterization of water quality in Florida Bay and Whitewater Bay by multivariate analyses: Zones of similar influence. *Estuaries*, 20, 743–758.
- BOYER, J. N., 2006. Shifting N and P limitation along a north-south gradient of mangrove estuaries in South Florida. *Hydrobiologia*, 569, 167–177.
- BRAND, L. E., 1984. The salinity tolerance of forty-six marine phytoplankton isolates. *Estuarine, Coastal and Shelf Science*, 18(5), 543–556. doi:10.1016/0272-7714(84)90089-1
- BRILLOUIN, L., 1956. Science and information theory. Academic Press, New York, pp. 320.
- BROECKER, W. S., 1998. Paleocean circulation during the Last Deglaciation: A bipolar seesaw? *Paleoceanography*, 13(2), 119–121. doi:10.1029/97pa03707
- BUŽANČIĆ, M., NINČEVIĆ GLADAN, Ž., MARASOVIĆ, I., KUŠPILIĆ, G., GRBEC, B., 2016. Eutrophication influence on phytoplankton community composition in three bays on the eastern Adriatic coast. *Oceanologia*. 58(4), 302–316. doi: 10.1016/j.oceano.2016.05.003.
- CABRAL, A., BONETTI, C. H. C., GARBOSSA, L. H. P., PEREIRA-FILHO, J., BESEN, K., FONSECA, A. L., 2020. Water masses seasonality and meteorological patterns drive the biogeochemical processes of a subtropical and urbanized watershed-bay-shelf continuum. *Science of the Total Environment*, 749, 141553. doi:10.1016/j.scitotenv.2020.141553
- CABRITA, M. T., 2014. Phytoplankton community indicators of changes associated with dredging in the Tagus estuary (Portugal). *Environmental Pollution*. 191, pp. 17–24. doi:10.1016/j.envpol.2014.04.001
- CARDINALE, B. J., DUFFY, J. E., GONZALEZ, A., HOOPER, D. U., PERRINGS, C., VENAIL, P., NARWANI, A., MACE, G. M., TILMAN, D., WARDLE, D. A., KINZIG, A. P., DAILY, G. C., LOREAU, M., GRACE, J. B., LARIGAUDERIE, A., SRIVASTAVA, D. S., NAEEM, S., 2012. Biodiversity loss and its impact on humanity. *Nature*, 486(7401), 59–67. doi:10.1038/nature11148
- CARSTENSEN, J., SÁNCHEZ-CAMACHO, M., DUARTE, C. M., KRAUSE-JENSEN, D., MARBÀ, N., 2011. Connecting the Dots: Responses of Coastal Ecosystems to Changing Nutrient Concentrations. *Environmental Science & Technology*, 45(21), 9122–9132. doi:10.1021/es202351y
- CARSTENSEN, J., KLAIS, R., CLOERN, J. E., 2015. Phytoplankton blooms in estuarine and coastal waters: seasonal patterns and key species. *Estuarine, Coastal and Shelf Science*. 162, 98–109. doi: 10.1016/j.ecss.2015.05.005.
- CAVALCANTI, L. F., AZEVEDO-CUTRIM, A. C. G., OLIVEIRA, A. L. L., FURTADO, J. A., ARAÚJO, B. DE O., SÁ, A. K. D.-S., FERREIRA, F. S., SANTOS, N. G. R., DIAS, F. J. S., CUTRIM, M. V. J., 2018. Structure of microphytoplankton community and environmental variables in a macrotidal estuarine complex, São Marcos Bay, Maranhão – Brazil. *Brazilian Journal of Oceanography*, 66(3), 283–300. doi: 10.1590/s1679-87592018021906603.

CAVALCANTI, L. F., CUTRIM, M. V. J., LOURENÇO, C. B., SÁ, A. K. D. S., OLIVEIRA, A. L. L., DE AZEVEDO-CUTRIM, A. C. G., 2020. Patterns of phytoplankton structure in response to environmental gradients in a macrotidal estuary of the Equatorial Margin (Atlantic coast, Brazil). *Estuarine, Coastal and Shelf Science*, 245, 106969. doi:10.1016/j.ecss.2020.106969

CHAI, Z. Y., WANG, H., DENG, Y., HU, Z., TANG, Y. Z., 2020. Harmful algal blooms significantly reduce the resource use efficiency in a coastal plankton community. *Science of the Total Environment*, 704, 135381. doi:10.1016/j.scitotenv.2019.135381

CHALAR, G., 2009. The use of phytoplankton patterns of diversity for algal bloom management. *Limnologica*, 39(3), 200–208. doi:10.1016/j.limno.2008.04.001

CHÍCHARO, L., BEN HAMADOU, R., AMARAL, A., RANGE, P., MATEUS, C., PILÓ, D., MARQUES, R., MORAIS, P. AND ALEXANDRA CHÍCHARO, M., 2009. Application and demonstration of the Ecohydrology approach for the sustainable functioning of the Guadiana estuary (South Portugal). *Ecohydrology & Hydrobiology*, 9(1), 55–71. doi: 10.2478/v10104-009-0039-3.

CLARKE, K. R., 1990. Comparisons of dominance curves. *Journal of Experimental Marine Biology and Ecology*. 138, 143–157. doi: 10.1016/0022-0981(90)90181-B.

CLARKE, K. R., WARWICK, R. M., 2001. In: Changes in marine Communities: an Approach to Statistical Analysis and Interpretation, first ed. Plymouth Marine Laboratory, Plymouth.

CLOERN, J. E., 1996. Phytoplankton bloom dynamics in coastal ecosystems: A review with some general lessons from sustained investigation of San Francisco Bay, California. *Reviews of Geophysics*. 34 (2), 127–168. doi:10.1029/96RG00986

COZZOLI, F., STANCA, E., SELMECZY, G.B., FRANCÉ, J., VARKITZI, I., BASSET, A., 2017. Sensitivity of phytoplankton metrics to sample-size: A case study on a large transitional water dataset (WISER). *Ecological Indicators*, 82, 558–573.
<https://doi.org/10.1016/j.ecolind.2017.07.022>

CUTRIM, M. V. J., FERREIRA, F. S., DUARTE DOS SANTOS, A. K., CAVALCANTI, L. F., ARAÚJO, B. DE O., DE AZEVEDO-CUTRIM, A. C. G., FURTADO, J. A., OLIVEIRA, A. L. L., 2019. Trophic state of an urban coastal lagoon (northern Brazil), seasonal variation of the phytoplankton community and environmental variables. *Estuarine, Coastal and Shelf Science*, 216, 98–109. doi:10.1016/j.ecss.2018.08.013

DIAS, F. J. DA S., CASTRO, B. M., LACERDA, L. D., MIRANDA, L. B., MARINS, R. V., 2016. Physical characteristics and discharges of suspended particulate matter at the continent-ocean interface in an estuary located in a semiarid region in northeastern Brazil. *Estuarine, Coastal and Shelf Science*, 180, 258–274. doi:10.1016/j.ecss.2016.08.006

DUARTE-DOS-SANTOS, A. K., OLIVEIRA, A. L. L., FURTADO, J. A., FERREIRA, F. S., ARAÚJO, B. O., CORRÊA, J. J. M., CAVALCANTI, L. F., CUTRIM, A. C. G. A., CUTRIM, M. V. J., 2017. Spatial and seasonal variation of microphytoplankton community and the correlation with environmental parameters in a hypereutrophic tropical estuary -

Maranhão - Brazil, Brazilian Journal of Oceanography. 65(3), 356–372. doi:10.1590/s1679-87592017134406503.

EWAID, S.H., ABED, S.A., KADHUM, S.A., 2018. Predicting the Tigris River water quality within Baghdad, Iraq by using water quality index and regression analysis. Environ. Technol. Innov. 11, 390–398.

FARIAS, G., B., MOLINERO, J.C. CARRÉ, C., BERTRAND, A., BEC, B., CASTRO-MELO, P. A. M., 2022. Uncoupled changes in phytoplankton biomass and size structure in the western tropical Atlantic. Journal of Marine Systems. 227, 103696. doi.org/10.1016/j.jmarsys.2021.103696

FELD, C. K., SEGURADO, P., GUTIÉRREZ-CÁNOVAS, C., 2016. Analysing the impact of multiple stressors in aquatic biomonitoring data: A “cookbook” with applications in R. Science of The Total Environment, 573, 1320–1339. doi:10.1016/j.scitotenv.2016.06.243

FRANCÉ, J., VARKITZI, I., STANCA, E., COZZOLI, F., SKEJIĆ, S., UNGARO, N., VASCOTTO, I., MOZETIĆ, P., NINČEVIĆ GLADAN, Ž., ASSIMAKOPOULOU, G., PAVLIDOU, A., ZERVOUDAKI, S., PAGOU, K., & BASSET, A., 2021. Large-scale testing of phytoplankton diversity indices for environmental assessment in Mediterranean sub-regions (Adriatic, Ionian and Aegean Seas). Ecological Indicators, 126, 107630. <https://doi.org/10.1016/j.ecolind.2021.107630>

FU, R., DICKINSON, R. E., CHEN, M., WANG, H., 2001. How Do Tropical Sea Surface Temperatures Influence the Seasonal Distribution of Precipitation in the Equatorial Amazon? Journal of Climate. 14(20), 4003–4026. doi:10.1175/1520-0442(2001)014<4003:hdtss>2.0.co;2

GAMEIRO, C., CARTAXANA, P., BROTHAS, V., 2007. Environmental drivers of phytoplankton distribution and composition in Tagus Estuary, Portugal. Estuarine, Coastal and Shelf Science. 75(1-2), 21–34. doi:10.1016/j.ecss.2007.05.014

GOES, J. I., GOMES, H. DO R., CHEKALYUK, A. M., CARPENTER, E. J., MONTOYA, J. P., COLES, V. J., YAGER, P. L., BERELSON, W. M., CAPONE, D. G., FOSTER, R. A., STEINBERG, D. K., SUBRAMANIAM, A., HAFEZ, M. A., 2014. Influence of the Amazon River discharge on the biogeography of phytoplankton communities in the western tropical north Atlantic. Progress in Oceanography, 120, 29–40. doi:10.1016/j.pocean.2013.07.010

GRASSHOFF, K., EHRHARDT, M. AND KREMLING, K., 1983. Methods of Seawater Analysis. 2nd Edition, Verlag Chemie, New York, vol. 16 (3), 581–614.

GUIRY, M. D., GUIRY, G. M., 2020. AlgaeBase. World-wide electronic publication, National University of Ireland, Galway. <https://www.algaebase.org>. (Accessed 08 October 2020).

HAQUE, M.A., JEWEL, M.A.S., AKHI, M.M. et al. 2021. Seasonal dynamics of phytoplankton community and functional groups in a tropical river. Environ Monit Assess, 193(704), 1-16. doi.org/10.1007/s10661-021-09500-5

- HASTIE, T., TIBSHIRANI, R., 1986. Generalized additive models. *Statistical science* 297–310.
- HAZIN, M.C., 2008. Sítio Ramsar APA das Reentrâncias Maranhenses – MA: planejamento para o sucesso de conservação. Brasília: Ministério do Meio Ambiente. 24 p.
- HEATH, M.R., RICHARDSON, K., KIORBOE, T., 1990. Optical assessment of phytoplankton nutrient depletion. *Journal of Plankton Research*, 12 (2), 381-396.
- HEIP, C.H.R., HERMAN, P.M.J., SOETAERT, K., 1998. Indices of diversity and evenness. *Oceanis* 24 (4), 61-87.
- HOOPER, D. U., ADAIR, E. C., CARDINALE, B. J., BYRNES, J. E. K., HUNGATE, B. A., MATULICH, K. L., GONZALEZ, A., DUFFY, J. E., GAMFELDT, L., O'CONNOR, M. I., 2012. A global synthesis reveals biodiversity loss as a major driver of ecosystem change. *Nature*, 486(7401), 105–108. doi:10.1038/nature11118
- HUTCHINSON, G.E., 1961. The Paradox of the Plankton. *The American Naturalist*. 95, 137–145.
- HOWARTH, R., ANDERSON, D., CLOERN, J., ELFRING, C., HOPKINSON, C., LAPOINTE, B., MALONE, T., MARCUS, N., MCGLATHERY, K., SHARPLEY, A., WALKER, D., 2000. Nutrient pollution of coastal rivers, bays, and seas. *Issues Ecol.* 7, 1-15.
- IBAÑEZ, M. S. R., CAVALCANTE, P. R. S., COSTA NETO, J. P., BARBIERI, R., PONTES, J. P., SANTANA, S. C. C., SERRA, C. L. M., NAKAMOTO N., MITAMURA O., 2000. Limnological characteristics of three aquatic systems of the pre-amazonian floodplain, Baixada Maranhense (Maranhão, Brazil). *Aquatic Ecosystem Health & Management*, 3(4), 521-531. doi:10.1080/14634980008650689
- JIN, J., LIU, S., REN, J., 2021. Phosphorus utilization by phytoplankton in the Yellow Sea during spring bloom: Cell surface adsorption and intracellular accumulation. *Marine Chemistry*, 231, p. 103935. doi: 10.1016/j.marchem.2021.103935.
- JYOTHIBABU, R., ARUNPANDI, N., JAGADEESAN, L., KARNAN, C., LALLU, K. R., VINAYACHANDRAN, P. N., 2018. Response of phytoplankton to heavy cloud cover and turbidity in the northern Bay of Bengal. *Scientific Reports*, 8(1). doi:10.1038/s41598-018-29586-1
- KANG, L., HE, Y., DAI, L., HE, Q., AI, Q., YANG, G., LIU, M., JIANG, HONG W.L., 2019. Interactions between suspended particulate matter and algal cells contributed to the reconstruction of phytoplankton communities in turbulent waters. *Water Research*. 149, 251–262. doi:10.1016/j.watres.2018.11.003.
- KNAPP, S., SCHWEIGER, O., KRABERG, A., ASMUS, H., ASMUS, R., BREY, T., FRICKENHAUS, S., GUTT, J., KÜHN, I., LIESS, M., MUSCHE, M., PÖRTNER, H.-O., SEPPELT, R., KLOTZ, S., KRAUSE, G., 2017. Do drivers of biodiversity change differ in importance across marine and terrestrial systems — Or is it just different research communities perspectives? *Science of The Total Environment*, 574, 191–203. doi:10.1016/j.scitotenv.2016.09.002

- KONAR, M., JASON TODD, M., MUNEEPEERAKUL, R., RINALDO, A., RODRIGUEZ-ITURBE, I., 2013. Hydrology as a driver of biodiversity: Controls on carrying capacity, niche formation, and dispersal. *Advances in Water Resources*, 51, 317–325. doi:10.1016/j.advwatres.2012.02.009
- KORHONEN, J. J., WANG, J., SOININEN, J., 2011. Productivity-Diversity Relationships in Lake Plankton Communities, Solan, M. (ed.) PLoS ONE. 6(8), p. e22041. doi: 10.1371/journal.pone.0022041.
- KOROLEFF, K., 1983. Determination of phosphorus. In: GRASSHOFF, K., EHRHARDT, M., KREMLING, K. (Eds.), *Methods of Seawater Analysis*, second ed. Verlag Chemie, Weinheim, pp. 125–139.
- KWAK, T.J., PETERSON, J.T., 2007. Community indices, parameters, and comparisons. In: GUY, C.S., BROWN, M.L. (Eds.), *Analysis and Interpretation of Freshwater Fisheries Data*. American Fisheries Society, Bethesda, MD, pp. 677–763.
- LANCELOT, C., MUYLAERT, K., 2011. Trends in Estuarine Phytoplankton Ecology. In: WOLANSKI, E., MCLUSKY, D. (Eds.), *Treatise on Estuarine and Coastal Science*. Elsevier Inc., pp. 5–15. doi: 10.1016/B978-0-12-374711-2.00703-8
- LANE, R. R., DAY, J. W., MARX, B. D., REYES, E., HYFIELD, E., DAY, J. N., 2007. The effects of riverine discharge on temperature, salinity, suspended sediment and chlorophyll *a* in a Mississippi delta estuary measured using a flow-through system. *Estuarine, Coastal and Shelf Science*, 74(1-2), 145–154. doi:10.1016/j.ecss.2007.04.008
- LEACH, T. H., BEISNER, B. E., CAREY, C. C., PERNICA, P., ROSE, K. C., HUOT, Y., BRENTROP, J. A., DOMAIZON, I., GROSSART, H.-P., IBELINGS, B. W., JACQUET, S., KELLY, P. T., RUSAK, J. A., STOCKWELL, J. D., STRAILE, D., VERBURG, P., 2018. Patterns and drivers of deep chlorophyll maxima structure in 100 lakes: The relative importance of light and thermal stratification. *Limnology and Oceanography*, 63(2), 628–646. doi:10.1002/lno.10656
- LEFÈVRE, N., DA SILVA DIAS, F. J., DE TORRES, A. R., NORIEGA, C., ARAUJO, M., DE CASTRO, A. C. L., ROCHA, C., JIANG, S., IBÁNHEZ, J. S. P., 2017. A source of CO₂ to the atmosphere throughout the year in the Maranhense continental shelf (2°30'S, Brazil). *Continental Shelf Research*. 141, 38–50. doi: 10.1016/j.csr.2017.05.004.
- LEMLEY, D. A., ADAMS, J. B., STRYDOM, N. A., 2017. Testing the efficacy of an estuarine eutrophic condition index: Does it account for shifts in flow conditions? *Ecological Indicators*. 74, 357–370. doi:10.1016/j.ecolind.2016.11.034
- LILLEBØ, A. I., SOMMA, F., NORÉN, K., GONÇALVES, J., ALVES, M. F., BALLARINI, E., BENTES, L., BIELECKA, M., CHUBARENKO, B. V., HEISE, S., KHOKHLOV, V., KLAUDATOS, D., LLORET, J., MARGONSKI, P., MARÍN, A., MATCZAK, M., OEN, A. M., PALMIERI, M. G., PRZEDRZYMIRSKA, J., ... ZAUCHA, J., 2016. Assessment of marine ecosystem services indicators: Experiences and lessons learned from 14 European case studies. *Integrated Environmental Assessment and Management*, 12(4), 726–734. <https://doi.org/10.1002/team.1782>

- LIU, X., XIAO, W., LANDRY, M.R., CHIANG, K.-P., WANG, L., HUANG, B., 2016. Responses of phytoplankton communities to environmental variability in the East China Sea. *Ecosystems*, 19 (5), 832–849. <https://doi.org/10.1007/s10021-016-9970-5>
- MADHU, N. V., JYOTHIBABU, R., MAHESWARAN, P. A., JOHN GERSON, V., GOPALAKRISHNAN, T. C., NAIR, K. K. C., 2006. Lack of seasonality in phytoplankton standing stock (chlorophyll *a*) and production in the western Bay of Bengal, *Continental Shelf Research*. 26(16), 1868–1883. doi: 10.1016/j.csr.2006.06.004.
- MALVIYA, S., SCALCO, E., AUDIC, S., VINCENT, F., VELUCHAMY, A., POULAIN, J., WINCKER, P., IUDICONE, D., DE VARGAS, C., BITTNER, L., ZINGONE, A., BOWLER, C., 2016. Insights into global diatom distribution and diversity in the world's ocean. *Proceedings of the National Academy of Sciences*. 113(11), E1516–E1525. doi: 10.1073/pnas.1509523113.
- MARTINS, M. B., OLIVEIRA, T. G., 2011. Amazônia Maranhense: diversidade e conservação. Belém: MPEG, 329 p.
- MARGALEF, R., 1958. Information theory in ecology. *Gen. Sys.* 3, 36–71.
- MATOS, J. B., OLIVEIRA, S. M. O. D., PEREIRA, L. C. C., COSTA, R. M. D., 2016a. Structure and temporal variation of the phytoplankton of a macrotidal beach from the Amazon coastal zone. *Anais da Academia Brasileira de Ciências*. 88(3), 1325–1339. doi: 10.1590/0001-3765201620150688.
- MATOS, J. B., OLIVEIRA, A. R. G., TRINDADE, W. N., LEITE, N. R., KOENING, M. L., PEREIRA, L. C. C., DA COSTA, R. M., 2016b. Phytoplankton Dynamics in Three Metropolitan Beaches of the Amazon Littoral (São Luís-Maranhão), *Journal of Coastal Research*. 75, 413–417. doi: 10.2112/si75-083.1.
- MCQUATTERS-GOLLOP, A., GILBERT, A. J., MEE, L. D., VERMAAT, J. E., ARTIOLI, Y., HUMBORG, C., WULFF, F., 2009. How well do ecosystem indicators communicate the effects of anthropogenic eutrophication? *Estuarine, Coastal and Shelf Science*, 82(4), 583–596. doi:10.1016/j.ecss.2009.02.017
- MENHINICK, E.F., 1964. A comparison of some species-individuals diversity indices applied to samples of field insects. *Ecology*, 45, 859–861. doi:10.2307/1934933.
- NASCIMENTO, W. R., SOUZA-FILHO, P. W. M., PROISY, C., LUCAS, R. M., ROSENQVIST, A., 2013. Mapping changes in the largest continuous Amazonian mangrove belt using object-based classification of multisensor satellite imagery. *Estuarine, Coastal and Shelf Science*. 117, 83–93. doi: 10.1016/j.ecss.2012.10.005.
- NITTROUER, C. A., DEMASTER, D. J., 1996. The Amazon shelf setting: tropical, energetic, and influenced by a large river. *Continental Shelf Research*, 16(5-6), 553–573. doi:10.1016/0278-4343(95)00069-0
- OLLI, K., PAERL, H. W., KLAIS, R., 2015. Diversity of coastal phytoplankton assemblages – Cross ecosystem comparison. *Estuarine, Coastal and Shelf Science*. 162, 110–118. doi: 10.1016/j.ecss.2015.03.015.

- PAERL, H. W., VALDES-WEAVER, L. M., JOYNER, A. R., WINKELMANN, V., 2007. Phytoplankton indicators of ecological change in the eutrophying pamlico sound system, North Carolina. *Ecological Applications*, 17(sp5), S88–S101. doi:10.1890/05-0840.1
- PAPRY, R. I., OMORI, Y., FUJISAWA, S., AL MAMUN, M. A., MIAH, S., MASHIO, A. S., MAKI, T., HASEGAWA, H., 2020. Arsenic biotransformation potential of marine phytoplankton under a salinity gradient. *Algal Research*, 47, 101842. doi:10.1016/j.algal.2020.101842
- PARSONS, T.R., MAITA, Y., LAILI, C.M., 1984. A manual of chemical and biological methods for seawater analysis. Pergamon Press, Oxford, 173pp.
- PASEK, M. A., SAMPSON, J. M., ATLAS, Z., 2015. Redox chemistry in the phosphorus biogeochemical cycle. *Proc. Natl. Acad. Sci. U. S. A.*, 111 (43), 15468–15473.
- PAVLIDOU, A., SIMBOURA, N., ROUSSELAKI, E., TSAPAKIS, M., PAGOU, K., DRAKOPOULOU, P., ASSIMAKOPOULOU, G., KONTOYIANNIS, H., PANAYOTIDIS, P., 2015. Methods of eutrophication assessment in the context of the water framework directive: examples from the Eastern Mediterranean coastal areas. *Cont. Shelf Res.*, 108, 156–168.
- PEREIRA, L. C. C., OLIVEIRA, S. M. O. DE, COSTA, R. M. DA, COSTA, K. G. DA, VILA-CONCEJO, A., 2013. What happens on an equatorial beach on the Amazon coast when La Niña occurs during the rainy season? *Estuarine, Coastal and Shelf Science*, 135, 116–127. doi:10.1016/j.ecss.2013.07.017
- PIELOU, E. C., 1984. Mathematical Ecology. John Wiley and Sons, USA.
- PIELOU, E.C., 1975. Ecological Diversity. Wiley InterScience, New York.
- POFF, N. L., 1997. Landscape Filters and Species Traits: Towards Mechanistic Understanding and Prediction in Stream Ecology. *Journal of the North American Benthological Society*, 16(2), 391–409. doi:10.2307/1468026
- POOLE, H. H., ATKINS, W. R. G., 1929. Photo-electric Measurements of Submarine Illumination throughout the Year. *Journal of the Marine Biological Association of the United Kingdom*, 16(1), 297–324. doi:10.1017/s0025315400029829
- REDFIELD, A.C., 1958. The biological control of chemical factors in the environment. *Am. Sci.* 46, 205–221.
- REED, M. L., PINCKNEY, J. L., KEPPLER, C. J., BROCK, L. M., HOGAN, S. B., GREENFIELD, D. I., 2016. The influence of nitrogen and phosphorus on phytoplankton growth and assemblage composition in four coastal, southeastern USA systems. *Estuarine, Coastal and Shelf Science*. 177, 71–82. doi: 10.1016/j.ecss.2016.05.002.
- ROMBOUTS, I., SIMON, N., AUBERT, A., CARIOU, T., FEUNTEUN, E., GUÉRIN, L., HOEBEKE, M., MCQUATTERS-GOLLOP, A., RIGAUT-JALABERT, F., ARTIGAS, L. F., 2019. Changes in marine phytoplankton diversity: Assessment under the Marine Strategy

Framework Directive. Ecological Indicators, 102, 265–277.
doi:10.1016/j.ecolind.2019.02.009

SANTANA, R. M. DA C., DOLBETH, M., DE LUCENA BARBOSA, J. E., PATRÍCIO, J., 2018. Narrowing the gap: Phytoplankton functional diversity in two disturbed tropical estuaries. Ecological Indicators. 86, pp. 81–93. doi:10.1016/j.ecolind.2017.12.003

SANTOS, V. H. M., DIAS, F. J. S., TORRES, A. R., SOARES, R. A., TERTO, L. C., DE CASTRO, A. C. L., SANTOS, R. L., CUTRIM, M. V. J., 2020. Hydrodynamics and suspended particulate matter retention in macrotidal estuaries located in Amazonia-semiarid interface (Northeastern-Brazil), International Journal of Sediment Research. 35(4), 417–429. doi: 10.1016/j.ijsrc.2020.03.004.

SHANNON, C.E., WEAVER, W., 1949. The Mathematical Theory of Communication. University of Illinois Press, Urbana.

SHIKATA, T., NAGASOE, S., MATSUBARA, T., YOSHIKAWA, S., YAMASAKI, Y., SHIMASAKI, Y., OSHIMA, Y., JENKINSON, I. R., HONJO, T., 2008. Factors influencing the initiation of blooms of the raphidophyte *Heterosigma akashiwo* and the diatom *Skeletonema costatum* in a port in Japan, Limnology and Oceanography. 53(6), 2503–2518. doi: 10.4319/lo.2008.53.6.2503.

SIMPSON, E.H., 1949. Measurement of diversity. Nature, 163, 688.

SMITH, V.H., TILAMAN, G.D., XELAILA, J.C., 1999. Eutrophication: Impacts of excess nutrient inputs on freshwater, marine and terrestrial ecosystems. Fisheries Bulletin. 100, 179–196.

SOKAL, R. R., ROHLF, F. J., 1994. Biometry: The Principles and Practices of Statistics in Biological Research. New York: W. H. Freeman. 880 p.

SOMMER, U., WORM, B., 2002. Competition and Coexistence. Springer-Verlag Berlin Heidelberg. doi: 10.1007/978-3-642-56166-5

SPATHARIS, S., TSIRTSIS, G., 2010. Ecological quality scales based on phytoplankton for the implementation of Water Framework Directive in the Eastern Mediterranean, Ecological Indicators. 10(4), 840–847. doi: 10.1016/j.ecolind.2010.01.005.

STEIN, A., GERSTNER, K., KREFT, H., 2014. Environmental heterogeneity as a universal driver of species richness across taxa, biomes and spatial scales, Arita, H. (ed.) Ecology Letters. 17(7), 866–880. doi: 10.1111/ele.12277.

STRICKLAND, J.D.H., PARSONS, T.R., 1972. A Practical Handbook of Seawater Analysis. J. C. STEVENSON AND J. WATSON, editors. 2nd ed. Ottawa (ON): Fisheries Research Board of Canada, vol. 167 (2), 205.

THOMPSON, P. A., O'BRIEN, T. D., PAERL, H. W., PEIERLS, B. L., HARRISON, P. J., ROBB, M., 2015. Precipitation as a driver of phytoplankton ecology in coastal waters: A climatic perspective. Estuarine, Coastal and Shelf Science, 162, 119–129. doi:10.1016/j.ecss.2015.04.004

- TILMAN, D., REICH, P. B., ISBELL, F., 2012. Biodiversity impacts ecosystem productivity as much as resources, disturbance, or herbivory. *Proceedings of the National Academy of Sciences*, 109(26), 10394–10397. doi:10.1073/pnas.1208240109
- UTERMÖHL, H., 1958. Zur Vervollkommnung der quantitativen Phytoplankton Methodik. *Mitt Int. Verein. Theor. Angew. Limnology and Oceanography*. 9, 1-38.
- VALE, C., SUNDBY, B., 1987. Suspended sediment fluctuations in the Tagus estuary on semi-diurnal and fortnightly time scales. *Estuarine, Coastal and Shelf Science*, 25(5), 495–508. doi:10.1016/0272-7714(87)90110-7
- VAN DER HOUT, C. M., WITBAARD, R., BERGMAN, M. J. N., DUINEVELD, G. C. A., ROZEMEIJER, M. J. C., GERKEMA, T., 2017. The dynamics of suspended particulate matter (SPM) and chlorophyll- a from intratidal to annual time scales in a coastal turbidity maximum. *Journal of Sea Research*, 127, 105–118. doi:10.1016/j.seares.2017.04.011
- VARONA-CORDERO, F., GUTIERREZ-MENDIETA, F. J., MEAVE DEL CASTILLO, M. E., 2010. Phytoplankton assemblages in two compartmentalized coastal tropical lagoons (Carretas-Pereyra and Chantuto-Panzacola, Mexico). *Journal of Plankton Research*. 32(9), 1283–1299. doi:10.1093/plankt/fbq043
- VERITY, P. G., BLANTON, J. O., AMFT, J., BARANS, C., KNOTT, D., STENDER, B., WENNER, E., 1998. Influences of physical oceanographic processes on chlorophyll distributions in coastal and estuarine waters of the South Atlantic Bight. *Journal of Marine Research*, 56(3), 681–711. doi:10.1357/002224098765213630
- VILLAFAÑE, V. E., REID, F. M. H., 1995. Métodos de microscopía para la cuantificación del fitoplancton. In: ALVEAR, K., FERRARIO, M. E., OLIVEIRA FILHO, E. C., SARS, E. (Eds.), *Manual de métodos ficológicos*. Universidad de Concepción, Chile, pp. 169–185.
- WANG, J., SHEN, J., WU, Y., TU, C., SOININEN, J., STEGEN, J. C., HE, J., LIU, X., ZHANG, L., ZHANG, E., 2013. Phylogenetic beta diversity in bacterial assemblages across ecosystems: deterministic versus stochastic processes. *The ISME Journal*, 7(7), 1310–1321. doi:10.1038/ismej.2013.30
- WETZ, M. S., YOSKOWITZ, D. W., 2013. An “extreme” future for estuaries? Effects of extreme climatic events on estuarine water quality and ecology. *Marine Pollution Bulletin*, 69(1-2), 7–18. doi:10.1016/j.marpolbul.2013.01.020
- WILSEY, B.J., POTVIN, C., 2000. Biodiversity and ecosystem functioning: importance of species evenness in an old field. *Ecology*, 81 (4), 887–892. doi:10.1890/0012-9658(2000)081[0887:Baefio]2.0.Co;2
- WIRTZ, K. W., WILTSHERE, K., 2005. Long-term shifts in marine ecosystem functioning detected by inverse modeling of the Helgoland Roads time-series. *Journal of Marine Systems*. 56 (3-4), pp. 262–282. doi:10.1016/j.jmarsys.2004.11.002
- WOLANSKI, E., SPAGNOL, S., 2003. Dynamics of the turbidity maximum in King Sound, tropical Western Australia. *Estuarine, Coastal and Shelf Science*, 56(5-6), 877–890. doi:10.1016/s0272-7714(02)00214-7

- WOLANSKI, E., ELLIOTT, M., 2015. Estuarine Ecohydrology: An Introduction. Elsevier, Amsterdam, p. 322.
- WOOD, S.N., 2011. Fast stable restricted maximum likelihood and marginal
- YANG, J. R., YU, X., CHEN, H., KUO, Y.-M., YANG, J., 2021. Structural and functional variations of phytoplankton communities in the face of multiple disturbances. *Journal of Environmental Sciences*, 100, 287–297. doi:10.1016/j.jes.2020.07.026
- YE, L., CHANG, C., MATSUZAKI, S. S., TAKAMURA, N., WIDDICOMBE, C. E., HSIEH, C., 2019. Functional diversity promotes phytoplankton resource use efficiency. *Journal of Ecology*, 107(5), 2353–2363. doi:10.1111/1365-2745.13192
- YELLEN, B., WOODRUFF, J. D., RALSTON, D. K., MACDONALD, D. G., JONES, D. S., 2017. Salt wedge dynamics lead to enhanced sediment trapping within side embayments in high-energy estuaries. *Journal of Geophysical Research: Oceans*, 122(3), 2226–2242. doi:10.1002/2016jc012595
- YIN, K., ZHANG, J., QIAN, P.-Y., JIAN, W., HUANG, L., CHEN, J., WU, M. C. S., 2004. Effect of wind events on phytoplankton blooms in the Pearl River estuary during summer. *Continental Shelf Research*. 24 (16), pp. 1909–1923. doi: 10.1016/j.csr.2004.06.015
- XIONG, L., FANG, S., LI, K., WU, Z., MIN, X., LIU, J., XING, J., DENG, Y., GUO, Y., 2021. Temporal distribution patterns of phytoplankton and their drivers in Lake Poyang (China) – A monthly study from 2011 to 2019. *Ecological Indicators*, 133, 108435. doi.org/10.1016/j.ecolind.2021.108435
- ZHANG, M., YU, Y., YANG, Z., KONG, F., 2016. Deterministic diversity changes in freshwater phytoplankton in the Yunnan–Guizhou Plateau lakes in China. *Ecological Indicators*, 63, 273–281. doi:10.1016/j.ecolind.2015.12.017
- ZHANG, J., ZHI, M., ZHANG, Y., 2021. Combined Generalized Additive model and Random Forest to evaluate the influence of environmental factors on phytoplankton biomass in a large eutrophic lake. *Ecological Indicators*, 130, 108082. doi:10.1016/j.ecolind.2021.108082
- ZHONG, M., ZHANG, H., SUN, X., WANG, Z., TIAN, W., HUANG, H., 2018. Analyzing the significant environmental factors on the spatial and temporal distribution of water quality utilizing multivariate statistical techniques: a case study in the Balihe Lake, China. *Environ. Sci. Pollut. R.* 25 (29), 29418–29432
- ZHOU, W., GAO, J., LIAO, J., SHI, R., LI, T., GUO, Y., LONG, A., 2016. Characteristics of Phytoplankton Biomass, Primary Production and Community Structure in the Modaomen Channel, Pearl River Estuary, with Special Reference to the Influence of Saltwater Intrusion during Neap and Spring Tides. *PLoS ONE*. 11(12), p. e0167630. doi: 10.1371/journal.pone.0167630.

6 ARTIGO 2

Effects of climate, spatial and hydrological processes on shaping phytoplankton community structure and β -diversity in an estuary-ocean continuum (Amazon continental shelf, Brazil)



Manuscript published in Journal of Sea Research

Published: 6 May 2023

<https://doi.org/10.1016/j.seares.2023.102384>

ABSTRACT

This study investigated the influence of the estuarine plume from the Maranhense Gulf on the phytoplankton community structure and β -diversity. To understand the effects of the regulation mechanisms on shaping phytoplankton community structure and β -diversity along an estuary-ocean continuum in the eastern sector of the Amazon shelf, this study considered spatiotemporal analyses of physical, chemical, and biological variables from May 2019 to June 2020. High temporal environmental heterogeneity was identified in Cumã Bay and significant spatial environmental variability in the estuary-ocean continuum. Based on the thermohaline properties, an estuarine plume was observed alongshore at a distance of approximately 60 km from the coastline. Both phytoplankton community structure and β -diversity varied in time and space. From 189 taxa, thirty-nine indicator species were selected based on their functional traits and indicator value. *Skeletonema costatum* was considered the best phytoplankton indicator of the estuarine water influence. Turnover was the main component responsible for boosting β -diversity at spatial and temporal scales. The present study was the first performed on an Amazon estuary-ocean continuum which applied diversity metrics (β -diversity) to generate new information about loss of taxon richness and provided important information about spatiotemporal changes in phytoplankton community and environmental heterogeneity.

Keywords: Maranhão continental shelf, Macrotidal bay, Diatoms, Phytoplankton indicator, *Skeletonema costatum*, Turnover.

Introduction

Continental shelves are environments with strong biogeochemical activity, particularly those influenced by fluvial input from large rivers, which may substantially impact the open ocean by retaining, exchanging, or breaking down nutrients and organic carbon (Sharples et al., 2017). These ecosystems account for approximately 25% of annual global primary production (Lefèvre et al., 2017). Among the several producers that support food webs in coastal ecosystems, phytoplankton contributes $\sim 2.52 \text{ gC m}^{-2} \text{ yr}^{-1}$ to annual primary production (Cloern et al., 2014; Sweet et al., 2022).

River discharge mixes with shelf water. When discharge predominates over the tidal and wind effects, resulting in a plume of low-salinity water that spreads along-shelf and serves mainly as a source for “new” nitrogen, which is conducive to high trophic transfer from primary producers (i. e., phytoplankton) through zooplankton to fish (Cepeda et al., 2020).

Plumes are critical areas for land–ocean interaction, where transformation takes place for the export of sediments, nutrients, and organic material from the land to the oceans (Dagg et al., 2004). Water plumes are characterized by a higher amount of dissolved organic carbon compared with coastal waters (Wu et al., 2017) and might differ in the composition and abundance of organisms compared with those of marine waters (Kingsford and Suthers, 1994). Additionally, plumes can act as permeable or ‘soft’ aquatic barriers, which may significantly limit marine organisms' distribution (Luiz et al., 2012; Cowman and Bellwood, 2013). These barriers reduce the potential for ocean-wide colonization by near-shore organisms and consequently act as dispersal ‘filters’ that affect species with reduced mobility (Luiz et al., 2012; Tosetto et al., 2022).

Located in the equatorial Atlantic Ocean, the Amazon continental shelf experiences the highest river discharge worldwide, accounting for nearly 15–20% of all freshwater entering the equatorial Atlantic Ocean (Coles et al., 2013). This shelf is a highly dynamic environments subjects to hyper- and macrotides, strong ocean currents (North Brazil Current – NBC), and elevated fluvial discharge (Nittrouer and DeMaster, 1996; Aquino et al., 2022). Along the eastern sector of the Amazon shelf, there are numerous estuarine plumes fed by rivers that typically have maximum discharge rates on the order of $1,000 \text{ m}^3 \text{ s}^{-1}$. In the state of Maranhão, the Maranhense Gulf is a major source of nutrients and sediments in coastal waters (Lefèvre et al., 2017), which influences the productivity, structure, and diversity of coastal phytoplankton.

Phytoplankton encompasses an extremely diverse, polyphyletic group of organisms, demonstrating a wide array of morphological and physiological traits (Litchman and

Klausmeier, 2008). Moreover, phytoplankton can quickly react to sensitive ecological changes (Reynolds, 2006; Paerl et al., 2007). Hence, phytoplankton is regarded as a biological indicator for assessing ocean ecosystem alterations and water quality (Harris, 2012). Environmental and biological factors, as well as their interactions, may determine phytoplankton dynamics (Paerl et al., 2010), and changes in local climatic, physical, and chemical conditions can affect phytoplankton diversity, abundance, and biomass (Peierls et al., 2012; Thompson et al., 2015).

Improving the knowledge about the distributions of species, how they vary across spatial and temporal scales, and the mechanisms that influence them are the cornerstones of ecological research (Cottenie, 2005). In addition to local scale diversity (α -diversity), changes in community composition among sites and time (β -diversity) are important determinants of regional diversity (Baselga, 2010) and have crucial implications for biodiversity conservation and ecosystem management (Legendre et al., 2005). Studies have shown that partitioning β -diversity into their respective turnover (replacement of species between sites) and nestedness (species loss or gain) components facilitates the detection of ecological patterns in space and time and is essential for understanding central biogeographic, ecological, and conservation issues (Legendre, 2014; Baselga, 2010).

There have been some studies on phytoplankton dynamics in the nearshore waters of the Maranhão coast, with the majority focusing on the overall species composition and abundance patterns (Duarte-dos-Santos, et al., 2017; Carvalho et al., 2016; Cavalcanti et al., 2018; Cavalcanti et al., 2020; Costa and Cutrim, 2021; Sá et al., 2022b; Queiroz et al., 2022). However, information based on functional traits and phytoplankton β -diversity is currently scarce, particularly in the shelf area off the Maranhense Gulf. To our knowledge, this is the first study performed on an estuary-ocean continuum across the Amazon continental shelf (eastern sector) from the perspective of phytoplankton functional traits and β -diversity ecology to narrow this gap.

Considering the complex hydrodynamics of Amazon ecosystems and the essential ecosystem services provided, we hypothesized that synergistic effects among climatic factors, spatial extent, hydrodynamics, and environmental heterogeneity would shape phytoplankton community structure, functional traits, and β -diversity in macrotidal Amazon ecosystems. Therefore, this study aimed to i) investigate the influence of the estuarine plume from the Maranhense Gulf on the phytoplankton community structure and β -diversity along a temporal-spatial macroscale, ii) identify the dominant functional traits across temporal and spatial scales,

and iii) determine the primary factor responsible for boosting β -diversity through partitioning analysis.

Material and methods

Study area

The Amazon continental shelf is situated between 5°N and 2°S , comprising the continental shelves of the Brazilian states of Amapá, Pará, and Maranhão (Prestes et al., 2020; Aquino et al., 2022). The shelf is approximately 300 km long near the Amazon River mouth and the 100 m isobaths outline its break (Nittrouer and DeMaster, 1986). It also receives a freshwater discharge on the order of 10^5 to $10^6 \text{ m}^3 \text{ s}^{-1}$ from the Amazon and Pará rivers, whose plumes extend up to 250 km and 165 km, respectively, into the Atlantic Ocean (Lentz, 1995; Mascarenhas et al., 2016). Therefore, a major factor influencing the oceanographic processes of the Amazon coast is the high discharge of the Amazon River and of the dozens of other estuarine systems found across the region (Nittrouer et al., 1991; Oltman, 1968).

The area of interest is the Maranhão continental shelf (hereafter referred as MCS) located in the eastern sector of the Amazon continental shelf (Fig. 1a). The MCS comprises a surface of 55.70 Km^2 and the second longest coastline in Brazil ($\sim 640 \text{ km}$), which is bounded by Gurupi River (1°S) in the west and Parnaíba River (2.5°S) in the east (Gualberto and El-Robrini, 2005; Pereira et al., 2018). It is characterized as a shallow shelf that contains a complex mosaic of vitally important aquatic ecosystems, sheltering bays, islands, beaches, estuaries as well as extensive mangroves, forming the largest continuous and best-preserved worldwide mangrove belt (1,200 km long), which corresponds to approximately 75% of the Brazilian mangroves (Nascimento et al., 2013; Souza-Filho et al., 2009). Mangroves in the region are dominated by *Rhizophora mangle*, *R. racemosa*, *R. harrisonii*, *Avicennia germinans*, *A. schaueriana*, *Laguncularia racemosa*, and *Conocarpus erectus* (Martins and Oliveira, 2011).

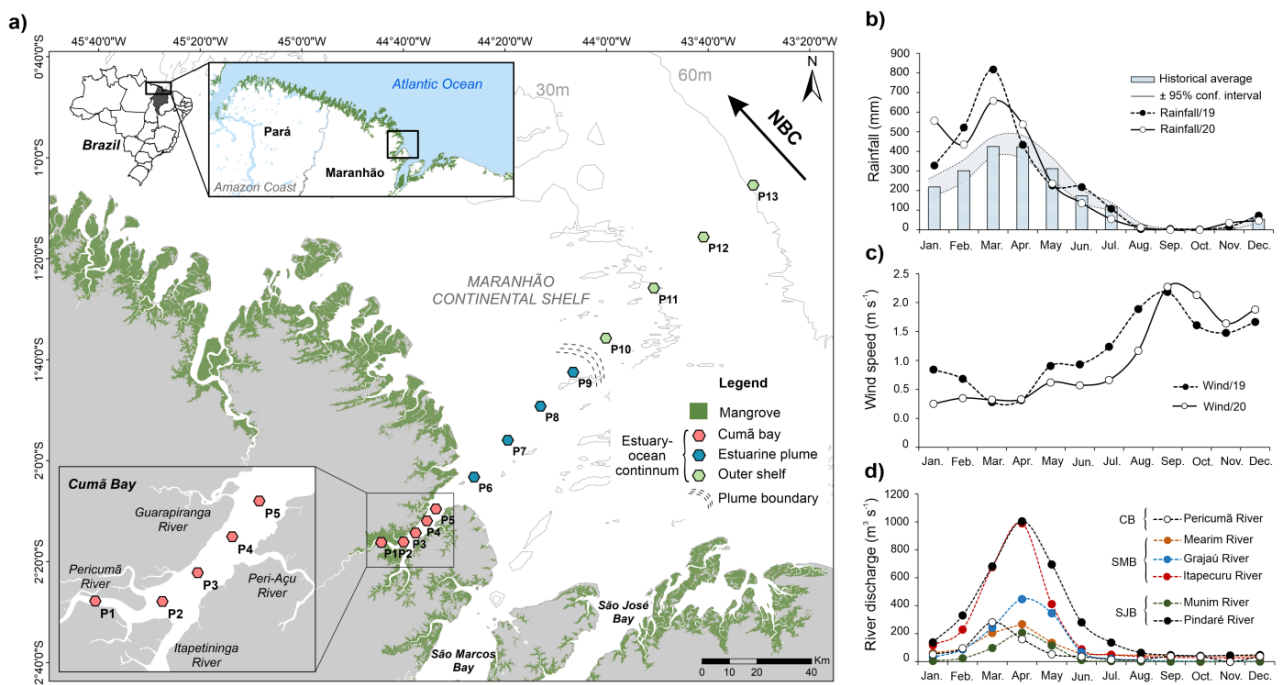
As the main reentrance of the Maranhão coast, the Maranhense Gulf consists of three main bays: Cumã, São Marcos and São José (Czizeweski et al., 2020). The domain receives high freshwater discharges from six main rivers: Pericumã River on Cumã Bay, Mearim, Grajaú, and Pindaré rivers on São Marcos Bay, and Itapecuru and Munim rivers on São José Bay, in addition to receiving contributions from other small basins and estuaries (Macedo, 1989; Czizeweski et al., 2020).

Cumã Bay is the second largest water body on the western coast of Maranhão, an area surrounded by mangrove forests and featuring semidiurnal macrotides (tidal range mean $> 4 \text{ m}$) associated with high river discharge of the Pericumã River basin. This basin is highly diverse

and covers 10,800 km² with a seasonal flooding cycle that annually overflows and inundates the lowland components of the fluvial network, resulting in the formation of temporary and permanent lakes (Ibañez et al., 2000). The bay is one of the best-conserved systems in the Maranhense Gulf and still preserves the characteristics of a pristine system. Table 1 summarizes some other relevant characteristics of the MCS and Cumã Bay.

The regional climate is tropical wet-dry (Aw), according to the Köppen classification, with predominantly northeasterly winds averaging 3.5 m s⁻¹ (Alvares et al., 2013). The annual average temperature is 26-27 °C and rainfall is > 2,000 mm, in which about 75-85% of the precipitation falls from January to May (INMET, 2019). Climatological variability in the Maranhense Gulf is caused by the seasonal transposition of the Intertropical Convergence Zone (ITCZ), which results in two well-defined seasons: the dry season that begins in August and extends to mid-December and the rainy season lasting from January to June.

Fig. 1. Map of the study area, including the positions of the 13 stations along the estuary-ocean continuum in the Amazon continental shelf (eastern sector). The North Brazil Current (NBC) is indicated in the map (a). The historical average and monthly rainfall (28-year historical series) (b) and wind speed (c) during the study period (January 2019 – December 2020). Monthly river discharge of the main rivers of Cumã Bay (CB), São Marcos Bay (SMB) and São José Bay (SJB) (c).



Source: The author (2023).

Table 1. Main physical and ecological characteristics of the Maranhão Continental Shelf and Cumã Bay.

Physical	
<i>Maranhão Continental Shelf</i>	
Location	
Latitude	0° 57' N – 3° 58' N
Longitude	47° 17' W – 42° 35' W
Surface area ^a	55.70 km ²
Tidal range ^b	3.0 to 5.0 m
Average annual freshwater discharge ^c	
Cumã bay	68.87 m ³ s ⁻¹ ;
São José bay	173.47 m ³ s ⁻¹ ;
São Marcos bay	140.57 m ³ s ⁻¹ ;
<i>Cumã Bay</i>	
Total area	205.72 km ²
Length	33.92 km
Tidal range ^b	4.0 m bay's entrance and < 2.0 m Pericumã river mouth
Surface current magnitude ^b	0.6 m s ⁻¹ outer bay, peak of 1.5 m s ⁻¹ bay's entrance, and 0.6 m s ⁻¹ Pericumã river mouth
Ecological	
Amazon Mangrove Coast area	7,210 km ²
Natural service	Ramsar site number 640 created in 1993 (Maranhão Reentrances - 2.680.911 ha) ^d

Source: The author (2023).

^a Gualberto and El-Robrini (2005).

^b Czizeweski et al. (2020).

^c Average freshwater discharge of the main bays connected to the continental shelf.

^d Convention on Wetlands (Ramsar, Iran, 1971).

Sampling strategy, climate and river discharge

To better analyze the fluctuations of phytoplankton and environmental variables, a temporal-spatial macroscale (Perillo and Piccolo, 2011) was considered in this study.

The spatial sampling strategy was carried out in the Maranhão Continental Shelf (MCS) (1° - 2°S) on board the *Ciências do Mar II* research and education vessel from the Brazilian Ministry of Education. This cruise was performed in May 2019, corresponding to the period when the MCS is under higher influence of the Maranhense Gulf estuarine plume and coinciding with the southernmost annual position of the Intertropical Convergence Zone (ITCZ). Sampling was conducted along one cross-shelf transect of approximately 100 nautical miles (192 km) that included 13 sampling sites, covering from the inner Cumã Bay portion towards to shelf-break (60 m isobaths) (hereafter estuary-ocean continuum). The temporal strategy was conducted in Cumã Bay, in which six surveys occurred along an annual cycle from

May 2019 to June 2020. Sampling encompassed rainy (May, March, and June) and dry (August, October, and December) seasons at five sampling sites along an ~ 27 km length during the flood and ebb tides.

A total of 61 samples were collected, with 13 samples from the estuary-ocean continuum and 48 from Cumã Bay, performed on the subsurface water with van Dorn oceanographic bottles (5 L) during the daytime neap tide. To facilitate spatial comparisons across the shelf, the study area was divided into three collection areas based on their thermohaline properties, which can differentiate the adjacent waters from the estuarine plume (Fig. 1a): (i) the bay itself (sites 1 to 5, depth < 17 m); (ii) the estuarine plume (sites 6 to 9; depth 20 – 24 m); and (iii) the outer shelf region (sites 10 to 13, depth 25 – 61 m).

The total precipitation in 2019 (2,753 mm) and 2020 (2,708 mm) was above the trend of the historical average (2,200 mm) based on the last 28 years. Peaks of precipitation were recorded in March of 2019 (818.2 mm) and 2020 (658.8 mm) during the rainy season, which were associated with lower wind speeds ($0.90 \pm 0.15 \text{ m s}^{-1}$). The dry season showed low precipitation levels (< 70 mm) with less than 10 mm of accumulated precipitation in August, September and October of 2019 and 2020 and higher wind speeds in September of 2019 (2.68 m s^{-1}) and 2020 (2.77 m s^{-1}) (Fig. 1b).

Considering the main rivers of the Maranhense Gulf, a marked seasonal pattern of freshwater discharge is observed during the study period where 89.22% of the freshwater discharge occurs in the rainy season ($245.54 \pm 182.47 \text{ m}^3 \text{ s}^{-1}$) of which 72.11% is concentrated between March and May 2019 (Fig. 1c). Historical precipitation and river discharge data were obtained from the National Institute of Meteorology (INMET, www.portal.inmet.gov.br/) and the National Agency for Water and Basic Sanitation (ANA, <https://www.snirh.gov.br/hidroweb>).

Hydrological conditions and nutrients

Salinity, temperature and pressure were measured *in situ* by a vertical profile of the water column using the CTD ([Conductivity, Temperature and Depth] - Castway, Sontek Instrument Company, USA) probe to physically characterize Cumã Bay and MCS. Dissolved oxygen (DO) concentrations and pH were measured with a Hanna multiparametric probe (HI-9828). Suspended particulate matter (SPM) was determined according to gravimetric analysis described by Strickland and Parsons (1972). All instruments were calibrated in the lab prior to each use.

The determination of nitrite (NO_2^-) and nitrate (NO_3^-) was based on Strickland and Parsons (1972); whereas orthophosphate (PO_4^{3-}) and silicate (SiO_2^-) measurements were derived according to Grasshoff et al. (1983) after filtration of the water samples through Whatman® GF/F glass fiber filters. The dissolved inorganic nutrients were categorized as dissolved inorganic nitrogen ($\text{DIN} = \text{NO}_3^- + \text{NO}_2^-$), dissolved inorganic phosphorus ($\text{DIP} = \text{PO}_4^{3-}$) and dissolved inorganic silicate ($\text{DSi} = \text{SiO}_2^-$). The precision was $\pm 0.02 \mu\text{mol}$ for NO_3^- , $\pm 0.02 \mu\text{mol}$ for NO_2^- and $0.01 \mu\text{mol}$ for PO_4^{3-} . The accuracy was $\pm 2\%$ for PO_4^{3-} and $\pm 3\%$ for NO_3^- and NO_2^- . All chemical analyses were performed following the recommendations of APHA (2005). Potentially limiting nutrients were evaluated by comparing water nutrient ratios with the Redfield proportions ($\text{DIN:DIP:DSi} = 16:1:16$).

Phytoplankton analysis

Water samples for the study of phytoplankton communities were collected from the subsurface and immediately fixed with Lugol's acid solution (1%). In the laboratory, a systematic analysis was performed to identify and count phytoplankton cells (20–200 μm cell size) following Utermöhl's technique (Utermöhl, 1958), using an inverted microscope (ZEISS Axiovert 100) at $400\times$ magnification. The equation of Villafaña and Reid (1995) was applied to calculate the phytoplankton abundance (cells L^{-1}). The synonyms and ecology of the taxa were updated using the AlgaeBase international database (Guiry and Guiry, 2020). The Shannon diversity index (Shannon, 1948) was applied to estimate the phytoplankton alpha diversity (α -diversity) and detect the random distribution of individuals.

To determine the phytoplankton biomass, in terms of chlorophyll-a concentration, samples (0.15 – 10.0 L) were filtered through Whatman® GF/F glass fiber filters 47 mm in diameter and to separate the microphytoplankton ($> 20 \mu\text{m}$) from the nanophytoplankton ($< 20 \mu\text{m}$) fraction, chlorophyll-a subsamples were passed through 20 μm mesh, and then filtered. Pigment extraction was performed in 10 mL of 90% (v/v) acetone in the dark at -18 °C for 24 h, and the fluorescence was measured both before and after acidification with 5% (v/v) HCl using a Turner Designs Trilogy Laboratory fluorimeter (Parsons et al., 1984), with the results expressed in mg m^{-3} .

Indicator species and functional traits

The indicator value method (IndVal) was then used to select the indicator phytoplankton species of the MCS. IndVal was calculated combining phytoplankton abundance with the

relative frequency of occurrence and expressed as the product of the specificity and fidelity for each taxon considering the temporal and spatial scales. The IndVal of species i for class j was obtained according to the following equation:

$$\text{Ind Val} = A_{ij} \times B_{ij} \times 100$$

where A_{ij} corresponds to specificity, and B_{ij} to fidelity (Dufrêne and Legendre, 1997). Species with $\text{IndVal} > 25\%$ and $p < 0.05$ according to a randomized distribution Monte Carlo test were considered the top indicators of the phytoplankton community.

The functional traits of the indicator phytoplankton community were determined from the maximum linear dimensions (MLD; Lewis, 1976) and classification in terms of life form, cell organization, and presence of flagella, mucilage and siliceous exoskeleton structures in accordance with the works of Kruk et al. (2010) and Santana et al. (2018).

Data analysis

Firstly, a permutational multivariate analysis of variance (PERMANOVA; Anderson, 2001) was applied to a Euclidean similarity matrix to evaluate the spatiotemporal differences of the hydrological variables and nutrients using three factors for Cumã Bay: i) seasons (rainy and dry), ii) months (May, March, June, August, October, and December) and iii) tides (ebb and flood). Zones (bay, plume and outer) was used as a factor for the estuary-ocean continuum.

To determine whether the Cumã Bay and the estuary-ocean continuum present high environmental heterogeneity (here measured through hydrological variables and nutrients), a permutational analysis of multivariate dispersion (PERMDISP; Anderson, 2006) was used. This analysis tested the dispersion homogeneity of those significant factors based on the distance between the variables and their centroids using one-way ANOVA and Tukey's HSD pairwise test ($p < 0.05$). Thus, the greater the distances are from samples to their group centroids, the greater is the environmental heterogeneity. A principal coordinate analysis (PCoA) was used to visualize the dispersion based on the environmental variables. For PERMANOVA and PERMDISP tests, a total of 999 unrestricted permutations of transformed data to log scale ($x + 1$) were used, applying the *betadisper* function in the 'vegan' R package (Oksanen et al., 2020).

After that, the normality and homoscedasticity of the variances were verified using the Shapiro-Wilk and Levene tests, respectively, and a non-parametric analysis (Kruskal-Wallis test) was used to test statistical differences for each variable, considering p values of ≤ 0.05 as

significant (IBM SPSS Statistics v.24). When significant, Dunn's post-hoc test was used to obtain pairwise comparison results.

The hierarchical cluster analysis, based on the Euclidian distance matrix and Ward method, was applied to examine the temporal and spatial variation in phytoplankton community abundance. For this analysis, taxa with low occurrence (<2%) and abundance (< 4.8×10^3 cells L⁻¹) were not included to diminish the effect of rare species (Legendre and Legendre, 1998). To evaluate community compositional changes among groups depicted in the cluster analyses, we used the β -diversity partitioning approach proposed by Baselga (2010). These metrics provide the total variation of the community in space and time (β_{Sor}) and the contribution of each diversity component that represents turnover (β_{Sim}) and nestedness (β_{Nes}). The Sørensen dissimilarity index was then used. β -diversity turnover and nestedness indices were calculated with *beta.pair* function in the 'betapart' R package (Baselga and Orme, 2012).

Finally, relative contributions of environmental (Env), spatial (Spa), climatic (Cli), and local hydrodynamic (Hyd) variables on phytoplankton community structure and β -diversity were further analyzed using distance-based redundancy analysis (db-RDA), which take the distance matrix as the response variables based on redundancy analysis. In the present study, phytoplankton distance matrices based on Euclidian (i.e., community structure) and Sørensen (i.e., β -diversity) dissimilarity were used as the response variables, and environmental (hydrological variables and nutrients), spatial (AEM eigenvectors), climatic (precipitation, wind), and local hydrodynamic (river discharge, tides) variables as predictors to perform db-RDA. To perform the db-RDA with the abundance data, a Hellinger transformation (Peres-Neto et al., 2006) was applied. A spatial matrix was submitted to the asymmetric eigenvectors maps (AEM) and the generated axes (eigenvectors) were considered the explanatory spatial variables (Blanchet et al., 2008a). Climatic variable was presented by a dummy variable differentiating the seasonal periods along the annual cycle based on precipitation and wind data. Multicollinearity of variables was evaluated by variance inflation factors (VIF, variables were excluded with VIF > 10). All the factors were subjected to a forward selection procedure proposed by Blanchet et al. (2008b) to determine the main variables to be included in the analyses. Then, variation partitioning analysis was used to calculate the unique and shared effects of variables (Peres-Neto et al., 2006). Variation partitioning analysis has been widely used in recent studies because it can flexibly integrate the effect of environmental models (local environmental factors) and different spatial and temporal models (e.g., dispersal models) (Dong et al., 2016; Rusanov et al., 2022). The variation partitioning was performed using the function

varpart in the ‘vegan’ R package (Oksanen et al., 2020). The components were tested with ANOVA, and significance was set at $p < 0.05$. These analyses were performed using R software (R Core Team, 2019).

Results

Cross-shelf environmental heterogeneity: from Cumã Bay to the shelf break

Highly significant variation in environmental conditions considering the temporal scale and tidal cycle in Cumã Bay was detected from PERMANOVA analysis based on the matrix of monthly campaigns of hydrological data ($P < 0.01$; Table 2). However, the interactions between these factors were not significant ($P > 0.05$). Considering the estuary-ocean continuum, the PERMANOVA analysis indicated that the spatial scale was an important source of variation in environmental conditions in the MCS ($P < 0.001$; Table 2).

Table 2. Summary of the permutational multivariate analysis of variance (PERMANOVA) results evaluating the variability of environmental conditions along the temporal scale (seasonal periods and months) and between tides cycle (flood and ebb) in Cumã Bay and the spatial scale (bay, plume and outer) in the estuary-ocean continuum in Maranhão continental shelf (MCS).

Cumã Bay PERMANOVA						
Source	df	SS	MS	F.Model	R ²	P
Seasonal	1	0.137	0.137	103.150	0.432	0.001***
Tide	1	0.008	0.008	5.955	0.025	0.003**
Month	4	0.107	0.027	20.122	0.337	0.001***
Sea vs. Tide	1	0.003	0.003	2.114	0.009	0.081
Tide vs. Months	2	0.004	0.002	1.636	0.014	0.137
Residuals	44	0.058	0.001		0.184	
Total	53	0.318			1.000	
Estuary-ocean continuum PERMANOVA						
Source	df	SS	MS	F.Model	R ²	P
Zones	3	0.189	0.063	44.121	0.868	0.001***
Residuals	20	0.028	0.001	0.131		
Total	23	0.217		1.000		

Source: The author (2023).

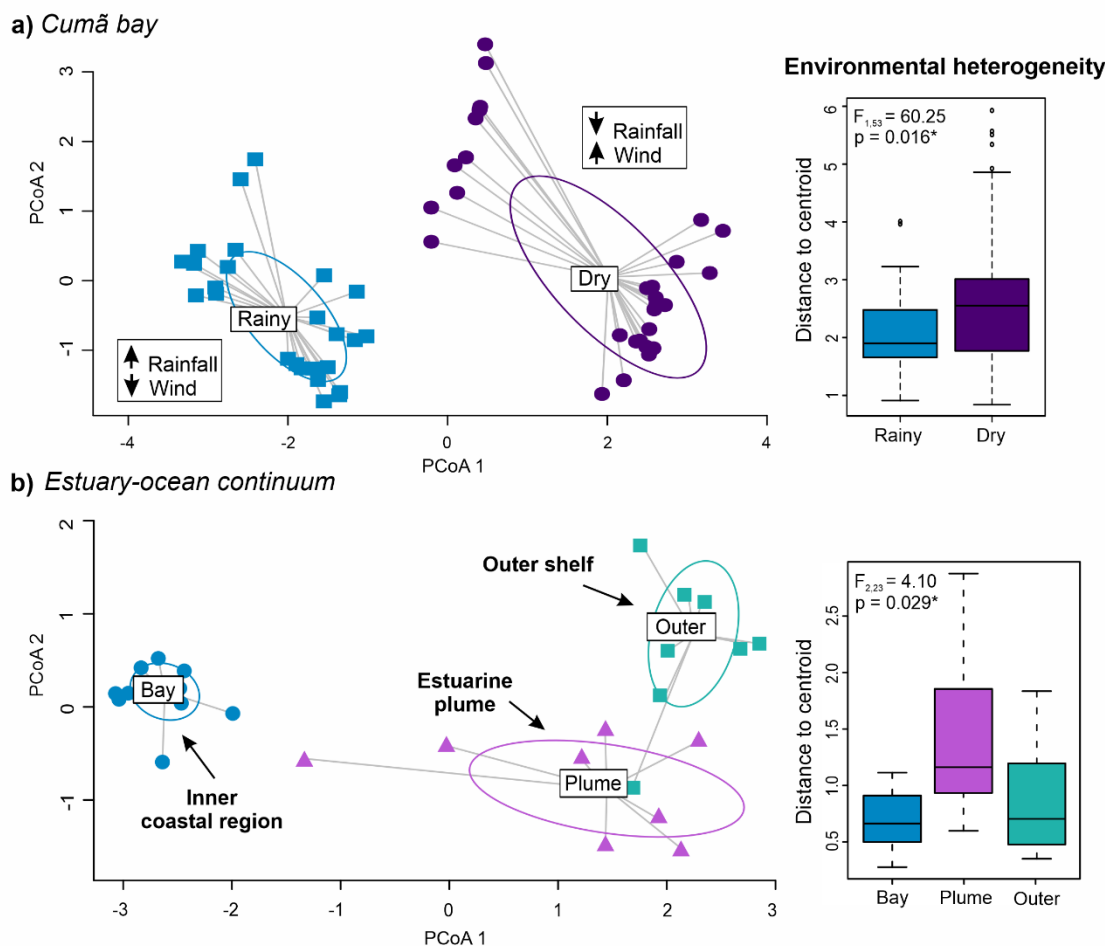
Statistically significant values are indicated with asterisks: * $p < 0.05$; ** $p < 0.01$; *** $p < 0.001$.

Environmental heterogeneity tested by PERMDISP (based on distance to centroid) indicated the effect on dispersion along the temporal ($p < 0.05$) and spatial ($p < 0.05$) scales (Fig. 2). In terms of temporal variation, environmental heterogeneity was identified in Cumã Bay ($F_{1,53} = 6.02$; $p = 0.016$), which was higher during the dry period (mean distance to centroid = 2.75) than during the rainy season (mean distance to centroid = 2.11) (Fig. 2a). However, low

dispersion and overlapping of the samples were observed among the studied months (May 2019 to June 2020) ($F_{5,48} = 0.56$; $p = 0.723$) and ebb and flood tides ($F_{1,53} = 0.26$; $p = 0.611$).

Along the estuary-ocean continuum, the hydrological conditions differed significantly ($F_{2,23} = 4.10$; $p < 0.05$) indicating high spatial heterogeneity mainly in the zone under a greater influence of the estuarine plume (mean distance to centroid = 1.42). The stations located close to the shelf break (mean distance to centroid = 0.86) and the innermost coastal region (mean distance to centroid = 0.69) showed lower dispersion, and consequently higher homogeneity (Fig. 2b).

Fig. 2. Dispersion of environmental variables through principal coordinate analysis (PCoA) and boxplot based on distance to centroid (environmental heterogeneity) considering the temporal scale in Cumã Bay (a) and spatial scale along the estuary-ocean continuum (b).



Source: The author (2023).

Temporal and tidal patterns of hydrological data and nutrients: Cumă Bay

Horizontal profiles of salinity and dissolved nutrients (nitrate, nitrite, orthophosphate, and silicate) were prepared to investigate temporal and tidal variations in Cumă Bay (Fig. 3). Table 3 presents descriptive statistics of the environmental and biological variables.

Thermohaline properties characterized the waters of the bay, which were typically estuarine in 79% of the samples, with an overall average salinity of 21.83 ± 8.40 and a temperature of $31.62 \pm 1.15^\circ\text{C}$. A marked seasonal pattern was observed in the salinity values, which were lower during the rainy season (15.44 ± 5.06) and higher during the dry season (26.83 ± 6.56) (Fig. 3a). The water temperature exhibited a narrow variation, with values of approximately $31.58 \pm 1.06^\circ\text{C}$ ($p > 0.05$). December 2019 recorded maximum salinity (34.03 ± 0.13) associated with relatively colder waters ($30.29 \pm 0.38^\circ\text{C}$), while in March 2020, the salinity reached a minimum of 12.00 ± 5.18 and was associated with warmer waters ($32.39 \pm 0.50^\circ\text{C}$) (Table 3), coinciding with the period of higher river discharge from the drainage basin.

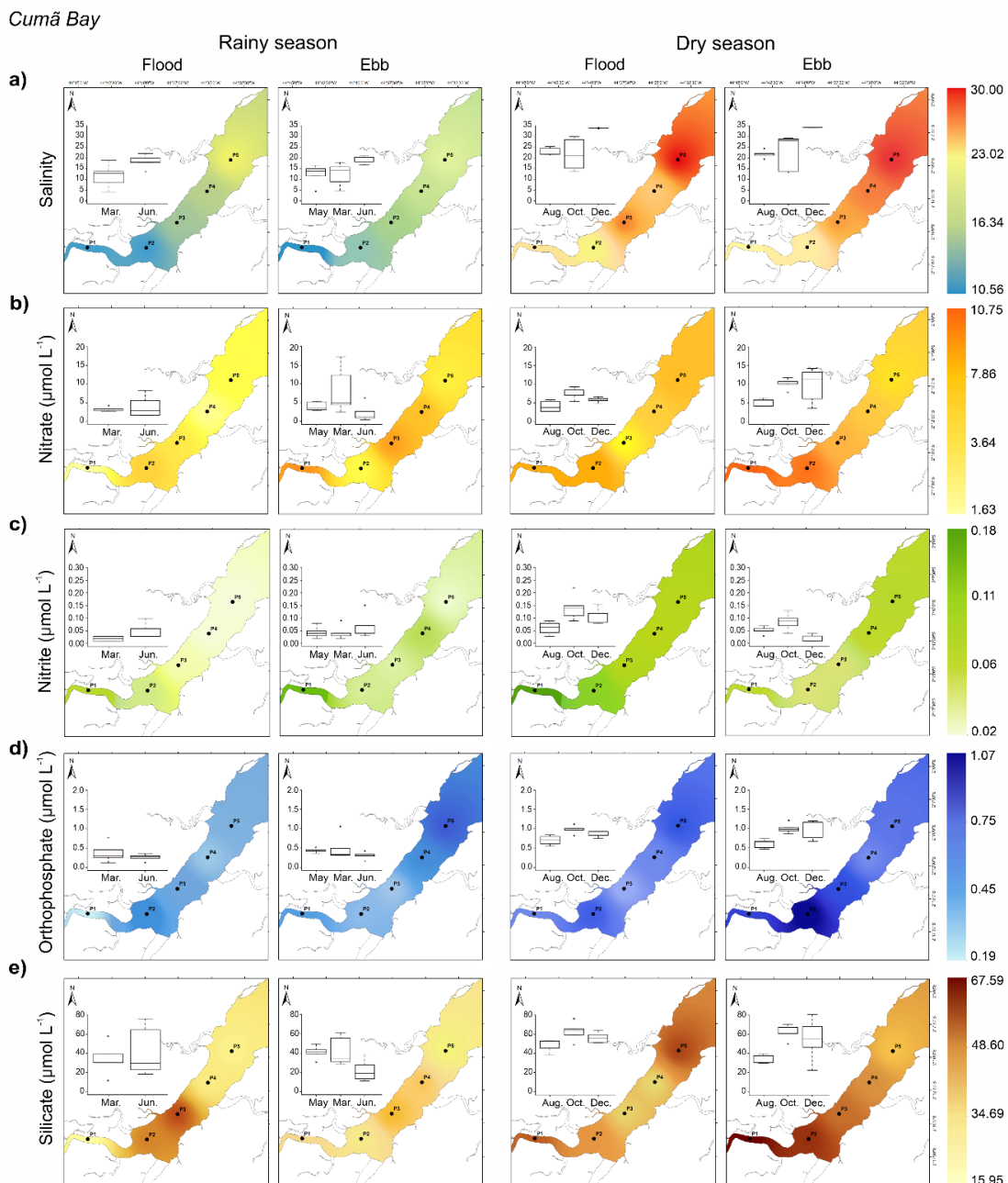
These seasonal dynamics influenced the pH and DO values, with a minor increase in the dry season, mainly in December, with a maximum of 7.46 ± 0.13 and $5.47 \pm 0.62 \text{ mg L}^{-1}$, respectively. SPM recorded concentrations $< 45 \text{ mg L}^{-1}$ in the rainy season, while more turbid waters ($\text{SPM} > 100 \text{ mg L}^{-1}$) were observed in the dry season, especially in December 2019, reaching averages of $208.46 \pm 129.49 \text{ mg L}^{-1}$ (Table 3).

Analyses of dissolved inorganic nutrients revealed that silicate was the most abundant nutrient in the bay, followed by nitrate, orthophosphate, and nitrite, which varied significantly over the months ($p < 0.01$) and seasonal periods ($p < 0.01$) (Fig. 3b–e). The highest nutrient concentrations (NO_3^- , NO_2^- , PO_4^{3-} , SiO_2^-) were recorded in October 2019, when the strongest winds occurred, whereas the minimum values occurred between March and June 2020 (Table 3).

The water nutrient ratios in Cumă Bay are compared in Fig. 6a-b. From the Redfield ratio data ($\text{DIN:DIP:DSi} = 16:1:16$), three areas were delimited, each characterized by a potentially limiting nutrient. The DIN:DSi ratios (overall mean 0.14 ± 0.07) were lower than 1 in 100% of the cases. The DSi:DIP ratios (overall mean 76.94 ± 41.45) were higher than 16 throughout the entire period of the study (100% of the samples), indicating that silicate was not a limiting factor. The DIN:DIP ratios were lower than 16 at most sampling sites in both the rainy (13.04 ± 13.28 ; 83% < 16) and dry (8.50 ± 1.93 ; 100% < 16) seasons, revealing that the bay was predominantly nitrogen-limited.

For the tidal regime, the highest averages of salinity (21.97 ± 8.32), temperature ($31.71 \pm 1.18^\circ\text{C}$), DO ($3.94 \pm 1.31 \text{ mg L}^{-1}$), pH (7.23 ± 0.31), nitrate ($6.90 \pm 4.50 \mu\text{mol L}^{-1}$) and orthophosphate ($0.69 \pm 0.34 \mu\text{mol L}^{-1}$) were recorded during the ebb tide. The SPM ($103.95 \pm 96.18 \text{ mg L}^{-1}$), nitrite ($0.08 \pm 0.05 \mu\text{mol L}^{-1}$), and silicate ($42.98 \pm 16.96 \mu\text{mol L}^{-1}$) concentrations were higher during the flood tide. However, between tides, no significant differences were recorded ($p < 0.05$).

Fig. 3. Temporal distribution of salinity (a) and nutrients (b–e) in Cumã Bay. Monthly distribution is indicated through boxplots



Source: The author (2023).

Table 3. Descriptive statistics (mean and standard deviation) of hydrological and biological variables and nutrients in Cumã Bay. Note: Ti: Tides. Temporal included seasonal (Se.) periods (rainy and dry) and months (Mo) (May to December).

Environmental variables	Tides			p	Temporal								p
	Flood	Ebb	Ti.		Rainy	Dry	May/19	Mar./20	Jun./20	Aug./19	Oct./19	Dec./19	Se.
Salinity	21.69±8.68	21.97±8.32	n.s.	15.30±5.19	26.34±7.16	12.42±4.70	12.00±5.18	18.60±2.42	22.40±1.82	22.20±7.51	34.03±0.13	***	***
Temperature (°C)	31.54±1.14	31.71±1.18	n.s.	31.50±1.00	31.72±1.26	31.77±0.27	32.39±0.50	30.61±0.32	32.43±0.19	32.50±1.15	30.29±0.38	n.s.	***
DO (mg L ⁻¹)	3.80±1.31	3.94±1.31	n.s.	3.99±0.84	3.79±1.55	4.52±0.54	4.19±0.90	3.78±0.77	2.84±0.36	3.86±0.20	5.47±0.62	n.s.	***
pH	7.22±0.33	7.23±0.31	n.s.	7.01±0.34	7.38±0.18	7.44±0.15	6.95±0.41	7.07±0.28	7.30±0.24	7.36±0.13	7.46±0.13	***	***
SPM (mg L ⁻¹)	103.95±96.18	83.52±83.93	n.s.	53.55±51.69	121.09±100.39	25.97±12.64	78.805±64.51	28.26±7.57	58.09±15.69	90.42±29.52	208.46±129.49	***	**
NO ₃ ⁻ (µmol L ⁻¹)	5.18±2.70	6.90±4.50	n.s.	4.08±4.17	7.42±2.86	3.96±1.18	5.39±5.14	2.78±2.54	4.88±1.20	9.09±1.55	8.04±3.43	***	***
NO ₂ ⁻ (µmol L ⁻¹)	0.08±0.05	0.06±0.04	n.s.	0.05±0.03	0.08±0.05	0.04±0.02	0.03±0.02	0.06±0.04	0.06±0.02	0.11±0.05	0.06±0.05	**	**
PO ₄ ³⁻ (µmol L ⁻¹)	0.63±0.31	0.69±0.34	n.s.	0.36±0.22	0.87±0.20	0.45±0.06	0.45±0.29	0.28±0.09	0.65±0.12	0.99±0.11	0.93±0.19	***	***
SiO ₂ ⁻ (µmol L ⁻¹)	42.98±16.96	42.43±18.90	n.s.	32.64±18.33	49.64±13.88	40.64±6.80	35.58±16.26	29.71±20.64	37.61±7.11	58.75±9.03	51.34±15.25	**	**
DIN:DIP ratio	9.48±5.32	11.19±11.20	n.s.	13.04±13.28	8.50±1.93	6.89±3.20	16.20±16.95	9.87±7.91	7.65±1.81	9.34±1.86	8.41±1.93	n.s.	n.s.
DIN:DSi ratio	0.13±0.06	0.16±0.08	*	0.13±0.10	0.15±0.03	0.74±0.68	0.16±0.12	0.10±0.07	0.13±0.03	0.16±0.01	0.16±0.04	**	*
DSi:DIP ratio	83.45±51.91	67.69±31.24	n.s.	101.33±57.55	57.53±10.03	41.54±44.53	96.49±55.92	106.18±61.74	57.62±4.92	59.82±11.76	55.16±11.87	**	*
Biological variables	Flood tide	Ebb tide	Ti.	Rainy	Dry	May/19	Mar./20	Jun./20	Aug./19	Oct./19	Dec./19	Se.	Mo.
Total Chl-a (mg m ⁻³)	13.64±9.60	12.08±6.90	n.s.	18.92±8.13	8.66±5.32	13.24±5.83	16.76±8.90	21.07±7.06	11.39±7.90	7.72±3.77	7.12±2.68	***	***
Abundance (x10 ⁵ cels L ⁻¹)	7.71±13.04	11.04±15.60	**	19.40±18.43	2.51±1.33	4.52±1.30	33.43±16.54	5.38±2.59	2.44±1.54	2.41±1.18	2.67±1.40	***	***
Shannon index (bits cell ⁻¹)	2.15±0.90	2.14±0.90	n.s.	1.75±1.15	2.50±0.31	1.73±0.54	0.60±0.50	2.92±0.36	2.54±0.38	2.46±0.30	2.49±0.28	n.s.	***

Source: The author (2023).

Statistically significant values are indicated with asterisks: * p <0.05; ** p <0.01; *** p <0.001; n.s.: non-significant.

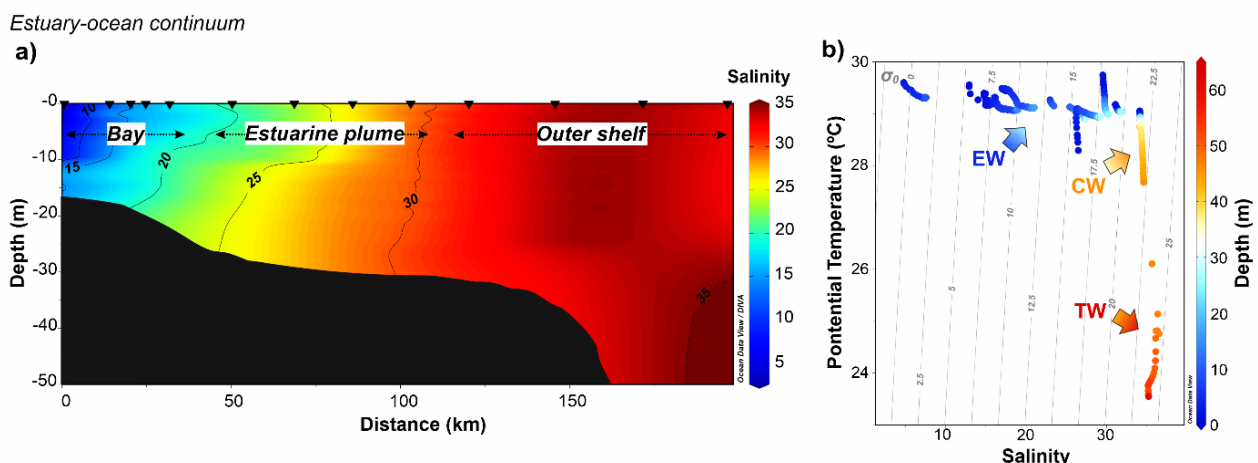
Cross-shelf distribution of hydrological variables and nutrients: estuary-ocean continuum

Vertical distribution of salinity and T-S diagram

The vertical structure of salinity along the estuary-ocean continuum showed typical estuarine waters from the innermost portion of the bay ($4.65 \leq S \leq 21$) to approximately 60 km away from the coastline ($21 \leq S \leq 30$) and marine waters with an increasing salinity gradient ($30.00 \leq S \leq 36.53$) towards the 60 m isobaths near the shelf break (Fig. 4a).

Based on the depth-referenced T-S diagram, the closed triangular structure in the density field of the water column is due to the mixing between three water masses that occupy different depths (Fig. 4b). Warmer water ($28 \leq T \leq 30^{\circ}\text{C}$) and less saline ($S \leq 30$) with densities lower than 20 ($\sigma_t \leq 20$) located in the upper water column, indicated the presence of an estuarine water mass (EW), showing a strong freshwater contribution to an adjacent continental shelf. More saline ($S \geq 35$) and colder ($T \leq 26^{\circ}\text{C}$) waters indicated the possible presence of the tropical water mass (TW) being restricted to isopycnics $22.5 \leq \sigma_t \leq 25$ and depths greater than 50 m. In contrast, the zone between isopycnics $20 \leq \sigma_t \leq 22.5$ shows a transitional zone between the area of the estuarine plume influence and the oceanic region, with typical coastal waters (CW).

Fig. 4. Vertical profile of salinity gradient (a) and depth-referenced T-S diagram (b) from the data collected during the cruise over the estuary-ocean continuum. Located at different water depths, three water masses are identified, the estuarine water (EW) in the upper water column, the coastal water (CW) at mid-depth, and the tropical water (TW) in the lower water column.



Source: The author (2023).

Horizontal distribution of hydrological variables and nutrients

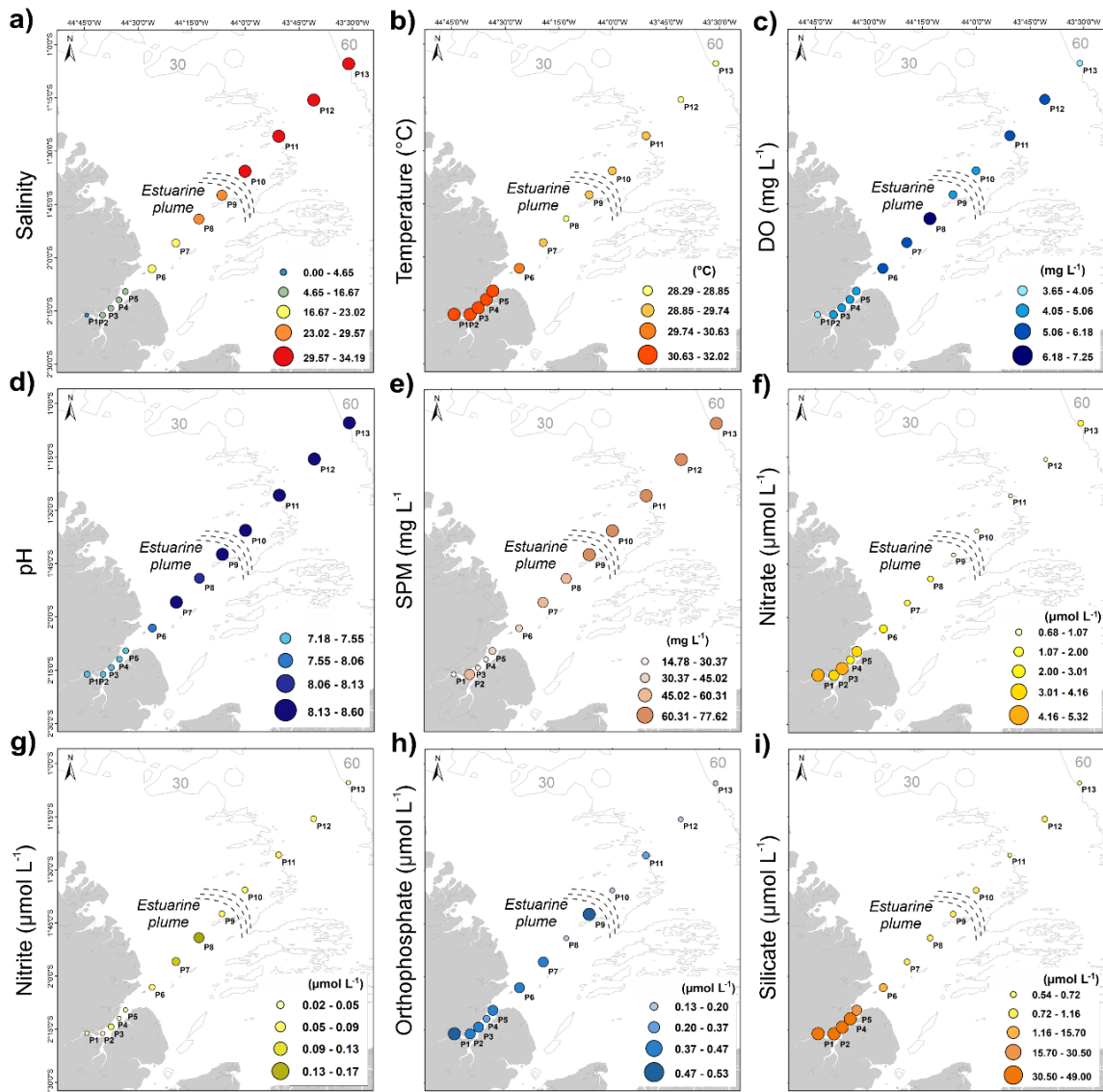
During the period of the highest river discharge in the MCS, significant cross-shelf variability in hydrological conditions was observed (Fig. 5). The pairwise test comparisons (bay *vs.* plume *vs.* outer) indicated higher environmental heterogeneity between the bay and the adjacent continental shelf (plume and outer shelf), revealing physical (salinity, temperature, and SPM) and chemical (pH, nitrate, and silicate) variables as tracers of water plume export (Table 4).

A marked salinity gradient is also observed. Surface salinity varied significantly from 4.65 to 34.19, decreasing towards the bay, and was associated with relatively warmer waters ($31.77 \pm 0.27^\circ\text{C}$) in the inner coastal region and lower temperatures in the outer shelf ($28.96 \pm 0.19^\circ\text{C}$), indicative of a surface estuarine plume (Fig. 4a–b).

Generally, DO concentrations were $> 3.6 \text{ mg L}^{-1}$, with waters slightly more oxygenated in the area of the estuarine plume influence ($5.99 \pm 1.00 \text{ mg L}^{-1}; p > 0.05$) (Fig. 4c). The pH was primarily alkaline (7.18–8.6), with typical seawater values (Fig. 4d). The greater contribution of the estuarine plume during this period promoted an increase in SPM values off the Cumă Bay mouth with values $> 50 \text{ mg L}^{-1}$ (Fig. 4e).

Fig. 5. Spatial distribution of salinity (a), water temperature (b), DO (c), pH (d), SPM (f) and nutrients (f–i) along the estuary-ocean continuum.

Estuary-ocean continuum



Source: The author (2023).

Among the nutrients, only nitrate and silicate showed significant spatial variation between the shelf zones ($p = 0.013$ and $p = 0.010$, respectively).

Among the different forms of dissolved inorganic nitrogen (DIN), nitrate was the predominant form in 100% of the data, with a maximum value recorded in the bay ($5.32 \mu\text{mol L}^{-1}$) and a minimum in the outer region ($0.68 \mu\text{mol L}^{-1}$). The analysis indicated low nitrite concentrations ($< 0.17 \mu\text{mol L}^{-1}$), with the highest value obtained near the estuarine plume boundary (P8). Orthophosphate and silicate exhibited a decreasing gradient from the inner

coast towards the 60 m isobaths, and higher concentrations were recorded in the bay ($0.45 \pm 0.06 \mu\text{mol L}^{-1}$ and $40.64 \pm 6.80 \mu\text{mol L}^{-1}$, respectively) being nearly depleted in the outer shelf (Fig. 4f–i).

DIN concentrations resulted in Redfield DIN:DIP ratios lower than 16 in 100% of the data (overall mean 6.89 ± 3.20) when associated with orthophosphate (DIP). The DSi:DIP ratio showed that Si was a potentially limiting nutrient in 54% of the samples (< 16). The DIN:DSi ratios were lower than 1 in the bay (0.10 ± 0.02) and estuarine plume (0.99 ± 0.62) and higher than 1 in the outer shelf (1.38 ± 0.48), indicating that the inner shelf was primarily nitrogen-limited and the outer shelf was silicate-limited (Fig. 6c).

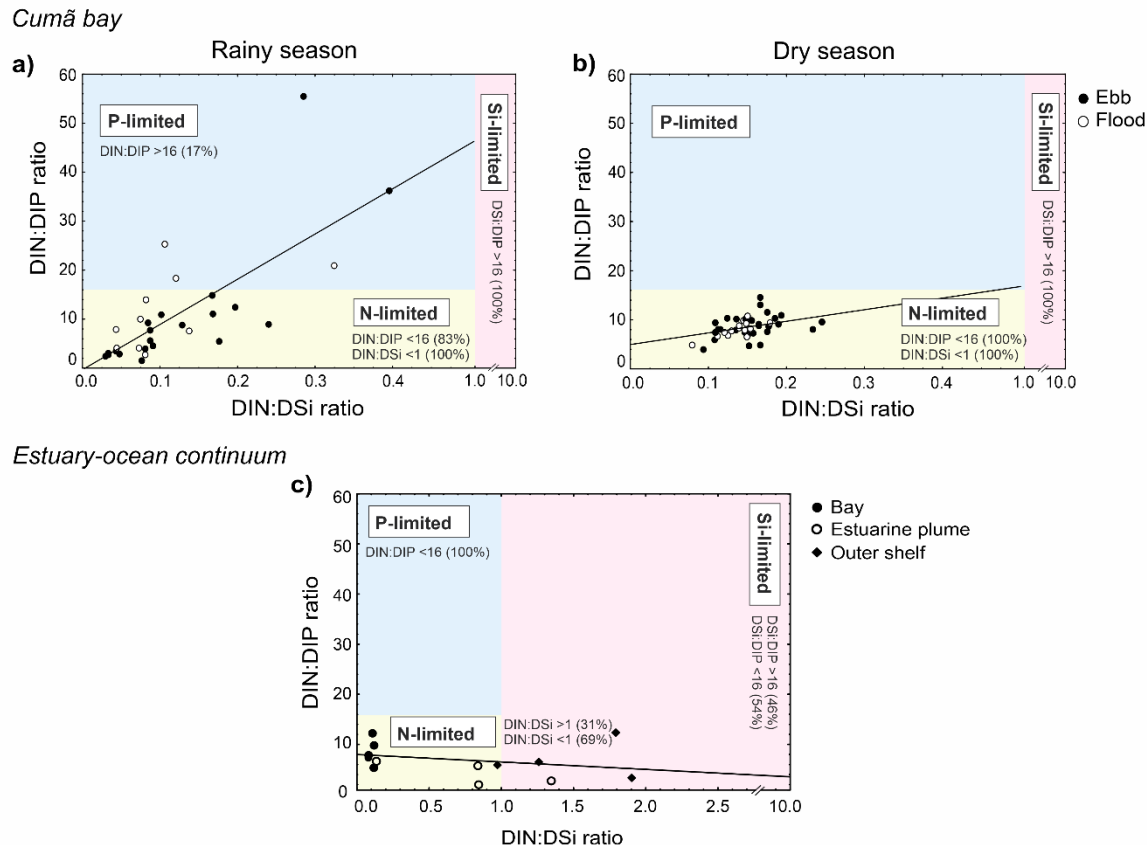
Table 4. Descriptive statistics (mean and standard deviation) and multiple comparisons (pairwise test) of hydrological and biological variables and nutrients along the estuary-ocean continuum.

<i>Hydrological variables</i>	Bay	Plume	Outer	<i>p</i> value
Salinity	12.42 ± 4.70	24.72 ± 4.20	33.40 ± 1.54	bay vs. plume*** bay vs. outer***
Temperature (°C)	31.77 ± 0.27	29.48 ± 0.98	28.96 ± 0.19	bay vs. plume*** bay vs. outer***
DO (mg L ⁻¹)	4.52 ± 0.54	5.99 ± 1.00	5.08 ± 0.83	n.s.
pH	7.44 ± 0.15	8.34 ± 0.28	8.54 ± 0.04	bay vs. plume*** bay vs. outer***
SPM (mg L ⁻¹)	25.97 ± 12.64	54.59 ± 11.44	69.59 ± 5.41	bay vs. plume** bay vs. outer***
NO ₃ ⁻ (μmol L ⁻¹)	3.96 ± 1.18	1.38 ± 0.51	0.89 ± 0.20	bay vs. plume*** bay vs. outer**
NO ₂ ⁻ (μmol L ⁻¹)	0.04 ± 0.02	0.11 ± 0.05	0.07 ± 0.02	n.s.
PO ₄ ³⁻ (μmol L ⁻¹)	0.45 ± 0.06	0.38 ± 0.17	0.19 ± 0.08	n.s.
SiO ₂ ⁻ (μmol L ⁻¹)	40.64 ± 6.80	4.67 ± 7.36	0.77 ± 0.17	bay vs. plume*** bay vs. outer***
DIN:DIP ratio	8.88 ± 2.22	5.92 ± 4.64	5.38 ± 1.36	n.s.
DIN:DSi ratio	0.10 ± 0.02	0.99 ± 0.62	1.38 ± 0.48	bay vs. plume* bay vs. outer**
DSi:DIP ratio	91.89 ± 18.65	15.20 ± 22.96	4.95 ± 2.21	bay vs. plume*** bay vs. outer***
<i>Biological variables</i>	Bay	Plume	Outer	<i>p</i> value
Total Chl-a (mg m ⁻³)	13.24 ± 5.83	21.44 ± 12.42	5.42 ± 7.26	plume vs. outer*
Abundance (x10 ⁵ cells L ⁻¹)	4.52 ± 1.30	2.71 ± 1.93	0.55 ± 0.64	bay vs. outer**
Shannon index (bits cell ⁻¹)	1.74 ± 0.54	2.29 ± 0.21	1.08 ± 0.55	plume vs. outer**

Source: The author (2023).

Statistically significant values are indicated with asterisks: * $p < 0.05$; ** $p < 0.01$; *** $p < 0.001$; n.s.: non-significant.

Fig. 6. Redfield ratios (DIN:DIP:DSi) in Cumã Bay (a-b) and along the estuary-ocean continuum (c). The potentially limiting nutrients are indicated in the three areas delimited by the Redfield ratio (P-limited: blue; N-limited: yellow; Si-limited: pink). (For interpretation of the references to colour in this figure legend, the reader is referred to the web version of this article.)



Source: The author (2023).

Distribution patterns of phytoplankton composition, abundance and biomass

A total of 189 phytoplankton taxa were identified in the MCS, distributed predominantly among Bacillariophyta (80.42%), Miozoa (13.23%), and Cyanobacteria (3.70%), while the other taxonomic groups contributed 2.65% to Euglenozoa, Ochrophyta, Chlorophyta, and Charophyta. Phytoplankton community diversity was notably spatiotemporally dominated by diatoms (152 taxa), with relative abundances ranging from 80.9 to 98.6% (Fig. 7 a,c). Dinoflagellates had the second highest contribution (25 taxa), with a relative density between 1.2 and 4.92%.

Phytoplankton abundance and biomass showed well-defined distribution patterns, exhibiting temporal (abundance $p < 0.001$; chlorophyll-a $p < 0.001$), spatial (abundance $p < 0.01$; chlorophyll-a $p < 0.05$), and tidal (abundance $p < 0.01$) heterogeneity (Fig. 7). The

results of pairwise tests confirmed significant spatial differences among the three zones (Table 4).

At the bay, the total abundance varied between $2.51 \pm 1.33 \times 10^5$ and $19.40 \pm 18.43 \times 10^5$ cells L⁻¹ in the dry and rainy periods, respectively, with higher values in the rainy season during the ebb tide (Fig. 7a). According to phytoplankton abundance and occurrence frequency, six diatoms were considered the dominant species in Cumā Bay. More details on species dominance are available in Supplementary Material (Fig. S1).

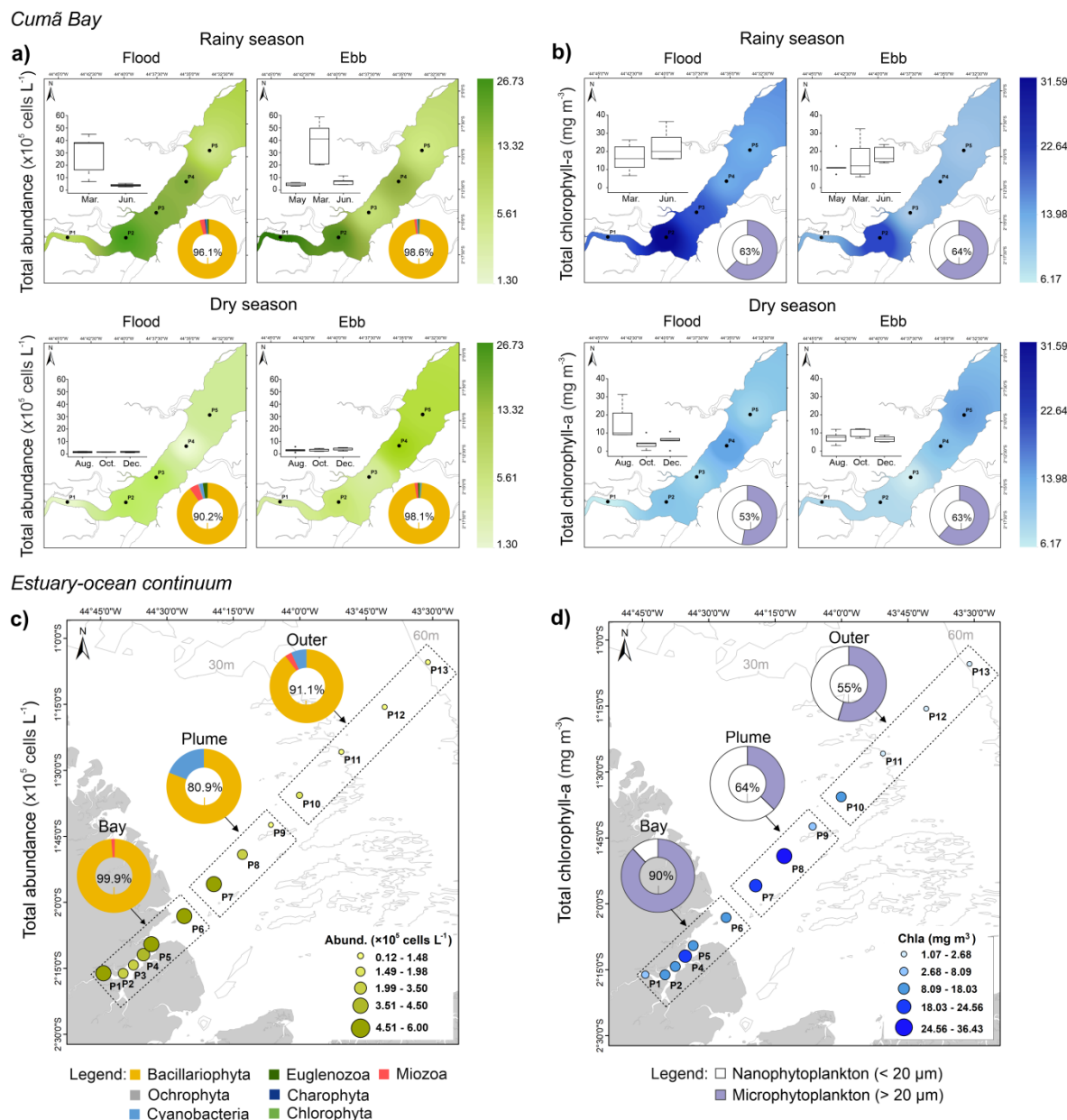
Fluctuations in the diatom domain were observed during the annual cycle (Fig. S1a). *Skeletonema costatum* blooms (305.64×10^5 cells L⁻¹), and a high abundance of *Thalassiosira gravida* (13.26×10^5 cells L⁻¹) were recorded in March 2020, which were the principal species responsible for the significant increase in abundance in the rainy season but dominance of a pennate diatom (*Thalassionema nitzschiooides*) was also identified in June 2020. The abundance of *Thalassiosira subtilis* increased during the dry season, peaking in December 2019 (6.52×10^5 cells L⁻¹). In addition, *Cyclotella litoralis* and *Cymatosira lorenziana* were dominant in August and December 2019, respectively.

At the estuary-ocean continuum, the cell abundance was mainly governed by the salinity gradient along the MCS with a significant decrease from the inner coastal region ($4.52 \pm 1.30 \times 10^5$ cells L⁻¹) towards the shelf break ($0.55 \pm 0.64 \times 10^5$ cells L⁻¹) following the water plume (Fig. 7c). The pairwise tests revealed dissimilarities between the bay and outer shelf ($p < 0.01$; Table 4). Six diatoms were considered the dominant species of the estuary-ocean continuum. The centric diatoms *Thalassiosira gravida* (11.69×10^5 cells L⁻¹) and *Cyclotella litoralis* (2.17×10^5 cells L⁻¹) were the most abundant species in the bay, decreasing gradually with distance from the coast. Variation in the abundance of *Skeletonema costatum* was observed among the three zones (bay: 1.71×10^5 cells L⁻¹; plume: 1.54×10^5 cells L⁻¹; outer: 0.58×10^5 cells L⁻¹) reaching up to 100 km (P11) from the coastline. The region over the plume influence was marked by the dominance of the diatoms *Leptocylindrus danicus* (1.32×10^5 cells L⁻¹) and *Pseudo-nitzschia pungens* (1.11×10^5 cells L⁻¹). *Thalassiosira oceanica* was present in the water plume (1.11×10^5 cells L⁻¹) and the outer shelf (0.06×10^5 cells L⁻¹). For more information, see Fig. S1b.

Shannon's diversity (α -diversity) of the phytoplankton community was marginally lower in the rainy season (1.75 ± 1.15 bits cell⁻¹) than in the dry season (2.50 ± 0.31 bits cell⁻¹), with a significant decrease in March 2020 (0.59 ± 0.50 bits cell⁻¹), indicating a potential ecological disturbance due to the diatom blooms. However, a high α -diversity was recorded

in June 2020 (2.92 ± 0.36 bits cell $^{-1}$). The spatial diversity had an overall average of 1.71 ± 0.66 bits cell $^{-1}$ and ranged between 0.59 (bay) and 2.53 bits cell $^{-1}$ (outer region), following the decreasing gradient from the inner coastal region to the outer shelf (Tables 2 and 3).

Fig. 7. Spatiotemporal distribution of phytoplankton abundance (a-b) and chlorophyll-a (c-d) in the MCS. Note: The pizza graphs attached to the abundance profiles represent the phytoplankton groups and those attached to the chlorophyll-a profiles represent the chlorophyll-a fractions.



Source: The author (2023).

Comparing the phytoplankton biomass (chlorophyll-a) with its composition, it can be noted that the temporal variability of total chlorophyll-a followed the abundance trend with peaks in the rainy season, mainly in June/20 ($21.07 \pm 7.06 \text{ mg m}^{-3}$), and a minimum value during the dry season (Fig. 7b). The distribution of chlorophyll-a along the cross-shelf transect followed the estuarine plume. The highest concentrations ($> 35 \text{ mg m}^{-3}$) were observed near the plume boundary (P8) ~ 40 km from the coastline, decreasing towards the 60 m isobath with a minimum of 1.08 mg m^{-3} (Fig. 7d). The pairwise test confirmed this spatial heterogeneity with significant differences ($p < 0.05$) between the plume and outer shelf (Table 3).

Regarding the contributions of the chlorophyll-a fractions, nanophytoplankton was the dominant fraction in 64% of the data across the temporal scale, with an average contribution ranging between 53 and 64% (Fig. 7b). This pattern was also observed across the continental shelf, with nanophytoplankton dominance in the inner coastal region (90%) and outer shelf (55%), except for the estuarine plume, in which microphytoplankton contributed 64% (Fig. 7d).

Phytoplankton community structure

Spatiotemporal changes in the distribution of phytoplankton were detected based on cluster analysis (Fig. 8). This analysis depicted three distinct groups (A, B and C) of phytoplankton assemblages with a dissimilarity level of ~ 3.7 units (Fig. 8a). In addition to phytoplankton assemblages, horizontal profiles were plotted to indicate their localization in the MCS (Fig. 8c).

Data for group A indicated a temporal pattern of phytoplankton assemblages, comprising 45 samples located in the inner coastal region, which where divided into five subgroups (A1, A2, A3, A4, and A5). Subgroup A1 included only samples from December 2019, a transitional month with higher salinity (> 34), SPM ($> 200 \text{ mg L}^{-1}$), and nutrient concentrations and had an average abundance of $2.67 \pm 1.40 \times 10^5 \text{ cells L}^{-1}$ and chlorophyll-a of $7.12 \pm 2.68 \text{ mg m}^{-3}$. Subgroups A2 and A4 were represented by samples from August and October 2019, when the wind reached the maximum speed, and the main tributary of the bay had the minimum freshwater discharge ($< 26 \text{ m}^3 \text{ s}^{-1}$), resulting in salinity values < 24 and high nutrient concentrations. The average abundance ($2.2 \pm 0.86 \times 10^5 \text{ cells L}^{-1}$) was relatively lower than that in the other groups, and chlorophyll-a was $9.53 \pm 6.39 \text{ mg m}^{-3}$. Subgroup A3 was formed mostly by samples from June 2020, showing a salinity < 19 and the lowest nutrient concentrations (nitrate, orthophosphate, and silicate). Abundance recorded an

average of $5.51 \pm 2.49 \times 10^5$ cells L⁻¹ and chlorophyll-a of 19.84 ± 7.86 mg m⁻³ in subgroup A3.

Subgroups A5 and B consisted of data collected in May 2019, which represented an evident spatial pattern with 13 samples situated across the estuary-ocean continuum. Subgroup A5 clustered only in inner coastal samples with an abundance ($4.10 \pm 1.55 \times 10^5$ cells L⁻¹) roughly double that in group B and chlorophyll-a of 14.04 ± 5.57 mg m⁻³.

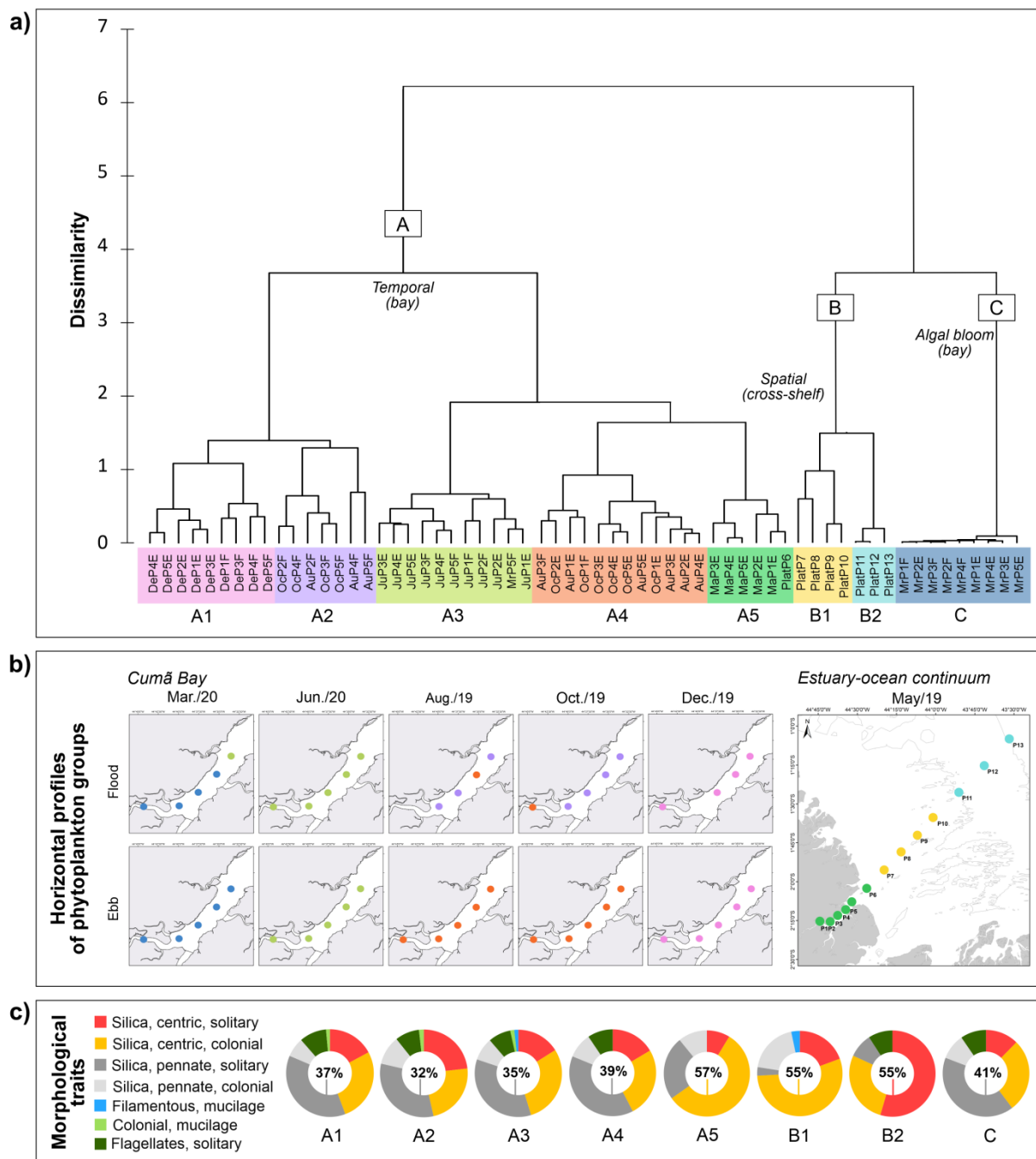
Group B was divided into B1 and B2, where subgroup B1 included samples under estuarine plume influence that showed a considerable peak of chlorophyll-a (20.99 ± 12.62 mg m⁻³) and an average abundance of $2.58 \pm 2.01 \times 10^5$ cells L⁻¹. Subgroup B2 was represented by stations near the shelf break between the 30 and 60 m isobaths and characterized by the lowest chlorophyll-a concentrations (1.80 ± 0.81 mg m⁻³) and abundance ($0.23 \pm 0.14 \times 10^5$ cells L⁻¹) when compared with other groups. The community structure showed a spatial distribution in response to the environmental gradients from Cumă Bay to the shelf break.

The phytoplankton assemblages sampled from March 2020 (nine samples) were classified into group C, which was characterized by the occurrence of potentially harmful algal blooms (HAB) and consequently had the highest cell abundance ($36.39 \pm 14.47 \times 10^5$ cells L⁻¹) and elevated chlorophyll-a concentrations (17.80 ± 8.78 mg m⁻³). The hydrological conditions of March 2020 were marked by the maximum river discharge (> 280 m³ s⁻¹) of the drainage basin, and salinity was < 11.

According to phytoplankton morphological traits, certain common dominant categories were identified across the temporal scale (Fig. 6b). For groups A1, A2, A3, A4, and C, most species had siliceous exoskeletons (diatoms) classified as solitary pennates with contributions ranging between 32 and 41%. Colonial centric species were the second most representative category, accounting for up to 31%. Along the estuary-ocean continuum, colonial centric diatoms dominated A5 (57%) and B1 (55%), and overlap of traits was observed in B2, with a predominance of solitary centric diatoms (55%) (Fig. 8c).

Phytoflagellates (dinoflagellates, euglenophytes, and ochrophytes) showed a solitary cell organization with a contribution of approximately 10%, with a wide occurrence throughout the groups, except in A5 and B1. Filamentous organisms with mucilage were recorded exclusively in A3 and B1, whereas mucilaginous colonies were observed in A1, A2, and A3. Both morphological traits comprise Cyanobacteria species and represent < 4% of their contribution.

Fig. 8. Synthesis of phytoplankton associations in Cumã Bay and MCS. Hierarchical clustering dendrogram of the phytoplankton assemblages (a), horizontal profiles of phytoplankton groups defined by cluster analysis (b), and morphological traits for each cluster group (c).



Source: The author (2023).

β -diversity across temporal and spatial scales

We calculated the mean pairwise β -diversity for each group depicted by cluster analysis (temporal and spatial scales). The monthly variations in β -diversity (β_{Sor}) among groups from the inner bay are compared in Fig. 9a. We found an increasing temporal trend along the annual cycle, with high levels of total β -diversity (> 0.41) among dry months (groups A1, A2, and A4) compared with rainy months (< 0.35). Considering the spatial variability, total β -diversity (β_{Sor}) displayed higher values (> 0.95) between the bay (A5) and outer stations (B2) (Fig. 9b).

The β -diversity partitioning patterns of the phytoplankton communities were similar. Turnover (β_{Sim}) was the main factor responsible for the differences in the species composition at both scales. At the temporal scale, species turnover contributed up to 73% of the total β -diversity, leaving 27% to nestedness (β_{Nes}). Between the bay and outer shelf, the turnover values reached 0.93, with considerably higher contributions ($> 90\%$), while the nestedness indices were always below 0.30. In general, consistently high between-station β -diversity was observed in the estuary-ocean continuum. In contrast, inter-month β -diversity in the bay was relatively low, even with an increasing temporal trend, suggesting a likely homogenization of the phytoplankton community.

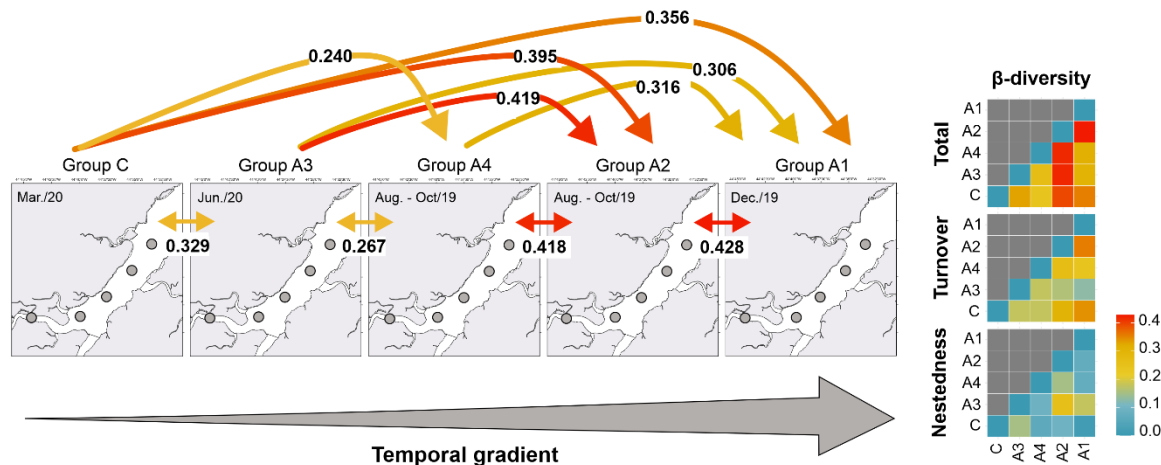
The exclusive and shared phytoplankton species in each group are summarized in Table S1. Temporally, the highest number of exclusive species (20.23%) was found in group A3 (June/20) compared with the other groups that contributed less than 4%, and 5.78% were shared with A4 (August–October/19). Group A2 (August–October/19) presented the lowest number of species shared with C (March/20; 1.16%) and A1 (December/19; 1.73%). No species were recorded sharing groups between A1 and C or A1 and A4. In addition, 27.43% of the species were exclusive to the rainy season and represented primarily by diatoms (20.57%). However, more than 50% shared both seasonal periods.

Among the identified species in the estuary-ocean continuum, 43.08% were found exclusively in group A5 (bay), and 24.62% were shared with B1 (estuarine plume). The bay shared only 1.54% of species with the outer shelf (B2). The estuarine plume presented 13.85% of exclusive species, including a filamentous cyanobacteria (*T. erythraeum*) and centric and pennate diatoms (*Dactyliosolen mediterraneus colonial*, *Hemiaulus hauckii*, *Neocalyprella robusta*, *Pseudo-nitzschia delicatissima*), which were considered plume tracers. The outer region comprised 4.62% of exclusive taxa, which included thecate dinoflagellates such as *Pyrophacus steinii* and *Protoperidinium* sp. Meanwhile, 6.15% of the taxa shared both groups

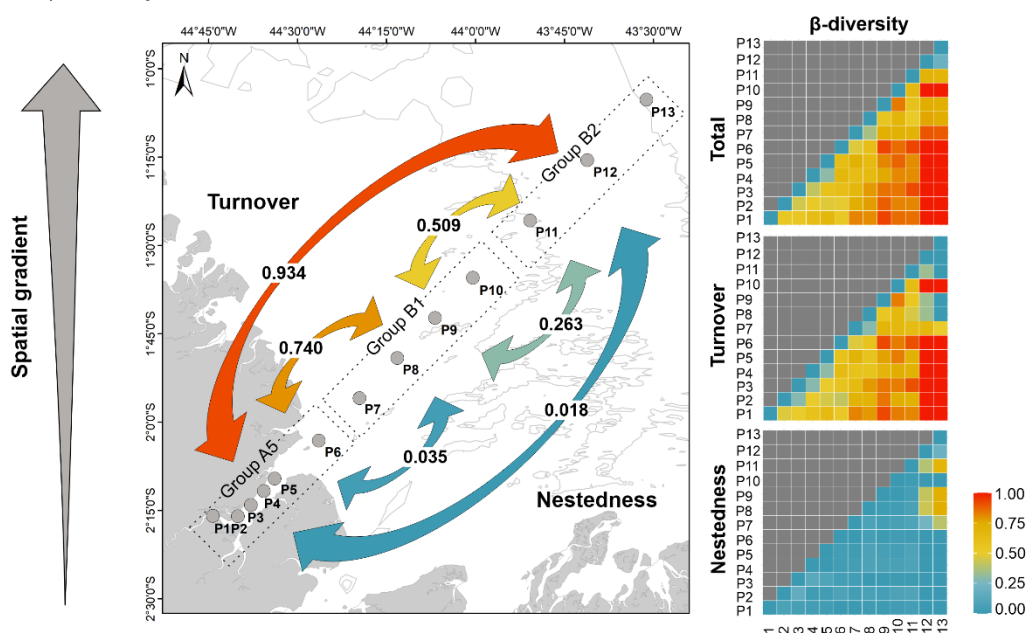
(A5, B1, and B2), characterized by centric diatoms (*Ditylum brightwellii*, *Trieves regia*, *S. costatum*, *Thalassiosira eccentrica*).

Fig. 9. Taxonomic β -diversity (β_{Sor}) partitioned into turnover (β_{Sim}) and nestedness (β_{Nes}) components considering the temporal scale in Cumã Bay (a) and spatial scale in the estuary-ocean continuum (b) for phytoplankton community. β -diversity heatmap comparing the groups depicted in the cluster analysis. Numbers under the arches on the temporal scale indicate total β -diversity. Upper and bottom arrowheads in spatial scale represent turnover and nestedness, respectively.

a) Temporal β -diversity



b) Spatial β -diversity



Source: The author (2023).

Ecological indicators and functional traits

Of the 139 species used to characterize the phytoplankton assemblages by cluster analysis, 39 taxa were selected as key indicators from the indicator value (IndVal) (IndVal > 25% at significance 0.05; Table 5). Due to their high cell abundance and specific occurrence, these taxa could best represent the spatial-temporal patterns of the phytoplankton community structure.

The phytoplankton indicator of group A1 was represented mostly by marine colonial diatoms (siliceous exoskeletons) and one freshwater euglenophyte (flagellate), both with relatively small maximum linear dimensions (MLD < 40 µm). The diatoms *Thalassiosira* sp3 (IndVal 57.82%; $p = 0.006$) and *Diploneis weissflogii* (IndVal 49.56%; $p = 0.001$) were selected as the main group indicators. Group A2 featured solitary diatoms, such as *Thalassiosira pacifica* (IndVal 42.86%; $p = 0.013$) and *Ulnaria ulna* (IndVal 36.95; $p = 0.012$), and visible variability in cell size (MLD: 17.5–225 µm).

Group A3 had a dominance of colonial centric diatoms and few flagellates with an average MLD of 81.7 ± 62.8 µm. The two highest IndVal values were associated with *Coscinodiscus granii* (IndVal 54.55%; $p = 0.003$) and *Thalassionema frauenfeldii* (IndVal 43.92; $p = 0.007$). The thecate dinoflagellates *Dinophysis norvegica* and *Tripos lineatus* also had high IndVal values (> 30%; $p < 0.05$). For group A4, only two colonial centric diatoms were selected with significant IndVal (> 34%; $p < 0.01$): the larger-celled diatom *Trieres chinensis* (MLD > 120 µm) and *Thalassiosira weissflogii* (MLD: 15 µm).

Along the estuary-ocean continuum, some differences were visible in the main traits of the indicators. Small diatoms dominated group A5, except for freshwater *Gyrosigma attenuatum* with MLD > 300 µm. The two highest IndVal taxa were *Thalassiosira gravida* (IndVal 46.7%; $p = 0.003$) and *Cylindrotheca closterium* (IndVal 45.51%; $p = 0.006$). Group B1 was formed by larger organisms (MLD: 85–505 µm), mostly colonial diatoms, such as *Proboscia alata* (IndVal 69.83%; $p = 0.001$), and one filamentous with mucilage (MLD > 250 µm), the cyanobacteria *Trichodesmium erythraeum* (IndVal 50.0%; $p = 0.004$). In group B2, the species decreased in size (MLD < 25 µm) and were dominated by solitary centric diatoms *Thalassiosira minuscula* (IndVal 52.79%; $p = 0.006$) and *Thalassiosira oceanica* (IndVal 44.34%; $p = 0.007$).

Group C was characterized by the dominance of the potentially harmful and bloom-forming diatom *S. costatum* (IndVal: 92.57%; $p = 0.001$), which was considered the best phytoplankton indicator. In addition to *S. costatum*, eight potential HAB species were

reported for the first time in Cumã Bay and MCS, including *D. norvegica*, *L. minimus*, *T. weissflogii*, *C. closterium*, *C. socialis*, *T. erythraeum*, *P. pungens*, and *T. minuscula*.

Based on ecological preferences, 79.49% of the indicators were marine species, whereas 20.51% comprised freshwater species (10.26%) and non-identified taxa ecology (10.26%).

Table 5. Indicator values (IndVal), phytoplankton abundance, functional traits, ecology and occurrence of phytoplankton species in the MCS.

Continue

Indicator species	Indv al (%)	p (MC)	Taxonomic group	APA (cell L ⁻¹)	PTA (%)	Morphological traits categories	MLD (μm)	Ecology	Occurrence
Group A1									
<i>Thalassiosira</i> sp ₃	57.82	0.006	Bacillariophyta	2,604	0.35	Silica, centric, colonial	27.5	--	Coast
<i>Diploneis weissflogii</i> (A.W.F.Schmidt) Cleve 1894	49.56	0.001	Bacillariophyta	2,959	0.4	Silica, pennate, solitary	52.4	Marine	Coast
<i>Nitzschia</i> sp.	43.42	0.012	Bacillariophyta	1,933	0.26	Silica, pennate, solitary	42.5	--	Coast
<i>Trachelomonas volvocina</i> (Ehrenberg) Ehrenberg 1834	34.64	0.034	Euglenozoa	1,381	0.19	Flagellate, solitary	31.0	Freshwater	Coast
<i>Thalassiosira subtilis</i> (Ostenfeld) Gran 1900	32.29	0.021	Bacillariophyta	34,245	4.67	Silica, centric, colonial	52.5	Marine	Coast
<i>Cymatosira lorenziana</i> Grunow 1862	30.21	0.046	Bacillariophyta	8,443	1.15	Silica, pennate, colonial	10.0	Marine	Coast
<i>Paralia sulcata</i> (Ehrenberg) Cleve 1873	27.66	0.039	Bacillariophyta	5,957	0.81	Silica, centric, colonial	45.3	Marine	Coast
Group A2									
<i>Thalassiosira pacifica</i> Gran & Angst 1931	42.86	0.013	Bacillariophyta	197	0.03	Silica, centric, solitary	17.5	Marine	Coast
<i>Ulnaria ulna</i> (Nitzsch) Compère 2001	36.95	0.012	Bacillariophyta	1,420	0.19	Silica, pennate, solitary	225.0	Freshwater	Coast
<i>Thalassiosira leptopus</i> (Grunow) Hasle & G.Fryxell 1977	26.25	0.049	Bacillariophyta	1,341	0.18	Silica, centric, solitary	60.0	Marine	Coast
Group A3									
<i>Coscinodiscus granii</i> L.F.Gough 1905	54.55	0.003	Bacillariophyta	513	0.07	Silica, centric, solitary	177.5	Marine	Coast
<i>Thalassionema frauenfeldii</i> (Grunow) Tempère & Peragallo 1910	43.92	0.007	Bacillariophyta	6,139	0.84	Silica, pennate, colonial	112.5	Marine	Coast/Plume
<i>Thalassionema nitzschiooides</i> (Grunow) Mereschkowsky 1902	43.68	0.006	Bacillariophyta	6,920	0.94	Silica, pennate, colonial	75.0	Marine	Coast/Plume
<i>Dinophysis norvegica</i> Claparède & Lachmann 1859	41.55	0.015	Miozoa	1,144	0.16	Flagellate, solitary, thecate*	37.5	Marine	Coast
<i>Cyclotella stylorum</i> Brightwell 1860	39.41	0.023	Bacillariophyta	2,722	0.37	Silica, centric, colonial	22.5	Marine	Coast
<i>Cyclotella</i> sp.	35.96	0.011	Bacillariophyta	4,300	0.59	Silica, centric, colonial	17.5	--	Coast
<i>Leptocylindrus minimus</i> Gran 1915	33.63	0.014	Bacillariophyta	6,155	0.84	Silica, centric, colonial*	15.0	Marine	Coast/Plume
<i>Odontella aurita</i> (Lyngbye) C.Agardh 1832	31.5	0.047	Bacillariophyta	5,760	0.78	Silica, centric, colonial	40.2	Marine	Coast
<i>Trieres regia</i> (M.Schultze) Ashworth & E.C.Theriot 2013	31.46	0.046	Bacillariophyta	10,644	1.45	Silica, centric, colonial	150.0	Marine	Coast/Plume
<i>Tripos lineatus</i> (Ehrenberg) F.Gómez 2021	30.39	0.041	Miozoa	355	0.05	Flagellate, solitary, thecate	165.2	Marine	Coast

										Conclusion
	<i>Trybliptychus cocconeiformis</i> (Grunow) Hendey 1958	30.26	0.036	Bacillariophyta	3,235	0.44	Silica, centric, solitary	30.0	Marine	Coast
	<i>Rhizosolenia hebetata</i> J.W.Bailey 1856	30.21	0.025	Bacillariophyta	552	0.08	Silica, centric, solitary	137.5	Marine	Coast
Group A4										
	<i>Trieres chinensis</i> (Greville) Ashworth & E.C.Theriot 2013	57.44	0.001	Bacillariophyta	5,121	0.7	Silica, centric, colonial	122.5	Marine	Coast
	<i>Thalassiosira weissflogii</i> (Grunow) G.A.Fryxell & Hasle 1977	34.8	0.017	Bacillariophyta	6,155	0.84	Silica, centric, colonial*	15.0	Marine	Coast
Group A5										
	<i>Thalassiosira gravida</i> Cleve 1896	46.7	0.003	Bacillariophyta	58,706	8	Silica, centric, colonial	5.0	Marine	Coast/Plume
	<i>Cylindrotheca closterium</i> (Ehrenberg) Reimann & J.C.Lewin 1964	45.51	0.006	Bacillariophyta	1,144	0.16	Silica, pennate, solitary*	36.0	Marine	Coast
	<i>Chaetoceros socialis</i> H.S.Lauder 1864	35.76	0.04	Bacillariophyta	3,709	0.51	Silica, centric, colonial*	7.5	Marine	Coast
	<i>Actinptychus</i> sp.	35.07	0.027	Bacillariophyta	671	0.09	Silica, centric, solitary	22.5	--	Coast
	<i>Gyrosigma attenuatum</i> (Kützing) Rabenhorst 1853	26.19	0.034	Bacillariophyta	118	0.02	Silica, pennate, solitary	350.0	Freshwater	Coast
Group B1										
Plume	<i>Proboscia alata</i> (Brightwell) Sundström 1986	69.83	0.001	Bacillariophyta	150	0.02	Silica, centric, colonial	505.0	Marine	Plume
	<i>Trichodesmium erythraeum</i> Ehrenberg ex Gomont 1892	50	0.004	Cyanobacteria	1,373	0.19	Filamentous, mucilage*	275.0	Marine	Plume
	<i>Leptocylindrus danicus</i> Cleve 1889	44.06	0.01	Bacillariophyta	2,801	0.38	Silica, centric, colonial	85.0	Marine	Plume
	<i>Pseudo-nitzschia pungens</i> (Grunow ex Cleve) Hasle 1993	42.91	0.01	Bacillariophyta	5,579	0.76	Silica, pennate, colonial*	100.0	Marine	Coast/Plume
	<i>Pseudosolenia calcar-avis</i> (Schultze) B.G.Sundström 1986	40.91	0.014	Bacillariophyta	197	0.03	Silica, centric, colonial	425.0	Marine	Plume
Group B2										
Outer	<i>Thalassiosira minuscula</i> Krasske 1941	52.79	0.006	Bacillariophyta	450	0.06	Silica, centric, solitary*	24.5	Marine	Plume/Offshore
	<i>Thalassiosira oceanica</i> Hasle 1983	44.34	0.007	Bacillariophyta	2,004	0.27	Silica, centric, solitary	12.5	Marine	Plume/ Offshore
Group C										
Bay	<i>Skeletonema costatum</i> (Greville) Cleve 1873	92.57	0.001	Bacillariophyta	535,808	73	Silica, centric, colonial*	7.5	Marine	Coast/Plume
	<i>Cocconeis placentula</i> Ehrenberg 1838	32.13	0.034	Bacillariophyta	829	0.11	Silica, pennate, solitary	22.5	Freshwater	Coast
	<i>Gyrosigma balticum</i> (Ehrenberg) Rabenhorst 1853	30.37	0.035	Bacillariophyta	316	0.04	Silica, pennate, solitary	300.0	Marine	Coast

Source: The author (2023).

Note: Monte Carlo permutation test (MC), average phytoplankton abundance (APA), and percentage of total abundance (PTA%). Potential harmful species first time reported in this area are indicated with an asterisk (*) and non-identified taxa ecology with double hyphen (--).

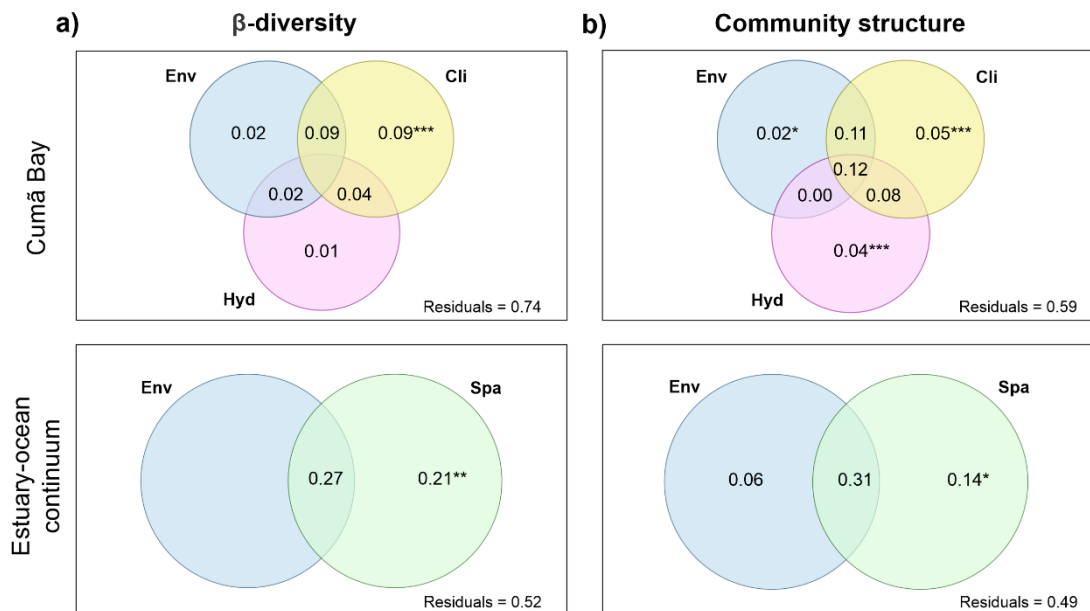
Relative contributions of factors in shaping phytoplankton β -diversity and community structure

According to the variation partitioning analysis performed for phytoplankton β -diversity, both climatic and spatial processes and environmental variability were important. However, their contributions varied between scales (Fig. 10a). In Cumă Bay, the climatic factor accounted for most of the variation (9%; adj. $R^2 = 0.09$, $p < 0.001$) in β -diversity, and the environmental (adj. $R^2 = 0.02$, $p > 0.05$) and hydrodynamic (adj. $R^2 = 0.01$, $p > 0.05$) variables contributed less than 3%. In the estuary-ocean continuum, the unique effect of spatial factors was dominant, which explained 21% (adj. $R^2 = 0.21$, $p < 0.001$) of the variation in β -diversity, whereas the unique effect of environmental variables was negligible. Moreover, the joint effects of the spatial and environmental variables explained an additional 27% of the variance.

Similarly, the results of the variation partitioning analysis performed for the phytoplankton community structure indicated a significant influence of climatic and spatial processes, in addition to hydrodynamic factors (Fig. 10b). Considering the scales separately, climatic (adj. $R^2 = 0.05$, $p < 0.001$) and hydrodynamic (adj. $R^2 = 0.04$, $p < 0.001$) factors were the main contributors, accounting for 9% of the variability in Cumă Bay. In comparison, unique spatial components are more important than environmental effects in the estuary-ocean continuum. Spatial variables independently accounted for 14% (adj. $R^2 = 0.14$, $p < 0.05$) of the variation in community structure, while the environment independently accounted for 6% (adj. $R^2 = 0.06$, $p < 0.05$). Additionally, the shared fraction between the environmental and spatial factors was substantially higher (31%) than that of the pure components.

For the environmental predictor variable group, six variables were selected by a forward selection procedure, including salinity, SPM, DO, and PO_4^{3-} to explain the variation in phytoplankton β -diversity, whereas salinity, SPM, DO, temperature, and SiO_2^- explained the community structure (Table S2). The spatial predictor set includes four AEM eigenvectors (AEM1, AEM2, AEM3, and AEM4). For the hydrodynamic predictor set, river discharge was the variable selected for β -diversity, whereas river discharge and tides (flood and ebb) explained the phytoplankton community structure. The climatic dummy variables are based on precipitation and wind variability during the annual cycle.

Fig. 10. Variation partitioning-based Venn diagrams showing the relative contribution of environmental variables (Env), spatial AEM eigenvectors (Spa), climatic variables (Cli) and local hydrodynamic factors (Hyd) for phytoplankton β -diversity (a) and community structure (b). Values represent the adjusted R^2 values. Negative fraction values are not presented. Statistical significance: * $p < 0.05$; ** $p < 0.01$; *** $p < 0.001$.



Source: The author (2023).

Discussion

The results found in this study improved our understanding of the coast-ocean interface processes responsible for the dynamics of the phytoplankton community and β -diversity on the Amazon continental shelf (eastern sector). We searched for the temporal and spatial patterns of phytoplankton in a tropical macroscale estuary-ocean continuum and assessed the effect of the relative contributions of the environment, space, and weather on shaping phytoplankton communities.

Environmental heterogeneity as a driving effect

The Maranhão continental shelf is located within an equatorial region that contains the wettest zone of the world associated with hydrodynamics, which is also distinct from those established in most other places worldwide. This shelf is characterized as a highly dynamic environment (macrotides > 7 m) and subject to elevated fluvial discharge largely from São Marcos, São José, Cumā bays, and small tributaries, which

are identified as the main regulators of the composition and diversity of plankton communities in the Amazon systems (Araújo et al., 2017; Santana et al., 2020; Otsuka et al., 2022).

The climatological pattern of the region accounted for an annual precipitation of > 2,300 mm, with monthly precipitation rates approximately twenty-fold higher during the rainy season. During the study period (2019–2020), the climatic regime was considered atypical, which can be explained by the La Niña event that caused a considerable increase in rainfall, as reported by Sá et al. (2022a). This unimodal rainfall pattern explains the significant environmental heterogeneity in Cumã Bay. This changed the hydrological conditions of the bay and consequently the adjacent shelf, exporting nutrients along the coast and decreasing salinity, pH, and SPM, which promoted phytoplankton production and algal blooms.

The main meteorological system responsible for Amazon rainfall patterns is the seasonal transposition of the ITCZ (Marengo, 1995). Therefore, the period the highest rainfall occurs when the ITCZ shifts southward (January to June) to the coasts of Maranhão and Pará. Between July and December, the ITCZ shifts to the Northern Hemisphere, resulting in higher air temperatures and lower rainfall rates (Fu et al., 2001; Pereira et al., 2012; Lefèvre et al., 2017). Our results showed this seasonal effect on local heterogeneity, in which higher dispersion of the data was detected during the dry season, and the hydrological variability and phytoplankton diversity decreased during the rainy season.

Elevated precipitation rates and freshwater discharges recorded between March and May appear to be primarily responsible for the lower environmental heterogeneity during the rainy period, particularly with minor variations in salinity, DO, and SPM. According to Brasil et al. (2020), rainfall events are important for re-establishing river networks and short-term hydrological connectivity between adjacent tributaries, which can lead to the homogenization of environmental conditions and communities between sites in aquatic ecosystems. Thus, homogenization and plankton dispersal are facilitated under high river flow conditions induced by rainfall (Chaparro et al., 2019; Rusanov et al., 2022).

In contrast, rainfall scarcity, greater wind speed, and seawater intrusion characterized the dry season and acted synergistically to promote the environmental gradients that drive plankton dynamics. This can be explained by the space-time variability of the western boundary current NBC, which intensifies during the early dry

season (July–August) and renews the Maranhense Gulf waters, pushing a larger seawater volume toward the inner coastal region (Lefèvre et al., 2017). Similar temporal patterns have been reported in other recent studies on Amazon coastal bays (Santos et al., 2020; Lima et al., 2021) and estuaries (Cavalcanti et al., 2020; Sá et al., 2022b), where lower precipitation and freshwater inputs resulted in salinity increases and penetration of seawater into the systems.

In addition, our study revealed a significant effect of spatial extent on environmental heterogeneity, indicating a trend of hydrological parameters with an increase in watercourse distance along the estuary-ocean continuum. This was predictable because the length of the studied cross-shelf transect was 192 km. The relative importance of spatial and environmental variables is directly related to the magnitude and frequency of precipitation to a broader spatial extent, which results in longitudinal changes in phytoplankton in large rivers (Rusanov et al., 2022).

During this period, warmer ($> 28^{\circ}\text{C}$) and less saline ($S \leq 30$) waters from the Maranhense Gulf were widely observed alongshore (Fig. 4), indicating the presence of estuarine water that penetrated the shelf at a distance of approximately 60 km from the coastline.

This behavior reflects the greater continental fluvial outflow over the Amazon shelf, especially during the rainy period, and is in accordance with the findings of Aquino et al. (2022) for the same period. Other authors, such as Carvalho et al. (2016) and Castro et al. (2018), have reported low salinities (< 30) in the inner MCS restricted to the São Marcos Bay mouth. Large-scale climate phenomena, such as El Niño Southern Oscillation (ENSO) events, may affect the annual variation in salinity in coastal ecosystems, particularly on the Amazon coast (Pereira et al., 2013; Sá et al., 2022a, Costa et al., 2022). Ibánhez et al. (2016) noted that a high correlation exists between rainfall and sea surface salinity in the area of plume influence and can affect $>16\%$ of the Amazon River plume region, for example.

Additionally, the high nutrient concentrations found in the innermost coastal region result from the presence of extensive mangroves throughout Cumã Bay and adjacent estuaries (Cavalcanti et al., 2022), which is a typical feature of the Amazon coastal region (Souza-Filho, 2005; Gomes et al., 2021). Moreover, tidal flux in macrotidal systems (Yellen et al., 2017) associated with wind speed may increase the resuspension of previously deposited material (Lancelot and Muylaert, 2011; Dias et al., 2016),

contributing to an increase in water turbidity and nutrient availability in the Amazon region (Goes et al., 2014).

In response to these high local hydrodynamics, we found high spatial heterogeneity, where the bay was characterized as chemically and physically distinct from the plume and outer shelf.

Factors responsible for temporal and spatial phytoplankton distribution

The study area is an ideal ecosystem for studying community ecology because of its location (Amazon shelf) and its importance for conservation (Ramsar site number 640). In this comprehensive study of phytoplankton that considered temporal and spatial scales, we detected 189 phytoplankton species and nine potential HAB species that were reported for the first time in the study area.

High diversity has also been reported in other Amazon macrotidal systems (Cavalcanti et al., 2018; Cavalcanti et al., 2020; Oliveira et al., 2022; Sá et al., 2022b), in the Amazon River plume (Araújo et al., 2017; Otsuka et al., 2022), and large river plumes worldwide (Zhong et al., 2020), thereby reflecting the biological integrity of these regions.

A major taxonomic group in the community was diatoms, which presented notable spatiotemporal dominance over the study period. The three main macrotidal bays bring nutrients to the waters off the Maranhense Gulf (Lefèvre et al., 2017), which, in combination with small estuaries, results in low salinity, high nutrient (mainly silicate), and SPM surface, which favors diatom growth. Both river and submarine groundwater discharge have been recognized as substantial terrestrial nutrient (nitrate and silicate) sources in coastal waters (Lecher et al., 2017) and consequently enhance phytoplankton abundance (Zhong et al., 2020).

The predominance of diatoms is a robust and well-known pattern built from multiyear sampling records across diverse coastal habitats (Carstensen et al., 2015). This diatom success is mostly attributed to their capacity to grow rapidly in turbulent high-nutrient environments (Marañón et al., 2012) associated with their euryhaline adaptation to cope with salinity fluctuations (Mukherjee et al., 2013). Diatoms also play a central role in silica cycling, which is essential for the synthesis of mineralized cell walls (Carstensen et al., 2015; Mayzel et al., 2021). Accordingly, Egge and Aksnes (1992) indicated that phytoplankton might shift from a diatom-dominated to a flagellate-dominated community under $\text{SiO}_2 < 2 \mu\text{M}$ conditions.

Significant temporal and spatial variations were observed in the phytoplankton community (Fig. 5). As the composition of phytoplankton assemblages is strongly associated with water masses (Liu et al., 2004), diluted waters positively influenced phytoplankton growth, as higher cell abundance ($> 19 \times 10^5$ cells L $^{-1}$) and biomass (> 18 mg m $^{-3}$) were observed during the rainy period. In addition, it has been reported that salinity could delineate the phytoplankton distribution in Cumã Bay (Cavalcanti et al., 2022).

The significant increase in abundance was due to small-celled and chain-forming diatom blooms (*S. costatum*) that developed in low-salinity water of the inner Cumã Bay during March 2020, a period when nutrient availability and light intensity were sufficient to support positive net production. The low N:P ratios and high phytoplankton abundance imply nutrient utilization for growth in the presence of increased light availability, depicted by the lower SPM. Similar findings were reported by Rath et al. (2021) in a tropical estuary from the east coast of India and Sá et al. (2022b) in a Brazilian macrotidal estuary.

In turbid and nutrient-rich estuarine systems, peaks in phytoplankton biomass and production often occur when irradiance is high (Gameiro et al., 2011). During the dry period, opposite patterns of phytoplankton abundance and biomass were observed. This might be a response of suspended solid resuspended sediments in the river flows of estuaries that absorb or disperse irradiance or both in the water column and constrain phytoplankton production (Cloern, 1987; Pan et al., 2016), which is particularly intense in macrotidal systems.

For the spatial scale, the marked decrease in cell abundance from the inner bay to the outer shelf followed nutrient gradients, which was consistent with the salinity gradient. The significant effect of spatial processes was statistically confirmed by variation-partitioning analysis. Notably, nutrient concentrations decreased across the estuary-ocean continuum because of dilution or removal, biologically and chemically, during estuarine mixing (Bharathi et al., 2018).

This is per Zhong et al. (2020), who examined the phytoplankton assemblages and the effect of diluted water from the Zhujiang (Pearl) River on them and reported higher diatom abundance (mostly chain-forming species) concentrated in coastal regions as a response to low salinity and high nutrients brought by estuarine plumes. Anglès et al. (2019) also reported this for the Mississippi River plume.

Our analysis also indicated a considerable peak in chlorophyll-a ($> 35 \text{ mg m}^{-3}$) near the plume boundary (P8). At the same station, deficits in orthophosphate ($< 0.14 \mu\text{mol L}^{-1}$) and nitrate ($< 1.43 \mu\text{mol L}^{-1}$) were observed, which may support the absorption by phytoplankton and an increase in chlorophyll-a. Chlorophyll-a was positively correlated with diatom abundance in the MCS (Carvalho et al., 2016). Therefore, fluctuations in chlorophyll-a dominated by microphytoplankton ($> 20\mu\text{m}$) accompanied changes in diatom abundance. High chlorophyll-a concentrations alongshore imply a highly productive region during periods of greater freshwater discharge.

Based on the variation partitioning analysis, the joint effects of the climatic, hydrodynamic, and spatial processes and local environmental heterogeneity governed the phytoplankton dynamics in terms of abundance and chlorophyll-a.

Ecological indicators and functional traits

The phytoplankton diversity in Cumã Bay and the adjacent continental shelf reflect ecological strategies that are compatible with the high hydrodynamics of the region, which is characterized by greater freshwater discharge and macrotidal-forced processes of intense mixing (Czizeweski et al., 2020; Cavalcanti et al., 2022).

Phytoplankton in the estuary-ocean continuum exhibited a series of functional traits that endowed them with some capacity to resist sinking. Thus, the predominance of solitary pennate and colonial centric diatoms (mainly chain-forming) in Cumã Bay, colonial centric diatoms and filamentous cyanobacteria along the estuarine plume, and solitary centric diatoms over the 30 and 60 m isobaths near the shelf break were notable (Fig. 6). Regarding cell size (MLD), larger diatoms and cyanobacteria dominated the estuarine plume (near the coast), and small single-celled centric diatoms dominated the outer shelf.

The dominance of pennate and colonial centric diatoms as an ecological strategy to adapt to the dynamics of coastal systems was also observed previously by studies in Drakes Bay along the United States west coast (Wilson et al., 2020), in the inner shelf of the East China Sea (Abate et al., 2016), and macrotidal (Cavalcanti et al., 2020) and tidal-forced (Aff et al., 2019) estuarine systems of Brazil.

The majority of pennate diatoms are benthic organisms that may enter the water column due to vertical currents (Koh et al., 2006) or resuspension of sediments, or both (Cavalcanti et al., 2018) and live temporarily as plankton, forming tychoplanktonic

diatom communities that are mostly immobile non-attached diatoms living between sediment particles (Zelnik et al., 2018).

Theoretically, under conditions of lower turbulence, larger cells sink faster than smaller cells, whereas greater water turbulence can favor the resuspension of larger cells (Margalef, 1978; Reynolds et al., 2002). For example, chain-forming species can control their chain size as a strategy to adapt to the dynamics of systems, as a longer chain will sink faster than a shorter chain of the same species (Gherardi et al., 2016; Bannon and Campbell, 2017). Variations in the chain size of chain-forming diatoms (e.g., *S. costatum*) were also detected during the different seasonal periods in this study. Chain-forming, which offers a better surface-volume ratio, is an adaptation to optimize the sinking rate to enhance nutrient absorption and rapid growth under turbulent conditions (Smayda, 1983), and is also an effective way to deter grazers (Wang and Tang, 2022).

Of the 39 taxa selected as key indicators, 10 potential HAB species were identified in this study, including eight centric diatoms, one dinoflagellate, and one filamentous cyanobacteria, nine of which were new records for the study area. As the most dominant species in the study, the small-celled chain-forming diatom *Skeletonema costatum* showed a higher abundance inside the bay than alongshore, with a strong preference for rainy months, when it reached a cell abundance of up to 3×10^7 cells L⁻¹.

Skeletonema costatum is a bloom-forming and typical estuarine diatom that gradually takes advantage of community competition in nutrient-enriched low-salinity turbid waters (Gao et al., 2022), such as the adaptable diatom that thrives in coastal waters globally (Carstensen et al., 2015; Liu et al., 2022; Lundsør et al., 2022). Additionally, this species, as an r-strategist, can rapidly multiply when the N/P ratio and temperature increase (Liu et al., 2002; Finkel et al., 2010).

Other chain-forming (*Chaetoceros socialis*, *Leptocylindrus minimus*) and pinnate (*Cylindrotheca closterium*) diatoms are among the newly detected phytoplankton species. Their occurrence was restricted to low abundance and did not develop blooms. The cosmopolitan distribution of these marine diatoms indicates considerable ecological plasticity (Degerlund et al., 2012; Yang et al., 2020).

The marine diatom *Pseudo-nitzschia pungens* and the dinoflagellate *D. norvegica* were also selected as ecological indicators; however, blooms were not observed. These HABs are known as a group that has the potential to produce toxins, which can pose toxic effects on human health through the food chain, such as diarrhetic shellfish poisoning producers *Dinophysis* spp. and domoic acid producers *Pseudo-nitzschia* spp. (Lundholm

et al., 2009 onwards). Santos et al. (2021) and Wang et al. (2022) stated that recurrent outbreaks of these HABs result in serious economic losses and sometimes coincide with human poisoning events. Thus, monitoring the occurrence of these species has become crucial as this region is an important fishing and aquaculture spot.

Thallasiosira species are also an indicator group in the study area. In particular, the occurrence of *T. subtilis*, *T. weissflogii*, *T. minuscula*, and *T. oceanica* was recorded here, with *T. subtilis* reported for the first time in the MCS by Carvalho et al. (2016). The environmental conditions found in dry months (high salinity, wind speed, and turbidity) favored the dominance of these colonial centric diatoms (*T. subtilis*, *T. weissflogii*) in the inner bay since the species shows the ability to associate with detrital and inorganic particles to minimize stress in turbulent ecosystems (Kang et al., 2019).

In contrast, the oligotrophic conditions found on the outer shelf favored the abundance of *T. minuscula* and *T. oceanica*. Unlike many other *Thallasiosira* species that are predominantly found in coastal waters, these small-celled diatoms are adapted to oligotrophic conditions and highly tolerant to iron limitation (Hoppenrath et al., 2007; Chappell et al., 2014). They have already been reported in Argentinean waters (Sar et al., 2002) and South Brazilian waters (Garcia and Odebrecht, 2009; Fernandes and Frassão-Santos, 2010).

The filamentous cyanobacteria *T. erythraeum* was also recorded near the estuarine plume boundary (P9–P10), where a deficit of nitrogen was identified, but also under low-salinity water influence ($S < 30$). This creates a distinct niche for N₂ fixation by diazotrophic organisms (Subramaniam et al., 2008; Araujo et al., 2017), as has been observed in other studies conducted in the Amazon River plume (Araujo et al., 2017; Lourenço, 2017; Otsuka et al., 2022).

Planktonic *Trichodesmium* species are globally distributed in tropical and subtropical oligotrophic oceans (Luo et al., 2012), and their wide occurrence may be due to their ability to fix molecular nitrogen (N₂) (Yeung et al., 2012) and resistance to grazing (Goes et al., 2014; Stukel et al., 2014). Despite the low abundance reported in this study, *Trichodesmium* spp. can develop blooms in other oligotrophic regions of Brazil, causing harmful effects on the components of marine biota and humans (Chellappa et al., 2005; Carvalho et al., 2008; Koenig et al., 2009; Aff et al., 2016).

Factors shaping phytoplankton β-diversity

In this study, phytoplankton β -diversity was synergistically driven by climatic and spatial processes associated with environmental variability. To the best of our knowledge, this is the first study to assess the influence of these processes on different β -diversity components in MCS.

Among the multiple factors accounting for variation in β -diversity, environmental heterogeneity is of supreme importance since it is defined as the variation in abiotic conditions among localities within a regional unit (Anderson et al., 2006). β -diversity was previously considered to be dependent on environmental heterogeneity (Astorga et al., 2014). Consequently, high environmental heterogeneity in water bodies is expected to promote high β -diversity (Tonkin et al., 2016). In this study, phytoplankton β -diversity was in accordance with the trend of environmental heterogeneity, indicating that the variability of environmental conditions in the MCS played a crucial role in driving the variation in species composition.

In Cumã Bay, β -diversity was governed primarily by climatic factors and environmental variability, while the spatial extent (spatial factor) accounted for most of the variation in phytoplankton across the estuary-ocean continuum. This finding suggests that the climatic pattern of the Amazon coast is the main driver of eco-hydrological interactions, including β -diversity, at small geographical scales. In contrast, the geographical distance was an important modulator of β -diversity patterns on large scales, as previously demonstrated by Wetzel et al. (2012), Zorzal-Almeida et al. (2017), Lansac-Tôha et al. (2019), and Zorzal-Almeida et al. (2021) for tropical and subtropical phytoplankton assemblages. Other studies of plankton β -diversity have revealed that environmental conditions have a more substantial effect than spatial distance (Diniz et al., 2021; Graco-Rosa et al., 2021; Diego et al., 2023).

Additionally, our results indicated a strong influence of the estuarine plume alongshore and on β -diversity, as was also observed by Tosetto et al. (2022) in studies on animal communities along the Tropical Western Atlantic coast. These authors associated the high endemism in Brazilian and Caribbean coastal habitats with the Amazon River Plume, which acts as a biogeographical barrier to marine species dispersal.

In this case, the estuarine plume from the Maranhense Gulf appears to act as a dispersal ‘filter’ resulting in differences in phytoplankton communities along the MCS since a high number of exclusive species was found inside the bay ($> 40\%$) and low richness along the adjacent shelf. Other studies have also argued that nearshore and offshore gradients in the physical and chemical properties of seawater can act as barriers

to cross-shelf exchanges of phytoplankton (d'Ovidio et al., 2010; Morales et al., 2012; Morales et al., 2017), and present different functional groups dominating coastal and oceanic zones (Menschel et al., 2016).

β -diversity partitioning analysis revealed that the turnover component was the main factor responsible for boosting taxonomic β -diversity at the spatial and temporal scales. Recent studies have shown that species turnover (defined here as the change in the identity of species and their relative proportions) is more sensitive to signal changes in biodiversity than richness measures (Dornelas et al., 2014; Hillebrand et al., 2018; Olli et al., 2022). In addition, Soininen et al. (2017) showed in a recent meta-analysis on taxonomic β -diversity partitioning that species turnover is consistently correlated with total β -diversity since it largely reflects dissimilarity between sites, being 5.7 times more important than richness differences.

Similar to the estuary-ocean continuum, species replacement appears to increase with larger geographical distances (Wetzel et al., 2012; Zorral-Almeida et al., 2021). Smith et al. (2005) stated that larger basins will likely enclose more types of habitats and facilitate colonization by species that have specialized habitat requirements, which may support our findings.

Turnover dominance implies that conservation incentives should involve as many sites as possible, whereas nestedness dominance suggests the conservation of the richest system (Socolar et al., 2016; Diniz et al., 2021). This fact reinforces the maintenance of conservation measures in the study area. As the species composition varies among stations and months, conservation measures should encompass as many sites as possible across the MCS during the entire annual cycle (rainy and dry periods).

Conclusions

This is the first study performed in Cumã Bay and the adjacent continental shelf from the perspective of phytoplankton functional traits and β -diversity ecology. Based on a synoptic evaluation of hydrological and biological variables in the study area, we showed the importance of considering the combined use of spatial, temporal, and hydrodynamic factors in the assessment of phytoplankton dynamics in Amazon ecosystems. Our results suggest that high freshwater discharge from the Maranhense Gulf and macrotidal dynamics substantially influence phytoplankton communities, β -diversity, and nutrient cycling in the MCS. In summary, we concluded that the study area is quite rich in terms of phytoplankton species diversity, with nine potential HABs reported as new records. In

terms of phytoplankton groups, diatoms were dominant, followed by dinoflagellates and cyanobacteria, presenting ecological strategies adapted to the highly dynamic environment, such as the ability to chain-forming and change cell size. The findings provided here are of particular value due to the good environmental status of the studied system, which can serve as an ideal ecosystem for a better understanding of the community ecology and predicting environmental changes that can occur in coastal regions as a result of impacts from human activities. Moreover, our findings suggest that this temporal-spatial approach to phytoplankton structure and β -diversity is feasible for assessing biotic heterogeneity and health in Amazon tropical ecosystems as other aquatic systems.

Acknowledgments

This research was supported by grant given by Coordination for the Improvement of Higher Education Personnel (CAPES) through the granting/concession of a doctoral scholarship to the first author. The authors would like to thank the Postgraduate Program in Oceanography (PPGO) as well as the Laboratory of Phytoplankton of Federal University of Pernambuco and Federal University of Maranhão for technical and structural support. We especially thank Leidiane P. Diniz for her contributions to the β -diversity analysis and statistical models. We would like to thank Editage (www.editage.com) for English language editing.

References

- ABATE, R., GAO, Y., CHEN, C., LIANG, J., MU, W., KIFILE, D., CHEN, Y., 2017. Decadal variations in diatoms and dinoflagellates on the inner shelf of the East China Sea, China. *Chinese Journal of Oceanology and Limnology*, 35, 1374–1386. <https://doi.org/10.1007/s00343-017-6029-1>.
- AFFE, H. M. J., CAIRES, T. A., SILVA, E. M., NUNES, J. M. C., 2016. Floración de *Trichodesmium erythraeum* en la región costera tropical de Brasil. *Revista de Biología Marina y Oceanografía*, 51, 175–179. <https://doi.org/10.4067/s0718-19572016000100017>.
- AFFE, H. M. J., PIEDRAS, F. R., SANTANA, L. M., MOSER, G. A. O., MENEZES, M., NUNES, J. M., 2019. Phytoplankton functional groups: Short-term variation in a tropical tidal-forced estuarine system. *Marine Ecology*, 40(4). Portico. <https://doi.org/10.1111/maec.12555>.
- ALVARES, C. A., STAPE, J. L., SENTELHAS, P. C., MORAES GONÇALVES, J. L., SPAROVEK, G., 2013. Köppen's climate classification map for Brazil. *Meteorologische Zeitschrift*, 22, 711–728.

- ANDERSON, M. J., 2001. A new method for non-parametric multivariate analysis of variance. *Austral. Ecol.* 26, 32–46. <https://doi.org/10.1111/j.1442-9993.2001.01070.pp.x>.
- ANDERSON, M. J., ELLINGSEN, K. E., MCARDLE, B. H., 2006. Multivariate dispersion as a measure of beta diversity. *Ecology Letters*, 9(6), 683–693. <https://doi.org/10.1111/j.1461-0248.2006.00926.x>.
- ANGLÈS, S., JORDI, A., HENRICHES, D. W., CAMPBELL, L., 2019. Influence of coastal upwelling and river discharge on the phytoplankton community composition in the northwestern Gulf of Mexico. *Progress in Oceanography*, 173, 26–36. <https://doi.org/10.1016/j.pocean.2019.02.001>.
- APHA., 2005. Standard Methods for the Examination of Water and Wastewater, 21st ed.
- AQUINO, R., NORIEGA, C., MASCARENHAS, A., COSTA, M., MONTEIRO, S., SANTANA, L., SILVA, I., PRESTES, Y., ARAUJO, M., ROLLNIC, M., 2022. Possible Amazonian contribution to Sargassum enhancement on the Amazon Continental Shelf. *Science of the Total Environment*, 853, 158432. <https://doi.org/10.1016/j.scitotenv.2022.158432>.
- ARAUJO, M., NORIEGA, C., HOUNSOU-GBO, G. A., VELEDA, D., ARAUJO, J., BRUTO, L., FEITOSA, F., FLORES-MONTES, M., LEFÈVRE, N., MELO, P., OTSUKA, A., TRAVASSOS, K., SCHWAMBORN, R., NEUMANN-LEITÃO, S., 2017. A Synoptic Assessment of the Amazon River-Ocean Continuum during Boreal Autumn: From Physics to Plankton Communities and Carbon Flux. *Frontiers in Microbiology*, 8. <https://doi.org/10.3389/fmicb.2017.01358>.
- ASTORGA, A., DEATH, R., DEATH, F., PAAVOLA, R., CHAKRABORTY, M., MUOTKA, T., 2014. Habitat heterogeneity drives the geographical distribution of beta diversity: the case of New Zealand stream invertebrates. *Ecology and Evolution*, 4(13), 2693–2702. Portico. <https://doi.org/10.1002/ece3.1124>.
- BANNON, C. C., CAMPBELL, D. A., 2017. Sinking towards destiny: High throughput measurement of phytoplankton sinking rates through time-resolved fluorescence plate spectroscopy. *PLoS ONE*, 12(10), e0185166. <https://doi.org/10.1371/journal.pone.0185166>.
- BASELGA, A., 2010. Partitioning the turnover and nestedness components of beta diversity. *Glob. Ecol. Biogeogr.* 19, 134–143. <https://doi.org/10.1111/j.1466-8238.2009.00490.x>.
- BASELGA, A. AND ORME, C. D. L., 2012. betapart: an R package for the study of beta diversity. *Methods in Ecology and Evolution*, 3(5), 808–812. Portico. <https://doi.org/10.1111/j.2041-210x.2012.00224.x>.
- BHARATHI, M. D., SARMA, V. V. S. S., RAMANESWARI, K., 2018. Intra-annual variations in phytoplankton biomass and its composition in the tropical estuary: Influence of river discharge. *Marine Pollution Bulletin*, 129(1), 14–25. <https://doi.org/10.1016/j.marpolbul.2018.02.007>.

- BLANCHET, F. G., LEGENDRE, P. AND BOCARD, D., 2008a. Modelling directional spatial processes in ecological data. *Ecological Modelling*, 215, 325–336.
- BLANCHET, F. G., LEGENDRE, P. AND BOCARD, D., 2008b. Forward selection of spatial explanatory variables. *Ecology*, 89, 2623–2632.
- BRASIL, J., SANTOS, J. B. O., SOUSA, W., MENEZES, R. F., HUSZAR, V. L. M., ATTAYDE, J. L., 2019. Rainfall leads to habitat homogenization and facilitates plankton dispersal in tropical semiarid lakes. *Aquatic Ecology*, 54(1), 225–241. <https://doi.org/10.1007/s10452-019-09738-9>.
- CARSTENSEN, J., KLAIS, R., CLOERN, J. E., 2015. Phytoplankton blooms in estuarine and coastal waters: Seasonal patterns and key species. *Estuarine, Coastal and Shelf Science*, 162, 98–109. <https://doi.org/10.1016/j.ecss.2015.05.005>.
- CARVALHO, M., GIANESELLA, S. M. F., SALDANHA-CORRÊA, F. M. P., 2008. *Trichodesmium erythraeum* Bloom on the Continental Shelf off Santos, Southeast Brazil. *Brazilian Journal of Oceanography*, 56(4), 307–311. <https://doi.org/10.1590/s1679-87592008000400006>.
- CARVALHO, R. C. Q., CUTRIM, M. V. J., ESCHRIQUE, S. A., AZEVEDO CUTRIM, A. C. G., MOREIRA, E. G., SILVEIRA, P. C. A., COELHO, J. M., 2016. Microphytoplankton composition, chlorophyll a concentration and environmental variables of the Maranhão Continental Shelf, Northern Brazil. *Latin American Journal of Aquatic Research*, 44(2), 256–266. <https://doi.org/10.3856/vol44-issue2-fulltext-7>.
- CASTRO, A. L. C., ESCHRIQUE, S. A., SILVEIRA, P. C. A., AZEVEDO, J. W. J., FERREIRA, H. R. S., SOARES, L. S., MONTELES, J. S., ARAÚJO, M. C., NUNES, J. L., SILVA, M. H. L., 2018. Physicochemical properties and distribution of nutrients on the inner continental shelf adjacent to the gulf of maranhão (Brazil) in the equatorial atlantic. *Applied Ecology and Environmental Research*, 16(4), 4829–4847. https://doi.org/10.15666/aeer/1604_48294847.
- CAVALCANTI, L. F., AZEVEDO-CUTRIM, A. C. G., OLIVEIRA, A. L. L., FURTADO, J. A., ARAÚJO, B. DE O., SÁ, A. K. D. S., FERREIRA, F. S., SANTOS, N. G. R., DIAS, F. J. S., CUTRIM, M. V. J., 2018. Structure of microphytoplankton community and environmental variables in a macrotidal estuarine complex, São Marcos Bay, Maranhão - Brazil. *Brazilian Journal of Oceanography*, 66(3), 283–300. <https://doi.org/10.1590/s1679-87592018021906603>.
- CAVALCANTI, L. F., CUTRIM, M. V. J., LOURENÇO, C. B., SÁ, A. K. D. S., OLIVEIRA, A. L. L., DE AZEVEDO-CUTRIM, A. C. G., 2020. Patterns of phytoplankton structure in response to environmental gradients in a macrotidal estuary of the Equatorial Margin (Atlantic coast, Brazil). *Estuarine, Coastal and Shelf Science*, 245, 106969. <https://doi.org/10.1016/j.ecss.2020.106969>.
- CAVALCANTI, L. F., DO N FEITOSA, F. A., CUTRIM, M. V. J., MONTES, M. J. F., LOURENÇO, C. B., FURTADO, J. A., DOS S SÁ, A. K. D., 2022. Drivers of phytoplankton biomass and diversity in a macrotidal bay of the Amazon Mangrove Coast,

a Ramsar site. *Ecohydrology and Hydrobiology*, 22(3), 435–453. <https://doi.org/10.1016/j.ecohyd.2022.02.002>.

CEPEDA, G. D., VIÑAS, M. D., MOLINARI, G. N., HOZBOR, M. C., SILVA, R. I., MARTÍNEZ, A., ACHA, E. M., 2020. The impact of Río de la Plata plume favors the small-sized copepods during summer. *Estuarine, Coastal and Shelf Science*, 245, 107000. <https://doi.org/10.1016/j.ecss.2020.107000>.

CHAPARRO, G., O'FARRELL, I., HEIN, T., 2019. Multi-scale analysis of functional plankton diversity in floodplain wetlands: Effects of river regulation. *Science of the Total Environment*, 667, 338–347. <https://doi.org/10.1016/j.scitotenv.2019.02.147>.

CHAPPELL, P. D., WHITNEY, L. P., WALLACE, J. R., DARER, A. I., JEAN-CHARLES, S., JENKINS, B. D., 2014. Genetic indicators of iron limitation in wild populations of *Thalassiosira oceanica* from the northeast Pacific Ocean. *The ISME Journal*, 9(3), 592–602. <https://doi.org/10.1038/ismej.2014.171>.

CHELLAPPA, N.T., LIMA, A.K.A. CHELLAPPA, T., 2005. Occurrence and dominance of an invasive toxin producing marine cyanobacteria into mangrove environment of the Potengi river estuary, in Natal, Rio Grande do Norte State, Brazil. *Arquivos de Ciências do Mar* 38: 19-27.

CLOERN, J. E., 1987. Turbidity as a control on phytoplankton biomass and productivity in estuaries. *Continental Shelf Research*, 7(11–12), 1367–1381. [https://doi.org/10.1016/0278-4343\(87\)90042-2](https://doi.org/10.1016/0278-4343(87)90042-2).

CLOERN, J. E., FOSTER, S. Q., KLECKNER, A. E., 2014. Phytoplankton primary production in the world's estuarine-coastal ecosystems. *Biogeosciences* 11, 2477–2501.

COLES, V. J., BROOKS, M., HOPKINS, J., STUKEL, M., YAGER, P., HOOD, R., 2013. The pathways and properties of the Amazon river plume in the tropical North Atlantic Ocean. *J. Geophys. Res. Oceans* 118 (12), 6894–6913. <https://doi.org/10.1002/2013JC008981>.

COSTA, D. S., CUTRIM, M. V. J., 2021. Spatial and seasonal variation in physicochemical characteristics and phytoplankton in an estuary of a tropical delta system. *Regional Studies in Marine Science*, 44, 101746. <https://doi.org/10.1016/j.rsma.2021.101746>.

COSTA, Á. K. R., PEREIRA, L. C. C., JIMÉNEZ, J. A., DE OLIVEIRA, A. R. G., DE JESUS FLORES-MONTES, M., DA COSTA, R. M., 2022. Effects of Extreme Climatic Events on the Hydrological Parameters of the Estuarine Waters of the Amazon Coast. *Estuaries and Coasts*, 45(6), 1517–1533. <https://doi.org/10.1007/s12237-022-01056-y>.

COTTENIE, K., 2005. Integrating environmental and spatial processes in ecological community dynamics. *Ecol. Lett.* 8, 1175–1182. <https://doi.org/10.1111/j.1461-0248.2005.00820.x>.

COWMAN, P. F., BELLWOOD, D. R., 2013. Vicariance across major marine biogeographic barriers: temporal concordance and the relative intensity of hard versus

soft barriers. *Proceedings of the Royal Society B: Biological Sciences*, 280(1768), 20131541. <https://doi.org/10.1098/rspb.2013.1541>.

CZIZEWESKI, A., PIMENTA, F. M., SAAVEDRA, O. R., 2020. Numerical modeling of Maranhão Gulf tidal circulation and power density distribution. *Ocean Dynamics*, 70(5), 667–682. <https://doi.org/10.1007/s10236-020-01354-8>.

D'ovidio, F., De Monte, S., Alvain, S., Dandonneau, Y., Lévy, M., 2010. Fluid dynamical niches of phytoplankton types. *Proceedings of the National Academy of Sciences*, 107(43), 18366–18370. <https://doi.org/10.1073/pnas.1004620107>.

Dagg, M., Bennerb, R., Lohrenzc, S., Lawrence, D., 2004. Transformation of dissolved and particulate materials on continental shelves influenced by large rivers: plume processes. *Continent. Shelf Res.* 24, 833–858. <https://doi.org/10.1016/j.csr.2004.02.003>.

Degerlund, M., Husaby, S., Zingone, A., Sarño, D., Landfald, B., 2012. Functional diversity in cryptic species of *Chaetoceros socialis* Lauder (Bacillariophyceae). *Journal of Plankton Research*, 34 (5), 416–431. <https://doi.org/10.1093/plankt/fbs004>.

DIAS, F. J. DA S., CASTRO, B. M., LACERDA, L. D., MIRANDA, L. B., MARINS, R. V., 2016. Physical characteristics and discharges of suspended particulate matter at the continent-ocean interface in an estuary located in a semiarid region in northeastern Brazil. *Estuarine, Coastal and Shelf Science*, 180, 258–274. <https://doi.org/10.1016/j.ecss.2016.08.006>.

Diego, F., Alfonso, P., Gisela, M. AND Gutierrez, M. F., 2023. Eutrophication as a homogenizer process of phytoplankton β -diversity in lowland streams. *Limnologica*. <https://doi.org/10.1016/j.limno.2023.126058>.

Diniz, L. P., Braghin, L. DE S. M., Pinheiro, T. S. A., Melo, P. A. M. DE C., Bonecker, C. C., Melo Júnior, M., 2021. Environmental filter drives the taxonomic and functional β -diversity of zooplankton in tropical shallow lakes. *Hydrobiologia*, 848(8), 1881–1895. <https://doi.org/10.1007/s10750-021-04562-5>.

Dong, X., Li, B., He, F., Gu, Y., Sun, M., Zhang, H., Tan, L., Xiao, W., Liu, S. AND CAI, Q., 2016. Flow directionality, mountain barriers and functional traits determine diatom metacommunity structuring of high mountain streams. *Scientific Reports*, 6(1). <https://doi.org/10.1038/srep24711>.

Dornelas, M., Gotelli, N. J., McGill, B., Shimadzu, H., Moyes, F., Sievers, C., Magurran, A. E., 2014. Assemblage Time Series Reveal Biodiversity Change but Not Systematic Loss. *Science*, 344(6181), 296–299. <https://doi.org/10.1126/science.1248484>.

Duarte-Dos-Santos, A. K., Oliveira, A. L. L., Furtado, J. A., Ferreira, F. S., Araújo, B. O., Corrêa, J. J. M., Cavalcanti, L. F., AZEVEDO-CUTRIM, A. C. G., CUTRIM, M. V. J., 2017. Spatial and seasonal variation of microphytoplankton community and the correlation with environmental parameters in a hypereutrophic

tropical estuary - Maranhão - Brazil. Brazilian Journal of Oceanography, 65(3), 356–372. <https://doi.org/10.1590/s1679-87592017134406503>.

DUFRÊNE, M., LEGENDRE, P., 1997. Species assemblages and indicator species: the need for a flexible asymmetrical approach. Ecol. Monogr. 67 (3), 345–366. <https://doi.org/10.1890/0012-9615>.

EGGE, J., AKSNES, D., 1992. Silicate as regulating nutrient in phytoplankton competition. Marine Ecology Progress Series, 83, 281–289. <https://doi.org/10.3354/meps083281>.

FERNANDES, L. F., FRASSÃO-SANTOS, E. K., 2011. Mucilaginous species of *Thalassiosira* Cleve emend: hasle (Diatomeae) in South Brazilian waters. Acta Botanica Brasilica, 25(1), 31–42. <https://doi.org/10.1590/s0102-33062011000100006>.

FINKEL, Z.V., J. BEARDALL, K.J. FLYNN, A. QUIQQ, T.A. REES, AND J.A. RAVEN., 2010. Phytoplankton in a changing world: Cells size and elemental stoichiometry. Journal of Plankton Research 32 (1): 119–137. <https://doi.org/10.1093/plankt/fbp098>.

FU, R., DICKINSON, R.E., CHEN, M., WANG, H., 2001. How Do Tropical Sea Surface Temperatures Influence the Seasonal Distribution of Precipitation in the Equatorial Amazon? Journal of Climate 14 (20), 4003 – 4026. [https://dx.doi.org/10.1175/1520-0442\(2001\)014<4003:HDTSS>2.0.CO;2](https://dx.doi.org/10.1175/1520-0442(2001)014<4003:HDTSS>2.0.CO;2).

GAO, Y., JIANG, Z., CHEN, Y., LIU, J., ZHU, Y., LIU, X., SUN, Z., ZENG, J., 2022. Spatial Variability of Phytoplankton and Environmental Drivers in the Turbid Sanmen Bay (East China Sea). Estuaries and Coasts, 45(8), 2519–2533. <https://doi.org/10.1007/s12237-022-01104-7>.

GARCIA, M., ODEBRECHT, C., 2009. Morphology and ecology of *Thalassiosira* Cleve (Bacillariophyta) species rarely recorded in Brazilian coastal waters. Brazilian Journal of Biology, 69(4), 1059–1071. <https://doi.org/10.1590/s1519-69842009000500009>.

GHERARDI, M., AMATO, A., BOULY, J.-P., CHEMINANT, S., FERRANTE, M. I., D'ALCALÁ, M. R., IUDICONE, D., FALCIATORE, A., COSENTINO LAGOMARSINO, M., 2016. Regulation of chain length in two diatoms as a growth-fragmentation process. Physical Review E, 94(2). <https://doi.org/10.1103/physreve.94.022418>.

GOES, J. I., GOMES, H. DO R., CHEKALYUK, A. M., CARPENTER, E. J., MONTOYA, J. P., COLES, V. J., YAGER, P. L., BERELSON, W. M., CAPONE, D. G., FOSTER, R. A., STEINBERG, D. K., SUBRAMANIAM, A., HAFIZ, M. A., 2014. Influence of the Amazon River discharge on the biogeography of phytoplankton communities in the western tropical north Atlantic. Progress in Oceanography, 120, 29–40. <https://doi.org/10.1016/j.pocean.2013.07.010>.

GOMES, V. J. C., ASP, N. E., SIEGLE, E., GOMES, J. D., SILVA, A. M. M., OGSTON, A. S., NITTROUER, C. A., 2021. Suspended-Sediment Distribution Patterns in Tide-

Dominated Estuaries on the Eastern Amazon Coast: Geomorphic Controls of Turbidity-Maxima Formation. *Water*, 13(11), 1568. <https://doi.org/10.3390/w13111568>.

GRACO-ROZA, C., SOININEN, J., CORRÊA, G., PACHECO, F. S., MIRANDA, M., DOMINGOS, P., MARINHO, M. M., 2021. Functional rather than taxonomic diversity reveals changes in the phytoplankton community of a large dammed river. *Ecological Indicators*, 121, 107048. <https://doi.org/10.1016/j.ecolind.2020.107048>.

GRASSHOFF, K., EHRHARDT, M., KREMLING, K., 1983. Methods of Seawater Analysis. Verlag Chemie, New York, pp. 581–614 vol. 16 (3).

GUALBERTO, L.P.S., EL-ROBRINI, M., 2005. Faciologia da Cobertura Sedimentar Superficial da Plataforma Continental do Maranhão. *Estudos Geológicos*, 15, 234-243.

GUIRY, M.D. GUIRY, G.M., 2020. AlgaeBase. World-wide electronic publication. National University of Ireland, Galway.

HARRIS, G., 2012. Phytoplankton Ecology: Structure, Function and Fluctuation. Springer Science Business Media, Amesterdam.

HILLEBRAND, H., BLASIUS, B., BORER, E. T., CHASE, J. M., DOWNING, J. A., ERIKSSON, B. K., FILSTRUP, C. T., HARPOLE, W. S., HODAPP, D., LARSEN, S., LEWANDOWSKA, A. M., SEABLOOM, E. W., VAN DE WAAL, D. B., RYABOV, A. B., 2018. Biodiversity change is uncoupled from species richness trends: Consequences for conservation and monitoring. *Journal of Applied Ecology*, 55(1), 169–184. Portico. <https://doi.org/10.1111/1365-2664.12959>.

HOPPENRATH, M., BESZTERI, B., DREBES, G., HALLIGER, H., VAN BEUSEKOM, J. E. E., JANISCH, S., WILTSHERE, K. H., 2007. Thalassiosiralespecies (Bacillariophyceae, Thalassiosirales) in the North Sea at Helgoland (German Bight) and Sylt (North Frisian Wadden Sea) – a first approach to assessing diversity. *European Journal of Phycology*, 42(3), 271–288. <https://doi.org/10.1080/09670260701352288>.

IBAÑEZ, M.S.R., CAVALCANTE, P.R.S., COSTA NETO, J.P., BARBIERI, R., PONTES, J.P., SANTANA, S.C.C., SERRA, C.L.M., NAKAMOTO, N., MITAMURA, O., 2000. Limnological characteristics of three aquatic systems of the pre Amazonian floodplain, Baixada Maranhense (Maranhão, Brazil). *Aquatic Ecosystem Health Management* 3 (4), 521–531. <https://doi.org/10.1080/14634980008650689>.

IBÁÑEZ, J. S. P., ARAUJO, M., LEFÈVRE, N., 2016. The overlooked tropical oceanic CO₂ sink. *Geophysical Research Letters*, 43(8), 3804–3812. Portico. <https://doi.org/10.1002/2016gl068020>.

INMET. Instituto Nacional de Meteorologia., 2019. Monitoramento das estações automáticas. Accessed at <http://www.inmet.gov.br/sonabra/maps/automaticas.php> on 2019-12-11.

KANG, L., HE, Y., DAI, L., HE, Q., AI, H., YANG, G., LIU, M., JIANG, W., LI, H., 2019. Interactions between suspended particulate matter and algal cells contributed to the

reconstruction of phytoplankton communities in turbulent waters. *Water Research*, 149, 251–262. <https://doi.org/10.1016/j.watres.2018.11.003>.

KINGSFORD, M.J., SUTHERS, I.M., 1994. Dynamic estuarine plumes and fronts: importance to small fish and plankton in coastal waters of NSW, Australia. *Continent. Shelf Res.* 14, 655–672. [https://doi.org/10.1016/0278-4343\(94\)90111-2](https://doi.org/10.1016/0278-4343(94)90111-2).

KOENING, M. L., WANDERLEY, B. E., MACEDO, S. J., 2009. Microphytoplankton structure from the neritic and oceanic regions of Pernambuco State - Brazil. *Brazilian Journal of Biology*, 69(4), 1037–1046. <https://doi.org/10.1590/s1519-69842009000500007>.

KOH, C., KHIM, J., ARAKI, H., YAMANISHI, H., MOGI, H., KOGA, K., 2006. Tidal resuspension of microphytobenthic chlorophyll a in a Nanaura mudflat, Saga, Ariake Sea, Japan: flood-ebb and spring-neap variations. *Marine Ecology Progress Series*, 312, 85–100. <https://doi.org/10.3354/meps312085>.

LANCELOT, C., MUYLAERT, K., 2011. Trends in Estuarine Phytoplankton Ecology. *Treatise on Estuarine and Coastal Science*, 5–15. <https://doi.org/10.1016/b978-0-12-374711-2.00703-8>.

LANSAC-TÔHA, F. M., HEINO, J., QUIRINO, B. A., MORESCO, G. A., PELÁEZ, O., MEIRA, B. R., RODRIGUES, L. C., JATI, S., LANSAC-TÔHA, F. A., VELHO, L. F. M., 2019. Differently dispersing organism groups show contrasting beta diversity patterns in a dammed subtropical river basin. *Science of The Total Environment*, 691, 1271–1281. <https://doi.org/10.1016/j.scitotenv.2019.07.236>.

LECHER, A., MACKEY, K., PAYTAN, A., 2017. River and Submarine Groundwater Discharge Effects on Diatom Phytoplankton Abundance in the Gulf of Alaska. *Hydrology*, 4(4), 61. <https://doi.org/10.3390/hydrology4040061>.

LEFÈVRE, N., DA SILVA DIAS, F. J., DE TORRES, A. R., NORIEGA, C., ARAUJO, M., DE CASTRO, A. C. L., ROCHA, C., JIANG, S., IBÁNHEZ, J. S. P., 2017. A source of CO₂ to the atmosphere throughout the year in the Maranhense continental shelf (2°30'S, Brazil). *Continental Shelf Research*, 141, 38–50. <https://doi.org/10.1016/j.csr.2017.05.004>.

LEGENDRE, P. AND LEGENDRE, L., 1998. Numerical Ecology. *Developments in Environmental Modelling* 20. Elsevier Science, Amsterdam pp .853.

LEGENDRE, P., BORCARD, D. AND PERES-NETO, P.R., 2005. Analysing beta diversity: partitioning the spatial variation of community composition data. *Ecol. Monogr.* 75, 435–450.

LEGENDRE, P., 2014. Interpreting the replacement and richness difference components of beta diversity. *Glob. Ecol. Biogeogr.* 23, 1324–1334. <https://doi.org/10.1111/geb.12207>.

LENTZ, S. J., 1995. The Amazon River plume during AmasSeds: Subtidal current variability and the importance of wind forcing. *J. Geophys. Res.*, 100, 2377–2390.

- LEWIS, W. M., 1976. Surface/volume ratio: implications for phytoplankton morphology. *Science*, 192, 885–887.
- LIMA, H. P., DIAS, F. J. S., TEIXEIRA, C. E. P., GODOI, V. A., TORRES, A. R., ARAÚJO, R. S., 2021. Implications of turbulence in a macrotidal estuary in northeastern Brazil — The São Marcos Estuarine Complex. *Regional Studies in Marine Science*, 47, 101947. <https://doi.org/10.1016/j.rsma.2021.101947>.
- LITCHMAN, E., KLAUSMEIER, C. A., 2008. Trait-based community ecology of phytoplankton. *Annual Review of Ecology, Evolution, and Systematics* 39: 615–639.
- LIU, D. Y., SUN, J., LIU, Z., CHEN, H. T, WEI, H, ZHANG, J., 2004. The effects of spring-neap tide on the phytoplankton community development in the Jiaozhou Bay, China. *Acta Oceanologica Sinica*, 23 (4): 687-697.
- LIU, D., SUN, J., CHEN, Z.T., 2002. Effect of N/P ratio on the growth of a red tide diatom *Skeletonema costatum*. *Trans Oceanol Limnol*. 2, 39-44. <https://10.13984/j.cnki.cn37-1141.2002.02.006>.
- LIU, S., CUI, Z., ZHAO, Y., CHEN, N., 2022. Composition and spatial-temporal dynamics of phytoplankton community shaped by environmental selection and interactions in the Jiaozhou Bay. *Water Research*, 218, 118488. <https://doi.org/10.1016/j.watres.2022.118488>.
- LOURENÇO, C.B., 2017. Variabilidade temporal da comunidade fitoplanctônica no continuum estuário-oceano na Plataforma Continental Amazônica. Thesis (PhD in Science). São Paulo University, São Paulo.
- LUIZ, O. J., MADIN, J. S., ROBERTSON, D. R., ROCHA, L. A., WIRTZ, P., FLOETER, S. R., 2011. Ecological traits influencing range expansion across large oceanic dispersal barriers: insights from tropical Atlantic reef fishes. *Proceedings of the Royal Society B: Biological Sciences*, 279(1730), 1033–1040. <https://doi.org/10.1098/rspb.2011.1525>.
- LUNDHOLM, N., CHURRO, C., FRAGA, S., HOPPENRATH, M., IWATAKI, M., LARSEN, J., MERTENS, K., MOESTRUP, Ø., ZINGONE, A. (Eds) (2009 onwards). IOC-UNESCO Taxonomic Reference List of Harmful Micro Algae. <https://doi.org/10.14284/362>. Accessed at <https://www.marinespecies.org/hab> on 2022-08-07.
- LUNDSØR, E., EIKREM, W., STIGE, L. C., ENGESMO, A., STADNICZEŃKO, S. G., EDWARDSEN, B., 2022. Changes in phytoplankton community structure over a century in relation to environmental factors. *Journal of Plankton Research*, 44 (6), 854–871. <https://doi.org/10.1093/plankt/fbac055>.
- LUO, Y.-W., DONEY, S. C., ANDERSON, L. A., BENAVIDES, M., BERMAN-FRANK, I., BODE, A., BONNET, S., BOSTRÖM, K. H., BÖTTJER, D., CAPONE, D. G., CARPENTER, E. J., CHEN, Y. L., CHURCH, M. J., DORE, J. E., FALCÓN, L. I., FERNÁNDEZ, A., FOSTER, R. A., FURUYA, K., GÓMEZ, F., ... ZEHR, J. P., 2012.

Database of diazotrophs in global ocean: abundance, biomass and nitrogen fixation rates. *Earth System Science Data*, 4(1), 47–73. <https://doi.org/10.5194/essd-4-47-2012>.

MACEDO, L. A. A., 1989. Controle ambiental do Golfão Maranhense. *DAE*, 49 (155), 1-7.

MARAÑÓN, E., CERMEÑO, P., LATASA, M., TADONLÉKÉ, R. D., 2012. Temperature, resources, and phytoplankton size structure in the ocean. *Limnology and Oceanography*, 57(5), 1266–1278. Portico. <https://doi.org/10.4319/lo.2012.57.5.1266>.

MARENGO, J. A., 1995. Interannual variability of deep convection over the tropical South American sector as deduced from ISCCP C2 data. *International Journal of Climatology*, 15(9), 995–1010. <https://doi.org/10.1002/joc.3370150906>.

MARGALEF, R., 1978. Life-forms of phytoplankton as survival alternatives in an unstable environment. *Oceanologica Acta*, 1(4), 493–509.

MARTINS, M.B., OLIVEIRA, T.G., 2011. Amazônia Maranhense: diversidade e conservação. MPEG, Belém, p. 329.

MASCARENHAS, A. C. C., GOMES, G. S., LIMA, A. P. Y., DA SILVA, H. K. N., SANTANA, L. S., ROSÁRIO, R. P., ROLLNIC, M., 2016. Seasonal Variations of the Amazon River Plume with Focus on the Eastern Sector. *Journal of Coastal Research*, 75(sp1), 532–536. <https://doi.org/10.2112/si75-107.1>.

MAYZEL, B., ARAM, L., VARSANO, N., WOLF, S. G., GAL, A., 2021. Structural evidence for extracellular silica formation by diatoms. *Nature Communications*, 12(1). <https://doi.org/10.1038/s41467-021-24944-6>.

MENSCHEL, E., GONZÁLEZ, H. E., GIESECKE, R., 2016. Coastal-oceanic distribution gradient of coccolithophores and their role in the carbonate flux of the upwelling system off Concepción, Chile (36°S). *Journal of Plankton Research*, 38(4), 798–817. <https://doi.org/10.1093/plankt/fbw037>.

MORALES, C. E., ANABALÓN, V., BENTO, J. P., HORMAZABAL, S., CORNEJO, M., CORREA-RAMÍREZ, M. A., SILVA, N., 2017. Front-Eddy Influence on Water Column Properties, Phytoplankton Community Structure, and Cross-Shelf Exchange of Diatom Taxa in the Shelf-Slope Area off Concepción (~36–37°S). *Journal of Geophysical Research: Oceans*, 122(11), 8944–8965. Portico. <https://doi.org/10.1002/2017jc013111>.

MORALES, C. E., HORMAZABAL, S., CORREA-RAMIREZ, M., PIZARRO, O., SILVA, N., FERNANDEZ, C., ANABALÓN, V., TORREBLANCA, M. L., 2012. Mesoscale variability and nutrient–phytoplankton distributions off central-southern Chile during the upwelling season: The influence of mesoscale eddies. *Progress in Oceanography*, 104, 17–29. <https://doi.org/10.1016/j.pocean.2012.04.015>.

MUKHERJEE, A., CHAKRABORTY, S., DAS, S., DE, T. K., 2013. Salinity might be the most influential governing factor of cell surface size of *Coscinodiscus* in well mixed tropical estuarine waters. *International Journal for Life Sciences and Education Research*, 1(2), 81–90. <https://doi.org/10.6084/m9.figshare.15073509.v1>.

- NASCIMENTO, W.R., SOUZA-FILHO, P.W.M., PROISY, C., LUCAS, R.M., ROSENQVIST, A., 2013. Mapping changes in the largest continuous Amazonian mangrove belt using object-based classification of multisensory satellite imagery. *Estuarine, Coastal and Shelf Science*, 117, 83–93. <https://doi.org/10.1016/j.ecss.2012.10.005>.
- NITTROUER, C.A., DEMASTER, D.J., 1996. The Amazon shelf setting tropical, energetic, and influenced by a large river. *Cont. Shelf Res.* 16, 553–574.
- NITTROUER, C.A., DEMASTER, D.J., 1986. Sedimentary processes on the Amazon continental shelf: past, present and future research. *Continental Shelf Research*, 6, 5–30. [https://doi.org/10.1016/0278-4343\(86\)90051-8](https://doi.org/10.1016/0278-4343(86)90051-8).
- NITTROUER, C.A., DEMASTER, D.J., FIGUEIREDO, A.G., RINE, J.M., 1991. AmasSeds: an interdisciplinary investigation of a complex coastal environment. *Oceanography*, 4, 3–7.
- OKSANEN, J., BLANCHET, F. G., FRIENDLY, M., KINDT, R., LEGENDRE, P., MCGLINN, D., MINCHIN, P.R., O'HARA, B., SIMPSON, G. L., SOLYMOS, P., STEVENS, M. H. H., SZOECS, E., WAGNER, H., 2020. vegan: Community Ecology Package. R package version 2, 5-7. <https://cran.r-project.org>.
- OLIVEIRA, A. R. G., ODEBRECHT, C., PEREIRA, L. C. C., COSTA, R. M., 2022. Phytoplankton variation in an Amazon estuary with emphasis on the diatoms of the Order Eupodiscales. *Ecohydrology and Hydrobiology*, 22(1), 55–74. <https://doi.org/10.1016/j.ecohyd.2021.12.001>.
- OLLI, K., NYMAN, E., TAMMINEN, T., 2022. Half-century trends in alpha and beta diversity of phytoplankton summer communities in the Helsinki Archipelago, the Baltic Sea. *Journal of Plankton Research*. <https://doi.org/10.1093/plankt/fbac029>.
- OLTMAN, R.E., 1968. Reconnaissance Investigations of the Discharge and Water Quality of the Amazon River. U.S. Geological Survey, Circular, 552, 16pp.
- OTSUKA, A., NORIEGA, C., FEITOSA, F., BORGES, G., MONTES, M. F., ARAUJO, M., SILVA-CUNHA, M. G., 2022. Characterization of microphytoplankton associations on the Amazon continental shelf and in the adjacent oceanic region. *Journal of Sea Research*, 189, 102271. <https://doi.org/10.1016/j.seares.2022.102271>.
- PAERL, H. W., VALDES-WEAVER, L. M., JOYNER, A. R., WINKELMANN, V., 2007. Phytoplankton indicators of ecological change in the eutrophying Pamlico sound system, North Carolina. *Ecological Applications*, 17(sp5), S88–S101. <https://doi.org/10.1890/05-0840.1>.
- PAERL, H. W., ROSSIGNOL, K. L., HALL, S. N., PEIERLS, B. L., WETZ, M. S., 2010. Phytoplankton Community Indicators of Short- and Long-term Ecological Change in the Anthropogenically and Climatically Impacted Neuse River Estuary, North Carolina, USA. *Estuaries and Coasts*, 33(2), 485–497. <https://doi.org/10.1007/s12237-009-9137-0>.

- PAN, C.W., CHUANG, Y.L., CHOU, L.S., CHEN, M.H., LIN, H.J., 2016. Factors governing phytoplankton biomass and production in tropical estuaries of western Taiwan. *Continental Shelf Research*, 118, 88–99. <https://doi.org/10.1016/j.csr.2016.02.015>.
- PARSONS, T.R., MAITA, Y., LAILI, C.M., 1984. A manual of chemical and biological methods for seawater analysis. Pergamon Press, Oxford, p. 173.
- PEREIRA, L. C. C., SILVA, N. I. S., COSTA, R. M., ASP, N. E., COSTA, K. G., VILA-CONCEJO, A., 2012. Seasonal changes in oceanographic processes at an equatorial macrotidal beach in northern Brazil. *Continental Shelf Research*, 43, 95–106. <https://doi.org/10.1016/j.csr.2012.05.003>.
- PEREIRA, L. C. C., OLIVEIRA, S. M. O. DE, COSTA, R. M. DA, COSTA, K. G. DA, VILA-CONCEJO, A., 2013. What happens on an equatorial beach on the Amazon coast when La Niña occurs during the rainy season? *Estuarine, Coastal and Shelf Science*, 135, 116–127. <https://doi.org/10.1016/j.ecss.2013.07.017>.
- PEREIRA, L. C. C., SOUSA-FELIX, R. C., COSTA, R. M., JIMENEZ, J. A., 2018. Challenges of the recreational use of Amazon beaches. *Ocean Coastal Management*, 165, 52–62. <https://doi.org/10.1016/j.ocecoaman.2018.08.012>.
- PERES-NETO, P. R., LEGENDRE, P., DRAY, S. AND BORCARD, D., 2006. Variation partitioning of species data matrices: estimation and comparison of fractions. *Ecology*, 87, 2614–2625. [https://doi.org/10.1890/0012-9658\(2006\)87\[2614:VPOSDM\]2.0.CO;2](https://doi.org/10.1890/0012-9658(2006)87[2614:VPOSDM]2.0.CO;2)
- PERILLO, G. M. E., PICCOLO, M. C., 2011. Global Variability in Estuaries and Coastal Settings. *Treatise on Estuarine and Coastal Science*, 7–36. <https://doi.org/10.1016/b978-0-12-374711-2.00102-9>.
- PEIERLS, B. L., HALL, N. S. AND PAERL, H. W., 2012. Non-monotonic Responses of Phytoplankton Biomass Accumulation to Hydrologic Variability: A Comparison of Two Coastal Plain North Carolina Estuaries. *Estuaries and Coasts*, 35(6), 1376–1392. <https://doi.org/10.1007/s12237-012-9547-2>.
- PRESTES, Y. O., BORBA, T. A. C., SILVA, A. C., ROLLNIC, M., 2020. A discharge stationary model for the Pará-Amazon estuarine system. *Journal of Hydrology: Regional Studies*, 28, 100668. <https://doi.org/10.1016/j.ejrh.2020.100668>.
- QUEIROZ, J. B. M., OLIVEIRA, A. R. G. DE, COSTA, K. G. DA, BRITO, E. P., FERNANDES, F. D. DOS S., NUNES, Z. M. P., KOENING, M. L., PEREIRA, L. C. C., DA COSTA, R. M., 2022. Phytoplankton of the shipping sector of São Marcos Bay (Amazon Coast): A potential risk area for the establishment of non-indigenous species. *Regional Studies in Marine Science*, 49, 102121. <https://doi.org/10.1016/j.rsma.2021.102121>.
- R CORE TEAM, 2019. R: A language and environment for statistical computing. R Foundation for Statistical Computing. www.R-project.org/.
- RATH, A. R., MITBAVKAR, S., ANIL, A. C., 2021. Response of the phytoplankton community to seasonal and spatial environmental conditions in the Haldia port ecosystem

located in the tropical Hooghly River estuary. *Environmental Monitoring and Assessment*, 193(9). <https://doi.org/10.1007/s10661-021-09255-z>.

REYNOLDS, C. S., HUSZAR, V., KRUK, C., NASELLI-FLORES, L., MELO, S., 2002. Towards a functional classification of the freshwater phytoplankton. *Journal of Plankton Research*, 24(5), 417–428. <https://doi.org/10.1093/plankt/24.5.417>.

REYNOLDS, C.S., 2006. *The Ecology of Phytoplankton*. Cambridge Univ. Press, Cambridge, UK, p. 550.

RUSANOV, A. G., BÍRÓ, T., KISS, K. T., BUCZKÓ, K., GRIGORSZKY, I., HIDAS, A., DULEBA, M., TRÁBERT, Z., FÖLDI, A., ÁCS, É., 2022. Relative importance of climate and spatial processes in shaping species composition, functional structure and beta diversity of phytoplankton in a large river. *Science of The Total Environment*, 807, 150891. <https://doi.org/10.1016/j.scitotenv.2021.150891>.

SÁ, A. K. D. S., CUTRIM, M. V. J., DO NASCIMENTO FEITOSA, F. A., DE JESUS FLORES-MONTES, M., CAVALCANTI, L. F., DOS SANTOS COSTA, D., DA CRUZ, Q. S., 2022a. Multiple stressors influencing the general eutrophication status of transitional waters of the Brazilian tropical coast: An approach utilizing the pressure, state, and response (PSR) framework. *Journal of Sea Research*, 189, 102282. <https://doi.org/10.1016/j.seares.2022.102282>.

SÁ, A. K. D. S., FEITOSA, F. A. N., CUTRIM, M. V. J., FLORES-MONTES, M. J., COSTA, D.S., CAVALCANTI, L. F., 2022b. Phytoplankton community dynamics in response to seawater intrusion in a tropical macrotidal river-estuary continuum. *Hydrobiologia*. <https://doi.org/10.1007/s10750-022-04851-7>.

SANTANA, R. M. C., DOLBETH, M., BARBOSA, J. E. L., PATRÍCIO, J., 2018. Narrowing the gap: Phytoplankton functional diversity in two disturbed tropical estuaries. *Ecological Indicators*, 86, 81–93. <https://doi.org/10.1016/j.ecolind.2017.12.003>.

SANTANA, C. S., LIRA, S. M. DE A., VARONA, H. L., NEUMANN-LEITÃO, S., ARAUJO, M., SCHWAMBORN, R., 2020. Amazon River plume influence on planktonic decapods in the tropical Atlantic. *Journal of Marine Systems*, 212, 103428. <https://doi.org/10.1016/j.jmarsys.2020.103428>.

SANTOS, V. H. M., DIAS, F. J. S., TORRES, A. R., SOARES, R. A., TERETO, L. C., CASTRO, A. C. L., SANTOS, R. L., CUTRIM, M. V. J., 2020. Hydrodynamics and suspended particulate matter retention in macrotidal estuaries located in Amazonia-semiarid interface (Northeastern-Brazil). *International Journal of Sediment Research*, 35(4), 417–429. <https://doi.org/10.1016/j.ijsrc.2020.03.004>.

SAR, E. A., SUNESEN, I. L., 2002. The diatom genus *Thalassiosira*: species from the northern San Matias Gulf (Rio Negro, Argentina). *Nova Hedwigia*, 74(3–4), 373–386. <https://doi.org/10.1127/0029-5035/2002/0074-0373>.

SHANNON, C.E., 1948. A mathematical theory of communication. *Bell Syst. Tech. J* 27, 379–423.

- SHARPLES, J., MIDDELBURG, J.J., FENNEL, K., JICKELLS, T.D., 2017. What proportion of riverine nutrients reaches the open ocean? *Global Biogeochemical Cycles*, 31(1), 39–58. <https://doi.org/10.1002/2016gb005483>
- SMAYDA, T. J., 1983. The phytoplankton of estuaries (pp. 65–112). Amsterdam, the Netherlands: Elsevier Press.
- SMITH, V. H., FOSTER, B. L., GROVER, J. P., HOLT, R. D., LEIBOLD, M. A., DENOYELLES, F., 2005. Phytoplankton species richness scales consistently from laboratory microcosms to the world's oceans. *Proceedings of the National Academy of Sciences*, 102(12), 4393–4396. <https://doi.org/10.1073/pnas.0500094102>.
- SOCOLAR, J. B., GILROY, J. J., KUNIN, W. E., EDWARDS, D. P., 2016. How Should Beta-Diversity Inform Biodiversity Conservation? *Trends in Ecology Evolution*, 31(1), 67–80. <https://doi.org/10.1016/j.tree.2015.11.005>.
- SOININEN, J., HEINO, J., WANG, J., 2017. A meta-analysis of nestedness and turnover components of beta diversity across organisms and ecosystems. *Global Ecology and Biogeography*, 27(1), 96–109. Portico. <https://doi.org/10.1111/geb.12660>.
- SOUZA-FILHO, P. W. M., 2005. Costa de manguezais de macromaré da Amazônia: cenários morfológicos, mapeamento e quantificação de áreas usando dados de sensores remotos. *Revista Brasileira de Geofísica*, 23(4), 427–435. <https://doi.org/10.1590/s0102-261x2005000400006>.
- SOUZA-FILHO, P. W. M., LESSA, G. C., COHEN, M. C. L., COSTA, F. R., LARA, R. J., 2009. The Subsiding Macrotidal Barrier Estuarine System of the Eastern Amazon Coast, Northern Brazil. *Lecture Notes in Earth Sciences*, 107, 347–375. https://doi.org/10.1007/978-3-540-44771-9_11.
- STRICKLAND, J. D. H. T. R. PARSONS., 1972. A practical handbook of seawater analysis. *Bulletin Fisheries Research Board of Canada*, Ottawa 167: 1–205.
- STUKEL, M. R., COLES, V. J., BROOKS, M. T., HOOD, R. R., 2014. Top-down, bottom-up and physical controls on diatom-diazotroph assemblage growth in the Amazon River lume. *Biogeosciences*, 11(12), 3259–3278. <https://doi.org/10.5194/bg-11-3259-2014>.
- SUBRAMANIAM, A., YAGER, P. L., CARPENTER, E. J., MAHAFFEY, C., BJÖRKMAN, K., COOLEY, S., KUSTKA, A. B., MONTOYA, J. P., SAÑUDO-WILHELMY, S. A., SHIPE, R., CAPONE, D. G., 2008. Amazon River enhances diazotrophy and carbon sequestration in the tropical North Atlantic Ocean. *Proceedings of the National Academy of Sciences*, 105(30), 10460–10465. <https://doi.org/10.1073/pnas.0710279105>.
- SWEET, J. A., BARGU, S., MORRISON, W. L., PARSONS, M., PATHARE, M. G., ROBERTS, B. J., SONIAT, T. M., STAUFFER, B. A., 2022. Phytoplankton dynamics in Louisiana estuaries: Building a baseline to understand current and future change. *Marine Pollution Bulletin*, 175, 113344. <https://doi.org/10.1016/j.marpolbul.2022.113344>.

- THOMPSON, P. A., O'BRIEN, T. D., PAERL, H. W., PEIERLS, B. L., HARRISON, P. J. AND ROBB, M., 2015. Precipitation as a driver of phytoplankton ecology in coastal waters: A climatic perspective. *Estuarine, Coastal and Shelf Science*, 162, 119–129. <https://doi.org/10.1016/j.ecss.2015.04.004>.
- TONKIN, J. D., STOLL, S., JÄHNIG, S. C., HAASE, P., 2015. Contrasting metacommunity structure and beta diversity in an aquatic-floodplain system. *Oikos*, 125(5), 686–697. Portico. <https://doi.org/10.1111/oik.02717>.
- TOSETTO, E. G., BERTRAND, A., NEUMANN-LEITÃO, S., NOGUEIRA JÚNIOR, M., 2022. The Amazon River plume, a barrier to animal dispersal in the Western Tropical Atlantic. *Scientific Reports*, 12(1). <https://doi.org/10.1038/s41598-021-04165-z>.
- UTERMÖHL, H., 1958. Zur Vervollkommnung der quantitativen Phyto-plankton Methodik. *Mitt Int. Verein. Theor. Angew. Limnology and Oceanography*. 9, 1–38.
- VILLAFAÑE, V.E. REID, F.M.H., 1995. Métodos de microscopía para la cuantificación del fitoplancton. In: ALVEAR, K., FERRARIO, M.E., OLIVEIRA FILHO, E.C., SARS, E. (Eds.), *Manual de métodos ficológicos*. Universidad de Concepción, Chile, pp. 169–185.
- WANG, X., TANG, K. W., 2022. Chain or sphere? Perspectives on colony shapes and sizes in microalgae. *Journal of Plankton Research*, 44(4), 521–527. <https://doi.org/10.1093/plankt/fbac032>.
- WANG, Z., LIU, L., TANG, Y., LI, A., LIU, C., XIE, C., XIAO, L., LU, S., 2022. Phytoplankton community and HAB species in the South China Sea detected by morphological and metabarcoding approaches. *Harmful Algae*, 118, 102297. <https://doi.org/10.1016/j.hal.2022.102297>.
- WETZEL, C. E., BICUDO, D. DE C., ECTOR, L., LOBO, E. A., SOININEN, J., LANDEIRO, V. L., BINI, L. M., 2012. Distance Decay of Similarity in Neotropical Diatom Communities. *PLoS ONE*, 7(9), e45071. <https://doi.org/10.1371/journal.pone.0045071>.
- WILSON, J. R., WILKERSON, F. P., BLASER, S. B., NIELSEN, K. J., 2020. Phytoplankton Community Structure in a Seasonal Low-Inflow Estuary Adjacent to Coastal Upwelling (Drakes Estero, CA, USA). *Estuaries and Coasts*, 44(3), 769–787. <https://doi.org/10.1007/s12237-020-00792-3>.
- WU, K., DAI, M., LI, X., MENG, F., CHEN, J., LIN, J., 2017. Dynamics and production of dissolved organic carbon in a large continental shelf system under the influence of both river plume and coastal upwelling. *Limnol. Oceanogr.* 62, 973–988. <https://doi.org/10.1002/lno.10479>.
- YANG, X., TAN, Y., LI, K., ZHANG, H., LIU, J., XIANG, C., 2020. Long-term changes in summer phytoplankton communities and their influencing factors in Daya Bay, China (1991–2017). *Marine Pollution Bulletin*, 161, 111694. <https://doi.org/10.1016/j.marpolbul.2020.111694>.

YELLEN, B., WOODRUFF, J. D., RALSTON, D. K., MACDONALD, D. G., JONES, D. S., 2017. Salt wedge dynamics lead to enhanced sediment trapping within side embayments in high-energy estuaries. *Journal of Geophysical Research: Oceans*, 122(3), 2226–2242. Portico. <https://doi.org/10.1002/2016jc012595>.

YEUNG, L. Y., BERELSON, W. M., YOUNG, E. D., PROKOPENKO, M. G., ROLLINS, N., COLES, V. J., MONTOYA, J. P., CARPENTER, E. J., STEINBERG, D. K., FOSTER, R. A., CAPONE, D. G., YAGER, P. L., 2012. Impact of diatom-diazotroph associations on carbon export in the Amazon River plume. *Geophysical Research Letters*, 39(18). Portico. <https://doi.org/10.1029/2012gl053356>.

ZELNIK, I., BALANČ, T., TOMAN, M., 2018. Diversity and Structure of the Tychoplankton Diatom Community in the Limnocrene Spring Zelenci (Slovenia) in Relation to Environmental Factors. *Water*, 10(4), 361. <https://doi.org/10.3390/w10040361>.

ZHONG, Q., XUE, B., NOMAN, M. A., WEI, Y., LIU, H., LIU, H., ZHENG, L., JING, H., SUN, J., 2020. Effect of river plume on phytoplankton community structure in Zhujiang River estuary. *Journal of Oceanology and Limnology*, 39(2), 550–565. <https://doi.org/10.1007/s00343-020-9213-7>.

ZORZAL-ALMEIDA, S., BARTOZEK, E. C. R., BICUDO, D. C., 2021. Homogenization of diatom assemblages is driven by eutrophication in tropical reservoirs. *Environmental Pollution*, 288, 117778. <https://doi.org/10.1016/j.envpol.2021.117778>.

ZORZAL-ALMEIDA, S., BINI, L. M., BICUDO, D. C., 2017. Beta diversity of diatoms is driven by environmental heterogeneity, spatial extent and productivity. *Hydrobiologia*, 800(1), 7–16. <https://doi.org/10.1007/s10750-017-3117-3>.

7 CONSIDERAÇÕES FINAIS

A Baía de Cumã e plataforma continental adjacente fazem parte de uma área privilegiada da costa maranhense por ser considerada Sítio Ramsar e oferecer importantes serviços ecossistêmicos à população local, além de fazer parte da maior faixa contínua de manguezais do mundo. A fim de preencher uma lacuna sobre o conhecimento do fitoplâncton na região, este estudo é a primeira contribuição científica que buscou compreender os padrões da dinâmica fitoplanctônica (diversidade, estrutura e biomassa) avaliada em escala espacial e temporal e sua relação com aspectos hidrológicos fortemente influenciados por fatores climáticos (elevada precipitação anual) e hidrodinâmicos (regimes de macromarés) característicos da Costa Norte Amazônica.

Assim, a partir de uma abordagem eco-hidrológica utilizada na Baía de Cumã foi possível identificar uma comunidade com predomínio de diatomáceas altamente diversas. A variabilidade temporal das condições ambientais foi o principal controlador da distribuição da comunidade fitoplanctônica, demonstrando um padrão sazonal marcante, com predomínio de águas mais salinas e com menor temperatura e maior disponibilidade de luz durante o período chuvoso e na estiagem foi notável a maior incidência dos ventos, influência de macromarés e intrusão de águas marinhas no ecossistema costeiro. Tais condições favoreceram a ocorrência de florações eventuais de *Skeletonema costatum* no período chuvoso e altas densidades de *Thalassiosira subtilis* na estiagem, consideradas espécies-chaves dos diferentes períodos sazonais investigados.

Em nossas observações, as métricas de diversidade também responderam às flutuações sazonais das condições hidrológicas apontando o índice de riqueza de Menhinick e o índice de diversidade de Shannon como os mais sensíveis a estas mudanças ambientais. Além disso, observou-se que a alta biomassa fitoplanctônica (clorofila-a) e o bom estado fisiológico das células fitoplanctônicas atuaram como indicadores do bom estado de conservação desse ecossistema tropical amazônico.

Tendo em vista investigar o status ecológico do fitoplâncton (traços funcionais, espécies indicadoras e diversidade beta) e os seus processos determinantes ao longo de um *continuum* estuário-oceano, os resultados revelaram que a intensa drenagem continental sobre a costa maranhense promove gradientes ambientais que influenciam substancialmente a ciclagem de nutrientes, comunidade fitoplanctônica e diversidade beta.

Então, a partir disso foi identificada uma heterogeneidade espacial das condições hidrológicas (gradiente de salinidade, disponibilidade de luz e nutrientes) desde a porção interna da baía, área de influência da pluma estuarina e porção externa da plataforma que condicionaram os principais grupos fitoplanctônicos.

Neste estudo, foi possível selecionar 39 espécies indicadoras do fitoplâncton que foram sensíveis às mudanças nos gradientes ambientais apresentando traços funcionais típicos de ecossistemas altamente dinâmicos. Nesse contexto, identificou-se o predomínio de diatomáceas penadas solitárias e cêntricas coloniais na Baía de Cumã, diatomáceas cêntricas coloniais e cianobactérias filamentosas ao longo da pluma estuarina e diatomáceas cêntricas solitárias na porção externa da plataforma, além de nove novos registros para a região de espécies potencialmente tóxicas e formadoras de *blooms*, o que indica a necessidade de monitoramento dessas espécies na área estudada por ser uma importante região de pesca.

Por fim, a análise de diversidade beta foi uma importante ferramenta para avaliar mudanças nas escalas espaciais e temporais, sendo aplicada para entender os padrões de heterogeneidade ambiental os quais se tornam cruciais para compreender ambientes costeiros dinâmicos. A substituição de espécies foi o principal componente responsável por impulsionar a diversidade beta total ao longo das escalas estudadas, sendo explicada pelo efeito sinergético dos processos do ponto de vista espacial, ambiental, climatológico e hidrológico.

Além disso, este estudo reforça a importância da manutenção de séries temporais para melhor compreensão da dinâmica da comunidade fitoplanctônica em ambientes de alta complexidade como os encontrados na Costa Norte Amazônica. Estudos adicionais sobre a comunidade fitoplanctônica como a avaliação da produtividade primária, quantificação do picofitoplâncton, bem como estudos sobre a trofodinâmica do plâncton e o monitoramento de floração sazonal poderão fornecer mais orientações para o manejo sustentável dos ecossistemas costeiros amazônicos.

REFERÊNCIAS

- ABONYI, A.; DESCY, J. P.; BORICS, G.; SMETI, E. From historical backgrounds towards the functional classification of river phytoplankton sensu Colin S. Reynolds: what future merits the approach may hold? **Hydrobiologia**, v. 848, n. 1, p. 131–142, 2021. DOI: 10.1007/s10750-020-04300-3.
- ALMEIDA-FUNO, I. C. S.; PINHEIRO, C. U. B.; MONTELES, J. S. Identificação de tensores ambientais nos ecossistemas aquáticos da área de proteção ambiental (APA) da Baixada Maranhense. **Revista Brasileira de Agroecologia**, v. 5, n. 1, p. 74-85, 2010.
- ANDERSON, M. J.; ELLINGSEN, K. E.; MCARDLE, B. H. Multivariate dispersion as a measure of beta diversity. **Ecology Letters**, v. 9, n. 6, p. 683–693, 2006. DOI: <https://doi.org/10.1111/j.1461-0248.2006.00926.x>.
- AQUINO, R.; NORIEGA, C.; MASCARENHAS, A.; COSTA, M.; MONTEIRO, S.; SANTANA, L.; SILVA, I.; PRESTES Y.; ARAUJO, M.; ROLLNIC, M. Possible Amazonian contribution to Sargassum enhancement on the Amazon Continental Shelf. **Science of the Total Environment**, v. 853, e158432, 2022. DOI: <https://doi.org/10.1016/j.scitotenv>.
- ARAUJO, M.; NORIEGA, C.; HOUNSOU-GBO, G. A.; VELEDA, D.; ARAUJO, J., BRUTO, L.; FEITOSA, F.; FLORES-MONTES, M.; LEFÈVRE, N.; MELO, P., OTSUKA, A.; TRAVASSOS, K.; SCHWAMBORN, R.; NEUMANN-LEITÃO, S. A Synoptic Assessment of the Amazon River-Ocean Continuum during Boreal Autumn: From Physics to Plankton Communities and Carbon Flux. **Frontiers in Microbiology**, v. 8, e 1358, 2017. DOI: <https://doi.org/10.3389/fmicb.2017.01358>.
- AZEVEDO, A. C. G DE; FEITOSA, F. A. N.; KOENING, M. L. Distribuição espacial e temporal da biomassa fitoplanctônica e variáveis ambientais no Golfão Maranhense, Brasil. **Acta Botanica Brasilica**, v. 22, n. 3, p. 870-877, 2008. DOI: <https://doi.org/10.1590/s0102-33062008000300022>.
- AZHIKODAN, G.; YOKOYAMA, K. Spatio-temporal variability of phytoplankton (Chlorophyll-a) in relation to salinity, suspended sediment concentration, and light intensity in a macrotidal estuary. **Continental Shelf Research**, v. 126, p. 15–26, 2016. DOI: <https://doi.org/10.1016/j.csr.2016.07.006>.
- BAO, L.; CHEN, J.; TONG, H.; QIAN, J.; LI, X. Phytoplankton dynamics and implications for eutrophication management in an urban river with a series of rubber dams. **Journal of Environmental Management**, v. 311, e114865, 2022. DOI: <https://doi.org/10.1016/j.jenvman.2022.114865>.
- BASELGA, A. Partitioning the turnover and nestedness components of beta diversity. **Global Ecology Biogeography**, v. 19, n. 134–143, 2010. DOI: <https://doi.org/10.1111/j.1466-8238.2009.00490.x>.
- BRADBURY, I. R.; LAUREL, B.; SNELGROVE, P. V. R.; BENTZEN, P.; CAMPANA, S. E. Global patterns in marine dispersal estimates: the influence of geography, taxonomic category and life history. **Proceedings of the Royal Society B: Biological Sciences**, v. 275, n. 1644, p. 1803–1809, 2008. DOI: <https://doi.org/10.1098/rspb.2008.0216>

- RANDINI, F.P.; LOPES, R.M.; GUTSEIT, K.S.; SPACH, H.L.; SASSI, R. **Planctonologia na plataforma continental do Brasil: diagnose e revisão bibliográfica.** Fundação de Estudos do Mar- FEMAR. Rio de Janeiro. 255p., 1997.
- BRASIL. Instituto Brasileiro dos Recursos Naturais. Secretaria de Estado do Meio Ambiente e Turismo. **Diagnóstico dos principais problemas ambientais do estado do Maranhão.** São Luís: SEMATUR, 1991.
- BRASIL, J.; SANTOS, J. B. O.; SOUSA, W.; MENEZES, R. F.; HUSZAR, V. L. M.; ATTAYDE, J. L. Rainfall leads to habitat homogenization and facilitates plankton dispersal in tropical semiarid lakes. **Aquatic Ecology**, v. 54, n.1, p. 225–241, 2019. DOI: <https://doi.org/10.1007/s10452-019-09738-9>.
- BRUNSKILL, G. Tropical margins. In: LIU, K.; ATKINSON, L.; QUINONES, R.; TALAUE-MCMANUS, L. (Ed.) **Carbon and Nutrient Fluxes in Continental Margins - A Global Synthesis.** Springer, 2010. p. 423–426.
- CARVALHO, J. V.; SILVA, T. R. C.; CORDEIRO, A. F. Modificações socioambientais decorrentes da construção da barragem do Rio Pericumã, na área de influência da cidade de Pinheiro-Estado do Maranhão-Brasil. **Revista Geográfica de América Central**, número especial EGAL, p. 1-16, 2011. ISSN-2115-2563
- CASTRO, B.M.; MIRANDA, L.B. Physical oceanography of the western Atlantic Continental Shelf located between 4° N and 34° S. In: ROBINSON, A.R.; BRINK, K. H. (Ed.). **The sea.** New York: John Wile, 1998. p. 209- 251.
- CASTRO, L. S.; SOUZA LOPES, A. A.; COLARES, L.; PALHETA, L.; DE SOUZA MENEZES, M.; FERNANDES, L. M.; DUNCK, B. Dam promotes downriver functional homogenization of phytoplankton in a transitional river-reservoir system in Amazon. **Limnology**, v. 22, n. 2, p. 245–257, 2021. DOI: <https://doi.org/10.1007/s10201-021-00650-6>.
- CAVALCANTI, L. F.; AZEVEDO-CUTRIM, A. C. G.; OLIVEIRA, A. L. L.; FURTADO, J. A.; ARAÚJO, B. DE O.; SÁ, A. K. D.-S.; FERREIRA, F. S.; SANTOS, N. G. R.; DIAS, F. J. S.; CUTRIM, M. V. J. Structure of microphytoplankton community and environmental variables in a macrotidal estuarine complex, São Marcos Bay, Maranhão - Brazil. **Brazilian Journal of Oceanography**, v. 66, n. 3, p. 283–300, 2018. DOI: <https://doi.org/10.1590/s1679-87592018021906603>.
- CAVALCANTI, L. F.; CUTRIM, M. V. J.; LOURENÇO, C. B.; SÁ, A. K. D. S.; OLIVEIRA, A. L. L.; AZEVEDO-CUTRIM, A. C. G. Patterns of phytoplankton structure in response to environmental gradients in a macrotidal estuary of the Equatorial Margin (Atlantic coast, Brazil). **Estuarine, Coastal and Shelf Science**, 245, e106969, 2020. DOI: <https://doi.org/10.1016/j.ecss.2020.106969>.
- CHÉRUBIN, L. M.; RICHARDSON, P. L. Caribbean current variability and the influence of the Amazon and Orinoco freshwater plumes. **Deep Sea Research Part I: Oceanographic Research Papers**, v. 54, n. 9, p. 1451–1473, 2007. DOI: <https://doi.org/10.1016/j.dsr.2007.04.021>.

- CLOERN, J. E.; FOSTER, S. Q.; KLECKNER, A. E. Phytoplankton primary production in the world's estuarine-coastal ecosystems. **Biogeosciences**, v. 11, p. 2477–2501, 2014.
- COLES, V.J.; BROOKS, M.T.; HOPKINS, J.; STUKEL, M.R.; YAGER, P.L.; HOOD, R.R. The pathways and properties of the Amazon River plume in the tropical North Atlantic Ocean. **Journal of Geophysical Research Oceans**, v. 118, p. 6894–6913, 2013. DOI: <https://doi.org/10.1002/2013JC008981>.
- CORDEIRO, C. A. M. M.; QUIMBAYO, J. P.; NUNES, J. A. C. C.; NUNES, L. T.; SISSINI, M. N.; SAMPAIO, C. L. S.; MORAIS, R. A.; HORTA, P. A.; AUED, A. W.; CARRARO, J. L.; HAJDU, E.; ROCHA, L. A.; SEGAL, B.; FLOETER, S. R. Conservation status of the southernmost reef of the Amazon Reef System: the Parcel de Manuel Luís. **Coral Reefs**, v. 40, n. 1, p. 165–185, 2020. DOI: <https://doi.org/10.1007/s00338-020-02026-1>.
- COSTA, A. P. T.; CROSSETTI, L. O.; HARTZ, S. M.; BECKER, F. G.; HEPP, L. U.; BOHNENBERGER, J. E.; LIMA, M. S.; GUIMARÃES, T.; SCHNECK, F. Land cover is the main correlate of phytoplankton beta diversity in subtropical coastal shallow lakes. **Aquatic Ecology**, v. 54, n. 4, p. 1015–1028, 2020. DOI: <https://doi.org/10.1007/s10452-020-09790-w>.
- COSTA, D. DOS S.; CUTRIM, M. V. J. Spatial and seasonal variation in physicochemical characteristics and phytoplankton in an estuary of a tropical delta system. **Regional Studies in Marine Science**, v. 44, e101746, 2021. DOI: <https://doi.org/10.1016/j.rsma.2021.101746>.
- CZIZEWESKI, A.; PIMENTA, F. M.; SAAVEDRA, O. R. Numerical modeling of Maranhão Gulf tidal circulation and power density distribution. **Ocean Dynamics**, v. 70, n. 5, p. 667–682, 2020. DOI: <https://doi.org/10.1007/s10236-020-01354-8>.
- D'ALESSANDRO, E. B.; NOGUEIRA, I. D. S.; HOFFMANN, N. K. S. DEL A. Variability in phytoplankton community structure and influence on stabilization pond functioning. **Ambiente e Água - An Interdisciplinary Journal of Applied Science**, v. 15, n. 2, p. 1-13, 2020. DOI: <https://doi.org/10.4136/ambi-agua.2507>.
- DINIZ, L. P.; BRAGHIN, L. S. M.; PINHEIRO, T. S. A.; MELO, P. A. M. C.; BONECKER, C. C.; MELO JÚNIOR, M. Environmental filter drives the taxonomic and functional β-diversity of zooplankton in tropical shallow lakes. **Hydrobiologia**, v. 848, n. 8, p. 1881–1895, 2021. DOI: <https://doi.org/10.1007/s10750-021-04562-5>.
- DUARTE-DOS-SANTOS, A. K.; OLIVEIRA, A. L. L.; FURTADO, J. A.; FERREIRA, F. S.; ARAÚJO, B. O.; CORRÊA, J. J. M.; CAVALCANTI, L. F.; AZEVEDO-CUTRIM, A. C. G.; CUTRIM, M. V. J. Spatial and seasonal variation of microphytoplankton community and the correlation with environmental parameters in a hypereutrophic tropical estuary - Maranhão - Brazil. **Brazilian Journal of Oceanography**, v. 65, n. 3, p. 356–372, 2017. DOI: <https://doi.org/10.1590/s1679-87592017134406503>.
- EKAU, W.; KNOPPERS, B. An introduction to the pelagic system of the East and Northeast Brazilian shelf. **Archive of Fishery and Marine Research**, v. 47, p. 113-132, 1999.

FALKOWSKI, P.G. The ocean's invisible forest - Marine phytoplankton play a critical role in regulating the earth's climate: Could they also be used to combat global warming. **Scientific American**, v. 287, p. 54-61, 2002.

FALKOWSKI, P. Ocean Science: the power of plankton. **Nature**, v. 483, n. 7387, S17–S20, 2012.

FLAGG, C. N.; GORDON, R. L; McDOWELL, S. Hydrographic and Current Observations on the Continental Slope and Shelf of the Western Equatorial Atlantic. **Journal of Physical Oceanography**, v. 16, p. 1412-1429, 1986.

FRAU, D., PINEDA, A., MAYORA, G., GUTIERREZ, M. F. Eutrophication as a homogenizer process of phytoplankton β-diversity in lowland streams. **Limnologica**, v. 99, e126058, 2023. DOI: <https://doi.org/10.1016/j.limno.2023.126058>.

GOES, J. I.; GOMES, H. DO R.; CHEKALYUK, A. M.; CARPENTER, E. J.; MONTOYA, J. P.; COLES, V. J.; YAGER, P. L.; BERELSON, W. M.; CAPONE, D. G.; FOSTER, R. A.; STEINBERG, D. K.; SUBRAMANIAM, A.; HAFEZ, M. A. Influence of the Amazon River discharge on the biogeography of phytoplankton communities in the western tropical north Atlantic. **Progress in Oceanography**, v. 120, p. 29–40, 2014. DOI: <https://doi.org/10.1016/j.pocean.2013.07.010>.

GOES, E. R.; FERREIRA JÚNIOR, A. V. Caracterização Morfosedimentar da Plataforma Continental Brasileira (Morphosedimentary characterization of the Brazilian Continental Shelf). **Revista Brasileira de Geografia Física**, v. 10, n. 5, e1595, 2017. DOI: <https://doi.org/10.26848/rbgf.v.10.5.p1595-1613>.

GRACO-ROZA, C.; SOININEN, J.; CORRÊA, G.; PACHECO, F. S.; MIRANDA, M.; DOMINGOS, P.; MARINHO, M. M. Functional rather than taxonomic diversity reveals changes in the phytoplankton community of a large dammed river. **Ecological Indicators**, v. 121, e107048, 2021. DOI: <https://doi.org/10.1016/j.ecolind.2020.107048>.

GUALBERTO, L.P.S.; EL-ROBRINI, M. Faciologia da Cobertura Sedimentar Superficial da Plataforma Continental do Maranhão. **Estudos Geológicos**, v. 15, p. 234-243, 2005.

HAYASHI, S. N.; SOUZA-FILHO, P. W. M.; NASCIMENTO, W. R.; FERNANDES, M. E. B. The effect of anthropogenic drivers on spatial patterns of mangrove land use on the Amazon coast. **PLOS ONE**, v. 14, n. 6, e0217754, 2019. DOI: <https://doi.org/10.1371/journal.pone.0217754>.

HOLLIGAN, P.M.; DE BOOIS, H. **Land-Ocean Interactions in the Coastal Zone: science plan and implementation strategy**. In: KREMER, H.H.; LE TISSIER, M.D.A.; BURBRIDGE, P.R.; TALAUE-MCMANUS, L.; RABALAIS, N.N.; PARSLAW, J.; CROSSLAND, C.J., YOUNG, B. (Eds.), IGBP Report 51; IHDP Report 18. International Geosphere-Biosphere Programme - Science Plan, p. 25-50, Stockholm, 1993.

IBGE - INSTITUTO BRASILEIRO DE GEOGRAFIA E ESTATÍSTICA. **Censo demográfico 2010**. Rio de Janeiro: IBGE, 2017.

JARDILLIER, L.; ZUBKOV, M. V.; PEARMAN, J.; SCANLAN, D. J. Significant CO₂ fixation by small prymnesiophytes in the subtropical and tropical northeast Atlantic

Ocean. **The ISME Journal**, v. 4, n. 9, p.1180–1192, 2010. DOI: <https://doi.org/10.1038/ismej.2010.36>.

JYRKÄNKALLIO-MIKKOLA, J.; SILJANDER, M.; HEIKINHEIMO, V.; PELLIKKA, P.; SOININEN, J. Tropical stream diatom communities – The importance of headwater streams for regional diversity. **Ecological Indicators**, v. 95, p. 183–193, 2018. DOI: <https://doi.org/10.1016/j.ecolind.2018.07.030>.

KANG, Y.; MOON, C. H.; KIM, H. J.; YOON, Y. H.; KANG, C. K. Water Quality Improvement Shifts the Dominant Phytoplankton Group From Cryptophytes to Diatoms in a Coastal Ecosystem. **Frontiers in Marine Science**, v. 8, e710891, 2021. DOI: <https://doi.org/10.3389/fmars.2021.710891>.

KAHSAY, A.; LEMMENS, P.; TRIEST, L.; DE MEESTER, L.; KIBRET, M.; VERLEYEN, E.; ADGO, E.; WONDIE, A.; STIERS, I. Plankton Diversity in Tropical Wetlands Under Different Hydrological Conditions (Lake Tana, Ethiopia). **Frontiers in Environmental Science**, v. 10, e816892, 2022. DOI: <https://doi.org/10.3389/fenvs.2022.816892>.

KOURAFALOU, V. H.; OEHY, L. Y.; WANG, J. D.; LEE, T. N. The fate of river discharge on the continental shelf. 1. Modeling the river pluma and the inner shelf coastal current. **Journal of Geophysical Research**, v. 101, n. 2, p. 3415-3434, 1996.

KRUK, C.; DEVERCELLI, M.; HUSZAR, V. L. Reynolds functional groups: a trait-based pathway from patterns to predictions. **Hydrobiologia**, v. 848, p. 113–129, 2021. DOI: <https://link.springer.com/article/10.1007/s10750-020-04340-9>.

LANSAC-TÔHA, F. M.; HEINO, J.; QUIRINO, B. A.; MORESCO, G. A.; PELÁEZ, O.; MEIRA, B. R.; RODRIGUES, L. C.; JATI, S.; LANSAC-TÔHA, F. A.; VELHO, L. F. M. Differently dispersing organism groups show contrasting beta diversity patterns in a dammed subtropical river basin. **Science of The Total Environment**, v. 691, p. 1271–1281, 2019. DOI: <https://doi.org/10.1016/j.scitotenv.2019.07.236>.

LEFÈVRE, N.; DA SILVA DIAS, F. J.; DE TORRES, A. R.; NORIEGA, C.; ARAUJO, M.; DE CASTRO, A. C. L.; ROCHA, C.; JIANG, S.; IBÁNHEZ, J. S. P. A source of CO₂ to the atmosphere throughout the year in the Maranhense continental shelf (2°30'S, Brazil), **Continental Shelf Research**, v.141, p. 38–50, 2017. DOI: [10.1016/j.csr.2017.05.004](https://doi.org/10.1016/j.csr.2017.05.004).

LEGENDRE, P. Interpreting the replacement and richness difference components of beta diversity. **Global Ecology and Biogeography**, v. 23, p. 1324–1334, 2014.

LENTZ, S. J. The Amazon River plume during AmasSeds: Subtidal current variability and the importance of wind forcing. **Journal of Geophysical Research**, 100, 2377–2390, 1995.

LIMA, H. P., DIAS, F. J. S., TEIXEIRA, C. E. P., GODOI, V. A., TORRES, A. R., ARAÚJO, R. S. Implications of turbulence in a macrotidal estuary in northeastern Brazil - The São Marcos Estuarine Complex. **Regional Studies in Marine Science**, 47, 101947, 2021. DOI: <https://doi.org/10.1016/j.rsma.2021.101947>.

LIU, S.; CUI, Z.; ZHAO, Y.; CHEN, N. Composition and spatial-temporal dynamics of phytoplankton community shaped by environmental selection and interactions in the Jiaozhou Bay. **Water Research**, v. 218, e118488, 2022. DOI: <https://doi.org/10.1016/j.watres.2022.118488>.

LOPES, P. M.; CALIMAN, A.; CARNEIRO, L. S.; BINI, L. M.; ESTEVES, F. A.; FARJALLA, V.; BOZELLI, R. L. Concordance among assemblages of upland Amazonian lakes and the structuring role of spatial and environmental factors. **Ecological Indicators**, v. 11, n. 5, p.1171–1176, 2011. DOI: <https://doi.org/10.1016/j.ecolind.2010.12.017>.

LOURENÇO, C. B. **O fitoplâncton na Zona Costeira Amazônica Brasileira: Biodiversidade, distribuição e estrutura no continuum estuário-oceano.** 2016. Tese (Doutorado em Ecologia Aplicada) - Ecologia de Agroecossistemas, Universidade de São Paulo, Piracicaba, 2016. DOI: 10.11606/T.91.2017.tde-05012017-142253.

LUIZ, O. J.; MADIN, J. S.; ROBERTSON, D. R.; ROCHA, L. A.; WIRTZ, P., FLOETER, S. R. Ecological traits influencing range expansion across large oceanic dispersal barriers: insights from tropical Atlantic reef fishes. **Proceedings of the Royal Society B: Biological Sciences**, v. 279, n. 1730, p. 1033–1040, 2011. DOI: <https://doi.org/10.1098/rspb.2011.1525>.

MACEDO, L. A. A. Controle ambiental do Golfão Maranhense. **DAE**, v. 49, n. 155, p. 1-7, 1989.

MARANHÃO. Atlas do Maranhão. **Gerência de Planejamento e Desenvolvimento Econômico/Laboratório de Geoprocessamento - UEMA**. São Luís: GEPLAN, 44p., 2002.

MARTINS, M. B.; OLIVEIRA, T.G. **Amazônia Maranhense: diversidade e conservação.** Belém: MPEG, 2011. 328 p.

MASCARENHAS, A. C. C.; GOMES, G. S.; LIMA, A. P. Y.; DA SILVA, H. K. N.; SANTANA, L. S.; ROSÁRIO, R. P.; ROLLNIC, M. Seasonal Variations of the Amazon River Plume with Focus on the Eastern Sector. **Journal of Coastal Research**, v. 75, n. 1, p. 532–536, 2016. DOI: <https://doi.org/10.2112/si75-107.1>.

MENEZES, M. P. M.; BERGER, U.; MEHLIG, U. Mangrove vegetation in Amazonia: a review of studies from the coast of Pará and Maranhão States, north Brazil. **Acta Amazonica**, v. 38, n. 3, p. 403–420, 2008. DOI: <https://doi.org/10.1590/s0044-59672008000300004>.

MOURA, W. B.; DA SILVA, P. R. L.; BAUMGARTNER, G.; BUENO, N. C.; BORTOLINI, J. C. Site contributions to phytoplankton beta diversity along two subtropical reservoirs. **Aquatic Sciences**, v. 84, n. 4, p. 1-18, 2022. DOI: <https://doi.org/10.1007/s00027-022-00890-3>.

MOUSING, E. A.; RICHARDSON, K.; BENDTSEN, J.; CETINIĆ, I.; PERRY, M. J. Evidence of small-scale spatial structuring of phytoplankton alpha- and beta-diversity in the open ocean. **Journal of Ecology**, v. 104, n. 6, p. 1682–1695, 2016. DOI: <https://doi.org/10.1111/1365-2745.12634>.

NABOUT, J. C.; DE NOGUEIRA, I. S.; DE OLIVEIRA, L. G.; MORAIS, R. R. Phytoplankton diversity (alpha, beta, and gamma) from the Araguaia River tropical floodplain lakes (central Brazil). **Hydrobiologia**, v. 575, n. 1, p. 455–461, 2006. <https://doi.org/10.1007/s10750-006-0393-8>.

NASCIMENTO, W. R.; SOUZA-FILHO, P. W. M.; PROISY, C.; LUCAS, R. M.; ROSENQVIST, A. Mapping changes in the largest continuous Amazonian mangrove belt using object-based classification of multisensor satellite imagery. **Estuarine, Coastal and Shelf Science**, v. 117, p. 83–93, 2013. DOI: <https://doi.org/10.1016/j.ecss.2012.10.005>.

NASELLI-FLORES, L.; PADISÁK, J. Ecosystem services provided by marine and freshwater phytoplankton. **Hydrobiologia**, v. 28, p. 1-16, 2022. DOI: <https://doi.org/10.1007/s10750-022-04795-y>.

NETO, J.A.B.; SILVA, C.G. Morfologia do fundo oceânico. In: NETO, J.A.B.; PONZI, V.R.A.; SICHEL, S E. (Ed.). **Introdução à geologia marinha**. Rio de Janeiro: Editora Interciênciac, 2004. 279p.

NETO, A. A.; FALCÃO, L. C.; AMARAL, P. J. T. Caracterização de ecofácies na margem continental norte Brasileira: estado do conhecimento. **Revista Brasileira de Geofísica**, v. 27, n. 1, 2009. DOI: <https://doi.org/10.1590/S0102-261X2009000500008>.

NITTROUER, C.A.; DEMASTER, D.J.; FIGUEIREDO, A.G.; RINE, J.M. AmasSeds: an interdisciplinary investigation of a complex coastal environment. **Oceanography**, v. 4, p. 3–7, 1991.

NITTROUER, C. A.; DeMASTER, D. J. The Amazon shelf setting: tropical, energetic, and influenced by a large river. **Continental Shelf Research**, v. 16, n. 5-6, p. 553–573, 1996. DOI: [10.1016/0278-4343\(95\)00069-0](https://doi.org/10.1016/0278-4343(95)00069-0).

NWE, L.W.; YOKOYAMA, K.; AZHIKODAN G. Phytoplankton habitats and size distribution during a neap-spring transition in the highly turbid macrotidal Chikugo River estuary. **Science of The Total Environment**, v. 850, e157810, 2022. DOI: <https://doi.org/10.1016/j.scitotenv.2022.157810>.

OLIVEIRA, P. H. F. DE; MACHADO, K. B.; TERESA, F. B.; HEINO, J.; NABOUT, J. C. Spatial processes determine planktonic diatom metacommunity structure of headwater streams. **Limnologica**, v. 84, e125813, 2020. DOI: <https://doi.org/10.1016/j.limno.2020.125813>.

OLLI, K.; NYMAN, E.; TAMMINEN, T. Half-century trends in alpha and beta diversity of phytoplankton summer communities in the Helsinki Archipelago, the Baltic Sea. **Journal of Plankton Research**, efbac029, 2022. DOI: <https://doi.org/10.1093/plankt/fbac029>.

OTSUKA, A.; NORIEGA, C.; FEITOSA, F.; BORGES, G.; MONTES, M. F.; ARAUJO, M.; SILVA-CUNHA, M. G. Characterization of microphytoplankton associations on the Amazon continental shelf and in the adjacent oceanic region. **Journal of Sea Research**, v. 189, e102271, 2022. DOI: <https://doi.org/10.1016/j.seares.2022.102271>.

PADISÁK, J.; CROSSETTI, L. O.; NASELLI-FLORES, L. Use and misuse in the application of the phytoplankton functional classification: a critical review with updates. **Hydrobiologia**, v. 621, p. 1–19, 2009.

PAERL, H. W.; VALDES, L. M.; PINCKNEY, J. L.; PIEHLER, M. F.; DYBLE, J.; MOISANDER, P. H. Phytoplankton photopigments as indicators of estuarine and coastal eutrophication. **AIBS Bull**, v. 53, p. 953–964, 2003. DOI: 10.1641/0006-3568(2003)053[0953:ppaioe]2.0.co;2

PAERL, H. W.; ROSSIGNOL, K. L.; HALL, N. S.; PEIERLS, B. L.; WETZ, M. S. Phytoplankton community indicators of short- and long-term ecological change in the anthropogenically and climatically impacted Neuse River Estuary, North Carolina, USA. **Estuaries and Coasts**, v. 33, p. 485–497, 2010. DOI: <https://doi.org/10.1007/s12237-009-9137-0>.

PALMA, J. J. C. **Geomorfologia da Plataforma Continental Brasileira**, In: CHAVES, H. A. F. (ed.). Geomorfologia da margem continental brasileira e das áreas adjacentes. (Relatório Final). PETROBRÁS/CENPES/DINTEP. Projeto REMAC. Rio de Janeiro, p. 25-51, 1979.

PEREIRA, L. C. C.; DIAS, J. A.; DO CARMO, J. A.; POLETTE, M. A Zona costeira amazônica brasileira. **Revista de Gestão Costeira Integrada**, v. 9, n. 2, p. 3-7, 2009.

PEREIRA, L.C.C.; VILA-CONCEJO, A.; TRINDADE, W.N.; SHORT, A.D. Influence of high-energy conditions on beach changes in tide-dominated (Amazon, Brazil) and wave-dominated (NSW, Australia) coastal environments. **Journal of Coastal Research**, v. 64, p. 115–119, 2011.

PEREIRA, L. C. C.; SOUSA-FELIX, R. C.; COSTA, R. M.; JIMENEZ, J. A. Challenges of the recreational use of Amazon beaches. **Ocean Coastal Management**, v. 165, p. 52–62, 2018. DOI: <https://doi.org/10.1016/j.ocecoaman.2018.08.012>.

PRESTES, Y. O.; BORBA, T. A. C.; SILVA, A. C.; ROLLNIC, M. A discharge stationary model for the Pará-Amazon estuarine system. **Journal of Hydrology: Regional Studies**, v. 28, e100668, 2020. DOI: <https://doi.org/10.1016/j.ejrh.2020.100668>.

PTACNIK, R.; SOLIMINI, A. G.; ANDERSEN, T.; TAMMINEN, T.; BRETTUM, P.; LEPISTO, L.; WILLE'N, E. REKOLAINEN, S. Diversity predicts stability and resource use efficiency in natural phytoplankton communities. **Proceedings of the National Academy of Sciences**, v. 105, p. 5134–5138, 2008.

QUEIROZ, J. B. M.; OLIVEIRA, A. R. G. DE; COSTA, K. G. DA; BRITO, E. P.; FERNANDES, F. D. DOS S.; NUNES, Z. M. P.; KOENING, M. L.; PEREIRA, L. C. C.; DA COSTA, R. M. Phytoplankton of the shipping sector of São Marcos Bay (Amazon Coast): A potential risk area for the establishment of non-indigenous species. **Regional Studies in Marine Science**, v. 49, e102121, 2022. DOI: <https://doi.org/10.1016/j.rsma.2021.102121>.

RAMESH, R.; CHEN, Z.; CUMMINS, V.; DAY, J.; D'ELIA, C.; DENNISON, B.; FORBES, D. L.; GLAESER, B.; GLASER, M.; GLAVOVIC, B.; KREMER, H.; LANGE, M.; LARSEN, J. N.; LE TISSIER, M.; NEWTON, A.; PELLING, M.;

PURVAJA, R.; WOLANSKI, E. Land–Ocean Interactions in the Coastal Zone: Past, present and future. **Anthropocene**, v. 12, p. 85–98, 2015. DOI: <https://doi.org/10.1016/j.ancene.2016.01.005>.

REYNOLDS, C. S.; HUSZAR, V.; KRUK, C.; NASELLI-FLORES, L. MELO, S. Towards a functional classification of the freshwater phytoplankton. **Journal of Plankton Research**, v. 24, p. 417–428, 2002.

REYNOLDS, C.S. **Ecology of Phytoplankton** (Ecology, Biodiversity and Conservation). Cambridge: Cambridge University Press, 2006. 552p.

RODRIGUES, E. I.; CUTRIM, M. V. J. Relações entre as variáveis físicas, químicas e fitoplanctônicas de três áreas estuarinas da costa norte do Brasil - São José de Ribamar, Cedral e Cajapió, MA. **Arquivos Ciências do Mar**, v. 43, n. 2, p. 45-54, 2010.

ROMBOUTS, I.; SIMON, N.; AUBERT, A.; CARIOU, T.; FEUNTEUN, E.; GUÉRIN, L.; HOEBEKE, M.; MCQUATTERS-GOLLOP, A.; RIGAUT-JALABERT, F.; ARTIGAS, L. F. Changes in marine phytoplankton diversity: Assessment under the Marine Strategy Framework Directive. **Ecological Indicators**, v. 102, p. 265–277, 2019. DOI: <https://doi.org/10.1016/j.ecolind.2019.02.009>.

RUSANOV, A. G.; BÍRÓ, T.; KISS, K. T.; BUCZKÓ, K.; GRIGORSZKY, I.; HIDAS, A.; DUŁEBA, M.; TRÁBERT, Z.; FÖLDI, A.; ÁCS, É. Relative importance of climate and spatial processes in shaping species composition, functional structure and beta diversity of phytoplankton in a large river. **Science of The Total Environment**, v. 807, e150891, 2022. DOI: <https://doi.org/10.1016/j.scitotenv.2021.150891>.

RYTHER, J. H. Photosynthesis and Fish Production in the Sea. **Science**, v. 166, n. 3901, p. 72–76, 1969. DOI: <https://doi.org/10.1126/science.166.3901.72>.

SAMPAIO, M. F.; FERREIRA, P. C.; VEIGA LUDWIG, T. A.; PADIAL, A. A. Temporal stability in beta diversity does not guarantee surrogacy or compositional stability in a micro-phytoplankton metacommunity. **Limnetica**, v. 42, n. 1, p. 127-141, 2023. DOI: <https://doi.org/10.23818/limn.42.10>.

SÁ, A. K. D. S.; FEITOSA, F. A. N.; CUTRIM, M. V. J.; FLORES-MONTES, M. J.; COSTA, D.S.; CAVALCANTI, L. F. Phytoplankton community dynamics in response to seawater intrusion in a tropical macrotidal river-estuary continuum. **Hydrobiologia**, [S.I.], 2022. DOI: <https://doi.org/10.1007/s10750-022-04851-7>.

SANTOS, J. B. O.; SILVA, L. H. S.; BRANCO, C. W. C.; HUSZAR, V. L. M. The roles of environmental conditions and geographical distances on the species turnover of the whole phytoplankton and zooplankton communities and their subsets in tropical reservoirs. **Hydrobiologia**, v. 764, n. 1, p. 171–186, 2015. DOI: <https://doi.org/10.1007/s10750-015-2296-z>.

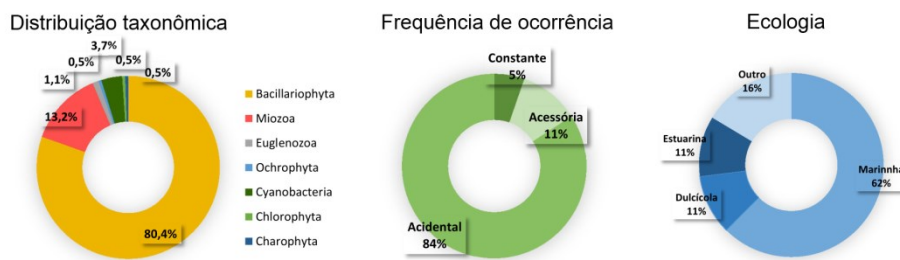
SANTOS, V. H. M.; DIAS, F. J. S.; TORRES, A. R.; SOARES, R. A.; TERTO, L. C.; DE CASTRO, A. C. L.; SANTOS, R. L.; CUTRIM, M. V. J. Hydrodynamics and suspended particulate matter retention in macrotidal estuaries located in Amazonia-semiarid interface (Northeastern-Brazil). **International Journal of Sediment Research**, v. 35, n. 4, p. 417–429, 2020. DOI: 10.1016/j.ijsrc.2020.03.004.

- SATHICQ, M. B.; GÓMEZ, N.; BAUER, D. E.; DONADELLI, J. Use of phytoplankton assemblages to assess the quality of coastal waters of a transitional ecosystem: río de La Plata estuary. **Continental Shelf Research**, v. 150, p. 10–17, 2017. DOI: 10.1016/j.csr.2016.08.009.
- SCHUSTER, K. F.; TREMARIN, P. I.; SOUZA-FRANCO, G. M. DE. Alpha and beta diversity of phytoplankton in two subtropical eutrophic streams in southern Brazil. **Acta Botanica Brasilica**, v. 29, n. 4, p. 597–607, 2015. DOI: <https://doi.org/10.1590/0102-33062015abb0060>.
- SHARPLES, J.; MIDDELBURG, J.J.; FENNEL, K.; JICKELLS, T.D. What proportion of riverine nutrients reaches the open ocean? **Global Biogeochemical Cycles**, v. 31, n. 1, p. 39–58, 2017. DOI: <https://doi.org/10.1002/2016gb005483>.
- SILVA, E. A. C. **Influência da pluma do Rio Amazonas na distribuição da abundância dos organismos zooplânctônicos na Plataforma Continental Amazônica (Pará, Brasil)**. Trabalho de Conclusão de Curso (Graduação em Engenharia de Pesca). Universidade Federal Rural da Amazônia. Belém, 2019. 34 f.
- SILVEIRA, I. C. A.; BROWN, W. S.; FLIERL, G. Dynamics of the North Brazil Current Retroflection Region from the WESTRAX Observations. **Journal of Geophysical Research**, v.99, p, 28559-28583, 2000.
- SIMON, N.; CRAS, A.L.; FOULON, E.; LEMEE, R. Diversity and evolution of marine phytoplankton. **Comptes Rendus Biologies**, v. 332, n. 2–3, p. 159–170, 2009.
- SMITH JR, W. O.; DEMASTER, D. J. Phytoplankton biomass and productivity in the Amazon River plume: correlation with seasonal river discharge. **Continental Shelf Research**, v.16, n. 3, p. 291-319, 1996.
- SOCOLAR, J. B.; GILROY, J. J.; KUNIN, W. E.; EDWARDS, D. P. How Should Beta-Diversity Inform Biodiversity Conservation? **Trends in Ecology Evolution**, v. 31, n. 1, p. 67–80, 2016. DOI: <https://doi.org/10.1016/j.tree.2015.11.005>.
- SOUZA-FILHO, P. W. M.; LESSA, G. C.; COHEN, M. C. L.; COSTA, F. R.; LARA, R. J. The Subsiding Macrotidal Barrier Estuarine System of the Eastern Amazon Coast, Northern Brazil. **Lecture Notes in Earth Sciences**, v. 107, p. 347–375, 2009. DOI: https://doi.org/10.1007/978-3-540-44771-9_11.
- SPALDING, M. D.; FOX, H. E.; ALLEN, G. R.; DAVIDSON, N.; FERDAÑA, Z. A.; FINLAYSON, M.; HALPERN, B. S.; JORGE, M. A.; LOMBANA, A.; LOURIE, S. A.; MARTIN, K. D.; MCMANUS, E.; MOLNAR, J.; RECCHIA, C. A.; ROBERTSON, J. Marine Ecoregions of the World: A Bioregionalization of Coastal and Shelf Areas. **BioScience**, v. 57, n. 7, p. 573–583, 2007. DOI: <https://doi.org/10.1641/b570707>.
- STEFANIDOU, N.; KATSIAPI, M.; TSIANIS, D.; DEMERTZIOGLOU, M.; MICHALOUDI, E.; MOUSTAKA-GOUNI, M. Patterns in Alpha and Beta Phytoplankton Diversity along a Conductivity Gradient in Coastal Mediterranean Lagoons. **Diversity**, v. 12, n. 1, p. 1-16, 2020. DOI: <https://doi.org/10.3390/d12010038>.

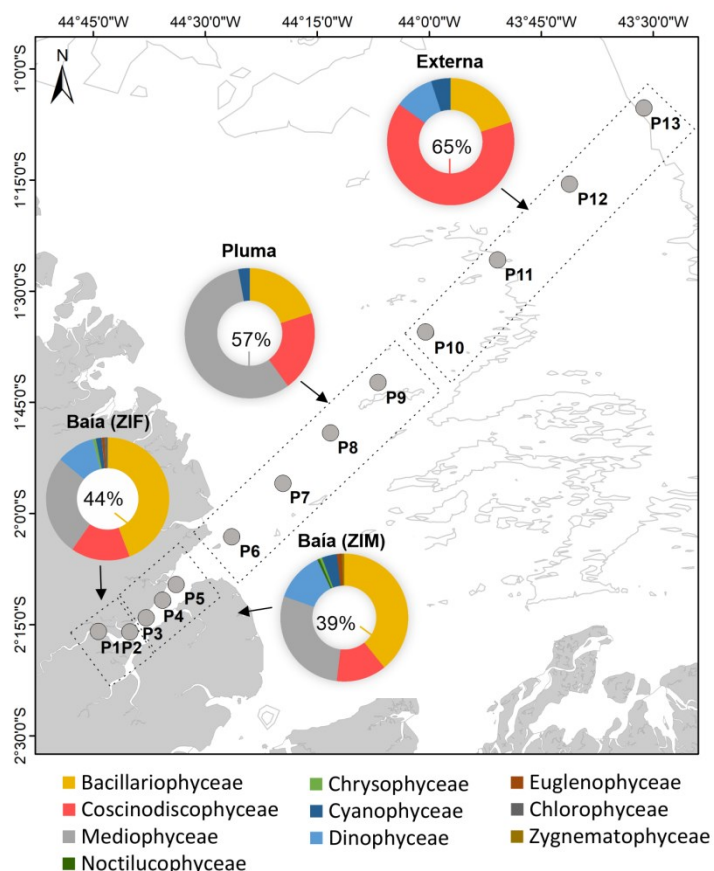
- THOMPSON, P.A.; O'BRIEN, T.D.; PAERL, H.W.; PEIERLS, B.L.; HARRISON, P.J.; ROB, M. Precipitation as a driver of phytoplankton ecology in coastal waters: a climatic perspective. **Estuarine, Coast and Shelf Science**, v. 162, p. 119–129, 2015.
- TONKIN, J. D.; STOLL, S.; JÄHNIG, S. C.; HAASE, P. Contrasting metacommunity structure and beta diversity in an aquatic-floodplain system. **Oikos**, v. 125, n. 5, p. 686–697, 2015. DOI: <https://doi.org/10.1111/oik.02717>.
- TOSETTO, E. G.; BERTRAND, A.; NEUMANN-LEITÃO, S.; NOGUEIRA JÚNIOR, M. The Amazon River plume, a barrier to animal dispersal in the Western Tropical Atlantic. **Scientific Reports**, v. 12, n. 1, 2022. <https://doi.org/10.1038/s41598-021-04165-z>.
- VAN DER MOST, H.; MARCHAND, M. Management of the Sustainable Development of Deltas. **Treatise on Estuarine and Coastal Science**, p. 179–204, 2011. DOI: <https://doi.org/10.1016/b978-0-12-374711-2.01111-6>.
- WETZEL, C. E.; BICUDO, D. DE C.; ECTOR, L.; LOBO, E. A.; SOININEN, J.; LANDEIRO, V. L.; BINI, L. M. Distance Decay of Similarity in Neotropical Diatom Communities. **PLoS ONE**, v. 7, n. 9, e45071, 2012. DOI: <https://doi.org/10.1371/journal.pone.0045071>.
- WHITTAKER, R. H. Evolution and measurement of species diversity. **TAXON**, v. 21, n. 2–3, p. 213–251, 1972. DOI: <https://doi.org/10.2307/1218190>.
- WOJCIECHOWSKI, J.; HEINO, J.; BINI, L. M.; PADIAL, A. A. Temporal variation in phytoplankton beta diversity patterns and metacommunity structures across subtropical reservoirs. **Freshwater Biology**, v. 62, n. 4, p. 751–766, 2017. DOI: <https://doi.org/10.1111/fwb.12899>.
- XU, Q.; HUANG, M.; YANG, S.; LI, X.; ZHAO, H.; TANG, J.; JIANG, G.; LI, Z.; HUANG, Y.; DONG, K.; HUANG, L.; LI, N. Ecological stoichiometry influences phytoplankton alpha and beta diversity rather than the community stability in subtropical bay. **Ecology and Evolution**, v. 12, n. 9, 2022. DOI: <https://doi.org/10.1002/ece3.9301>.
- ZHANG, Y.; PENG, C.; HUANG, S.; WANG, J.; XIONG, X.; LI, D. The relative role of spatial and environmental processes on seasonal variations of phytoplankton beta diversity along different anthropogenic disturbances of subtropical rivers in China. **Environmental Science and Pollution Research**, v. 26, n. 2, p. 1422–1434, 2018. DOI: <https://doi.org/10.1007/s11356-018-3632-4>.
- ZHONG, Q.; XUE, B.; NOMAN, M. A.; WEI, Y.; LIU, H.; LIU, H.; ZHENG, L.; JING, H.; SUN, J. Effect of river plume on phytoplankton community structure in Zhujiang River estuary. **Journal of Oceanology and Limnology**, v. 39, n. 2, p. 550–565, 2021. DOI: <https://doi.org/10.1007/s00343-020-9213-7>.
- ZORZAL-ALMEIDA, S.; BARTOZEK, E. C. R.; BICUDO, D. C. Homogenization of diatom assemblages is driven by eutrophication in tropical reservoirs. **Environmental Pollution**, v. 288, e117778, 2021. DOI: <https://doi.org/10.1016/j.envpol.2021.117778>

APÊNDICE A – IMPLICAÇÕES ECOLÓGICAS DA COMUNIDADE FITOPLANCTÔNICA GERAL (DISTRIBUIÇÃO TAXONÔMICA, FREQUÊNCIA DE OCORRÊNCIA E ECOLOGIA) E DISTRIBUIÇÃO TAXONÔMICA POR CLASSES AO LONGO DO CONTINUUM ESTUÁRIO-OCEANO

Comunidade fitoplancônica geral



Distribuição fitoplancônica ao longo do continuum estuário-oceano



Fonte: Autoria própria (2023).

APÊNDICE B – SINOPSE DOS TÁXONS IDENTIFICADOS NA BAÍA DE CUMÃ E PLATAFORMA CONTINENTAL MARANHENSE

Continua

CYANOBACTERIA	
Classe Cyanophyceae	<i>Nitzschia vidovichii</i> (Grunow) Grunow 1881
Ordem Synechococcales	<i>Nitzschia</i> sp1
Família Merismopediaceae	<i>Nitzschia</i> sp2
<i>Aphanocapsa incerta</i> (Lemmermann) G.Cronberg & Komárek 1994	<i>Pseudo-nitzschia delicatissima</i> (Cleve) Heiden 1928
Ordem Chroococcales	<i>Pseudo-nitzschia seriata</i> (Cleve) H.Peragallo 1899
Família Microcystaceae	<i>Pseudo-nitzschia pungens</i> (Grunow ex Cleve) Hasle 1993
<i>Microcystis aeruginosa</i> (Kützing) Kützing 1846	<i>Tryblionella compressa</i> (Bailey) Poulin 1990
<i>Microcystis</i> sp.	<i>Tryblionella granulata</i> (Grunow) D.G.Mann 1990
Ordem Nostocales	<i>Tryblionella hantzschiana</i> Grunow 1862
Família Aphanizomenonaceae	<i>Tryblionella punctata</i> W.Smith 1853
<i>Dolichospermum</i> sp.	Ordem Cymbellales
Ordem Oscillatoriales	Família Cymbellaceae
Família Oscillatoriaceae	<i>Cymbella</i> sp.
<i>Oscillatoria</i> sp.	Ordem Fragilariales
Família Microcoleaceae	Família Fragilariae
<i>Trichodesmium erythraeum</i> Ehrenberg ex Gomont 1892	<i>Synedra ulna</i> (Nitzsch) Ehrenberg 1832
Ordem Synechococcales	<i>Synedra</i> sp1
Família Merismopediaceae	<i>Synedra</i> sp2
<i>Synechocystis aquatilis</i> Sauvageau 1892	Família Staurosiraceae
EUGLENOZOA	<i>Opephora</i> sp.
Classe Euglenophyceae	Ordem Lyrellales
Ordem Euglenida	Família Lyrellaceae
Família Euglenidae	<i>Lyrella clavata</i> var. <i>subconstricta</i> (Hustedt) Moreno 1996
<i>Trachelomonas volvocina</i> (Ehrenberg) Ehrenberg 1834	Ordem Naviculares
<i>Trachelomonas</i> sp.	Família Amphipleuraceae
BACILLARIOPHYTA	<i>Frustulia interposta</i> (Lewis) De Toni 1891
Classe Bacillariophyceae	Família Diplopodiaceae
Ordem Achnanthales	<i>Diploneis bombus</i> (Ehrenberg) Ehrenberg 1853
Família Cocconeidaceae	<i>Diploneis decipiens</i> A.Cleve 1915
<i>Cocconeis placentula</i> Ehrenberg 1838	<i>Diploneis ovalis</i> (Hilse) Cleve 1891
<i>Cocconeis fluminensis</i> (Grunow) H.Peragallo & M.Peragallo 1897	<i>Diploneis splendida</i> Cleve 1894
<i>Cocconeis</i> sp.	<i>Diploneis vacillans</i> (A.W.F.Schmidt) Cleve 1894
Ordem Bacillariales	<i>Diploneis weissflogii</i> (A.W.F.Schmidt) Cleve 1894
Família Bacillariaceae	<i>Diploneis</i> sp.
<i>Alveus marinus</i> (Grunow) Kaczmarska & Fryxell 1996	Família Naviculaceae
<i>Bacillaria paxillifera</i> (O.F.Müller) T.Marsson 1901	<i>Caloneis permagna</i> (Bailey) Cleve 1894
<i>Cylindrotheca closterium</i> (Ehrenberg) Reimann & J.C.Lewin 1964	<i>Gyrosigma attenuatum</i> (Kützing) Rabenhorst 1853
<i>Nitzschia acicularis</i> (Kützing) W.Smith 1853	<i>Gyrosigma balticum</i> (Ehrenberg) Rabenhorst 1853
<i>Nitzschia dissipata</i> (Kützing) Rabenhorst 1860	<i>Gyrosigma eximium</i> (Thwaites) Boyer 1927
<i>Nitzschia frustulum</i> (Kützing) Grunow 1880	<i>Gyrosigma tenuissimum</i> (W.Smith) J.W.Griffith & Henfrey 1856
<i>Nitzschia granulata</i> Grunow 1880	<i>Navicula gottlandica</i> Grunow 1880
<i>Nitzschia grossstriata</i> Hustedt 1955	<i>Navicula lanceolata</i> Ehrenberg 1838
<i>Nitzschia linearis</i> W.Smith 1853	<i>Navicula polae</i> Heiden 1903
<i>Nitzschia longa</i> Grunow 1880	<i>Navicula</i> sp1
<i>Nitzschia longissima</i> (Brébisson) Ralfs 1861	<i>Navicula</i> sp2
<i>Nitzschia obtusa</i> W.Smith 1853	Família Pinnulariaceae
<i>Nitzschia palea</i> (Kützing) W.Smith 1856	<i>Pinnularia</i> sp.
<i>Nitzschia pacifica</i> Cupp 1943	Família Pleurosigmataceae
<i>Nitzschia sigma</i> (Kützing) W.Smith 1853	<i>Pleurosigma acutum</i> Norman ex Ralfs 1861
	<i>Pleurosigma angulatum</i> (J.T.Quekett) W.Smith 1852
	<i>Pleurosigma elongatum</i> W.Smith 1852
	<i>Pleurosigma formosum</i> W.Smith 1852
	<i>Pleurosigma normanii</i> Ralfs 1861

Continuação

<i>Pleurosigma</i> sp.	<i>Pseudosolenia calcar-avis</i> (Schultz) B.G.Sundström 1986= <i>Rhizosolenia calcar-avis</i> Schultz 1858
Família Stauroneidaceae	<i>Rhizosolenia hebetata</i> J.W.Bailey 1856
<i>Craticula cuspidata</i> (Kutzing) D.G.Mann 1990	<i>Rhizosolenia setigera</i> Brightwell 1858= <i>Sundstroemia setigera</i> (Brightwell) Medlin 2021
<i>Prestauroneis crucicula</i> (W.Smith) Genkal & Yarushina 2017	<i>Rhizosolenia striata</i> Greville 1865
Ordem Rhaphoneidales	Ordem Triceratiales
Família Asterionellopsidaceae	Família Triceratiaceae
<i>Asterionellopsis glacialis</i> (Castracane) Round 1990	<i>Triceratium favus</i> Ehrenberg 1839
Família Rhaphoneidaceae	Classe Mediophyceae
<i>Rhaphoneis amphiceros</i> (Ehrenberg) Ehrenberg 1844	Ordem Chaetocerotales
Ordem Surirellales	Família Chaetocerotaceae
Família Entomoneidaceae	<i>Bacteriastrum hyalinum</i> Lauder 1864
<i>Entomoneis alata</i> (Ehrenberg) Ehrenberg 1845	<i>Chaetoceros abnormis</i> Proshkina-Lavrenko 1953
Família Surirellaceae	<i>Chaetoceros affinis</i> Lauder 1864
<i>Petrodictyon gemma</i> (Ehrenberg) D.G.Mann 1990	<i>Chaetoceros atlanticus</i> Cleve 1873
<i>Tryblioptychus coccineiformis</i> (Grunow) Hendey 1958	<i>Chaetoceros compressus</i> Lauder 1864
Ordem Thalassionematales	<i>Chaetoceros curisetus</i> Cleve 1889
Família Thalassionemataceae	<i>Chaetoceros debilis</i> Cleve 1894
<i>Thalassionema frauenfeldii</i> (Grunow) Tempère & Peragallo 1910	<i>Chaetoceros lorenzianus</i> Grunow 1863
<i>Thalassionema nitzschiooides</i> (Grunow)	<i>Chaetoceros pendulus</i> Karsten 1905
Mereschkowsky 1902	<i>Chaetoceros peruvianus</i> Brightwell 1856
<i>Thalassionema</i> sp.	<i>Chaetoceros socialis</i> H.S.Lauder 1864
<i>Thalassiothrix longissima</i> Cleve & Grunow 1880	<i>Chaetoceros subtilis</i> Cleve 1896
Ordem Thalassiphysales	<i>Chaetoceros teres</i> Cleve 1896
Família Catenulaceae	<i>Chaetoceros</i> sp.
<i>Amphora</i> sp.	Família Leptocylindraceae
Classe Coscinodiscophyceae	<i>Leptocylindrus danicus</i> Cleve 1889
Ordem Coscinodiscales	<i>Leptocylindrus minimus</i> Gran 1915
Família Coscinodiscaceae	Ordem Biddulphiales
<i>Coscinodiscus centralis</i> Ehrenberg 1839	Família Bellerocheaceae
<i>Coscinodiscus concinnus</i> W.Smith 1856	<i>Bellerochea malleus</i> (Brightwell) Van Heurck 1885
<i>Coscinodiscus granii</i> L.F.Gough 1905	Família Biddulphiacea
<i>Coscinodiscus oculus-iridis</i> (Ehrenberg) Ehrenberg 1840	<i>Biddulphia</i> sp.
<i>Coscinodiscus radiatus</i> Ehrenberg 1840	Ordem Cymatosira
<i>Coscinodiscus rothii</i> (Ehrenberg) Grunow 1878	Família Cymatosiraceae
<i>Coscinodiscus</i> sp.	<i>Campylosira cymbelliformis</i> (A.W.F.Schmidt) Grunow ex Van Heurck 1885
Família Hemidiscaceae	<i>Cymatosira lorenziana</i> Grunow 1862
<i>Actinocyclus octonarius</i> Ehrenberg 1837	Ordem Eupodiscales
Família Heliopeltaceae	Família Odontellaceae
<i>Actinopytchus annulatus</i> (Wallich) Grunow 1883	<i>Odontella turgida</i> (Ehrenberg) Kützing 1844
<i>Actinopytchus campanulifer</i> Schmidt 1875	<i>Odontella aurita</i> (Lyngbye) C.Agardh 1832
<i>Actinopytchus minutus</i> Greville 1866	<i>Odontella minuta</i> (Greville) Andrews 1990
<i>Actinopytchus senarius</i> (Ehrenberg) Ehrenberg 1843	<i>Odontella</i> sp.
<i>Actinopytchus</i> sp.	Família Parodontellaceae
Ordem Crysanthemodiscales	<i>Trieres mobilensis</i> (Bailey) Ashworth & E.C.Theriot 2013
Família Chrysanthemodiscaceae	<i>Trieres regia</i> (M.Schultze) Ashworth & E.C.Theriot 2013
<i>Melchersiela hexagonalis</i> C. Teixeira 1958	<i>Trieres chinensis</i> (Greville) Ashworth & E.C.Theriot 2013
Ordem Melosirales	Ordem Hemiaulales
Família Melosiraceae	Família Hemiaulaceae
<i>Melosira nummuloides</i> C.Agardh 1824	<i>Hemiaulus hauckii</i> Grunow ex Van Heurck 1882
Ordem Paraliales	Ordem Lithodesmiales
Família Paraliaceae	Família Lithodesmiaceae
<i>Paralia sulcata</i> (Ehrenberg) Cleve 1873	<i>Ditylum brightwellii</i> (T.West) Grunow 1885
Ordem Rhizosoleniales	<i>Helicotheca tamesis</i> (Shrubsole) M.Ricard 1987
Família Rhizosoleniaceae	<i>Lithodesmium undulatum</i> Ehrenberg 1839
<i>Guinardia flaccida</i> (Castracane) H.Peragallo 1892	Ordem Probosciales
<i>Guinardia striata</i> (Stolterfoth) Hasle 1996	Família Probosciaceae
<i>Dactyliosolen mediterraneus</i> (H.Peragallo) H.Peragallo 1892	<i>Proboscia alata</i> (Brightwell) Sundström 1986
<i>Neocalyptrella robusta</i> (G.Norman ex Ralfs)	Ordem Stephanodiscales
Hernández-Becerril & Meave 1997	

Família Stephanodiscaceae	<i>Gonyaulax</i> sp.
<i>Cyclotella delicatula</i> Hustedt 1952	
<i>Cyclotella litoralis</i> Lange & Syvertsen 1989	
<i>Cyclotella meneghiniana</i> Kützing 1844	
<i>Cyclotella striata</i> (Kützing) Grunow 1880	
<i>Cyclotella stylorum</i> Brightwell 1860	
<i>Cyclotella</i> sp.	
Ordem Thalassiosirales	
Família Lauderiacae	
<i>Lauderia annulata</i> Cleve 1873	
Família Skeletonemataceae	
<i>Skeletonema costatum</i> (Greville) Cleve 1873	
Família Thalassiosiraceae	
<i>Conticribra weissflogii</i> (Grunow) Stachura-Suchoples & D.M.Williams 2009	
<i>Thalassiosira delicatula</i> Ostenfeld 1908	
<i>Thalassiosira leptopus</i> (Grunow) Hasle & G.Fryxell 1977	
<i>Thalassiosira lineata</i> Jousé 1968	
<i>Thalassiosira eccentrica</i> (Ehrenberg) Cleve 1904	
<i>Shionodiscus oestruppii</i> (Ostenfeld) A.J.Alverson, S.-H.Kang & E.C.Theriot 2006=	
<i>Thalassiosira oestruppii</i> (Ostenfeld) Proshkina-Lavrenko ex Hasle 1960	
<i>Thalassiosira pacifica</i> Gran & Angst 1931	
<i>Thalassiosira plicata</i> H.J.Schrader 1974	
<i>Thalassiosira gravida</i> Cleve 1896	
<i>Thalassiosira simonsenii</i> Hasle & G.Fryxell 1977	
<i>Thalassiosira subtilis</i> (Ostenfeld) Gran 1900	
<i>Thalassiosira</i> sp ₁	
<i>Thalassiosira</i> sp ₂	
<i>Thalassiosira</i> sp ₃	
Ordem Toxariales	
Família Ardissonaceae	
<i>Ardissonia crystallina</i> (C.Agardh) Grunow 1880	
MIOZOA	
Classe Dinophyceae	
Ordem Dinophysales	
Família Dinophysaceae	
<i>Dinophysis caudata</i> Kent 1881	
<i>Dinophysis norvegica</i> Claparède & Lachmann 1859	
<i>Dinophysis tripos</i> Gourret 1883	
Ordem Gymnodiniales	
Família Gymnodiniaceae	
<i>Gymnodinium mitratum</i> J.Schiller 1932	
<i>Gymnodinium</i> sp ₁	
<i>Gymnodinium</i> sp ₂	
Ordem Gonyaulacales	
Família Ceratiaceae	
<i>Triplos furca</i> (Ehrenberg) F.Gómez 2013= <i>Neoceratium furca</i> (Ehrenberg) F.Gómez, D.Moreira & P.López-Garcia 2010	
<i>Triplos lineatus</i> (Ehrenberg) F.Gómez 2021= <i>Neoceratium lineatum</i> (Ehrenberg) F.Gómez, D.Moreira & P.López-Garcia 2010	
Família Gonyaulacaceae	
<i>Gonyaulax spinifera</i> (Claparède & Lachmann) Diesing 1866= <i>Peridinium spiniferum</i> Claparède & Lachmann 1859	
Gonyaulax sp.	
Família Pyrocystaceae	
<i>Pyrophacus steinii</i> (Schiller) Wall & Dale 1971= <i>Pyrophacus horogium</i> var. <i>steinii</i> J.Schiller 1935	
Ordem Peridiniales	
Família Heterocapsaceae	
<i>Heterocapsa psammophila</i> M.Tamura, M.Iwataki & M.Horiguchi 2006	
<i>Heterocapsa rotundata</i> (Lohmann) Gert Hansen 1995	
<i>Heterocapsa</i> sp.	
Família Oxytoxaceae	
<i>Oxytoxum crassum</i> J.Schiller 1937	
Família Peridiniaceae	
<i>Peridinium</i> sp.	
Família Protoperidiniaceae	
<i>Protoperidinium crassipes</i> (Kofoid) Balech 1974= <i>Peridinium crassipes</i> Kofoid 1907	
<i>Protoperidinium pyriforme</i> (Paulsen) Balech 1974= <i>Peridinium pyriforme</i> Paulsen 1907	
<i>Protoperidinium trochoideum</i> (Stein) Lemmermann, 1910	
<i>Archaeoperidinium minutum</i> (Kofoid) Jørgensen 1912= <i>Protoperidinium minutum</i> (Kofoid)	
A.R.Loeblitch 1970	
<i>Protoperidinium</i> sp.	
Ordem Prorocentrales	
Família Prorocentraceae	
<i>Prorocentrum micans</i> Ehrenberg 1834	
<i>Prorocentrum gracile</i> F.Schütt 1895	
Ordem Thoracosphaerales	
Família Thoracosphaeraceae	
<i>Scrippsiella acuminata</i> (Ehrenberg) Kretschmann, Elbrächter, Zinssmeister, S.Soehner, Kirsch, Kusber & Gottschling 2015	
Classe Noctilucophyceae	
Ordem Noctilucales	
Família Noctilucaceae	
<i>Noctiluca scintillans</i> (Macartney) Kofoid & Swezy 1921	
CHLOROPHYTA	
Classe Chlorophyceae	
Ordem Sphaeropteales	
Família Hydrodictyaceae	
<i>Pediastrum boryanum</i> (Turpin) Meneghini 1840	
CHAROPHYTA	
Classe Zygnematophyceae	
Ordem Desmidiales	
Família Desmidiaceae	
<i>Bambusina borreri</i> (Ralfs) Cleve 1864	
OCHROPHYTA	
Classe Chrysophyceae	
Ordem Chromulinales	
Família Chromulinaceae	
<i>Chromulina</i> sp.	

Fonte: Autoria própria (2023).

**APÊNDICE C – DISTRIBUIÇÃO E IMPLICAÇÕES ECOLÓGICAS DO FITOPLÂNCTON NA BAÍA DE CUMA E PLATAFORMA
CONTINENTAL MARANHENSE**

Continua

CATEGORIA TAXONÔMICA	Baía ZIF	Baía ZIM	Pluma	Plat. externa	Abund. ($\times 10^3$ cel L $^{-1}$)	PAT (%)	Freq. (%)	Índice Const.	Ecologia
Bacillariophyta									
<i>Actinocyclus octonarius</i> Ehrenberg 1837	+	-	-	-	0,12	0,01	1,64	Acidental	Marinha
<i>Actinoptychus annulatus</i> (Wallich) Grunow 1883	+	+	-	-	0,08	0,01	3,28	Acidental	Estuarina
<i>Actinoptychus splendens</i> (Shadbolt) Ralfs 1861	-	+	-	-	0,04	0,00	1,64	Acidental	Marinha
<i>Actinoptychus campanulifer</i> Schmidt 1875	+	-	-	-	0,08	0,01	1,64	Acidental	Marinha
<i>Actinoptychus minutus</i> Greville 1866	+	-	-	-	0,28	0,03	4,92	Acidental	Marinha
<i>Actinoptychus senarius</i> (Ehrenberg) Ehrenberg 1843	+	+	-	-	0,39	0,05	9,84	Acidental	Marinha
<i>Actinoptychus</i> sp.	+	+	+	-	0,67	0,08	11,48	Acidental	Outro
<i>Alveus marinus</i> (Grunow) Kaczmarska & Fryxell 1996	+	+	-	-	0,63	0,08	4,92	Acidental	Marinha
<i>Amphora</i> sp.	+	+	-	-	0,43	0,05	14,75	Acidental	Outro
<i>Ardissonea crystallina</i> (C.Agardh) Grunow 1880	-	+	-	-	0,04	0,00	1,64	Acidental	Estuarina
<i>Asterionellopsis glacialis</i> (Castracane) Round 1990	-	+	-	-	1,54	0,19	4,92	Acidental	Marinha
<i>Bacillaria paxillifera</i> (O.F.Müller) T.Marsson 1901	+	+	-	+	1,18	0,14	8,20	Acidental	Estuarina
<i>Bacteriastrum hyalinum</i> Lauder 1864	-	+	-	-	0,12	0,01	1,64	Acidental	Marinha
<i>Bellerochea malleus</i> (Brightwell) Van Heurck 1885	-	+	+	-	0,50	0,06	3,28	Acidental	Marinha
<i>Biddulphia</i> sp.	+	+	-	-	0,08	0,01	3,28	Acidental	Outro
<i>Caloneis permagna</i> (Bailey) Cleve 1894	+	+	-	-	0,32	0,04	9,84	Acidental	Estuarina
<i>Campylosira cymbelliformis</i> (A.W.F.Schmidt) Grunow ex Van Heurck 1885	+	+	-	-	1,10	0,14	9,84	Acidental	Marinha
<i>Chaetoceros abnormis</i> Proshkina-Lavrenko 1953	+	+	+	+	2,35	0,29	24,59	Acidental	Marinha
<i>Chaetoceros atlanticus</i> Cleve 1873	-	+	-	-	0,08	0,01	3,28	Acidental	Marinha
<i>Chaetoceros affinis</i> Lauder 1864	-	+	-	-	0,12	0,01	1,64	Acidental	Marinha
<i>Chaetoceros compressus</i> Lauder 1864	-	+	+	-	0,95	0,12	4,92	Acidental	Marinha
<i>Chaetoceros curvisetus</i> Cleve 1889	-	-	+	-	0,43	0,05	3,28	Acidental	Marinha
<i>Chaetoceros debilis</i> Cleve 1894	-	+	-	-	0,04	0,00	1,64	Acidental	Marinha
<i>Chaetoceros lorenzianus</i> Grunow 1863	-	+	-	-	0,95	0,12	8,20	Acidental	Marinha
<i>Chaetoceros pendulus</i> Karsten 1905	-	+	-	-	0,04	0,00	1,64	Acidental	Marinha
<i>Chaetoceros peruvianus</i> Brightwell 1856	-	-	+	-	0,08	0,01	1,64	Acidental	Marinha

Continuação

CATEGORIA TAXONÔMICA	Baía ZIF	Baía ZIM	Pluma	Plat. externa	Abund. ($\times 10^3$ cel L $^{-1}$)	PAT (%)	Freq. (%)	Índice Const.	Ecologia
<i>Chaetoceros socialis</i> H.S.Lauder 1864	+	+	-	-	3,71	0,46	14,75	Acidental	Marinha
<i>Chaetoceros subtilis</i> Cleve 1896	+	+	-	-	0,24	0,03	3,28	Acidental	Marinha
<i>Chaetoceros teres</i> Cleve 1896	-	-	+	-	0,24	0,03	3,28	Acidental	Marinha
<i>Chaetoceros</i> sp.	+	+	-	-	0,16	0,02	4,92	Acidental	Outro
<i>Cocconeis fluminensis</i> (Grunow) H.Peragallo & M.Peragallo 1897	-	+	-	-	0,04	0,00	1,64	Acidental	Marinha
<i>Cocconeis placentula</i> Ehrenberg 1838	-	+	-	-	0,83	0,10	6,56	Acidental	Dulcícola
<i>Cocconeis</i> sp.	+	+	-	+	0,80	0,10	19,67	Acidental	Outro
<i>Conticriba weissflogii</i> (Grunow) Stachura-Suchoples & D.M.Williams 2009	+	+	+	-	6,15	0,76	55,74	Constante	Estuarina
<i>Coscinodiscus centralis</i> Ehrenberg 1839	+	+	-	-	0,39	0,05	13,11	Acidental	Marinha
<i>Coscinodiscus concinnus</i> W.Smith 1856	+	+	-	+	0,38	0,05	9,84	Acidental	Estuarina
<i>Coscinodiscus granii</i> L.F.Gough 1905	+	+	-	-	0,51	0,06	14,75	Acidental	Marinha
<i>Coscinodiscus oculus-iridis</i> (Ehrenberg) Ehrenberg 1840	+	+	-	-	0,71	0,09	14,75	Acidental	Marinha
<i>Coscinodiscus radiatus</i> Ehrenberg 1840	-	+	-	+	0,13	0,02	4,92	Acidental	Marinha
<i>Coscinodiscus rothii</i> (Ehrenberg) Grunow 1878	+	+	-	-	0,24	0,03	9,84	Acidental	Marinha
<i>Coscinodiscus</i> sp.	+	-	-	-	0,24	0,03	6,56	Acidental	Outro
<i>Craticula cuspidata</i> (Kutzing) D.G.Mann 1990	+	+	-	-	0,20	0,02	6,56	Acidental	Dulcícola
<i>Cyclotella</i> sp.	+	+	-	-	4,30	0,53	49,18	Acessória	Outro
<i>Cyclotella delicatula</i> Hustedt 1952	+	-	-	-	0,47	0,06	1,64	Acidental	Dulcícola
<i>Cyclotella litoralis</i> Lange & Syvertsen 1989	+	+	+	-	13,14	1,62	55,74	Constante	Estuarina
<i>Cyclotella meneghiniana</i> Kützing 1844	+	+	-	-	0,59	0,07	11,48	Acidental	Estuarina
<i>Cyclotella striata</i> (Kützing) Grunow 1880	+	+	+	-	4,34	0,53	59,02	Constante	Dulcícola
<i>Cyclotella stylorum</i> Brightwell 1860	+	+	-	-	2,72	0,34	36,07	Acessória	Marinha
<i>Cylindrotheca closterium</i> (Ehrenberg) Reimann & J.C.Lewin 1964	+	+	+	-	1,14	0,14	21,31	Acidental	Marinha
<i>Cymatosira lorenziana</i> Grunow 1862	+	+	+	-	8,44	1,04	47,54	Acessória	Marinha
<i>Cymbella</i> sp.	-	+	-	-	0,08	0,01	3,28	Acidental	Outro
<i>Dactyliosolen mediterraneus</i> (H.Peragallo) H.Peragallo 1892	-	-	-	+	0,09	0,01	1,64	Acidental	Marinha
<i>Diploneis weissflogii</i> (A.W.F.Schmidt) Cleve 1894	+	+	-	-	2,96	0,36	34,43	Acessória	Marinha
<i>Diploneis bombus</i> (Ehrenberg) Ehrenberg 1853	+	+	-	-	2,09	0,26	40,98	Acessória	Marinha
<i>Diploneis decipiens</i> A.Cleve 1915	+	+	-	-	0,12	0,01	3,28	Acidental	Estuarina

Continuação

CATEGORIA TAXONÔMICA	Baía ZIF	Baía ZIM	Pluma	Plat. externa	Abund. (x10 ³ cel L ⁻¹)	PAT (%)	Freq. (%)	Índice Const.	Ecologia
<i>Diploneis ovalis</i> (Hilse) Cleve 1891	+	+	-	-	0,20	0,02	6,56	Acidental	Dulcícola
<i>Diploneis splendida</i> Cleve 1894	+	+	-	-	0,91	0,11	21,31	Acidental	Marinha
<i>Diploneis vacillans</i> (A.W.F.Schmidt) Cleve 1894	+	+	-	-	0,24	0,03	8,20	Acidental	Marinha
<i>Diploneis</i> sp.	+	+	-	-	0,39	0,05	13,11	Acidental	Outro
<i>Ditylum brightwellii</i> (T.West) Grunow 1885	+	+	+	+	1,56	0,19	39,34	Acessória	Marinha
<i>Entomoneis alata</i> (Ehrenberg) Ehrenberg 1845	+	+	-	-	0,12	0,01	4,92	Acidental	Marinha
<i>Frustulia interposita</i> (Lewis) De Toni 1891	+	+	-	-	0,16	0,02	4,92	Acidental	Dulcícola
<i>Guinardia flaccida</i> (Castracane) H.Peragallo 1892	+	+	+	-	2,60	0,32	16,39	Acidental	Marinha
<i>Guinardia striata</i> (Stolterfoth) Hasle 1996	+	+	+	+	2,19	0,27	16,39	Acidental	Marinha
<i>Gyrosigma attenuatum</i> (Kützing) Rabenhorst 1853	-	+	-	-	0,16	0,02	6,56	Acidental	Dulcícola
<i>Gyrosigma balticum</i> (Ehrenberg) Rabenhorst 1853	+	+	-	-	0,32	0,04	11,48	Acidental	Marinha
<i>Gyrosigma eximium</i> (Thwaites) Boyer 1927	+	-	-	-	0,04	0,00	1,64	Acidental	Estuarina
<i>Gyrosigma tenuissimum</i> (W.Smith) J.W.Griffith & Henfrey 1856	-	+	-	-	0,08	0,01	1,64	Acidental	Marinha
<i>Helicotheca tamesis</i> (Shrubsole) M.Ricard 1987	-	+	-	-	0,08	0,01	3,28	Acidental	Marinha
<i>Hemiaulus hauckii</i> Grunow ex Van Heurck 1882	-	-	+	-	0,09	0,01	1,64	Acidental	Marinha
<i>Lauderia annulata</i> Cleve 1873	-	+	-	-	0,04	0,00	1,64	Acidental	Marinha
<i>Leptocylindrus danicus</i> Cleve 1889	+	+	+	-	2,80	0,35	9,84	Acidental	Marinha
<i>Leptocylindrus minimus</i> Gran 1915	+	+	+	-	6,15	0,76	26,23	Acessória	Marinha
<i>Lithodesmium undulatum</i> Ehrenberg 1839	+	+	-	-	0,55	0,07	14,75	Acidental	Marinha
<i>Lyrella clavata</i> var. <i>subconstricta</i> (Hustedt) Moreno 1996	+	-	-	-	0,04	0,00	1,64	Acidental	Marinha
<i>Melchersiella hexagonalis</i> C. Teixeira 1958	+	-	-	-	0,04	0,00	1,64	Acidental	Marinha
<i>Melosira nummuloides</i> C.Agardh 1824	+	+	-	-	0,63	0,08	8,20	Acidental	Marinha
<i>Navicula gottlandica</i> Grunow 1880	+	+	-	-	0,39	0,05	6,56	Acidental	Dulcícola
<i>Navicula lanceolata</i> Ehrenberg 1838	+	+	-	-	0,71	0,09	9,84	Acidental	Dulcícola
<i>Navicula polae</i> Heiden 1903	-	+	-	-	0,08	0,01	1,64	Acidental	Marinha
<i>Navicula</i> sp1	+	+	-	-	0,51	0,06	9,84	Acidental	Outro
<i>Navicula</i> sp2	-	+	-	-	0,04	0,00	1,64	Acidental	Outro
<i>Neocalyprella robusta</i> (G.Norman ex Ralfs) Hernández-Becerril & Meave 1997	-	-	+	-	0,02	0,00	1,64	Acidental	Marinha
<i>Nitzschia acicularis</i> (Kützing) W.Smith 1853	+	+	-	-	0,36	0,04	6,56	Acidental	Estuarina
<i>Nitzschia dissipata</i> (Kützing) Rabenhorst 1860	-	+	-	-	0,04	0,00	1,64	Acidental	Dulcícola

Continuação

CATEGORIA TAXONÔMICA	Baía ZIF	Baía ZIM	Pluma	Plat. externa	Abund. ($\times 10^3$ cel L $^{-1}$)	PAT (%)	Freq. (%)	Índice Const.	Ecologia
<i>Nitzschia frustulum</i> (Kützing) Grunow 1880	+	+	-	-	0,20	0,02	4,92	Acidental	Estuarina
<i>Nitzschia granulata</i> Grunow 1880	+	+	-	-	0,32	0,04	6,56	Acidental	Dulcícola
<i>Nitzschia grossstriata</i> Hustedt 1955	+	-	-	-	0,08	0,01	1,64	Acidental	Marinha
<i>Nitzschia linearis</i> W.Smith 1853	+	+	-	-	0,12	0,01	3,28	Acidental	Estuarina
<i>Nitzschia longa</i> Grunow 1880	+	+	-	-	0,36	0,04	8,20	Acidental	Marinha
<i>Nitzschia longissima</i> (Brébisson) Ralfs 1861	+	+	-	+	2,77	0,34	21,31	Acidental	Marinha
<i>Nitzschia obtusa</i> W.Smith 1853	+	-	-	-	0,12	0,01	3,28	Acidental	Dulcícola
<i>Nitzschia pacifica</i> Cupp 1943	+	+	-	-	0,20	0,02	4,92	Acidental	Marinha
<i>Nitzschia palea</i> (Kützing) W.Smith 1856	-	+	-	-	0,08	0,01	1,64	Acidental	Dulcícola
<i>Nitzschia sigma</i> (Kützing) W.Smith 1853	+	+	-	-	0,51	0,06	13,11	Acidental	Estuarina
<i>Nitzschia vidovichii</i> (Grunow) Grunow 1881	+	+	-	-	0,36	0,04	9,84	Acidental	Marinha
<i>Nitzschia</i> sp1	+	+	-	-	1,93	0,24	27,87	Acessória	Outro
<i>Nitzschia</i> sp2	+	+	-	-	0,08	0,01	3,28	Acidental	Outro
<i>Odontella minuta</i> (Greville) Andrews 1990	+	+	-	-	0,39	0,05	4,92	Acidental	Marinha
<i>Odontella turgida</i> (Ehrenberg) Kützing 1844	+	+	-	-	0,16	0,02	4,92	Acidental	Marinha
<i>Odontella aurita</i> (Lyngbye) C.Agardh 1832	+	+	+	-	5,76	0,71	45,90	Acessória	Marinha
<i>Odontella</i> sp.	+	+	-	-	0,16	0,02	3,28	Acidental	Outro
<i>Opephora</i> sp.	-	+	-	-	0,04	0,00	1,64	Acidental	Outro
<i>Paralia sulcata</i> (Ehrenberg) Cleve 1873	+	+	-	-	5,96	0,73	52,46	Constante	Marinha
<i>Petrodictyon gemma</i> (Ehrenberg) D.G.Mann 1990	+	+	-	-	0,12	0,01	3,28	Acidental	Marinha
<i>Pinnularia</i> sp.	-	+	-	-	0,04	0,00	1,64	Acidental	Outro
<i>Pleurosigma normanii</i> Ralfs 1861	+	+	-	-	0,32	0,04	8,20	Acidental	Marinha
<i>Pleurosigma acutum</i> Norman ex Ralfs 1861	+	-	-	-	0,16	0,02	3,28	Acidental	Marinha
<i>Pleurosigma angulatum</i> (J.T.Quekett) W.Smith 1852	+	+	-	-	0,75	0,09	18,03	Acidental	Marinha
<i>Pleurosigma elongatum</i> W.Smith 1852	+	-	-	-	0,12	0,01	3,28	Acidental	Marinha
<i>Pleurosigma formosum</i> W.Smith 1852	+	-	-	-	0,20	0,02	4,92	Acidental	Marinha
<i>Pleurosigma</i> sp.	+	+	-	-	0,47	0,06	11,48	Acidental	Outro
<i>Prestauroneis crucicula</i> (W.Smith) Genkal & Yarushina 2017	+	+	+	-	2,09	0,26	29,51	Acessória	Estuarina
<i>Proboscia alata</i> (Brightwell) Sundström 1986	-	-	+	+	0,15	0,02	6,56	Acidental	Marinha
<i>Pseudo-nitzschia delicatissima</i> (Cleve) Heiden 1928	-	-	+	-	0,83	0,10	1,64	Acidental	Marinha

Continuação

CATEGORIA TAXONÔMICA	Baía ZIF	Baía ZIM	Pluma	Plat. externa	Abund. (x10 ³ cel L ⁻¹)	PAT (%)	Freq. (%)	Índice Const.	Ecologia
<i>Pseudo-nitzschia pungens</i> (Grunow ex Cleve) Hasle 1993	+	+	+	+	5,58	0,69	26,23	Acessória	Marinha
<i>Pseudo-nitzschia seriata</i> (Cleve) H.Peragallo 1899	+	+	+	-	0,40	0,05	6,56	Acidental	Marinha
<i>Pseudosolenia calcar-avis</i> (Schultze) B.G.Sundström 1986	-	+	+	-	0,20	0,02	6,56	Acidental	Marinha
<i>Rhaphoneis amphiceros</i> (Ehrenberg) Ehrenberg 1844	+	+	-	-	0,91	0,11	27,87	Acessória	Marinha
<i>Rhizosolenia hebetata</i> J.W.Bailey 1856	+	+	-	-	0,55	0,07	8,20	Acidental	Marinha
<i>Rhizosolenia striata</i> Greville 1865	-	+	-	-	0,08	0,01	1,64	Acidental	Marinha
<i>Shionodiscus oestrupii</i> (Ostenfeld) A.J.Alverson, S.-H.Kang & E.C.Theriot 2006	+	+	-	-	0,28	0,03	8,20	Acidental	Marinha
<i>Skeletonema costatum</i> (Greville) Cleve 1873	+	+	+	+	535,81	66,02	62,30	Constante	Marinha
<i>Sundstroemia setigera</i> (Brightwell) Medlin 2021	+	+	+	+	1,61	0,20	27,87	Acessória	Marinha
<i>Synedra ulna</i> (Nitzsch) Ehrenberg 1832	+	+	-	-	1,42	0,18	36,07	Acessória	Marinha
<i>Synedra</i> sp1	+	+	-	-	0,63	0,08	14,75	Acidental	Outro
<i>Synedra</i> sp2	+	+	-	-	0,28	0,03	8,20	Acidental	Outro
<i>Thalassionema frauenfeldii</i> (Grunow) Tempère & Peragallo 1910	+	+	+	-	6,14	0,76	54,10	Constante	Marinha
<i>Thalassionema nitzschiooides</i> (Grunow) Mereschkowsky 1902	+	+	+	-	6,92	0,85	54,10	Constante	Marinha
<i>Thalassionema</i> sp.	+	+	-	-	1,50	0,18	26,23	Acessória	Outro
<i>Thalassiosira subtilis</i> (Ostenfeld) Gran 1900	+	+	-	-	34,25	4,22	78,69	Constante	Marinha
<i>Thalassiosira delicatula</i> Ostenfeld 1908	+	-	-	-	0,04	0,00	1,64	Acidental	Marinha
<i>Thalassiosira eccentrica</i> (Ehrenberg) Cleve 1904	+	+	-	+	1,78	0,22	34,43	Acessória	Marinha
<i>Thalassiosira gravida</i> Cleve 1896	+	+	+	-	58,71	7,23	62,30	Constante	Marinha
<i>Thalassiosira leptopus</i> (Grunow) Hasle & G.Fryxell 1977	+	+	-	-	1,34	0,17	36,07	Acessória	Marinha
<i>Thalassiosira lineata</i> Jousé 1968	+	+	-	-	0,12	0,01	4,92	Acidental	Marinha
<i>Thalassiosira minuscula</i> Krasske 1941	-	-	+	+	0,45	0,06	8,20	Acidental	Outro
<i>Thalassiosira oceanica</i> Hasle 1983	-	-	+	+	2,00	0,25	9,84	Acidental	Outro
<i>Thalassiosira pacifica</i> Gran & Angst 1931	-	+	-	-	0,20	0,02	4,92	Acidental	Marinha
<i>Thalassiosira plicata</i> H.J.Schrader 1974	+	+	-	-	0,24	0,03	8,20	Acidental	Marinha
<i>Thalassiosira simonsenii</i> Hasle & G.Fryxell 1977	-	+	-	-	0,20	0,02	4,92	Acidental	Marinha
<i>Thalassiosira</i> sp1	+	+	-	-	2,60	0,32	21,31	Acidental	Outro
<i>Thalassiothrix longissima</i> Cleve & Grunow 1880	+	+	-	-	0,39	0,05	9,84	Acidental	Marinha
<i>Triceratium favus</i> Ehrenberg 1839	-	+	-	-	0,08	0,01	3,28	Acidental	Marinha
<i>Trieres chinensis</i> (Greville) Ashworth & E.C.Theriot 2013	+	+	+	-	5,12	0,63	47,54	Acessória	Marinha

Continuação

CATEGORIA TAXONÔMICA	Baía ZIF	Baía ZIM	Pluma	Plat. externa	Abund. (x10 ³ cel L ⁻¹)	PAT (%)	Freq. (%)	Índice Const.	Ecologia
<i>Trieres mobiliensis</i> (Bailey) Ashworth & E.C.Theriot 2013	+	+	-	-	0,75	0,09	26,23	Acessória	Marinha
<i>Trieres regia</i> (M.Schultze) Ashworth & E.C.Theriot 2013	+	+	+	+	10,64	1,31	59,02	Constante	Marinha
<i>Tryblionella hantzschiana</i> Grunow 1862	-	+	-	-	0,04	0,00	1,64	Acidental	Estuarina
<i>Tryblionella compressa</i> (Bailey) Poulin 1990	+	+	-	-	0,87	0,11	4,92	Acidental	Marinha
<i>Tryblionella granulata</i> (Grunow) D.G.Mann 1990	+	+	-	-	0,16	0,02	4,92	Acidental	Marinha
<i>Tryblionella punctata</i> W.Smith 1853	+	-	-	-	0,04	0,00	1,64	Acidental	Estuarina
<i>Tryblioptychus coccineiformis</i> (Grunow) Hendey 1958	+	+	-	-	3,24	0,40	40,98	Acessória	Marinha
Miozoa									
<i>Archaoperidinium minutum</i> (Kofoid) Jørgensen 1912	-	+	-	-	0,08	0,01	1,64	Acidental	Marinha
<i>Dinophysis caudata</i> Kent 1881	-	+	-	-	0,04	0,00	1,64	Acidental	Marinha
<i>Dinophysis norvegica</i> Claparède & Lachmann 1859	+	+	-	-	1,14	0,14	14,75	Acidental	Marinha
<i>Dinophysis tripos</i> Gourret 1883	+	-	-	-	0,04	0,00	1,64	Acidental	Marinha
<i>Gonyaulax</i> sp.	-	+	-	-	0,08	0,01	3,28	Acidental	Outro
<i>Gonyaulax spinifera</i> (Claparède & Lachmann) Diesing 1866	-	+	-	-	0,04	0,00	1,64	Acidental	Estuarina
<i>Gymnodinium mitratum</i> J.Schiller 1932	+	+	-	-	0,39	0,05	6,56	Acidental	Dulcícola
<i>Gymnodinium</i> sp1	-	+	-	-	0,16	0,02	3,28	Acidental	Outro
<i>Gymnodinium</i> sp2	-	+	-	-	0,08	0,01	3,28	Acidental	Outro
<i>Heterocapsa psammophila</i> M.Tamura, M.Iwataki & M.Horiguchi 2006	+	+	-	-	2,01	0,25	19,67	Acidental	Marinha
<i>Heterocapsa rotundata</i> (Lohmann) Gert Hansen 1995	+	+	-	-	0,67	0,08	8,20	Acidental	Marinha
<i>Heterocapsa</i> sp.	+	+	-	-	0,83	0,10	6,56	Acidental	Outro
<i>Noctiluca scintillans</i> (Macartney) Kofoid & Swezy 1921	-	+	-	-	0,04	0,00	1,64	Acidental	Marinha
<i>Oxytoxum crassum</i> J.Schiller 1937	-	+	-	-	0,16	0,02	3,28	Acidental	Marinha
<i>Peridinium</i> sp.	+	+	-	-	0,28	0,03	4,92	Acidental	Outro
<i>Prorocentrum gracile</i> F.Schütt 1895	+	-	-	-	0,08	0,01	3,28	Acidental	Marinha
<i>Prorocentrum micans</i> Ehrenberg 1834	+	+	-	-	0,43	0,05	11,48	Acidental	Marinha
<i>Protoperidinium crassipes</i> (Kofoid) Balech 1974	-	+	-	-	0,08	0,01	1,64	Acidental	Marinha
<i>Protoperidinium trochoideum</i> (Stein) Lemmermann, 1910	-	+	-	-	0,04	0,00	1,64	Acidental	Marinha
<i>Protoperidinium pyriforme</i> (Paulsen) Balech 1974	+	-	-	-	0,08	0,01	1,64	Acidental	Marinha
<i>Protoperidinium</i> sp.	+	+	-	+	0,28	0,04	11,48	Acidental	Outro
<i>Pyrophacus steinii</i> (Schiller) Wall & Dale 1971	-	-	-	+	0,02	0,00	1,64	Acidental	Marinha

Conclusão

CATEGORIA TAXONÔMICA	Baía ZIF	Baía ZIM	Pluma	Plat. externa	Abund. ($\times 10^3$ cel L $^{-1}$)	PAT (%)	Freq. (%)	Índice Const.	Ecologia
<i>Scrippsiella acuminata</i> (Ehrenberg) Kretschmann, Elbrächter, Zinssmeister, S.Soehner, Kirsch, Kusber & Gottschling 2015	-	+	-	-	0,04	0,00	1,64	Acidental	Marinha
<i>Triplos furca</i> (Ehrenberg) F.Gómez 2013	+	+	-	-	0,16	0,02	4,92	Acidental	Marinha
<i>Triplos lineatus</i> (Ehrenberg) F.Gómez 2021	+	+	-	-	0,36	0,04	8,20	Acidental	Marinha
Ochrophyta									
<i>Chromulina</i> sp.	+	+	-	-	0,12	0,01	3,28	Acidental	Dulcícola
Cyanobacteria									
<i>Aphanocapsa incerta</i> (Lemmermann) G.Cronberg & Komárek 1994	-	+	-	-	0,16	0,02	1,64	Acidental	Dulcícola
<i>Dolichospermum</i> sp.	-	+	-	-	0,12	0,01	1,64	Acidental	Outro
<i>Microcystis aeruginosa</i> (Kützing) Kützing 1846	+	+	-	-	0,08	0,01	3,28	Acidental	Estuarina
<i>Microcystis</i> sp.	-	+	-	-	0,04	0,00	1,64	Acidental	Outro
<i>Oscillatoria</i> sp.	-	+	-	-	0,04	0,00	1,64	Acidental	Outro
<i>Synechocystis aquatilis</i> Sauvageau 1892	+	+	-	-	0,59	0,07	3,28	Acidental	Dulcícola
<i>Trichodesmium erythraeum</i> Ehrenberg ex Gomont 1892	-	-	+	+	1,37	0,17	3,28	Acidental	Marinha
Euglenozoa									
<i>Trachelomonas volvocina</i> (Ehrenberg) Ehrenberg 1834	+	+	-	-	1,38	0,17	14,75	Acidental	Dulcícola
<i>Trachelomonas</i> sp.	-	+	-	-	0,04	0,00	1,64	Acidental	Outro
Chlorophyta									
<i>Pediastrum boryanum</i> (Turpin) Meneghini 1840	+	-	-	-	0,04	0,00	1,64	Acidental	Dulcícola
Charophyta									
<i>Bambusina borreri</i> (Ralfs) Cleve 1864	-	+	-	-	0,04	0,00	1,64	Acidental	Dulcícola

Fonte: Autoria própria (2023).

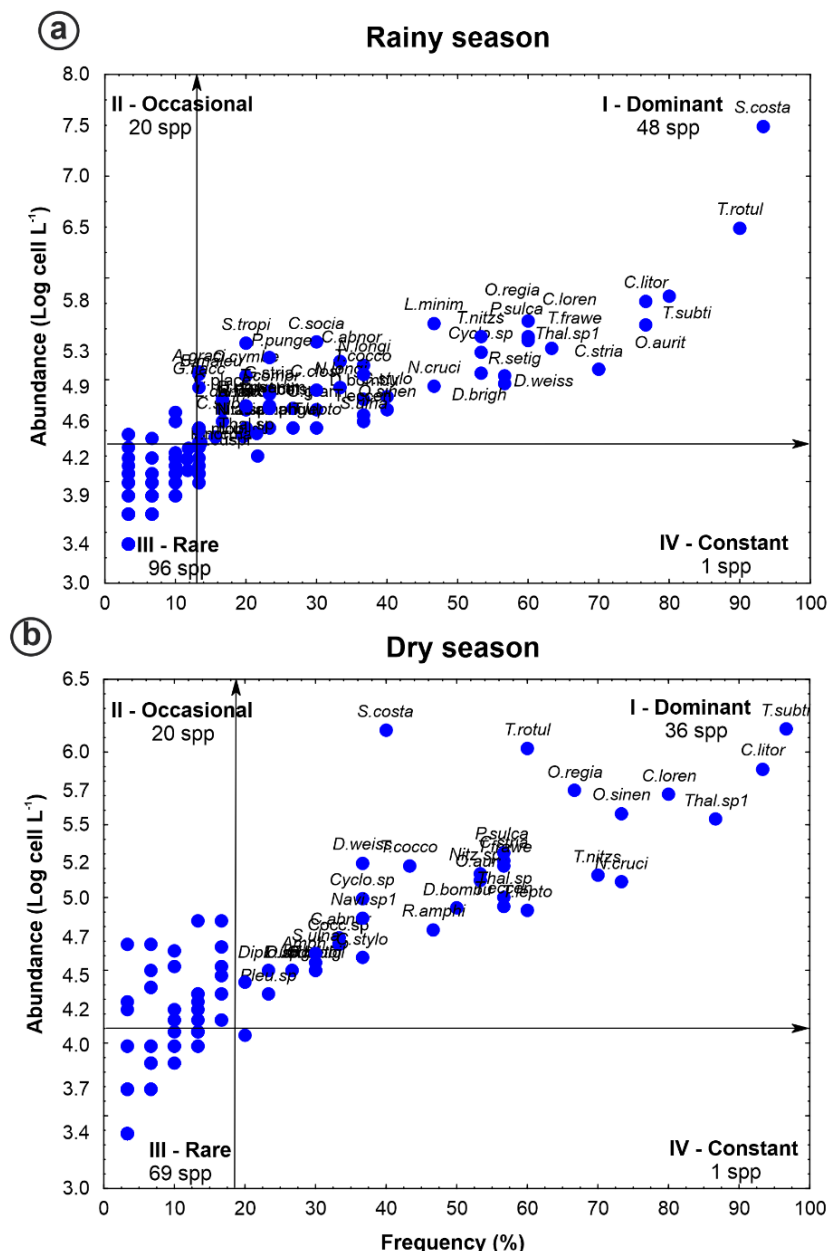
Nota: ZIF – Zona de maior influência fluvial; ZIM – Zona de maior influência marinha; Plat. Externa – Plataforma externa; Abund. – Abundância fitoplanctônica média; PAT – Porcentagem da Abundância Total; Freq. – Frequência de ocorrência; Índice Const. - Índice de Constância.

APÊNDICE D – ARTIGO 1

Drivers of phytoplankton biomass and diversity in a macrotidal bay of the Amazon Mangrove Coast, a Ramsar site

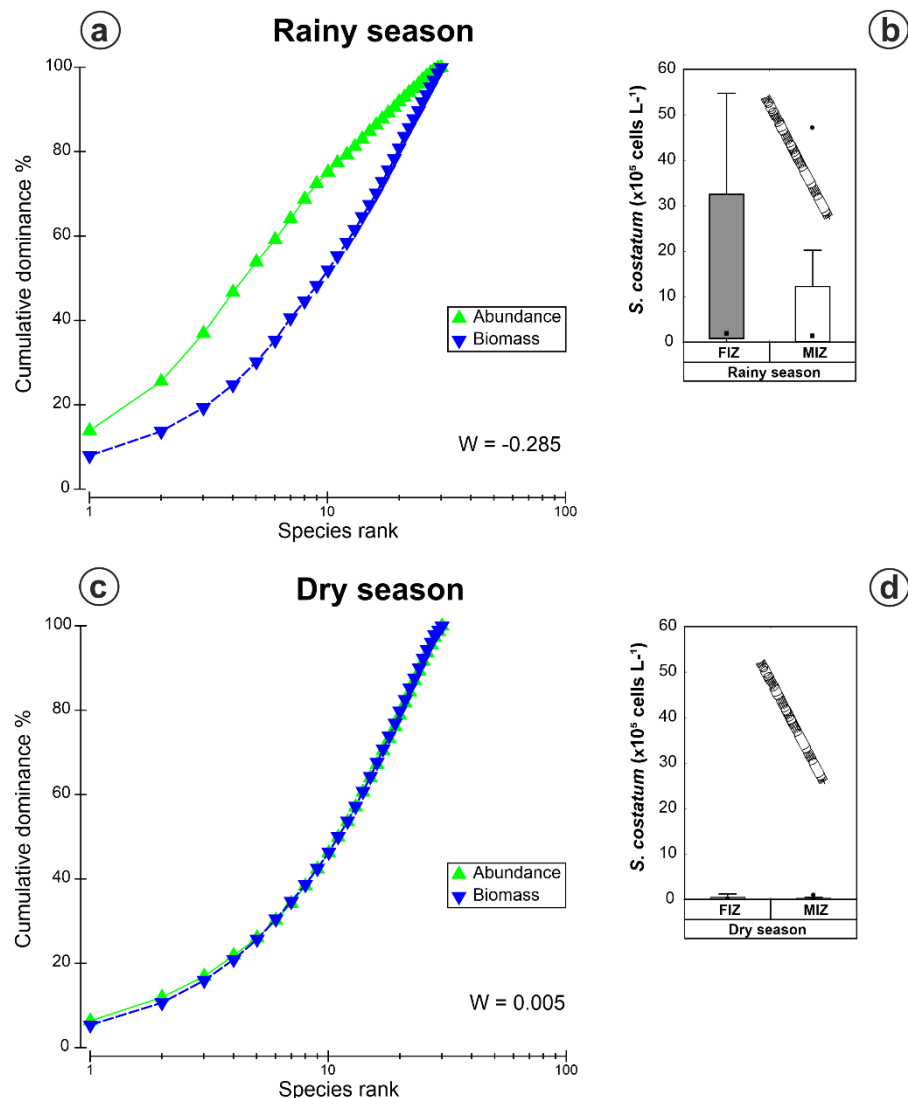
Supplementary Material

Supplementary Fig. 1. Olmstead and Tukey (O-T) diagram based on the correlation between phytoplankton abundance ($\log \text{cell L}^{-1}$) and frequency (%) in Cumã Bay during the seasonal periods: (a) rainy season and (c) dry season. Note: The arrows represent the mean values of phytoplankton abundance and frequency.



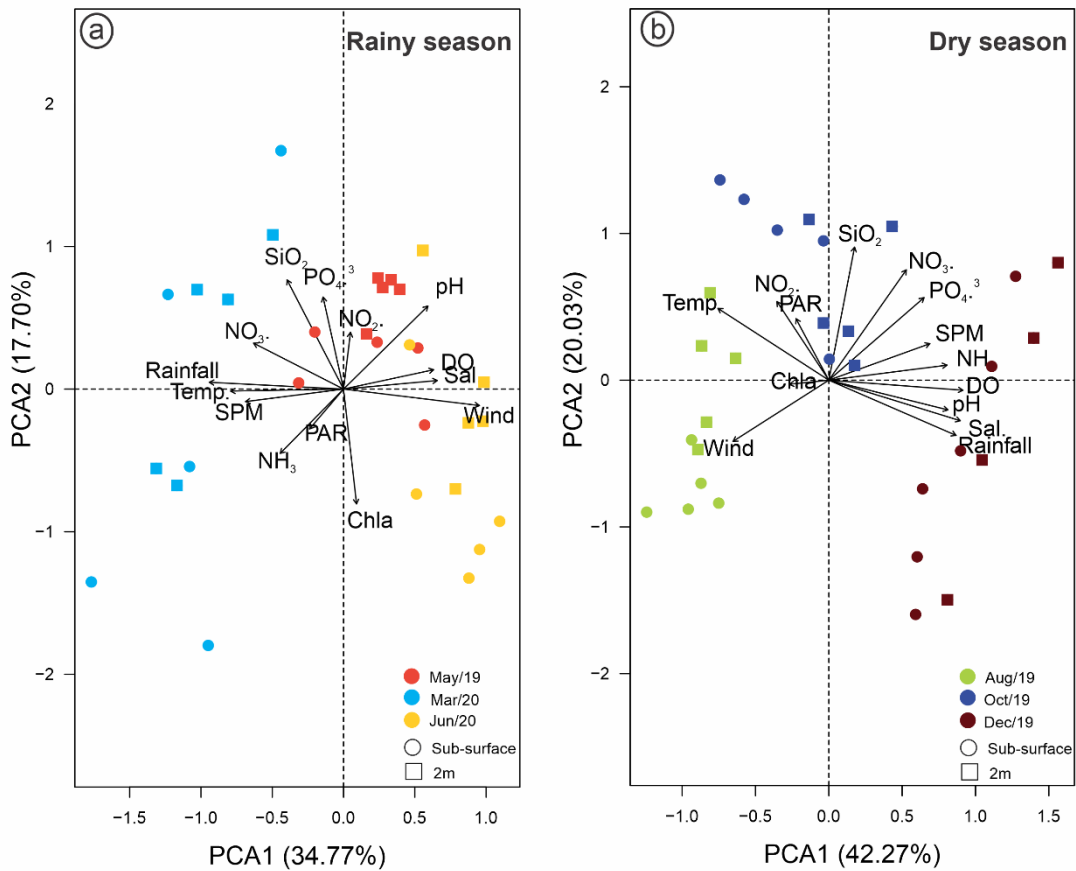
Fonte: Autoria própria (2023).

Supplementary Fig. 2. Abundance-Biomass comparison (ABC) curve by ranked species during the rainy (a) and dry (c) seasons and cell abundance of the most dominant species (*S. costatum*) (b, d) in Cumã Bay, Amazon Macrotidal Mangrove Coast.



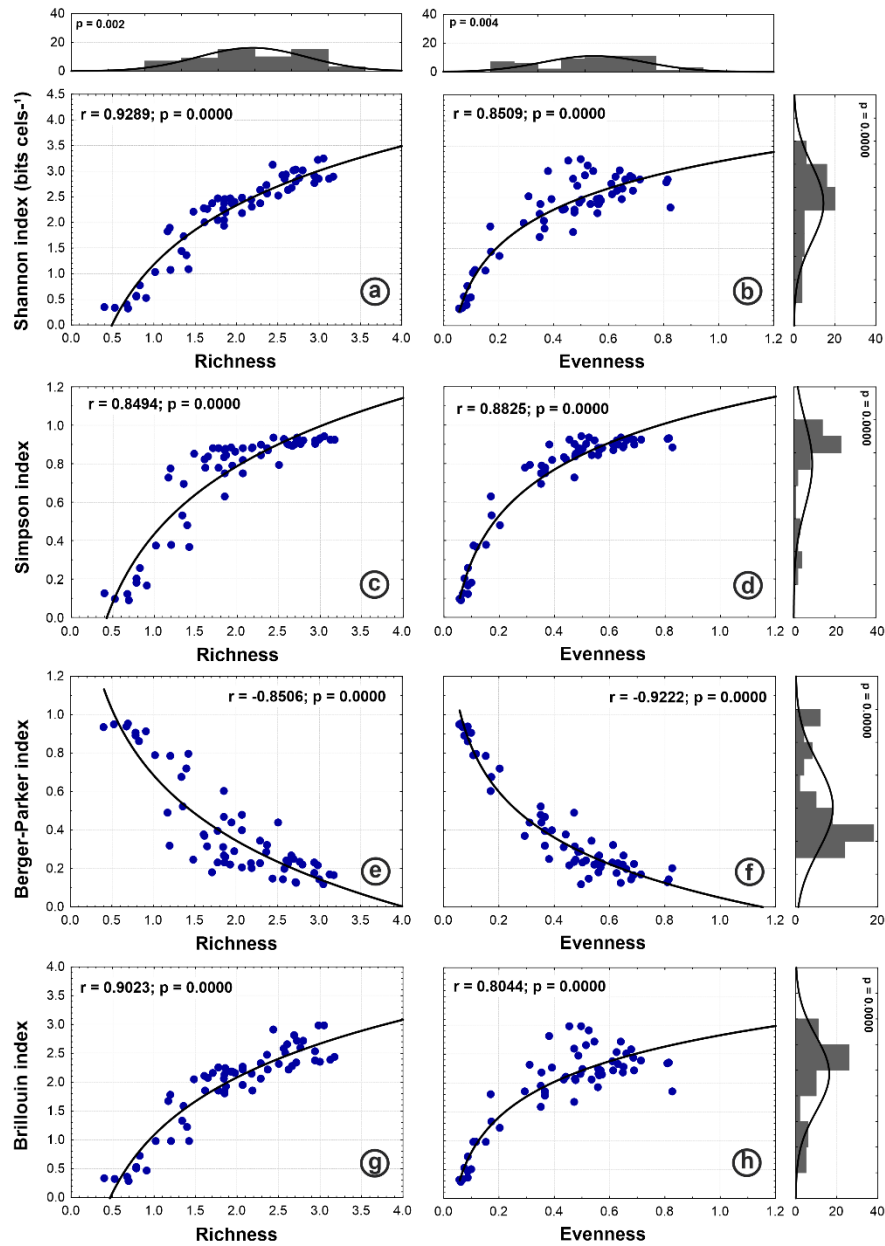
Fonte: Autoria própria (2023).

Supplementary Fig. 3. Principal Components Analysis (PCA) plot of hydrological variables and chlorophyll *a* for rainy (a) and dry (b) seasons in Cumã Bay, Amazon Macrotidal Mangrove Coast. Note: Sal = Salinity, Temp. = Temperature, Turb = Turbidity, Chla = Chlorophyll *a*.



Fonte: Autoria própria (2023).

Supplementary Fig. A. Changes in Shannon (H'), Simpson (λ), Berger-Parker (BP) and Brillouin (HB) indices along phytoplankton richness and evenness by linear regression equations in Cumã Bay.



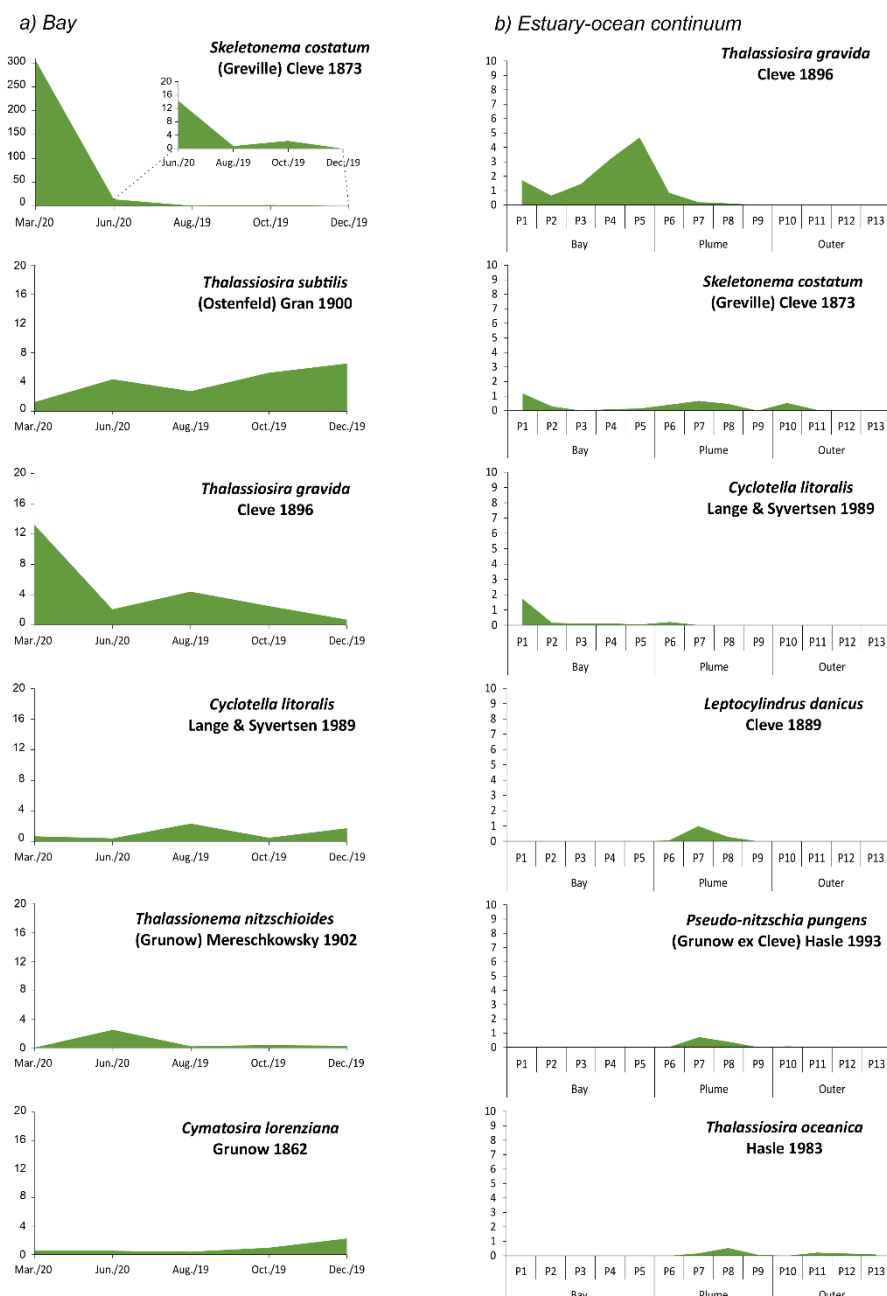
Fonte: Autoria própria (2023).

APÊNDICE E - ARTIGO 2

Effects of climate, spatial and hydrological processes on shaping phytoplankton community structure and β -diversity in an estuary-ocean continuum (Amazon continental shelf, Brazil)

Supplementary Material

Supplementary Material. Fig. S1. Phytoplankton succession of dominant species at Cumã Bay (a) and along the estuary-ocean continuum.



Fonte: Autoria própria (2023).

Supplementary Material. Table S1. Summary of exclusive and shared phytoplankton species (%) in each group defined by cluster analysis. *Shared species that occurred in at least 3 groups.

	Taxonomic groups	Temporal							Spatial		
		A1	A2	A3	A4	C	Rainy	Dry	Bay (A5)	Plume (B1)	Outer (B2)
EXCLUSIVE (%)	Bacillariophyta	1.73	1.73	14.45	1.16	1.73	20.57	7.43	41.54	12.31	1.54
	Miozoa	--	1.16	3.47	0.58	1.16	4.57	2.29	1.54	--	3.08
	Euglenozoa	--	--	0.58	--	--	0.57	--	--	--	--
	Ochrophyta	--	--	--	--	--	--	--	--	--	--
	Cyanobacteria	0.58	0.58	1.16	0.58	--	1.14	1.71	--	1.54	--
	Chlorophyta	--	--	--	0.58	--	--	0.57	--	--	--
	Charophyta	--	--	0.58	--	--	0.57	--	--	--	--
	Total	2.31	3.47	20.23	2.89	2.89	27.43	12.00	43.08	13.85	4.62
SHARED (%)	Taxonomic groups	C			A3				A5		B1/ B2
		A3	A4	A2	A1	A4	A2	A1	B1	B2	
	Bacillariophyta	4.05	1.73	1.16	--	4.05	1.73	2.89	27.69	1.54	6.15
	Miozoa	--	0.58	--	--	1.73	--	--	--	--	--
	Euglenozoa	--	--	--	--	--	--	0.58	--	--	--
	Ochrophyta	--	--	--	--	--	--	0.58	--	--	--
	Cyanobacteria	--	--	--	--	--	0.58	--	--	--	--
	Chlorophyta	--	--	--	--	--	--	--	--	--	--
	Charophyta	--	--	--	--	--	--	--	--	--	--
	Total	4.05	2.31	1.16	--	5.78	2.31	4.05	24.62	1.54	6.15
	Taxonomic groups	A4		A2/ A1	A1/A2/A3/ A4/C*		Rainy/ Dry		A5/B1/ B2		
		A2	A1	A2/ A1	A1/A2/A3/ A4/C*	A1/A2/A3/ A4/C*	Rainy	Dry	A5/B1/ B2		
	Bacillariophyta	2.31	--	1.16	40.46	40.46	52.57	--	6.15		
	Miozoa	--	--	0.58	4.05	4.05	6.29	--	--		
	Euglenozoa	--	--	--	--	--	0.57	--	--		
	Ochrophyta	--	--	--	--	--	0.57	--	--		
	Cyanobacteria	--	--	--	--	--	0.57	--	--		
	Chlorophyta	--	--	--	--	--	--	--	--		
	Charophyta	--	--	--	--	--	--	--	--		
	Total	2.31	--	1.73	44.51	44.51	60.57	--	6.15		

Fonte: Autoria própria (2023).

Supplementary Material. Table S2. Environmental (Env), climatic (Cli), spatial (Spa) variables and local hydrodynamic factors (Hyd) selected by forward selection for explaining variation in phytoplankton β -diversity and community structure.

Variables					
		Env	Cli	Spa	Hyd
β-diversity	Cumã Bay	Salinity, SPM, DO	Precipitation, wind	--	River discharge
	Estuary-ocean continuum	Salinity, PO_4^{3-}	--	AEM1, AEM2, AEM4	--
Community structure	Cumã Bay	Salinity, SPM, DO, Temp.	Precipitation, wind	--	River discharge, tides
	Estuary-ocean continuum	Salinity, SiO_2^-	--	AEM1, AEM2, AEM3	--

Fonte: Autoria própria (2023).

ANEXO A - DESENVOLVIMENTO DE ENSINO E PESQUISA DURANTE O DOUTORADO QUE CONTRIBUIU PARA A EXECUÇÃO DESTA TESE

ENSINO

1. CUTRIM, M. V. J.; CAVALCANTI, L. F.; CASTRO, A.C.L. Participação em banca de trabalho de conclusão de curso de Cybelle Cristina Silva Maciel. Variação espaço-temporal da diversidade fitoplanctônica e sua correlação com índices de estado trófico em um sistema estuarino regido por macromaré. Curso de Graduação em Oceanografia, Universidade Federal do Maranhão, MA. 2019.

PESQUISA

(i) Artigos publicados durante o curso de doutorado

1. CAVALCANTI, L. F.; AZEVEDO-CUTRIM, A. C. G.; OLIVEIRA, A. L. L.; FURTADO, J. A.; ARAÚJO, B. DE O.; SÁ, A. K. D.-S.; FERREIRA, F. S.; SANTOS, N. G. R.; DIAS, F. J. S.; CUTRIM, M. V. J. Structure of microphytoplankton community and environmental variables in a macrotidal estuarine complex, São Marcos Bay, Maranhão - Brazil. *Brazilian Journal of Oceanography*, v. 66, n. 3, p. 283–300, 2018. DOI: <https://doi.org/10.1590/s1679-87592018021906603>.
2. CAVALCANTI, L. F.; CUTRIM, M. V. J.; LOURENÇO, C. B.; SÁ, A. K. D. S.; OLIVEIRA, A. L. L.; AZEVEDO-CUTRIM, A. C. G. Patterns of phytoplankton structure in response to environmental gradients in a macrotidal estuary of the Equatorial Margin (Atlantic coast, Brazil). *Estuarine, Coastal and Shelf Science*, 245, e106969, 2020. DOI: <https://doi.org/10.1016/j.ecss.2020.106969>
3. CAVALCANTI, L. F.; CUTRIM, M. V. J.; MACIEL, C. C. S.; SÁ, A. K. D. S.; AZEVEDO-CUTRIM, A. C. G.; SANTOS, T. P.; CRUZ, Q. S. Application of multiple indices to the evaluation of trophic and ecological status in a tropical macrotidal estuary (Equatorial Margin, Brazil). *Chemistry and Ecology*, v. 38, n. 2, p. 122–144, 2022. DOI: <https://doi.org/10.1080/02757540.2021.2023509>
4. CUTRIM, M. V. J.; FERREIRA, F. S.; DUARTE DOS SANTOS, A. K.; CAVALCANTI, L. F.; ARAÚJO, B. O.; AZEVEDO-CUTRIM, A. C. G.; FURTADO, J. A.; OLIVEIRA, A. L. L. Trophic state of an urban coastal lagoon (northern Brazil), seasonal variation of the phytoplankton community and environmental variables. *Estuarine, Coastal and Shelf Science*, v. 216, p. 98–109, 2019. DOI: <https://doi.org/10.1016/j.ecss.2018.08.013>
5. SÁ, A. K. D. S.; CUTRIM, M. V. J.; COSTA, D. S.; CAVALCANTI, L. F.; FERREIRA, F. S.; OLIVEIRA, A. L. L.; SEREJO, J. H. F. Algal blooms and trophic state in a tropical estuary blocked by a dam (northeastern Brazil). *Ocean and Coastal Research*, v. 69, p. 1-16, 2021. DOI: <https://doi.org/10.1590/2675-2824069.20-006akddss>

6. SÁ, A. K. D. S.; FEITOSA, F. A. N.; CUTRIM, M. V. J.; FLORES-MONTES, M. J.; COSTA, D.S.; **CAVALCANTI, L. F.** Phytoplankton community dynamics in response to seawater intrusion in a tropical macrotidal river-estuary continuum. *Hydrobiologia*, [S.I.], 2022a. DOI: <https://doi.org/10.1007/s10750-022-04851-7>.
7. SÁ, A. K. D. S.; CUTRIM, M. V. J.; FEITOSA, F. A. N.: FLORES-MONTES, M. J.; **CAVALCANTI, L. F.**; COSTA, D. S.; CRUZ, Q. S. Multiple stressors influencing the general eutrophication status of transitional waters of the Brazilian tropical coast: An approach utilizing the pressure, state, and response (PSR) framework. *Journal of Sea Research*, v. 189, 102282, 2022b. DOI: <https://doi.org/10.1016/j.seares.2022.102282>
8. CRUZ, Q. S.; CUTRIM, M. V. J.; SANTOS, T. P.; SÁ, A. K. D. S.; **CAVALCANTI-LIMA, L. F.** Environmental heterogeneity of a tropical river-to-sea continuum and its relationship with structure and phytoplankton dynamics – Lençóis Maranhenses National Park. *Marine Environmental Research*, v. 187, 105950, 2023. DOI: <https://doi.org/10.1016/j.marenvres.2023.105950>

(ii) Capítulo de livro

1. **CAVALCANTI, L. F.**; OLIVEIRA, A. L. L.; ARAUJO, B. O.; FURTADO, J. A.; DUARTE-DOS-SANTOS, A. K.; FERREIRA, F. S.; CUTRIM, M. V. J. *Divisão Bacillariophyta (diatomáceas) e gradiente de salinidade em um estuário tropical (Estuário do Rio Paciência, Maranhão)*. In: SANTOS, M. E. M. (Org.). Tópicos multidisciplinares em ciências biológicas: trabalhando ensino, pesquisa e extensão. 1ed. SÃO LUÍS: Universidade Estadual do Maranhão - UEMA, v. 1, p. 13-24, 2018.
2. **CAVALCANTI, L. F.**; SÁ, A. K. D. S.; CRUZ, Q. S.; SANTOS, T. P.; OLIVEIRA, A. L. L.; COSTA, D. S.; BRITO, M. V.; FERREIRA, F. S.; AZEVEDO-CUTRIM, A. C.G.; CUTRIM, M. V. J. *Fitoplâncton da área portuária da Baía de São Marcos (Costa Norte do Brasil)*. In: SOUSA, D. B. P.; CASTRO, J. S.; JESUS, W. B. (Org.). Monitoramento Ambiental: metodologias e estudos de casos. 1ed. São Luís: i-EDUCAM, p. 1-183, 2022.
3. CUTRIM, M. V. J.; FERREIRA, F. S.; **CAVALCANTI, L. F.**; SÁ, A. K. D. S.; AZEVEDO-CUTRIM, A. C. G.; SANTOS, R. L. *Phytoplankton Biomass and Environmental Descriptors of Water Quality of an Urban Lagoon*. In: PAN, J.; DEVLIN, A. (Eds.) *Estuaries and Coastal Zones - Dynamics and Response to Environmental Changes*, p. 1-18, IntechOpen, 2019.

(iii) Premiação

1. Prêmio de 1º lugar na modalidade Pôster (Ciências Biológicas) na XIV Mostra Acadêmico-Científica e Cultural em Ciências Biológicas e IV Simpósio de Ciências Biológicas - Universidade Estadual do Maranhão (2019). Trabalho apresentado intitulado: “*Diversidade fitoplanctônica no Estuário do Rio Guarapiranga, Reentrâncias Maranhenses-Brasil*”.

(iv) Divulgação científica

1. Apresentação de trabalho para a Popularização da Ciência (Live) na Série: *Jovens Limnólogos - Fitoplâncton* pela Associação Brasileira de Limnologia (ABLimno) - 2020. Apresentação intitulada: “*Fitoplâncton como indicador de Bacias Urbanas do Maranhão*”.